Hydroxycinnamic acids in sunflower leaves as UV protecting secondary metabolites responsive to different abiotic stress conditions

Doctoral thesis for obtaining the academic degree

Doctor of Natural Sciences

(Dr. rer. nat.)

at the Faculty of Mathematics and Natural Science

of Christian-Albrechts-University, Kiel

Submitted by

Jana Stelzner

Kiel, 2023

Prüfungskommission

Vorsitz:	Prof. Dr. rer. nat. Regina Scherließ
Erstgutachten:	Prof. Dr. rer. nat. Wolfgang Bilger
Zweitgutachten:	Prof. Dr. rer. nat. Dietrich Ober
Beisitz:	Prof. Dr. rer. nat. Jennifer Selinski
Tag der Disputation:	04.07.2023

Content

1 Introduction

1.1 The plant's environment and responding metabolism

Each plant population – holding true for every other population – is exposed to a whole set of dynamic environmental parameters that the plants respond to on different time scales ensuring optimal performance in their habitat (Lüttge and Scarano 2004; Lambers and Oliveira 2019). The parameters involve both biotic and abiotic variables of which the first result from co-existing living organisms such as other plants, herbivores, fungi, viruses, or bacteria. Abiotic parameters, on the contrary, include physical variables such as the incident radiation (e.g. photosynthetically active and ultraviolet radiation), surrounding temperature (that of the soil and the air) and the inorganic soil composition (availability of water and nutrients). The individual variables undergo long-term and short-term changes resulting in a large spectrum of possible combinations characterizing specific seasons, daytimes or habitats and geographical sites (Barnes et al. 2013, 2016b; Duan et al. 2014; Mu et al. 2021; Pescheck and Bilger 2019; Price et al. 1999; Teixeira et al. 2020). If a particular abiotic parameter exists as stress, i.e. in a manner that an organism is not yet appropriately equipped for, the plants can experience strain that may cause severe negative effects on their physiological performance (Levitt 1980; Cramer et al. 2011; Lambers and Oliveira 2019). Considering the sessile nature of the plants, they need to adjust appropriately to their habitat in order to avoid or, at least, reduce the strain. Appropriate adjustment to a certain stress factor can result from genetic adaptation over generations if the stress persists and selects for strain-reducing mutations (Levitt 1980). Besides, phenotypic plasticity allows plants of the same genotype to respond variably to their environment on a short-term scale conferring the capability to recover their optimal performance – partially or fully – by physiological and morphological adjustment, i.e. acclimation (Piersma and Drent 2003; Lambers and Oliveira 2019). Thus, acclimation requires an interaction of the environment with the plant's metabolism at various coordinating points (Cramer et al. 2011; Sha Valli Khan et al. 2014; Pereira 2016). In general, the metabolism in plants can be subdivided into the so-called primary and secondary metabolism. While the former denominates the biochemical pathways that are essential for plant survival, growth and development including energy-delivering processes such as photosynthesis or glycolysis, secondary metabolism involves diverse partially inducible biochemical pathways that ensure optimal performance of plants in the given ecological context. Both primary and secondary metabolisms are intertwined and dependent on each other in a manner that is highly complex and the detailed description would go beyond the scope of the present work. The interactions of the environment and the plant's biochemistry that are assumed relevant for a comprehension of the experimental approach in this study are being described in excerpts in the following sections with a focus on secondary metabolic pathways.

1.1.1 The role of plant's metabolism for mankind

Before going into any further detail of interactions between the environment and plants secondary metabolism, a brief digression regarding the role of the latter for humankind will be introduced.

Humans have used a variety of selected plant species, most often herbs, for a long time as sources of (traditional) medicines, spices, dyes and perfumes likely centuries before the reasons for their pharmacological – or at least health benefiting – effects were scientifically explained (Bentley 1997; Verpoorte 2000; Kalemba and Kunicka 2003). Ongoing technical development of extraction, analysis and essay methods of plant metabolites has made it possible to identify plant's secondary metabolism as responsible for those effects. Secondary metabolites include a tremendously large variety of mono- or multifunctional molecules that fulfil diverse protective functions or act as signalling molecules integrating external stimuli to the plant's organism (Verpoorte 2000; Herms and Mattson 1992; Harborne 2007; Demain and Fang 2000; Rice-Evans et al. 1997). One well known example is salicylic acid from *Salix alba* as leading compound for ASA (acetylic salicylic acid) that is widely used in therapeutic medicine because of its analgesic, anti-inflammatory, antipyretic and blood thinning effect since the 19th century (Vane 1971; Roth et al. 1975; Alfonso et al. 2014). For the sake of completeness, it should be denoted without going into further detail that secondary metabolites may also have toxic or even lethal effects on the human organism as known from the famous cup of hemlock that Socrates was condemned to drink (Bentley 1997). Nowadays, a vast number of secondary metabolites is of high economic importance for mankind involving applications in medicine or in perfume, dye and food production (Verpoorte 2000; Kalemba and Kunicka 2003). Products of the phenylpropanoid metabolism, for example, include flavonoids and hydroxycinnamic acids, which are often reported to reduce the risk of particular diseases by their antioxidative, anti-inflammatory or antimicrobial properties (Hussein and El-Anssary 2018; dos Santos et al. 2006; Rice-Evans et al. 1997; Crozier et al. 2009; Scalbert and Williamson 2000; Vogt 2010). Besides acting as suitable candidates for serving as basis structure with diverse applications for pharmacological industry, the food industry also has a growing interest in these bioactive compounds that improve the nutritional values and stress tolerance of crops (Rice-Evans et al. 1996; Crozier et al. 1997; Grundy et al. 2015). Thus, research on the relationship between plant secondary metabolites and the environment and its underlying genetically determined regulation mechanisms is a necessary step towards further applications like targeted and specific manipulation of plants' metabolism for human usage (Grace et al. 1998; Verpoorte 2000). Whether the improvement occurs via biotechnological or less interventional approaches such as traditional breeding or application of specific growth conditions has to be a matter of a societal discussion.

1.2 The physiological relevance of terrestrial solar radiation for plants

Plants are photoautotrophic organisms and provide the energy they require themselves by light-driven carbon assimilation, i.e. oxygenic photosynthesis. This process constitutes an important –if not the most important – part of the primary metabolism involving the entirety of biochemical routes essential for growth, development and reproduction. During photosynthesis, light energy is successively converted into storable biochemical energy equivalents by pigment-protein complexes such as photosystem II and I (PS II and PS I) (Shevela et al. 2013). The particular driving force of photosynthesis is – as the name implies – photosynthetically active radiation (PAR). This radiation has

been defined as ranging from 400 to 700 nm in wavelength in accordance with action spectra of photosynthesis measured as either CO_2 assimilation or O_2 evolution and absorption spectra of the photosynthetic pigments (Inada 1976; McCree 1972; Govindjee et al. 1968). However, the sun emits a spectrum of electromagnetic radiation that is by far broader than the wavebands that drive photosynthesis (Fig. 1.1). The complete solar emission spectrum covers wavelengths from 200 nm to more than 5000 nm of which an approximate interval from 300 to 3000 nm, belonging to optical radiation, is transmitted through earth's atmosphere (Thekaekara 1974; Mecherikunnel and Richmond 1980; Liou 2002a, 2002b, 2002c). The radiation below 300 nm is absorbed mainly by ozone whereas some wavebands above 300 nm are filtered out especially by water vapour, oxygen and carbon dioxide (Mecherikunnel and Richmond 1980; U.S. Department of Energy (DOE)/NREL/ALLIANCE 2003). The spectral region of optical radiation with wavelengths longer than those of PAR is referred to as thermal or infrared radiation. The steady state of earth's infrared radiation (IR) resulting from reflectance by the earth's surface and absorption by the earth's atmosphere mainly determines the terrestrial air temperature (Pierrehumbert 2004). Plants are ectotherm organisms, which usually do not generate own body heat, so that the temperature of plants is – together with convective or evaporative heat flux processes – strongly dependent on the terrestrial air temperature. Thus, without substantially being absorbed by the plant's structures themselves, IR does not affect photosynthesis and other metabolic pathways (Lambers and Oliveira 2019).

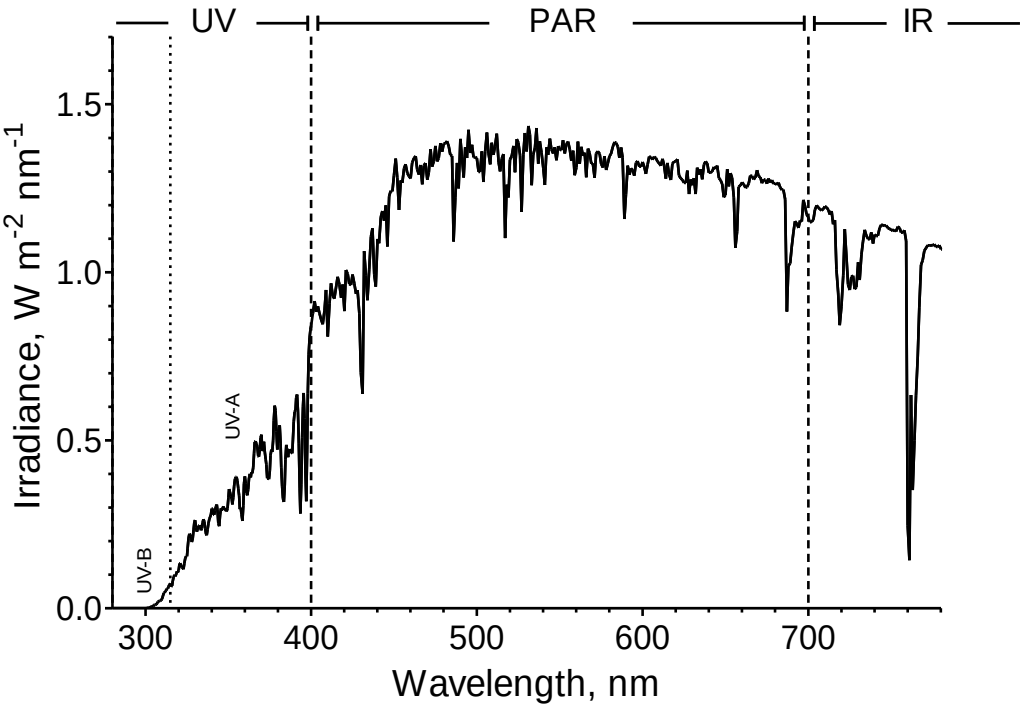

Figure 1.1 Terrestrial solar radiation from 290 to 790 nm based on the reference spectrum ASTM (American Society for Testing and Materials) G173-03 provided by the National Renewable Energy Laboratory of the U.S. Department of Energy, Office of Energy, Efficiency and Renewable Energy (U.S. Department of Energy (DOE)/NREL/ALLIANCE 2003) for direct and circumsolar irradiance.

Based on the visual properties of the human eye, the spectral part of electromagnetic radiation reaching the earth's surface below 400 nm has been defined as ultraviolet radiation (UVR, 280–400

nm). This region can be subdivided into UV-B ranging from 280 to 315 nm and UV-A with an interval from 315 to 400 nm (CIE, International Commission on Illumination 2014; Björn 2015) (Fig. 1.1). The amount of UVR is many times lower than that of PAR and IR with irradiance based ratios of UV-A/PAR=0.081 and UV-B/PAR=0.001, respectively (Mecherikunnel and Richmond 1980; Liou 2002c) and Table 1.1).

Table 1.1 Waveband-specific irradiance and photon flux density for terrestrial solar radiation

Terrestrial radiation	Waveband, nm	Irradiance, W m^{-2}	Proportion*, %	PFD, µmol m^{-2} s^{-1}
PAR + UV	280 – 700	404.37	100	1827
PAR	400 – 700	373.64	92.4	1731
Total UV	280 – 400	30.73	7.6	94
UV-A	315 – 400	30.34	7.5	93
UV-B	280 – 315	0.39	0.1	1

The irradiance and photon flux density (PFD) was calculated for 280 to 700 nm on the basis of the ASTM G173-03 reference spectrum *(U.S. Department of Energy (DOE)/NREL/ALLIANCE 2003)*. *Irradiance-based

However, this shortwave radiation is highly relevant for plant's survival and development. The physiological relevance of radiation ensues from being absorbed by physiologically important molecules as described in more detail in the following section and is based on the energy content of its photons (Cockell 1997). The more energy a photon possesses, the higher is the potential to cause destruction of chemical bonds. The energy content (E) of a mole of photons is the product of the Avogadro constant $N_a = 6.022 \times 10^{23}\ mol^{-1}$, the Planck's quantum of action $h = 6.626 \times 10^{-34}$ J s and the photons' frequency (ν) (equation (Eq.) 1). The latter is equal to the quotient of and the speed of light $c = 2.998 \times 10^{17}\ nm\ s^{-1}$ and the wavelength (λ) (Eq. 2).

(Eq. 1) $E = N_a \times h \times \nu$ and (Eq. 2) $\nu = {}^{c}/_{\lambda}$ gives

(Eq. 3) $E = N_a \times h \times \frac{c}{\lambda}$.

Equation 3 demonstrates that the energy content per mole photons increases with decreasing wavelengths. Accordingly, the ultraviolet spectral range contains photons with the highest energy levels.

1.2.1 Physiological consequences of ultraviolet radiation for plants

As shown in the previous section, terrestrial ultraviolet radiation poses a risk for plants. The understanding of how UV acts on plants remains an important factor especially for crop production (Norval et al. 2011; Bornman et al. 2019; Takshak and Agrawal 2019). Various cellular components and macromolecules lose their functionality upon the absorption of photons with wavelengths below 400 nm (Strid et al. 1994; Jansen et al. 1998). The UV absorptivity of these components is given especially by π-electron systems in e.g. nucleic acids, unsaturated membrane components including

phospho- or glycolipids or aromatic amino acids (Cockell 1997; Hollósy 2002). In addition, proteins often contain disulphide bonds that absorb UV as well (Cockell 1997). Besides, particularly those metalloenzymes are UV-susceptible of which the catalytic function depends on manganese as co-factor, independent of the content of UV-absorbing aromatic amino acids (Hakala 2006). The degree of the damage resulting from ultraviolet radiation increases with the absorbed energy content differentially for distinct metabolic processes and components such as DNA or the oxygen evolving complex (OEC) as shown by exposure to artificial UV radiation (Takahashi et al. 2010; Hakala et al. 2005; Quaite et al. 1992; Setlow 1974; Sarvikas et al. 2006). The action spectra of UV weighted for biological quantum efficiency on different physiological processes such as DNA damage, plant growth response or photoinhibition share the conclusion that UV-B must be regarded as the most hazardous natural radiation to living organisms (Quaite et al. 1992; Ghetti et al. 1999; Flint and Caldwell 2003; Takahashi et al. 2010). The potential of UV-A radiation to impair physiological processes is different from the biological effectiveness of UV-B radiation and underlying molecular and biochemical mechanisms are distinct from each other (Verdaguer et al. 2017). For example, UV-B radiation consistently causes a reduced size of leaves and biomass production of aerial parts, whereas leaf area and plant growth may be affected either positively or negatively among different species by UV-A (Panagopoulos et al. 1990; Tezuka et al. 1993; Krizek et al. 1997; Kataria et al. 2013; Verdaguer et al. 2017).

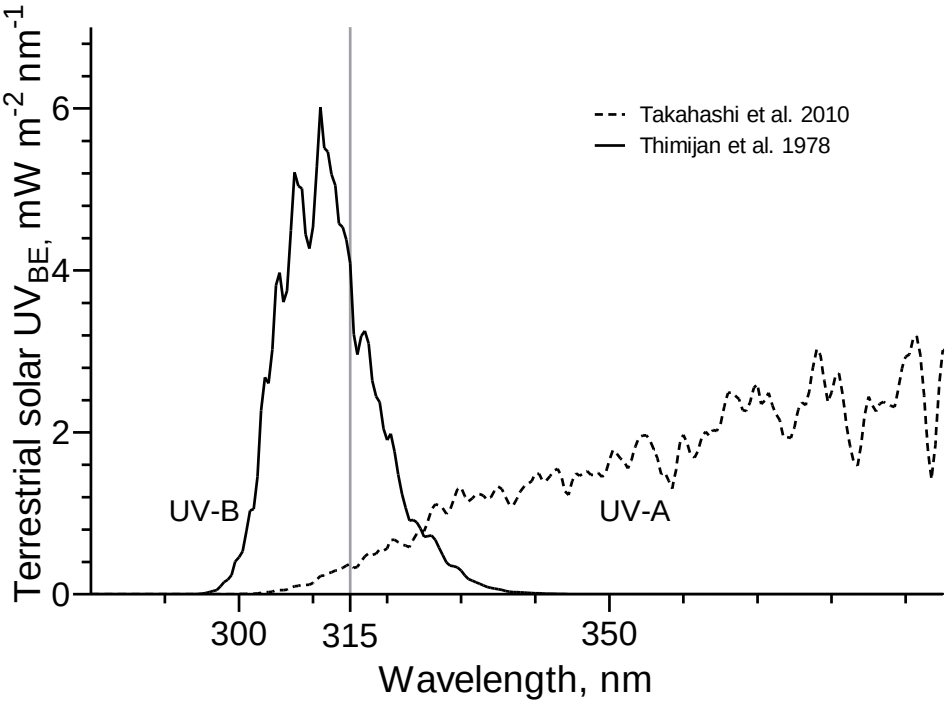

Figure 1.2 Solar UV action spectra weighted for biological effectiveness
Biological effectiveness was calculated as the product of terrestrial solar irradiance spectrum (ASTM G173-03) and the action spectrum for photoinhibtion published in Takahashi et al. (2010; dashed line) or by Thimijan et al. (1978, solid line). For a high resolution, the action spectrum of Takahashi et al. was fitted with the following exponential growth equation: $Photodamage\ efficiency = 5.019*10^{6*e-0.04075*\lambda}$. The published action spectrum of Thimijan (1978) included an equation, which was used for calculation. The grey vertical line marks 315 nm.

Although the damaging potential of UV-B photons strongly exceeds that of UV-A photons, both types of radiation are risky for plants since terrestrial irradiance of UV-A exceeds that of UV-B by far (Vass 2012; Verdaguer et al. 2017) (Table 1.1). Based on the higher irradiance, UV-A is proposed – especially in the context of photosynthesis – to be the more hazardous part of the solar ultraviolet spectrum for plants (Turcsányi and Vass 2000; Vass et al. 2002; Sarvikas et al. 2006; Hakala-Yatkin et al. 2010; Vass 2012). Dependent on published action spectra, the biologically effective doses of UV-A is as relevant as that of UV-B (Thimijan et al. 1978; Takahashi et al. 2010)(Fig. 1.2). Consistently, a loss of oxygen evolution and concomitantly decreased photosynthetic quantum efficiency was found under UV-A irradiation for isolated thylakoids, green algae and intact leaves (Herrmann et al. 1997; Turcsányi and Vass 2000; Vass et al. 2002; Hakala-Yatkin et al. 2010). At the same time, the degree of photoinhibition is directly dependent on the duration of irradiation suggesting a dose-dependency on absorbed ultraviolet photons (Vass et al. 2002). The reduced photosynthetic quantum efficiency was explained by possible indirect effects such as adjustment of stomatal aperture or leaf thickness as well as more direct damaging effects on molecular components of the photosynthetic apparatus due to absorption of UV-A photons or ROS production (Hollósy 2002; Vass 2012; Jansen et al. 2022). The molecular component mainly inactivated by UV-A is PS II whereas PS I functionality appears negligibly affected (Turcsányi and Vass 2000). For the UV-A induced loss of PS II electron transfer the most relevant target of destruction has been identified to be the OEC with the catalytic Mn_4O_5Ca cluster in mechanistic approaches in accordance with the absorbance of manganese cations (Vass et al. 2002; Hakala et al. 2005; Sarvikas et al. 2006; Sicora et al. 2006; Tyystjärvi 2008). Hence, the underlying molecular mechanism is proposed to occur via UV absorption by manganese inducing a break of a covalent bond within the catalytic cluster resulting in the loss of a Mn^{2+} ion (Hakala et al. 2005; Vass 2012). Other suggested UV-A induced mechanisms of PSII impairment involve the degradation of the D1 and D2 core proteins and alteration of binding affinity to Q_B at the acceptor binding site caused by molecular modifications (Greenberg et al. 1989; Turcsányi and Vass 2000; Vass et al. 2002; Nayak et al. 2003). In a few plant species UV-A affected photosynthesis in a positive manner when they had grown under natural UV-levels (Bernal et al. 2013; Tezuka et al. 1993, 1994; Verdaguer et al. 2017). These findings indicate the presence of resistance mechanisms in order to cope with UV involving both adaptation and acclimation.

1.3 Resistance strategies to cope with the risks of ultraviolet radiation

Plants have a variety of resistance strategies to cope with the physiological risk of high UV irradiance levels (Cockell 1997; Takahashi and Badger 2011). During evolution, plants developed specific and non-specific mechanisms counteracting or preventing UV-initiated cascades of damaging events such as inhibition of photosynthesis (Xiong and Day 2001; Hakala-Yatkin et al. 2010; Tohge et al. 2013). For example, a non-functional D1 protein of photosystem II can be replaced by functional one, a process known as the D1 repair cycle (Järvi et al. 2015). This repair cycle involves biochemical processes including D1-specific disassembly, enzymatic degradation and *de novo* synthesis that take effect when the high energy radiation has already been absorbed by the plant tissue and induced damage (Ohad et al. 1984; Cockell 1997; Theis and Schroda 2016). In contrast, preventing systems are

mechanisms that minimise absorption of incident UV radiation by sensitive cellular structures and their ensuing damaging effects as well as energetic costs of repair mechanisms (Cockell and Knowland 1999; Takahashi and Badger 2011). According to Lambert's cosine law, solar irradiation including ultraviolet radiation reaching a leaf can be attenuated by increasing the angle of incidence *via* leaf movements (Cockell and Knowland 1999; Lüders und Pohl 2006; Takahashi and Badger 2011). Another important and ubiquitously employed mechanism is the accumulation of UV screening pigments as produced by the secondary metabolism and specifically absorb UV (Cockell 1997; Takshak and Agrawal 2019).

1.3.1 Secondary metabolites as UV screening pigments

The accumulation of UV screening pigments in the epidermis, the outermost layer, of plants attenuates incident UV radiation before it can penetrate into the valuable inner tissue where photosynthesis and other essential metabolic processes take place (Hutzler 1998; Cockell and Knowland 1999; Kolb et al. 2001; Takahashi and Badger 2011). This effective strategy of UV attenuation by screening pigments is widely distributed among the plant kingdom. It has been shown for many higher plants and is also found in algae and cyanobacteria (Garcia-Pichel and Castenholz 1991; Day 1993; Day et al. 1993, 1994; Cockell and Knowland 1999; Rozema et al. 2002; Nybakken et al. 2004; Gao and Garcia-Pichel 2011; Pescheck 2019). A few common characteristics are required of molecules in order to function as UV screens (Cockell and Knowland 1999). The first – and most obvious – requirement is the general absorptivity of ultraviolet radiation. In a second criterion, this absorptivity is specified in so far that it should be physiologically effective. This can be considered the case when molecules are localized in the organism in a way that they reduce UV radiation at sensitive targets, for example in the epidermis (Hutzler et al. 1998; Takahashi and Badger 2011). Thirdly, their presence must protect against physiological UV damage so that individuals with UV pigments survive better under elevated UV radiation as compared to individuals in which UV pigments are absent or not sufficiently abundant. A further characteristic of a UV-protecting molecule is that its accumulation is inducible by UV radiation (Cockell and Knowland 1999). According to these authors, the UV-specific response presents "strong evidence" for a UV screening function, although it is not obligatory since constitutively present molecules can provide protection to the same extent (Cockell and Knowland 1999).

Compounds in plants that fulfil the criteria stated by Cockell and Knowland (1999) are flavonoids and hydroxycinnamic acids (HCAs), both diverse product groups of the phenylpropanoid biosynthetic pathway – and, thus, secondary metabolites (Robberecht and Caldwell 1978; Landry et al. 1995). Flavonoids and HCAs have a C6-C3 basic skeleton with an UV absorbing π-electron system in common and provide a physiologically effective UV protection – if localized in the epidermis – that ensures enhanced survival under ultraviolet radiation (Li et al. 1993; Landry et al. 1995). In the beginning of the research on UV protecting systems in plants, the epidermis and therein located flavonoids were identified as effective UV-B attenuators (Robberecht and Caldwell 1978; Caldwell et al. 1983). Further research showed that the epidermal UV-B and UV-A transmittance in rye and bean correlates

closely to the content of epidermal flavonoids but not to that of HCAs suggesting the latter to occur in other tissues than the epidermis or being present in non-variable amounts (Burchard et al. 2000; Bilger et al. 2001; Markstädter et al. 2001). Several years later, HCAs have been shown to be as screening pigments more relevant for protection against UV-B than flavonoids in *Arabidopsis* mutants (Chapple et al. 1992; Landry et al. 1995; Sheahan 1996). Consistently, the molar UV-B absorbance of flavonoids is lower than that of HCAs and different spectra of protection were proposed for both compound groups (Agati and Tattini 2010; Agati et al. 2012). Hence, epidermal flavonoids have been proposed as specific UV-A screens due to their maximal extinction around 350 nm whereas shielding of UV-B was mainly assigned to epidermal hydroxycinnamic acids since they absorb maximally at or below 330 nm (Agati et al. 2009; Pfündel et al. 2006; Agati et al. 2012; Agati and Tattini 2010). It is conceivable that plants ensure their UV protection over the whole bandwidth of UV-B and UV-A cost-effectively by synthesizing both groups since plant's phenolic compound patterns often involve both flavonoids and HCAs with flavonoids being more abundant (Cockell and Knowland 1999; Burchard et al. 2000; Bidel et al. 2007).

However, in several species, epidermal UV-B and UV-A absorbance correlated with the highest degree of accuracy to the sum of epidermal flavonoids and HCAs as compared to consideration of solely one compound group (Burchard et al. 2000; Kolb and Pfündel 2005). Precursors of both classes derive from the shikimic acid biosynthetic pathway and are further metabolized by the common enzymes phenylalanine ammonia lyase, cinnamate-4-hydroxylase and 4-coumarate-CoA ligase (PAL, C4H and 4CL) via phenylalanine to *p*-Coumaroyl-Coenzyme A (Bennett and Wallsgrove 1994; Petersen et al. 2009; Biała and Jasiński 2018) (Fig. 1.3). The latter molecule corresponds to the point at which the pathway divides in several branches of which two distinct ones lead to flavonoid and HCA biosynthesis (Vogt 2010; Liu et al. 2015a). One subclass of HCAs comprises caffeoylquinic acids (CQAs), which are ubiquitously present among the plant kingdom (Clifford 1999). Their biosynthesis involves the enzymes hydroxycinnamoyl-CoA:quinate transferase (HQT) and hydroxycinnamoyltransferase (HCT), which have been identified and characterised in a few species (Clifford 1999; Hoffmann et al. 2003; Hoffmann 2004; Niggeweg et al. 2004; Comino et al. 2007, 2009; Sonnante et al. 2010; Moglia et al. 2014; Cheevarungnapakul et al. 2019). Both enzymes share the conserved amino acid motifs HXXXD and DFGWG – likely conferring the acyltransferase activity (Brown et al. 1994; St-Pierre et al. 1998; Hoffmann et al. 2003; Niggeweg et al. 2004; Comino et al. 2007, 2009; Sonnante et al. 2010; Moglia et al. 2016; Cheevarungnapakul et al. 2019). A key role for HQT in the accumulation of the monocaffeoylquinic derivative chlorogenic acid was shown in transgenic potato and coffee plants (Lepelley et al. 2007; Payyavula et al. 2015). However, neither their sequential arrangement along the pathway nor specific reactions are yet fully understood so that several biosynthesis routes are proposed among different species (Niggeweg et al. 2004; Sonnante et al. 2010; Moglia et al. 2016; Cheevarungnapakul et al. 2019) (Fig. 1.3).

1.4 Regulation of UV screening by abiotic environmental parameters

The specific phenylpropanoid profiles of plants are tremendously diverse, strongly vary with individual taxonomical classification, and are furthermore subject of phenotypic plasticity (Dixon and Paiva 1995; Bentley 1997; Verpoorte 2000). The concrete combination of secondary metabolites may change among different tissues or organs and is a result of specific biosynthetic enzymes whose activity is regulated by abiotic – besides biotic – variables that underlie seasonal and daily rhythms and fluctuations (Bentley 1997; Verpoorte 2000; Medina-Sánchez et al. 2002; Barnes et al. 2016b; Pescheck and Bilger 2019). The knowledge of the regulation of epidermal UV screening by different abiotic parameters and linked UV pigment biosynthesis will be dealt in more detail in the next section.

1.4.1 Regulation of UV screening by single abiotic variables

The epidermal UV screening capacity of many higher plants is affected by various parameters of the abiotic environment (Pescheck and Bilger 2020). The presence of ultraviolet radiation, for instance, strongly induces an increase in epidermal UV absorbance in many higher plants of multiple families (Wilson et al. 2001; Kolb et al. 2001; Tegelberg et al. 2004; Morales et al. 2010; Agati et al. 2011a; Kaling et al. 2015; Csepregi et al. 2017; Rai et al. 2019). At the same time, the responsivity can vary widely among different species or even different accessions of one species (Kolb et al. 2001; Agati et al. 2011a, 2011b; Schulz et al. 2015; Bidel et al. 2020). Some plants responded rapidly to diurnal changes in UV levels by adjustment of leaf epidermal UV absorbance whereas the response of others, such as pea and blueberry cultivars (*Pisum sativum* cv. Meteor and *Vaccinium corymbosum* cv. Bluegold), was missing completely – even in long term observations (Barnes et al. 2016b, 2016a, 2013; Luengo Escobar et al. 2017; Siipola et al. 2015). Similarly, a species-specific increase in epidermal UV screening was observed when PAR levels were high or air temperature was low in the absence of UV (Kolb et al. 2001; Bilger et al. 2007; Agati et al. 2011a, 2011b; Bidel et al. 2020). The enhancement of epidermal UV absorbance – independent of which parameter induced it – was associated with an increase of epidermal phenylpropanoid contents confirming the close correlation between both parameters (Burchard et al. 2000; Kolb et al. 2001; Bilger et al. 2007; Morales et al. 2010; Agati et al. 2011a, 2011b; Nenadis et al. 2015; Bidel et al. 2020).

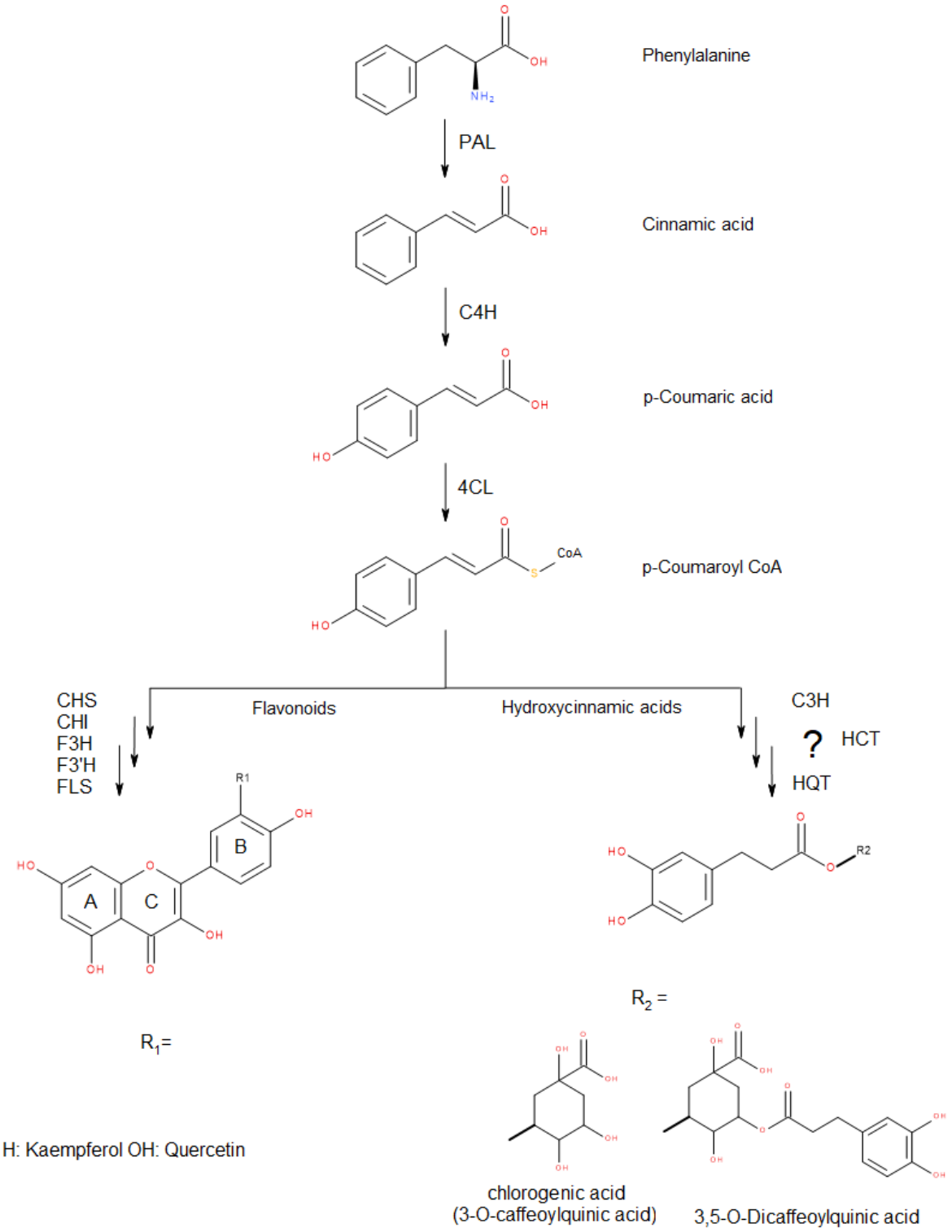

Figure 1.3 Schematic and simplified phenylpropanoid metabolism
Initial flavonoid and hydroxycinnamic acid (HCA) biosynthesis share one route involving activity of phenylalanine ammonia lyase (PAL), cinnamate-4-hydroxyylase (C4H) and 4-coumarate-CoA ligase (4CL). Subsequent biosynthesis occurs in two distinct branches via processing of p-coumaroyl-CoA. Intermediates of flavonoid biosynthesis via chalcone synthase (CHS), chalcone isomerase (CHI), flavanone-3-hydroxalase (F3H), flavonoid3'hydroxylase (F3'H) and flavonol synthase (FLS) are not depicted. The question mark at the HCA biosynthesis branch symbolizes the uncertainty of the sequential arrangement of coumarate-3-hydroxylase (C3H), hydroxycinnamoyl-CoA transferase (HCT) and hydroxycinnamoyl-CoA quinate hydroxycinnamoyl transferase (HQT). Modified after Neugart et al. (2016).

While the total amount of extractable leaf flavonoids is often increasing, the contents of different derivatives may change differentially for specific moiety patterns including hydroxylation, glycosylation, or acylation (Agati et al. 2011a, 2011b; Neugart et al. 2012, 2013, 2016, 2019; Nenadis et al. 2015). In *Ligustrum vulgare* for instance, flavonoids with an ortho-dihydroxylation at the B-ring were significantly upregulated by changes in UV or PAR irradiance whereas levels of flavonoids with another pattern of hydroxylation were not affected at all (Agati et al. 2011a, 2011b). A highly differential response among different flavonoids to changing PAR conditions was observed in *Brassica oleracea* as well; depending on glycosylation and acylation patterns, some derivatives increased after elevation of PAR whereas others increased upon lowering of PAR levels (Neugart et al. 2016). Similarly, how strong the content of particular flavonoids increased upon lowering the air temperature, depended on the glycosylation pattern in two Brassicacean species (Olsen et al. 2009; Neugart et al. 2016). An increase of flavonoid leaf contents depending on glycosylation as well as B-ring-hydroxylation was also found under limitation of nitrogen although data on epidermal UV absorbance is missing for most publications (Becker et al. 2015; Lea et al. 2007; Løvdal et al. 2010; Olsen et al. 2008, 2009). The simultaneous responses of different hydroxycinnamic acid levels in leaves to changes in UV, PAR, air temperature, or nitrogen depletion were much more variable suggesting a regulation that is less general than that in flavonoid biosynthesis. The foliar HCA contents remained stable, decreased or increased and they responded in a considerably smaller order of magnitude than the flavonoids in most species (Kolb et al. 2001; Morales et al. 2010; Agati et al. 2011a, 2011b; Neugart et al. 2013, 2016; Guidi et al. 2016; Rai et al. 2019; Bidel et al. 2020).

In contrast, changes of foliar HCA levels induced by nitrogen depletion were comparable to the order of magnitude of flavonoids but differed significantly among ten tomato cultivars, highlighting the variability (phenotypic plasticity) of HCA metabolism (Løvdal et al. 2010; Larbat et al. 2012a, 2012b).

For flavonoids, there is common consent that their accumulation is generally preceded by a transient transcriptional upregulation of corresponding biosynthesis enzymes (Ragg et al. 1981; Kreuzaler et al. 1983; Chappell and Hahlbrock 1984; Kuhn et al. 1984; Schmelzer et al. 1988; Ryan et al. 2002; Gutierrez et al. 2017). This upregulation has been proposed to occur in a cascade that is precisely coordinated with respect to the concrete position of the enzyme within the biosynthetic pathway (Ragg et al. 1981; Kubasek et al. 1992; Christie et al. 1994). Indeed, remarkably enhanced mRNA levels of phenylalanine ammonia lyase (PAL) and chalcone synthase (CHS) were found under the same abiotic conditions – such as high UV radiation or low temperature – that increased flavonoid pools (Kubasek et al. 1992; Christie et al. 1994; Leyva et al. 1995; Jaakola et al. 2004; Lillo et al. 2008; Løvdal et al. 2010; Schulz et al. 2015; Neugart et al. 2016; Rai et al. 2019). At the same time, the regulation may be differential among specific gene isoforms of the enzymes (Olsen et al. 2008; Neugart et al. 2016; Qian et al. 2019). Nevertheless, a few reports on the transcriptional upregulation of further downstream flavonoid biosynthesis enzymes appear conflicting with each other (Morales et al. 2010; Neugart et al. 2013, 2016; Rai et al. 2019). For example, long-and shortwave UV induced upregulation of several enzymes of the flavonoid biosynthetic pathway such as PAL, CHS, CHI and F3'H – involving early and late steps (Rai et al. 2019). In contrast, Morales and colleagues (2010) found significant upregulation of PAL solely under UV-B but not UV-A, whereas transcript levels of no

other downstream enzyme were affected under both conditions. However, high PAR induced significant upregulation of flavanone 3-hydroxylase, flavonol synthase and flavonoid 3'-hydroxylase (F3H, FLS and F3'H) in *Brassica oleracea* that was totally absent in another study in the same cultivar (Neugart et al. 2013, 2016). Regarding other flavonoid biosynthesis enzymes, the potential of induction by light was shown to depend on the seedling age (Kubasek et al. 1998). In the studies of Neugart and colleagues (2013, 2016), plants were at the same age, so that it became conceivable that different time points of sampling (7 days vs 4 weeks after shift to high PAR) led to deviating results. Nevertheless, in spite of missing puzzle pieces, the understanding of flavonoid biosynthesis and its regulation by the abiotic environment may nowadays be classified as extensive.

In contrast, – although analyses of epidermal absorbance and phytochemistry often find highly abundant hydroxycinnamic acids such as CQAs – knowledge on the regulation of HCA biosynthesis by abiotic environmental variables appears limited (Løvdal et al. 2010; Morales et al. 2010; Neugart et al. 2016). To date no consensus exists on enzymes and intermediates of the hydroxycinnamic acid biosynthetic pathway downstream of p-coumaroyl-CoA in higher plants and proposed routes differ from each other (Niggeweg et al. 2004; Moglia et al. 2016; Cheevarungnapakul et al. 2019). Exposure to radiation at 254 nm significantly increases transcript levels of *HCT* and *HQT* (Comino et al. 2009; Moglia et al. 2013). However, since UV-C is not included in the terrestrial solar spectrum, the physiological relevance of these results seems questionable. Thus, further data on environmental regulation of enzymes involved in CQA biosynthesis are needed.

1.4.2 Signal perception, transduction and crosstalk

The upregulation of UV screening pigments and linked phenylpropanoid biosynthesis enzymes in response to solar radiation including high UV and PAR levels, low temperature or low nitrogen availability requires sensing and integrating the response to each variable into their metabolism. In general, the transformation of external stimuli occurs via specific receptors and subsequent transduction into biochemical signals, i.e. a whole cascade of sequentially coordinated biochemical reactions, resulting in a systemic or tissue-specific physiological response mediated by altered gene expression (Mulligan et al. 1997). Consequently, several specific receptors and transduction cascades must be coupled to the adjustment of the phenylpropanoid biosynthesis. Different studies on the regulation of phenylpropanoid metabolism provide data on specific signals, their perception and transduction on a molecular level especially for flavonoids. These results imply an interaction between the plant's metabolism and its environment with crosstalk of different signal transduction pathways whose large complexity is beyond the scope of the present work (Kubasek et al. 1998; Løvdal et al. 2010; Nenadis et al. 2015; Bhatia et al. 2018; Pescheck and Bilger 2020).

However, perception of optical radiation comprises receptor proteins that undergo structural and conformational changes upon absorption of specific wavelengths. Nowadays, distinct photoreceptors sensing UV, blue or red light are known for plants (Jenkins et al. 2001; Paik and Huq 2019). The PAR-enhanced phenylpropanoid biosynthesis is mediated *via* light-dependent phosphorylation of the blue light receptor cryptochrome that was recently proposed to be activated by UV-A above 350 nm as

well (Engelsma and Meijer 1965; Engelsma 1974; Kubasek et al. 1992, 1998; Fuglevand et al. 1996; Yu et al. 2010; Siipola et al. 2015; Rai et al. 2019, 2020). Furthermore, there exists an – at least partially – distinct pathway involving a signalling cascade after monomerization of the inactive UVR8 protein dimer by UV-B and shortwave UV-A radiation (Fuglevand et al. 1996; Jenkins 2014; Jenkins et al. 2001; Kubasek et al. 1992; Rai et al. 2019, 2020; Vogt et al. 1991). In comparison to light sensing, sensing of temperature in plants is far less understood and likely involves the red-light receptor phytochrome as well (Schachtman and Shin 2007; Legris et al. 2016; Murray et al. 2017; Casal and Balasubramanian 2019). In addition, phytochrome is crucially involved in the light-dependent activation of nitrogen metabolism and sensing of external nitrogen has recently been ascribed to the membrane-located nitrogen transporters (Lillo 2008; Bouguyon et al. 2012; Larbat et al. 2016; O'Brien et al. 2016). Resulting signalling cascades triggered by either blue light/UV-A, UV-B, low temperature or nitrogen depletion finally result in an enhanced flavonoid biosynthesis, and must converge at some, yet unknown coordinating point and share common regulatory components. Currently, the regulatory network of MYB transcription factors and HYH/HY5 and COP1 is probably the most extensively investigated one (Bhatia et al. 2018, 2021; Catalá et al. 2011; Jenkins 2014; Lea et al. 2007; Lillo et al. 2008; Liu et al. 2015b; Rai et al. 2020, 2019; Schulz et al. 2016; Stracke et al. 2010). Similarly as for flavonoids, an induction of hydroxycinnamic acids was mediated by MYB transcription factors as well (Liu et al. 2015a). Consistently, *in silico* promoter analysis revealed presence of MYB binding elements in the gene of the key enzyme of caffeoylquinic acid formation HQT (Cheevarungnapakul et al. 2019). However, data on the link of abiotic factors and *HQT* gene expression is missing to date.

1.5 Research issues of the present work

The possibilities for providing an effective epidermal UV shielding are as least as diverse as the naturally occurring combinations of the products of phenylpropanoid biosynthesis in plant leaves. A large number of reports on phenylpropanoid profiles shows how diverse the composition of flavonoid and HCA derivatives under various physical parameters are among different species. This diversity and specificity of the composition must be reflected on the level of biosynthesis routes, so that phenylpropanoid biosynthesis appears only partially generalizable for plants. However, phenylpropanoid profiles of some important crop species and likewise their regulation by abiotic factors are less investigated than others are. One worldwide relevant crop involves *Helianthus annuus* (sunflower) accessions that derived from domestication of a wild progenitor by indigenous people (Heiser, 1951; Arias and Rieseberg 1995; Heiser et al. 2001; Rieseberg and Harter 2006). Sunflowers belong to the euasterid clade of eudicots and are nowadays taxonomically assigned to the Heliantheae tribe of the Asteraceaen family (Badouin et al. 2017; Gemeinholzer 2018). Other crop species of the euasterid clade and relative to the sunflower include for instance tomato, potato and tobacco that belong to the Solanaceae family (Gemeinholzer 2018). The origin of the wild form is thought to be Middle America with nowadays naturally occurring high levels of ultraviolet radiation making the evolution for genetic adaptation of UV protecting mechanisms likely (Barnes et al. 2013). Various recent cultivars are used either as ornamental plants or for agronomic industry (e.g.

Helianthus annuus (L.) cv. Peredovick as oilseed or cv. Sunrise for confectionery production) (Cronn et al. 1997). Different molecular markers have shown a close genetic relationship between domesticated and wild sunflowers (Rieseberg and Seiler 1990; Arias and Rieseberg 1995; Cronn et al. 1997). Preliminary studies conducted in the working group of Ecophysiology of Plants determining the epidermal UV-A absorbance of the sunflower cultivar Peredovick gave strong evidence that the leaves contain high amounts of UV-A screening pigments (Hoier 2012). UV-A screening is commonly attributed to the presence of flavonoids, which have an absorbance maximum around 350 nm, depending on their specific chemical nature (Agati et al. 2012). Flavonoids have been found in the epicuticular wax of leaves of various wild grown *Helianthus annuus* subspecies (Rieseberg et al. 1987). However, other studies showed that the phenylpropanoid pattern of sunflower leaves is dominated by hydroxycinnamic acids and flavonoids were only minor constituents of leaf extracts (Saftić-Panković et al. 2006; Hoier 2012; Gai et al. 2020). Although the phenylpropanoid composition may differ among subspecies, cultivars and accessions, reports on internal flavonoids or on alternative compounds, which could be considered as internal UV screens in sunflower, were missing when the present work was initiated (Rieseberg et al. 1987; Saftić-Panković et al. 2006; Cheevarungnapakul et al. 2019; Gai et al. 2020).

In order to identify UV screening pigments according to the criteria of Cockell and Knowland (1998), the phenylpropanoid profile of sunflower leaves was re-checked focussing on their identification, localization and physiological screening efficacy in a first part. In the study, the following research questions have been addressed:

Which internal, epidermal UV screening pigments do vegetative leaves of *Helianthus annuus* contain?

- Which phenylpropanoids can be found in sunflower leaves?
- Which phenylpropanoids are localized in the epidermis?
- Which phenylpropanoids contribute to the epidermal UV screening?
- Do epidermal phenylpropanoids protect UV susceptible components of photosynthesis (e.g. photosystem II) against UV induced damages?
- If epidermal phenylpropanoids protect against UV damage, to what extent do they protect?

Epidermal phenylpropanoids of sunflower leaves were hypothesized to contribute substantially to the epidermal UV screening according to their absorbance spectrum. Consequently, UV sensitive structures in the mesophyll should be protected against UV-induced damage in proportion to the concentration of the screening pigments. As sensitive structure, PS II was selected as its function can be rapidly and repeatedly assessed.

According to Cockell and Knowland (1999), UV inducible accumulation of a specific compound gives strong evidence of the compound acting as UV screening pigment. The content of hydroxycinnamic acids in seeds of field-grown sunflowers was positively correlated with increasing latitude pointing towards regulation by the abiotic environment but leaf-specific regulation has not been known yet (Dorrell 1976a, 1976b). Testing the hypotheses of the first section provided on one hand evidence

that the internal UV screening is provided solely by hydroxycinnamic acids and, on the other hand, a first indication that HCA concentrations were regulated by the abiotic environment. The positive effect of increasing PPFDs on HCA levels was reminiscent to that of flavonoids in many other higher plants suggesting other abiotic variables such as UV, low temperature or nitrogen starvation that are known as regulatory elements for accumulation of flavonoids to affect that of HCAs in sunflower as well.

The release of the sunflower genome in 2017 served as a basis for gene annotations and functional identification of key enzymes involved in hydroxycinnamic acid biosynthesis (Badouin et al. 2017; Cheevarungnapakul et al. 2019). Hence, the potential transcriptional upregulation of HCA biosynthetic key enzymes by the selected physical variables in analogy to that of flavonoids was addressed in further research issues:

Does the abiotic environment induce UV screening in sunflower?

- Do environmental factors such as high levels of ultraviolet and photosynthetically active radiation, low temperature and nitrogen starvation, which induce flavonoid accumulation, also induce HCA accumulation?
- What is the time course of the enhanced accumulation?
- Is an enhanced HCA accumulation preceded by a transient transcriptional upregulation of a key enzyme, as it is known for chalcone synthase in the flavonoid biosynthetic pathway?

It was hypothesized that UV screening and underlying HCA accumulation are increased by changes in the same abiotic environmental factors known to induce flavonoid formation. This response was expected to occur within days to weeks. In addition, it was speculated that the enhanced accumulation is preceded by a transient transcriptional upregulation of the biosynthesis key enzyme HQT.

2 Material and methods

2.1 Plant material and growth conditions

Prior to sowing, seeds of *Helianthus annuus* (L.) cv. Peredovick (Kiepenkerl, Everswinkel, Germany) were surface sterilized in NaClO (5-10 %; Carl Roth, Karlsruhe, Germany) with 2 % Tween 20 for 30 minutes on a rocking platform according to the protocol of Sauer and Burroughs (1986) followed by several washing steps with ddH_2O and then air-dried for storage. Subsequent cultivation of plants and growth light conditions, respectively, differed slightly between the two research foci. The sections of material and methods will refer to either analytical experiments for the characterisation of UV screening in sunflower leaves presented in chapter 3.1 or to analysis of regulation of epidermal UV screening that involve mainly shift experiments summarised in chapter 3.2.

For characterisation of foliar epidermal UV screening and photoinhibition experiments (chapter 3.1), dried seeds of the Peredovick cultivar were sown in TKS 2 (Floragard, HaGaFe GmbH, Saterland/Ramsloh, Germany) and separated when the first vegetative leaves after the cotyledons had emerged, so that one individual remained per pot. The cultivation took place in a climate chamber (Johnson Controls Systems & Service GmbH, Cork, Ireland) with a relative humidity (r. h.) of 60 % and a day/night-rhythm of 16h/8h. Growth temperature was at 21 °C and growth irradiance was provided by HQI lamps (CMT369 LS W BH 360W, EYE Iwasaki, IWASAKI ELECTRIC CO., LTD., Tokyo, Japan) with panels of UV blocking acrylic glass. Four different photosynthetic photon flux densities of PAR (PPFDs) were used as growth conditions by installing either transparent polyester foil for control conditions (Rachow Kunststoff-Folien GmbH, Hamburg, Germany) or one to four layers of neutral filter foils (NF; Llumar N1050 SR CDF, foliendealer.com, Berlin, Germany) above the plants for three shading conditions. Plants that grew at averaged PPFDs of 220 (± 30) µmol m^{-2} s^{-1} are defined in the following as high light (HL) grown or control plants. Moderate (ML), low (LL) and super low (SLL) light conditions refer to 160 (± 50) µmol m^{-2} s^{-1} (one layer), 40 (± 10) µmol m^{-2} s^{-1} (two layers) and 20 (± 2) µmol m^{-2} s^{-1} (four layers), respectively (irradiance spectra see Fig. 2.1A). Six plants were cultivated per growth condition.

For shift experiments presented in chapter 3.2, sunflowers were grown in climate cabinets (GroBank BB-XL3/M, CLF Plant Climatics, Wertingen, Germany) under low PPFDs provided by white light fluorescent tubes (PHILIPS F32T8/ TL741, Koninklijke PHILIPS N.V, Amsterdam, The Netherlands), if not stated otherwise. The ultraviolet part emitted from the fluorescence tubes was blocked by standard glass (Fig. 2.1B). In the distinct approaches, different substrate was applied. Which substrate was used is specified in the respective section.

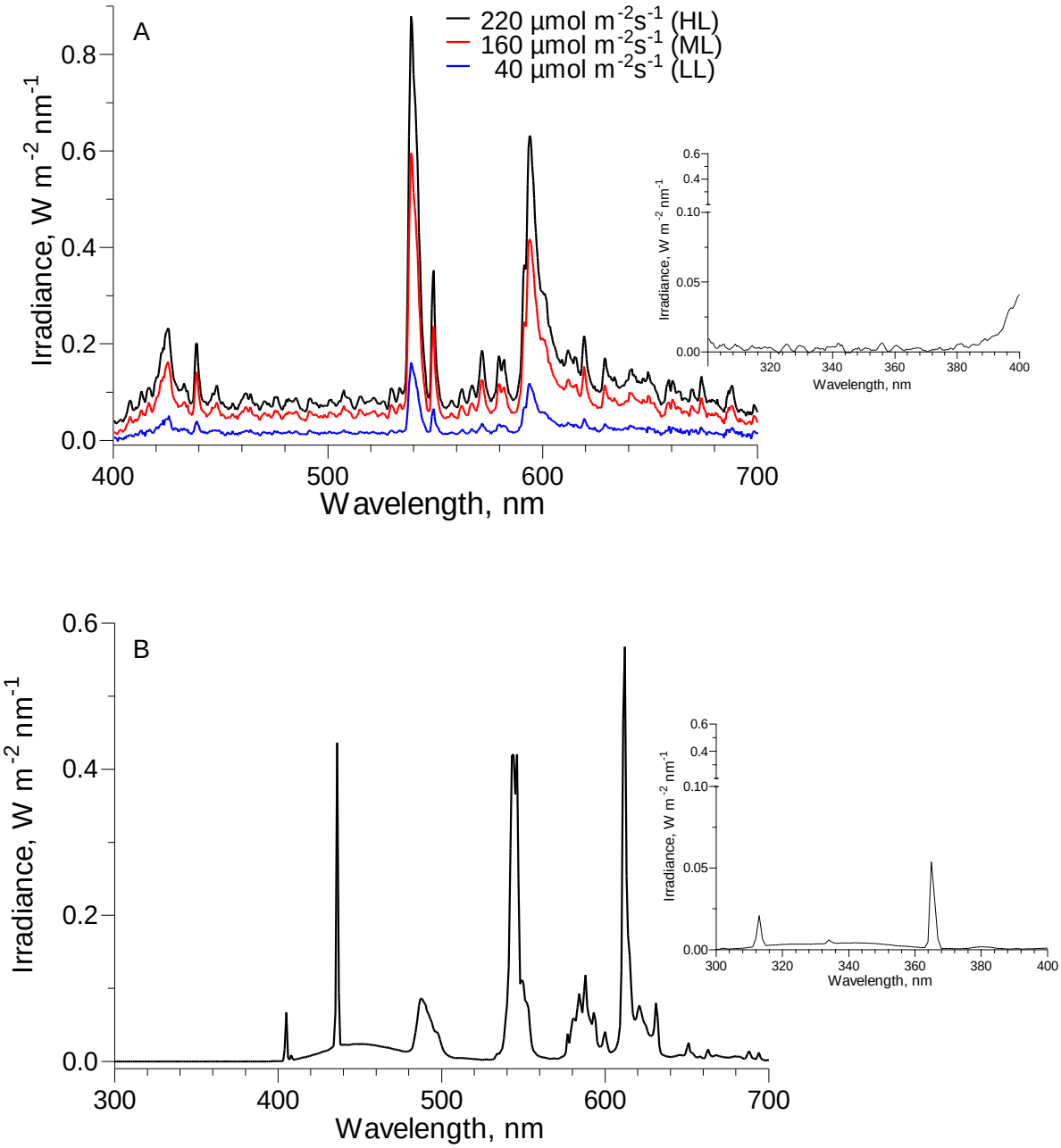

Figure 2.1 Irradiance spectra of HQI lamps in the climate chamber(A) and white light fluorescence tubes in the growth cabinet (B)

(A) For characterisation of UV screening, HQI lamps were combined with transparent filter or varying neutral filter foils in order to generate different PPFDs. Growth conditions were defined as high light (HL; black line; 220 (± 30) µmol m^{-2} s^{-1}), moderate light (ML; red line; 160 (± 50) µmol m^{-2} s^{-1}), low light (LL; blue line; 40 (± 10) µmol m^{-2} s^{-1}). The spectrum of super low light conditions (SLL; 20 (± 2) µmol m^{-2} s^{-1}) was nearly congruent to LL conditions. For clarity, the SLL spectrum is not shown. Each irradiance spectrum displays a single measurement recorded with a FLAME Extended Range Miniature spectroradiometer (OceanInsight, Orlando, USA). (B) The cabinet was equipped with white light fluorescence tubes with blocked UV radiation. The irradiance spectrum was measured once with a Bentham double monochromator spectroradiometer (DMc150, Bentham Instrument Ltd., Reading, United Kingdom) according to a PPFD of 25 µmol m^{-2} s^{-1}.The insets show the UV irradiance spectrum of HL conditions (A) or in experiments if UV was not blocked (B; described in chapter 2.2.1).

2.2 Treatments in shift experiments

For the analysis of induction by different abiotic parameters including UV and photosynthetically active radiation, low temperature and nitrogen depletion, plants were grown simultaneously in two to four groups (control and one to three treatments) for each parameter of interest. In principle, the groups were grown initially under identical abiotic conditions and the treatment groups were then shifted to either altered UV, PAR, temperature or nitrogen availability. The abiotic conditions in the shift experiments differed slightly among each other in the different experiments. The conditions are specified in the following sections.

2.2.1 Induction by different UV regions

For experiments analysing regulatory effects of UV (chapter 3.2), plants were grown simultaneously in groups of ten plants in a growth cabinet (CLF Laborgeräte GmbH). Surface-sterilized seeds were sown in TKS 2 (Floragard) and separated, so that ten individual plants per treatment group remained. Each treatment group was exposed to initially identical controlled growth conditions at 21 °C, 60 % r. h. and low PPFDs at a 16 h day/8 h night cycle for four weeks of growth.

Growth under UV-B

In a first approach, ten sunflower plants per treatment group grew at 60 µmol m^{-2} s^{-1} PAR without (control) or with supplemental UV above 280 nm at an irradiance of 1.6 W m^{-2} (1.0 W m^{-2} UV-B and 0.6 W m^{-2} UV-A). PAR irradiance was provided by white light fluorescence tubes (F32T8/TL741; PHILIPS, Amsterdam Netherlands), radiation below 400 nm was emitted by UV-B fluorescence tubes (TL40/12RS, PHILIPS). Control irradiance conditions were provided by installing UV blocking filter foil (226 LEE U.V, LMP Lichttechnik Vertriebs GmbH) and UV radiation for plants grown under UV-B was filtered through cellulose diacetate (90 µm thickness; Rachow Kunststoff-Folien GmbH).

Shift to UV-B

In a further approach, sunflowers were grown in under white fluorescence tubes (F32T8/TL741; PHILIPS) at 55 µmol m^{-2} s^{-1} PAR for the analysis of induction by UV-B. The uncovered white fluorescence tubes emitted 0.4 ± 0.1 W m^{-2} UV (0.05 ± 0.01 W m^{-2} UV-B + 0.34 ± 0.08 W m^{-2} UV-A). When three consecutive leaf generations had developed, ten plants were treated with UV-B. For UV-B treatment, UV-B fluorescence tubes (TL40/12RS, PHILIPS) were turned on, which were covered with cellulose diacetate (> 280 nm; Rachow Kunststoff-Folien GmbH), so that plants were exposed to 1.1 (± 0.03) W m^{-2} UV-B radiation. Because the treatment with UV-B also included radiation in the UV-A region (0.7 (± 0.02) W m^{-2}), the induction in the UV-B treatment group could have been a combined effect of both UV-B and UV-A radiation. In order to assign the induction solely to UV-B, the control group was exposed to the UV-A spectrum of the fluorescence tubes in absence of UV-B using polyester foil as a filter (> 320 nm; Rachow Kunststoff-Folien GmbH). The control was exposed to a comparable UV-A irradiance (0.9 ± 0.07 W m^{-2}).

Shift to UV-B, shortwave UV-A and longwave UV-A

In a third approach, the UV region was blocked by a filter foil (226 LEE U.V., LMP Lichttechnik Vertriebs GmbH) during growth. For the growth light, different fluorescence tubes were mixed (F32T8/TL741 (PHILIPS); UV-A-340 LAMP (Q-PANEL^{tm}, Q-Lab Corporation, Westlake, USA); UV 36W G13 120cm T8 (OMNILUX, Thomann GmbH, Burgebrach, Germany); T8 L 36W/73 (OSRAM GmbH, Munich, Germany). When plants had developed three consecutive leaf generations, the UV excluding foil was removed in order to begin 72 hours of exposure to four different UV treatments that had been previously installed. The treatments were provided by a combination of UV transparent acrylic glass and different filters specified in Table 2.1.

Table 2.1 UV irradiance and photon flux densities used in the UV shift experiment

Treatment	**control**	**UV-A_{lw}**	**UV-A_{sw}**	**UV-B**
Filter type / material	226 LEE U.V.	PETG	Polyester	Cellulose diacetate
$\lambda_{Cut\text{-}off}$[1], nm	390	350	320	290
$\lambda_{Half\ transmittance}$[2], nm	405	370	330	295
$Irr_{UV\text{-}A}$, W m^{-2}	0.03 (± 0.00)	0.09 (± 0.08)	0.46 (± 0.14)	1.14 (± 0.51)
$Irr_{UV\text{-}B}$, W m^{-2}	0.002 (± 0.0)	0.002 (± 0.0)	0.002 (± 0.0)	0.048 (± 0.02)
$PFD_{UV\text{-}A}$, µmol m^{-2} s^{-1}	0.1 (± 0.0)	0.3 (± 0.2)	1.4 (± 0.4)	3.4 (± 1.5)
$PFD_{UV\text{-}B}$, µmol m^{-2} s^{-1}	0.0 (± 0.0)	0.0 (± 0.0)	0.0 (± 0.0)	0.1 (± 0.1)
PFD_{PAR}, µmol m^{-2} s^{-1}	54 (± 12.5)	53 (± 16.2)	50 (± 13.7)	54 (± 15.1)

Four filter types with different cut-off wavelengths were installed below UV transmitting plexiglass and a combination of UV and PAR for either control, longwave (lw) UV-A, shortwave (sw) UV-A or UV-B treatment. Irradiance (Irr) and photon flux densities (PFDs) are given as average of ten plants per treatment group (± standard deviation). Measurements were conducted in technical duplicates for the second leaf generation. Waveband regions for calculation of Irradiance and PFD were defined as following: UV-B: 280−315 nm, UV-A: 315−400 nm and PAR: 400−700 nm.

[1] Transmittance < 5 %; [2] Transmittance = 50 %; PETG, Polyethylenterephtalatglycol

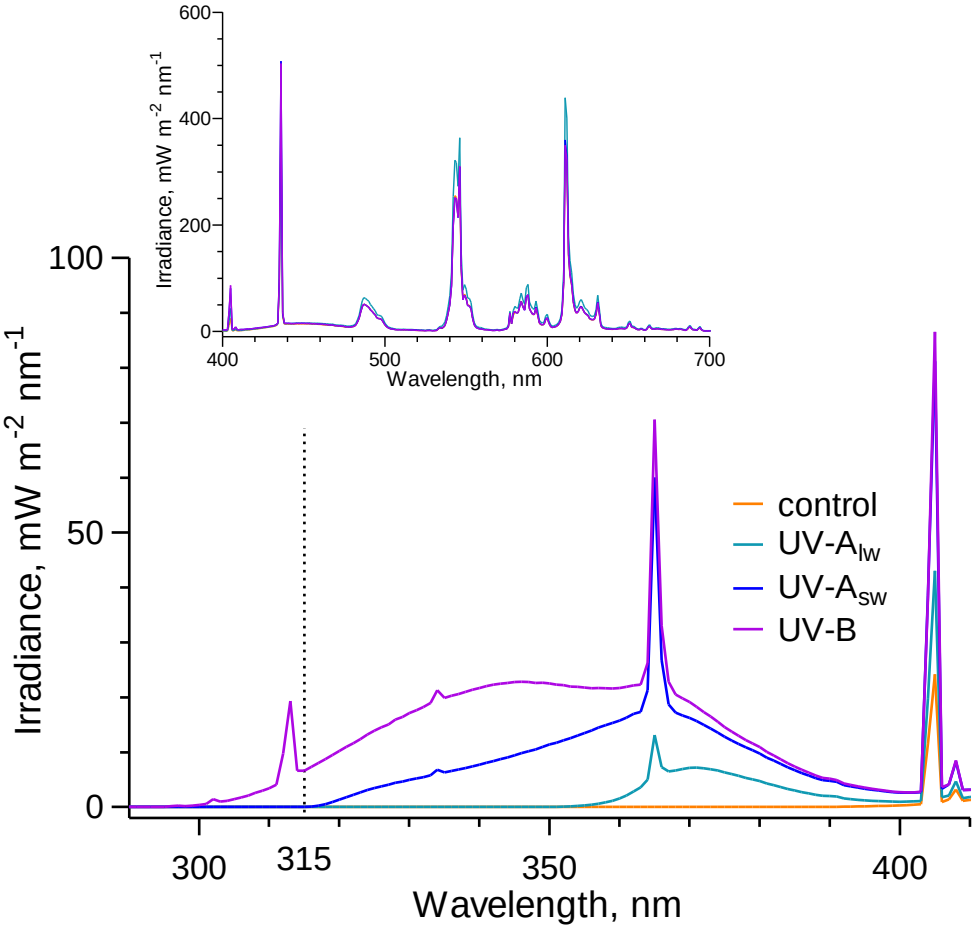

Fig. 2.2 Treatment irradiance spectra used in the UV shift experiment
Sunflowers with identical growth conditions for four weeks were exposed for 72 hours to different UV conditions: UV-B (magenta), UV-A_{sw} (blue), UV-A_{lw} (turquoise) and control (orange). Irradiance spectra were measured from 280 to 700 nm with a Bentham DMc150 spectroradiometer. Spectra in the PAR were nearly identical to each other (inset).

The filters were purchased from following companies: LMP Lichttechnik Vertriebs GmbH (226 LEE U.V.), Rachow Kunststoff-Folien GmbH (PETG, polyester and cellulose diacetate). The respective irradiance spectra were recorded using a double monochromator spectroradiometer (DMc150 FI, Bentham Ltd) and contained either λ > 390 nm (control), λ > 350 nm (longwave UV-A, UV-A_{lw}), λ > 320 nm (shortwave UV-A, UV-A_{sw}) or λ > 290 nm (UV-B) and nearly identical PAR spectra (Fig. 2.2). PPFD and intensity of UV-A and UV-B were monitored for each sampled leaf separately using a Li-250 quantum sensor (LI-COR, Lincoln, USA) and sensors specific for the UV-A (315-400 nm, TOCON-A, sglux, Berlin, Germany) and the UV-B (280-315 nm; Veit et al. 1996) region. The UV sensors were calibrated with the integral in the UV-A and UV-B, respectively, obtained from measurements with the Bentham spectroradiometer (Fig. 2.3A, B).

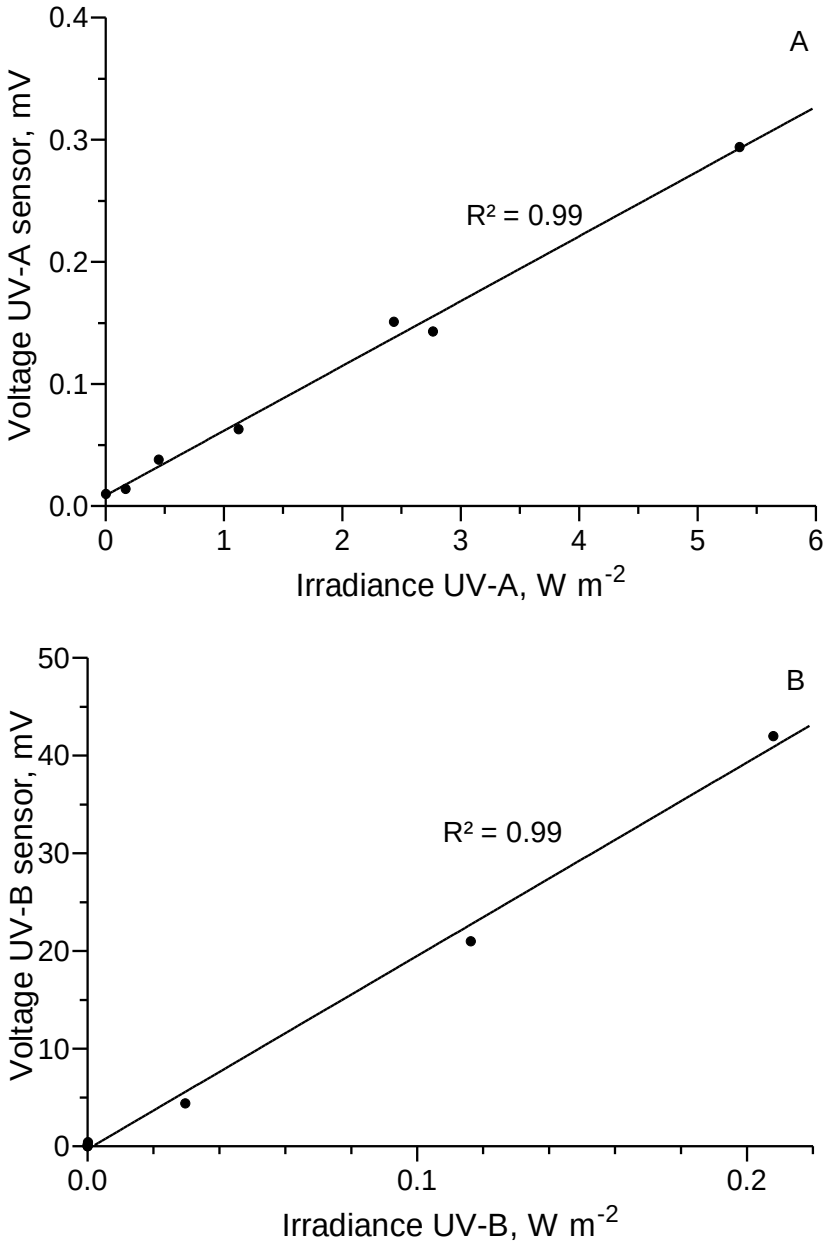

Figure 2.3 Calibration of UV-A (A) and UV-B (B) sensors
UV radiation of the different treatment spectra were measured simultaneously using the UV sensors and the Bentham spectroradiometer. Obtained voltages were correlated to the integral of UV irradiance over the region of UV-A (A; 315-400 nm) and UV-B (B; 280-315 nm), respectively. Each correlation was fitted with a linear regression (R^2 = 0.99 for both).

2.2.2 Induction by high PAR and low temperature

For analysis of the regulatory effect of either high PPFD or low temperature, one control and one treatment group was grown for each experiment simultaneously. Dried seeds were sown in TKS 2 (Floragard) and separated when first vegetative leaves after cotyledons had developed, so that ten individual plants per treatment group remained. Every plant group was exposed to identical conditions in a growth cabinet (GroBank BB-XL^3/M, CLF Laborgeräte GmbH) at 21 °C and 60 % relative humidity for three weeks. Growth light was provided by fluorescence tubes (F32T8/TL741, PHILIPS) and PPFD accounted for 50 (± 10) µmol m^{-2} s^{-1} as determined with a Li-250 quantum sensor (LI-COR) for all treatment groups. When necessary, PPFD was either adjusted by attenuating a

maximal PPFD output by neutral density filter foil (Llumar N1050 SR CDF, & Llumar N1020 SR CDF, Foliendealer Vertriebs GmbH). The day/night cycle was to 16 h/8h and the weak UV-B radiation emitted by the fluorescent tubes was blocked by standard glass. During the whole experiment, plants were watered three times per week with faucet water. When plants had emerged six vegetative leaves, the respective treatment group was either shifted to 375 (± 70) µmol m^{-2} s^{-1} and 21 °C by removing the neutral filter foil (high PPFD) or transferred to a further growth cabinet with a stable growth temperature at 9 °C and 45 (± 5) µmol m^{-2} s^{-1} (Mobylux GroBank, CLF Laborgeräte GmbH). The corresponding other growth parameters were not changed and the control group plants remained at initial conditions.

2.2.3 Induction by low nitrogen

For the nitrogen shift experiments, plants were initially sown and grown for four weeks in Vermiculite (Floragard) that was watered every second day with nutrient solution containing sufficient nitrogen (see +N/control in Table 2.3). Plants were grown in a growth cabinet (GroBank BB-XL^3/M, CLF Laborgeräte GmbH) at 21 °C, 60 % r. h. and 40 (± 5) µmol m^{-2} s^{-1} PPFD provided by fluorescence tubes. The day/night cycle was to 16 h/8 h and UV radiation was blocked by standard glass. When plants had developed three consecutive leaf generations, plants were transferred to hydroponic solution. The transfer to hydroponics was approximately one week before a change in nitrogen availability took place in order to give time for a potential adjustment to the hydroponic conditions. The nitrogen depletion was realized by transferring plants to a hydroponic solution devoid of any nitrogen source (see −N/shifted in Table 2.2).

Table 2.2 Compound composition for the hydroponic sunflower culture

Nutrient	Concentration (mM)	
	+ N	− N
NH_4NO_3	2	0
$MgSO_4 \times 7\ H_2O$	0.5	
$CaCl_2$	0.5	
K_2SO_4	0.5	
KH_2PO_4	0.5	
Fe-Chelate (Fe-EDTA)	0.09	
H_3BO_3	0.03	
$MnCl_2 \times 2\ H_2O$	0.0036	
$ZnSO_4 \times 7\ H_2O$	0.001	
$CuSO_4 \times 5\ H_2O$	0.001	
$Na_2MoO_4 \times 2\ H_2O$	0.002	
$NiSO_4 \times 6\ H_2O$	0.002	
$CoSO_4 \times 7\ H_2O$	0.0006	
Final adjustment of pH to 6.8		

Culture medium was replaced every two to three days in the experiment with plants shifted to nitrogen depletion. Elements were supplied at the same concentrations except for ammonium nitrate for + N (control) and – N (shifted).

2.3 Sampling strategy

In all experiments, single discs of one or two leaves per individual were taken with a cork borer (size no. 5, 0.68 cm^2, ca. 15 mg fresh weight). The centre of the top leaf of individuals avoiding any dominant veins stage was sampled. In order to analyse a potential direct correlation between UV screening capacity, phenolic content and key enzyme transcript levels, epidermal UV screening was determined as described in chapter 2.2 for the single leaf discs. Subsequently, discs were frozen in 2 mL tubes (Eppendorf, Hamburg, Germany) containing glass beads (Carl Roth, Karlsruhe, Germany) in liquid nitrogen and kept at −80 °C for storage until further analysis.

For experiments presented in chapter 3.1, the centre of the top leaf of individuals in the four-leaf stage was sampled whereas for experiments presented in chapter 3.2, one leaf at an intermediate insertion height at the stem per individual in the six-leaf stage was sampled for HPLC and RNA analysis per time point. The sampling was conducted at one initial (control, t_0) time point before the shift followed by five different time points (t_{1-5}) after the shift specified in table 2.4 for the respective analysed parameters. In the second approach of nitrogen depletion, a sixth time point of sampling was included at 144 hours after the shift for measurement of relative epidermal UV-A absorbance but no tissue was sampled.

Table 2.3 Time points of sampling in the different shift experiments

Time point of sampling	Hours after shift to			
	UV	High PPFD	Low temperature	N depletion
t_0	0	0	0	0
t_1	3	3	3	3
t_2	6	6	12	6
t_3	12	12	24	12
t_4	24	24	72	24
t_5	48	72	120	72
t_6	-	-	-	(144)*

*Epidermal screening was determined but no tissue sampling was done

2.4 Phytochemical analysis

2.4.1 HPLC analysis

Extraction and HPLC analysis of free phenolics

Frozen leaf discs were homogenised in a cell mill (MM2, Retsch GmbH, Haan, Germany) and extracted on ice subsequently according to a slightly modified protocol of Petridis et al. (2016). The leaf powder was first suspended in 250 mL of a cooled acidified aqueous methanolic solution (49,5 % MeOH / 49,5 % H_2O / 1 % HCl of a 36 % stock solution, MercK KGaA, Darmstadt, Germany). Subsequent centrifugation (Biofuge fresco, Heraeus, Hanau, Germany) was conducted at 16.500 g and 4 °C for 5 minutes. The supernatant was removed, collected in a further tube and the pellet was again resuspended in aqueous methanol. Centrifugation was repeated at identical settings as before

and supernatant was added to the previously collected. Afterwards, the pellet was resuspended in pure MeOH and once more centrifuged. The resulting supernatant was again added to the previously collected ones. The unified supernatant was centrifuged for 10 minutes at 4 °C and 16.500 g and 100 µL of that extract was transferred to vials for subsequent phytochemical analysis.

For HPLC analysis 40 µL of 100 µL were injected into the HPLC system (SCL-10A VP, SIL-10A VP, LC-10AT VP, FRC 10-A, RF-10A XL, Shimadzu, Duisburg, Germany). Phenolic compounds were separated using a LiChrospher 100 RP-18 column (4 × 250 mm, 5 µm particle size, Merck) and a gradient of 0.01 % phosphoric acid (H_3PO_4; eluent A) and acidified MeOH (90 % MeOH / 10 % H_3PO_4; eluent B) at a flow rate of 0.75 mL min^{-1}. At the time point of injection, the ratio of eluent A and B accounted for 80% / 20 %. The relative proportion of B increased linearly to 45 % within 12 minutes after injection and was kept constant for the next 13 minutes followed by a further linear gradient from 25 minutes to 40 minutes to 75 % of eluent B. Once more, the relative proportion of B rose in a linear manner from 40 to 42 minutes to 100 %. This proportion remained for the next 8 minutes followed by a return within 2 minutes to the initial composition of 80 % A / 20 % B and a subsequent post run time of 5 minutes. Detection of phenolics was conducted by a diode array detector (SPD-M10A VP, Shimadzu) at 330 and 360 nm.

The chromatograms and UV spectra of occurring peaks were analysed using LC software version 1.25 SP2 (Shimadzu). For comparison of retention times and UV spectra, a HPLC standard solution of chlorogenic acid (CGA; Carl Roth) diluted in acidified aqueous methanol (49.5 % MeOH/49. 5 % H_2O/1 % HCl) was used after compound identification by mass spectrometry analysis. The HPLC method was calibrated with that standard solution plotting peak area against defined injected amount of CGA. In order to calculate the quantity of caffeoylquinic acid residues, one molecule of dicaffeoylquinic acid was counted as two caffeoylquinic acid residues by taking into account that its UV absorbance was twice as high as that of CGA. The relative content of CGA and DCQA was calculated by referring the respective peak areas to the integral of all peaks at 330 nm. For expressing the content of CGA, DCQA and unidentified HCAs as fold-of-control, averaged peak areas at 330 nm of treated plants were referred to that of control plants.

Extraction and HPLC analysis of cell wall-bound phenolics

For the isolation of leaf cell walls and subsequent extraction of bound phenolics, the protocol of Harbaum et al. (2008) was slightly modified. A total amount of 30 g fresh leaf material of eight high-light grown plants (Flav index of 1.03 ± 0.07) was harvested, manually cut and subsequently homogenised in 60 mL of two-fold 1.5 % SDS-solution with 5 mM sodium metabisulphite (Merck) using an Ultra-Turrax (Janke & Kunkel GmbH & Co KG, Staufen, Germany) at 20000 U min^{-1} for 5 minutes. The obtained suspension was stirred for 15 minutes and then filtered through a nylon mesh with 40-µm mesh width. The remaining cell debris was washed three times with 0.5 % SDS solution containing 3 mM sodium metabisulphite followed by rinsing with 3 mM sodium metabisulphite and another rinsing step with distilled water. The residue was washed again three times with EtOH and then freeze-dried and ball-milled.

For cell wall digestion, 25 mg cell wall material was incubated in triplicates in 12.5 mL of ddH_2O with 10 µL of a cellulolytic enzyme mixture (Viscozym L, Merck) in a water bath at 30 °C for 24 hours. Subsequent saponification with 2 M NaOH (addition of 12.5 mL) was conducted in nitrogen atmosphere for 96 hours. The solution was extracted three times with ethyl acetate and the organic phases were collected, acidified with HCl and centrifuged at 11 000 rpm. The resulting organic phase was decanted, added to Na_2SO_4 for dehydration and evaporated followed by a further step of centrifugation at 11 000 rpm. In total 400 µL of 25 % aqueous MeOH was added and HPLC analysis with 100 µL was conducted following the protocol of Harbaum et al (2008) with 0.1% formic acid in water (HPLC grade) and 100 % acetonitrile at a flow rate of 0.7 mL/min using a linear gradient.

2.4.2 Mass spectrometry analysis

2.4.2.1 Settings of UPLC and tandem mass spectrometer

Free phenolics extracted as described in section 2.2.3.1 were analysed by a combination of Ultra-Performance Liquid Chromatography (UPLC) and tandem mass spectrometry (MS/MS) for a detailed identification of phenylpropanoids according to Oertel et al. (2017). Extracts were analysed in an Acquity UPLC system using an Acquity UPLC eλ photodiode array detector (Waters GmbH, Eschborn, Germany) that was coupled to an electrospray quadrupole tome-of-flight mass spectrometer (ESI-Q-TOF MS; maXis Impact, Bruker Daltonik GmbH, Bremen, Germany). Tandem mass spectrometry settings were according to the method in Brauch et al. (2018). For identification of the small peak at the approximate retention time of 20.4 minutes (peak 2), a specific protocol was used. The extracts of four samples with high phenolic contents were pooled. The pooled extracts were partially vaporised in a vacuum concentrator (Concentrator 5301, Eppendorf) to a final volume of 80 µL of which 50 µL were injected in an Alliance 2690 HPLC system with a PDA detector (Waters GmbH) for compound separation. Eluents, flow rate and separation gradient were according to the protocol in section 2.2.3.1 using the identical Lichrospher 100 18-RP column. For subsequent MS analysis, fractions containing the compound corresponding to peak 2 were collected and concentrated in the vacuum concentrator for 20 minutes. In order to remove the H_3PO_4-proportion of the HPLC run, the fractions containing phenolics were cleansed using a conditioned Chromafix C18 Cartridge (Macherey-Nagel GmbH & Co KG, Düren, Germany). The conditioning was conducted in a first step with 100 % MeOH followed by a step with 2 % MeOH. The purified phenolic fractions were solved with 1 mL of 100 % MeOH and concentrated to a final volume of 50 µL and 12.5 µL of 0.5% formic acid (HCOOH) was added for subsequent UPLC-PDA-ESI-QTOF-MS/MS analysis.

2.4.2.2 Data collection

Data was analysed and compounds were identified using the software packages Compass Data Analysis V4.4 and Metaboscape V3.0 Service Release 1 (Bruker Daltonik GmbH). The preliminary annotation of compounds according to the library of spectral data was confirmed by following authentic standards: 3-O-, 4-O-, trans-5-O-caffeoylquinic acids (Merck); 1,3-, 1,5-, 3,4,- 4,5-di-O-

caffeoylquinic acids (Carbosynth Ltd, Berkshire, United Kingdom); 3,5-di-O-caffeoylquinic acid, quercetin 3-O-galactoside, quercetin 3-O-rutinoside (Extrasynthese, Genay Cedex, France).

2.5 Analysis of relative gene expression of *HQT*

2.5.1 Selection and sequence research of sunflower genes

For partial analysis of transcriptional regulation of CQA biosynthesis, the key enzyme hydroxycinnamoyl CoA quinate transferase (HQT) was selected as gene of interest. Relative quantification of transcript levels requires the normalization to reference genes that are not regulated upon variable experimental factors such as developmental stage or differing abiotic conditions. Prior to the molecular laboratory work part of relative transcript level investigation, latest sequence information on this key enzyme and reference genes was required for target-specific primer design.

2.5.1.1 Genes of Interest

Literature was screened for hydroxycinnamoyl-quinate transferase (*HQT*) genes in sunflowers. Cheevarungnapakul and co-workers (2019) identified the Coding DNA sequences (CDSs) of three *HQT* sunflower genes based on nucleotide data of tomato and tobacco published in Niggeweg et al. (2004). The corresponding mRNA sequences are listed in the NCBI database under following entries: Accession (Acc.) MK598073.1, *HQT1* (1305 bp); Acc. MK598074.1, *HQT2* (1323 bp); Acc. MK598075.1, *HQT3* (1326 bp). In order to find out, whether sequences had been updated or annotations of potential new isoforms had been added, similar sequences were searched using Nucleotide BLAST® (blastn, National Center for Biotechnology Information (ncbi)) and the database "Helianthus annuus XRQr2.0 Genome Portal" released by the French National Research Institute for Agriculture, Food and Environment (INRAE; available at www.heliagene.org). The latter database includes a sunflower reference genome that was sequenced and has been made publicly available on heliagene.org (Badouin et al. 2017). For MK598073.1 the most similar mRNA sequence with an e-value of 0 corresponded to the locus tag HanXRQChr09g0244541 with 2 mismatches but no gaps. The next similar sequence displayed 277 mismatches in comparison to MK598073 making unspecific priming improbable. For MK598074.1, in total three sequences with an e-value of 0 were found. One (locus tag HanXRQChr10g0313671) was found to be identical over the whole sequence length. The other two candidates (locus tag HanXRQChr12g0357711 and HanXRQChr02g0055601) showed 183 mismatches and 7 gaps as well as 257 mismatches and 18 gaps, respectively. Searching sequences identical to that of MK598075.1 resulted likewise in three sequences with an e-value of zero. One sequence (locus tag HanXRQChr12g0357711) was found to be identical to MK598075.1 with no gaps or mismatches. The two next similar sequences (locus tag HanXRQChr12g0357711 and HanXRQChr10g0313671) possessed 253 mismatches and 19 gaps as well as 257 plus 18 gaps, respectively.

2.5.1.2 Reference genes

As in the publication of Cheeverungnapakul et al. (2919), one gene of the eukaryotic translation initiation factor 5A (*eIF5A*; XM_022156448.1) and of actin (*ACT7*; XM_022154554.1) were selected as reference genes. Ochogavía et al. (2017) had shown that the transcript levels of these genes are stably expressed in leaves of sunflowers at different developmental stages. The *elongation factor 2* (*EF2*; XM_022137686.1) has been included in preliminary analysis but was deselected since the relative transcript levels were not stable under the used treatment conditions. As proceeded for the genes of interest, NCBI and INRAE databases were checked for new or updated annotations. For *eIF5A* the sequences with the locus tags HanXRQChr15g0481661 and HanXRQChr15g0481631 were found (0 mismatches, 0 gaps in 480 bp). Next similar sequences with no gaps and more than 50 mismatches displayed the locus tag HanXRQChr16g0502561. For XM_022154554, the sequence with the locus tag HanXRQChr15g0463061 possessed neither mismatches nor gaps over 1083 bp. The next similar sequences with more than 80 % identity over 1083 bp included the tags HanXRQChr14g0446641, HanXRQChr08g0220711, HanXRQChr14g0457921 and HanXRQChr12g0370231 with no gaps and 88, 200, 207 and 211 mismatches respectively. The sequences with the identifiers HanXRQChr04g0124891, HanXRQChr02g0049231 and HanXRQChr09g0249361 with 2 or 4 gaps were aligned with 201, 197 and 203 mismatches. Since reference gene analysis was included for each sample, the stability of reference genes was validated for each of the conducted experiments.

2.5.2 Primer design and analysis of primer specificity

The sequences of MK598073.1, MK598074.1, MK598075.1, XM_022156448.1, XM_022154554.1 and the corresponding sequence entries of the INRA database were used for primer design by the Primer-BLAST (NCBI) software. Since there was no information available on alternative splicing of these genes, primers were designed for a single exon in order to target all splice variants. Amplicon length was set between 80 and 140 bp, melting temperature to 60 °C. The designed primers were used for a Nucleotide BLAST search to avoid amplification of unintended targets. Primer quality was checked using the AmplifX software V2.0.7 (© Nicolas Jullien 2004-2019). Sequences of each designed primer shown in Table 2.4 were re-checked *in silico* not to match similar targets (at least 3 mismatches) using the NCBI and INRAE database.

Table 2.4 Primers and corresponding target genes used for the analysis of relative gene expression

Target gene	Acc. number	Forward primer (5' → 3')	Reverse primer (5' → 3')
ACT7	XM_022156448.1	GCACCATTGAATCCCAAGGC	GCAACATACATGGCGGGAAC
eIF5A	XM_022154554.1	TCATCTACGCCTCTGCAGTC	CTGATGCTCTTCGTCCGACA
HQT1	MK598073.1	GATTGCCCCGTTGGAAAACC	TACGCACTTCCATCGCCTTT
HQT2	MK598074.1	GAGGAGTCGCACTTGGTTGT	ATGAACGGTGGGATGGCTAC
HQT3	MK598075.1	GAAGAAGGCGCTTGCAGATG	GGACTCGGCTTCGACAAACA

Prior to qRT-PCR, target specificity was proven in cDNA experimentally by PCR and subsequent gel-electrophoresis at a voltage of 70 V for 60 min (Böttcher 2020). PCR products were loaded together with a 50 bp DNA-marker (5 µL Gene Ruler 50 bp DNA Ladder, Thermo Fisher Scientific GmbH) and non-template controls (primer without cDNA) on an ethidium-bromide stained agarose (2 %) gel floating in 1 × TAE buffer (Carl Roth GmbH & Co. KG). Additionally, amplification efficiency was tested for comparability and is summarised in table 2.5 (Böttcher 2020).

Table 2.5 Averaged amplification efficiency of primers used for the qRT-PCR evaluated in a preliminary shift experiment with high PAR

	Amplification efficiency of primer pair for				
h after shift	***ACT7***	***eIF5A***	***HQT1***	***HQT2***	***HQT3***
0	1.99 ± 0.05 (6)	2.07 ± 0.08 (6)	1.94 ± 0.05 (6)	1.93 ± 0.02 (6)	1.95 ± 0.03 (6)
2	2.00 ± 0.05 (6)	2.02 ± 0.06 (5)	1.97 ± 0.01 (6)	1.91 ± 0.06 (6)	1.90 ± 0.06 (6)
6	1.99 ± 0.03 (6)	2.02 ± 0.16 (6)	1.88 ± 0.09 (6)	1.92 ± 0.09 (6)	1.85 ± 0.06 (6)
24	1.93 ± 0.09 (6)	2.00 ± 0.03 (6)	1.90 ± 0.06 (4)	1.92 ± 0.07 (4)	1.96 ± 0.10 (6)
72	2.00 ±0.06 (6)	1.99 ± 0.07 (6)	1.95 ± 0.04 (5)	1.89 ± 0.08 (6)	1.95 ± 0.04 (6)
96	1.97 ± 0.05 (6)	2.00 ± 0.05 (6)	2.00± 0.05 (6)	1.89 ± 0.06 (6)	1.84 ± 0.22 (6)

Values are given as average ± standard deviation for respective number of biological replicates (given in brackets) that were analysed in three technical replicates (Böttcher 2020). The amplification efficiency was evaluated by Carolin Böttcher and is redrawn from her bachelor thesis; h, hours

2.5.3 RNA-extraction, RNA concentration and integrity

Of the ten sampled plants, three representative ones were selected for analysis of relative gene expression. Selection based on relative epidermal absorbance with these three plants displaying absorbance values closest to the values averaged for all ten plants. A single leaf disc (0.68 cm^2, 15 mg) per sampling time point was used for RNA extraction. RNA was extracted using TriZol reagent (peqGOLD TriFast ^{TM}, VWR International GmbH, Darmstadt, Germany) following the manufacturers' protocol with slight modifications. Centrifugation was done at 13.000 rpm, washing of RNA was done with of 70 % EtOH and an additional precipitation step was included. For this step, 100 µL of the sample was mixed with 1.3 µL NaCl and 200 µL EtOH (100 %, p.a.) and incubated overnight at −20 °C followed by washing steps as described in the manufacturer's protocol. The concentration of RNA was measured by a NanoDrop 2000 spectrophotometer (Thermo Fisher Scientific Inc., Waltham, USA) in a 1.5 µL-sample in three technical replicates. Resulting 260/280 ratios were between 1.9 and 2.1. An amount of 300 ng RNA per sample was added to a MOPS-based loading buffer mixed with ethidium bromide and used to check for integrity by running electrophoresis on an agarose gel (1 %, v/v; Carl Roth). For a stock solution of 10.25 mL MOPS-based loading buffer 1 mL 10 × MOPS (3-(N-Morpholino)-propanesulfonic acid (Carl Roth) , 5 mL deionised formamide (Carl Roth), 1,75 mL formaldehyde solution (37 %; Carl Roth) and 2.5 mL 10 × bromophenol blue (Carl Roth) were mixed. Afterwards 3.6 µL of ethidium bromide (1 % stock solution, Carl Roth) was added to 500 µL of loading buffer. The photographed gels of selected samples are shown in the supplement (Fig. S7.8).

2.5.4 Synthesis of cDNA and subsequent qRT-PCR

For cDNA synthesis, 120 ng of extracted RNA per sample was used with the QuantiTect Reverse Transcription Kit (QIAGEN GmbH, Hilden, Germany) following the manufacturer's protocol with the slight modification that the incubation at 42 °C was extended to 5 min. Subsequent qRT-PCR was prepared using the QuantiNova SYBR Green RT-PCR Kit following the manufacturer's protocol (QIAGEN GmbH) and conducted in the RotorGene cycler 5-Plex HRM (QIAGEN GmbH) using a Three Step Cycling profile (45 cycles) with acquisition of melting curves. Analysis was done using the Rotor-Gene Q series software (QIAGEN GmbH, version 2.3.5).

2.5.5 Threshold-C_T-value and calculation of relative gene expression

The threshold of normalized fluorescence for determination of C_T was manually selected at a value where fluorescence curves became parallel to each other. This was identical for all PCR runs at a value of 0.5. The relative gene expression of HQT genes was then calculated according to Livak and Schmittgen (2001) using the averages of the technical duplicates. In a first step, a reference amount of copies ($\overline{x}(C_{T_X}ref)$) was calculated by averaging the C_T-values for the reference genes actin *(ACT7)* and eukaryotic translation initiation factor (*eIF5A)* of the six biological replicates over the six time points of sampling (equation 1). Then, the reference value was subtracted from the C_T-values of HQT1,2 or 3 for each biological replicate individually in order to obtain expression difference between the gene of interest and that of reference genes ($\Delta_{C_{T_x}}$). The expression difference was averaged for the three biological control replicates. In a subsequent step, the averaged control $\Delta_{C_{T_x}}$ were subtracted from $\Delta_{C_{T_x}}$ for each biological replicate and time point. The obtained $\Delta\Delta_{C_{T_X}}$ was then used as negative exponent for final calculation of relative gene expression.

$$\overline{x}(C_{T_X}ref) = \frac{\sum C_{T_X}(Actin) + \sum C_{T_X}(eIF5A)}{n}$$

$$\Delta_{C_{T_x}} = C_{T_X} - \overline{x}(C_{T_X}ref)$$

$$\Delta\Delta_{C_{T_X}} = \Delta_{C_{T_X}} - \Delta_{C_T}control$$

$$Relative\ gene\ expression = 2^{-\Delta\Delta C_T}$$

$$with\ X = sample\ and\ n = number\ of\ sampling\ time\ points$$

2.6 Chlorophyll fluorescence measurements

2.6.1 Determination of UV screening

For relative *in situ* quantification of UV-absorbing compounds, such as phenylpropanoids, in the leaf epidermis of higher plants, a non-invasive measurement of relative epidermal UV transmittance has been established making use of the Beer-Lambert law and chlorophyll fluorescence. According to the Beer-Lambert law, the absorbance at a particular wavelength increases linearly with the concentration of a specific compound in solution until other optical processes such as scattering become interfering. Analogously, the absorbance of ultraviolet radiation by the epidermis, thus its screening capacity, depends on the content of UV absorbing compounds, such as phenylpropanoids,

solved in the epidermal cells or bound to cell walls. The epidermal screening capacity can be determined *in situ* in higher plants making use of the Beer-Lambert law (Day et al. 1994). Different instruments share the same principle of measurement by determining the relative degree of UV attenuation in the epidermis via differentially excited chlorophyll autofluorescence originating from the underlying mesophyll (Bilger et al. 1997, 2001; Goulas et al. 2004). Leaf epidermal transmittance and absorbance, respectively, was determined as described by Bilger et al. (1997, 2001) with an updated reference measurement of chlorophyll fluorescence induced by red light (Nichelmann et al. 2016). Originally, a blue beam served as reference that was supposed to induce maximal chlorophyll fluorescence since it could pass the epidermis unhindered (Bilger et al. 1997, 2001). Later studies showed that different light acclimation states of plants interfered with the blue reference, although the latter was not absorbed by the epidermis. The differential light acclimation was accompanied by a shift in the pool size of blue light absorbing carotenoids in the mesophyll, especially those of the VAZ cycle (Marquardt and Hanelt 2004; Nichelmann et al. 2016). Thus, fluorescence induced by UV radiation with a wavelength of maximal excitation specific for the device is referred to that induced by red light (Table 2.6). The UV radiation is attenuated by the UV absorbing compounds in the epidermis (and potentially the cuticle) whereas red light can pass the outermost layer unhindered resulting in a maximum of chlorophyll fluorescence. The more UV absorbing compounds are present, the less UV excites chlorophyll resulting in a lower fluorescence. In an ideal model, the gradual increase of UV absorbing compounds yields in a correlated decrease of UV induced chlorophyll fluorescence, neglecting for example scattering of the measuring beams within the leaf tissue and different depth of penetration.

Table 2.6 Devices for determination of epidermal UV screening and corresponding measurement parameters

Instrument	UV excitation, λ_{max}, nm	Reference, λ_{max}, nm	Detection of chlorophyll fluorescence
Xenon-PAM fluorometer[1]	313, 366	650	Remitted
UV-A[2]- & Mini[1]-PAM fluorometer	375	650	Remitted
DUALEX®[3]	375	650	Transmitted
fluorescence spectrophotometer[4]	280 – 400	650	Remitted

[1]Heinz Walz GmbH, Effeltrich, Germany; [2]Gademann Instruments GmbH, Würzburg, Germany; [3]Force-A, Orsay Cedex, France; [4]Hitachi Ltd., Tokyo, Japan

For measurements using the fluorescence spectrophotometer (Hitachi Ltd., Tokyo, Japan), a leaf sample was put in a sample holder so that it had an angle of 45° to the excitation beam and towards the detector site. At the detector site, a 715 nm longpass filter (RG 715; Schott AG, Mainz, Germany) was installed to eliminate radiation other than chlorophyll fluorescence. An excitation spectrum of the leaf sample was conducted at a photomultiplier voltage of 950 V with 5 nm slit width for both excitation (280–500 nm) and emission (720 nm) and analysed via FL solution software (Hitachi Ltd.). Raw fluorescence data obtained from PAM fluorometer measurements was corrected for the device-internal noise and normalized using standard foils in which fluorescence is either minimal (green standard) or maximal (blue standard) (Bilger et al. 1997, 2001; Markstädter et al. 2001).

$$F(UV) = \frac{\mathrm{F(UV)_{leaf\ sample} - F(UV)_{green\ standard}}}{\mathrm{F(UV)_{blue\ standard} - F(UV)_{green\ standard}}}$$

$$F(R) = \frac{\mathrm{F(R)_{leaf\ sample} - F(R)_{green\ standard}}}{\mathrm{F(R)_{blue\ standard} - F(R)_{green\ standard}}}$$

The UV screening capacity is expressed either as relative epidermal transmittance (T_{UV}) or absorbance (A_{UV}) at the wavelength of UV measurement that are based on the obtained fluorescence ratios (Bilger et al. 1997, 2001). In order to calculate transmittance, the corrected fluorescence values were related to each other and resulting ratios were normalized to a so-called 100 % transmittance value ($T_{100\ \%}$) determined from leaves in which the epidermis was removed. $T_{100\ \%}$ considers optical properties of the epidermis itself.

$$T(UV) = \frac{F(UV)}{F(R)} * \frac{1}{T_{100\,\%}}$$

$$A(UV) = -\log(T)$$

Whereas the DUALEX® Scientific device gives relative absorbance units based on normalization to a device-internal $T_{100\ \%}$, the fluorescence ratios obtained from Xenon- and UV-A/Mini-PAM fluorometer measurements were referred to $T_{100\ \%}$ determined separately. The presented data in the results part was referred to *Vicia faba* leaves of which the epidermis has been removed since peeling of *Helianthus annuus* leaves was not possible. It was assumed that the fluorescence ratios between sunflowers and been diverge negligibly. When the fluorescence spectrophotometer was applied, an excitation spectrum of isolated chloroplasts on filter paper served as 100 % transmittance reference.
The DUALEX® and the combination of UV-A- and Mini-PAM fluorometer was used for measurements of leaf discs. The Flav index DUALEX measurements was correlated against calculated UV-A absorbance obtained from UV-A/mini-PAM measurements (Fig. 2.4).

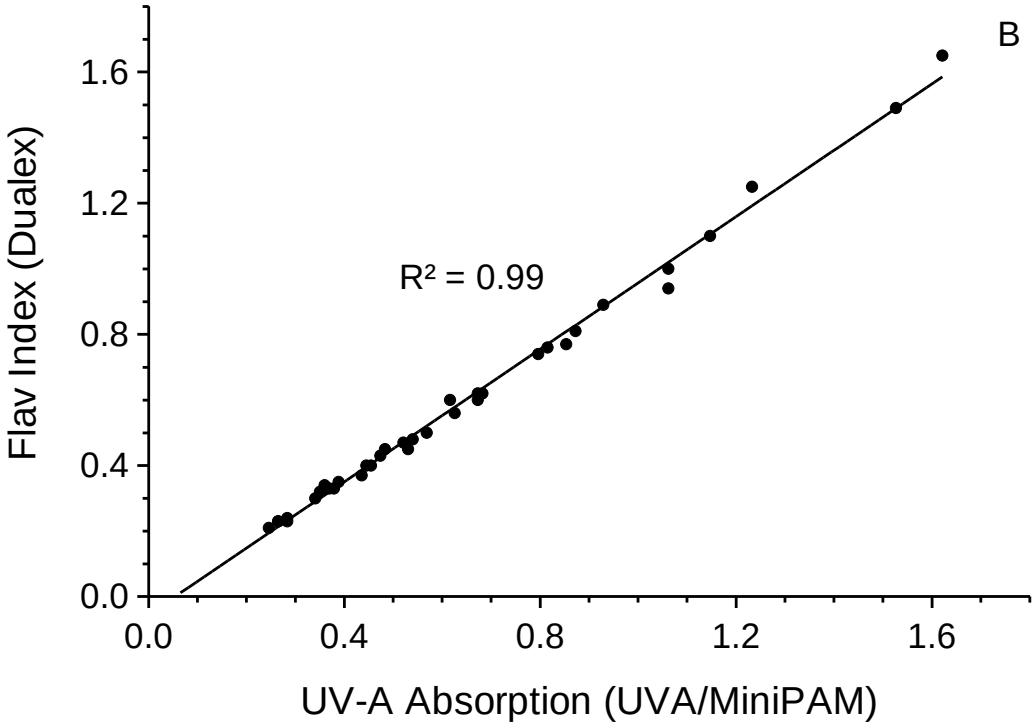

Figure 2.4 Correlation of epidermal UV-A absorbance obtained by two devices
Comparison of UV-A/Mini-PAM fluorometer and DUALEX measurement was done in leaves of 36 plants. The correlation of Dualex® versus UV-A/Mini-PAM fluorometers was fitted by a linear

regression (Flav index = 1.01 × A(UV-A_{375}) – 0.054; R^2 = 0.99).

2.6.2 Determination of photoinhibition

Prior to exposition to UV radiation, leaf epidermal UV transmittance was measured as described in chapter 2.6 and the maximal photochemical quantum yield F_V/F_M was determined. For the measurements of this parameter, chlorophyll fluorescence was measured with the saturation pulse method using an Imaging-PAM chlorophyll fluorometer (Heinz Walz GmbH) in dark-adapted leaves. The dark adaption took 15 to 20 minutes.

The degree of photoinhbition was determined in leaf discs, which had been incubated in lincomycin as described in chapter 2.7. The relative photodamage was calculated individually for each leaf disc with inhibited D1 repair with the initial F_V/F_M of the same leaf discs serving as 100 % reference so that the effect of lincomycin on F_V/F_M became irrelevant. Thus, it can be ruled out, that a differential rate of the D1 repair cycle could have affected the extent of PS II inactivation. F_V/F_M was measured before and after photoinhibition-inducing treatment. The intensity of the measuring light was adjusted such that F_O had values between 0.1 and 0.2 relative units. Obtained data was analysed using the software ImagingWin V2.41A (Heinz Walz GmbH). Relative PS II damage was calculated as

$$Relative\ PS\ II\ damage = \frac{\left(\frac{F_V}{F_M}\text{initial} - \frac{F_V}{F_M}\text{final}\right)}{\frac{F_V}{F_M}\text{initial}} * 100\ \%$$

2.7 Photoinhibition treatments

For the characterisation of the in vivo UV screening efficacy of CQAs (chapter 3.1.), three individual approaches for photoinhibition by different sources of ultraviolet radiation were conducted with leaf discs which differed in CQA content. For each photoinhibition experiment, leaf discs of high and low light grown were sampled. Photoinhibition was induced using either UV-A fluorescence tubes, solar radiation or a Xenon lamp. The bandwidth of the UV radiation was adjusted using different filter combinations as specified in the following sections. Prior to photoinhibition treatments, chloroplast encoded D1 repair was inhibited by lincomycin according to a slightly modified protocol of Bachmann et al. (2004). Leaf discs were incubated on moistened filter paper soaked with 4 mM lincomycin (AppliChem, Darmstadt, Germany) dissolved in ddH_2O for 4 hours under low light conditions (< 10 µmol m^{-2} s^{-1}). It has been shown that the D1 repair cycle involving the reassembly of destroyed, non-functional core proteins of PSII, is differentially efficient in high light and low light grown plants (Rintamäki et al. 1995). In order to diminish the divergent capacity of D1 repair cycle and to make the degree of photoinhibition more comparable, the D1 repair cycle was inhibited by treatment with lincomycin. Lincomycin did not affect epidermal absorbance and initial photochemical quantum yield was marginally reduced in leaves with high transmittance values. Photoinhibition was determined by measurements of the maximal photochemical quantum yield (F_V/F_M) via chlorophyll fluorescence. The details of the measurement and calculation of the photoinhibition parameter were described in chapter 2.6.2.

Photoinhibition by UV-A radiation

For photoinhibition induced by an artificial UV-A source of radiation, leaf discs of plants that grew under a gradient of PPFD (20 to 230 µmol m^{-2} s^{-1}; provided by HQI lamps) were placed on moistened filter paper under a fluorescence tube (T8 L 36W/73, OSRAM) for one hour without additional PAR. UV-B radiation was excluded using a polyester filter (Rachow Kunststoff-Folien GmbH) and the irradiance spectrum was recorded with a double monochromator spectroradiometer (DMc150, Bentham instrument Ltd.). The UV irradiance accounted to 25 W m^{-2} with a half bandwidth from 363 to 376 nm and a maximum at 365 nm (Fig. 2.5).

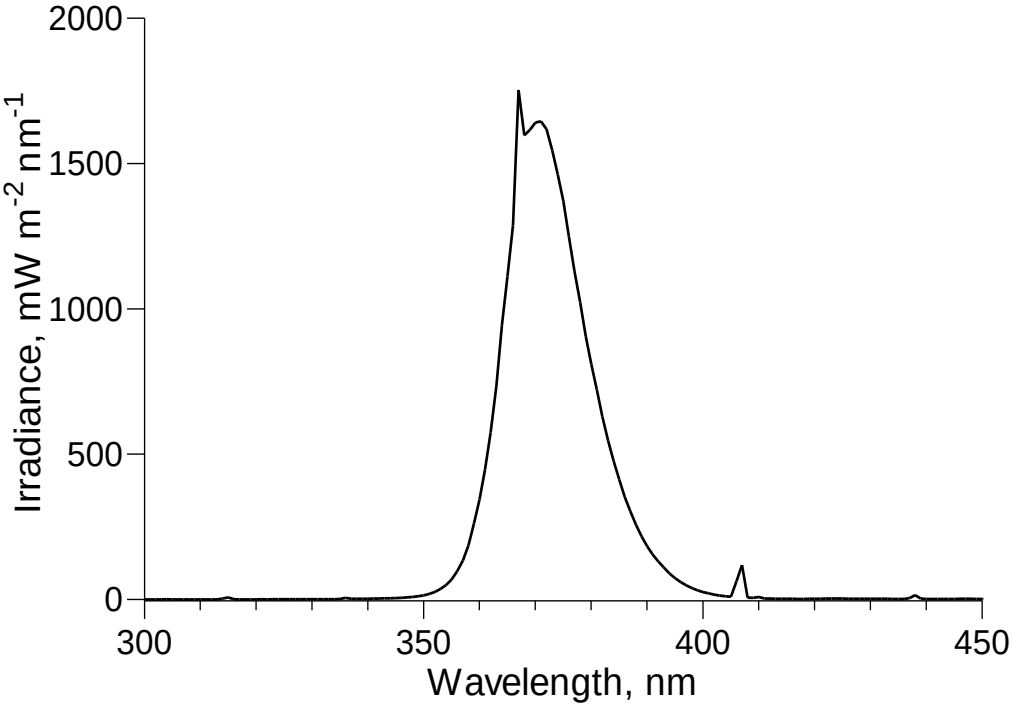

Figure 2.5 Irradiance spectra used for photoinhibtion driven by artificial UV-A
The irradiance spectrum was recorded with a Bentham double monochromator spectroradiometer. The integrated irradiance over 280 to 400 nm accounted to 25 W m^{-2} displayed a maximum at 365 nm with a half bandwidth from 363 to 376 nm.

Photoinhibition by solar UV-A radiation

For photoinhibition driven by solar UV-A, the leaf discs were arranged on moistened filter paper on a glass panel outdoors on a sunny day in July 2018 with a PPFD of 1400 µmo m^{-2} s^{-1} during the experiment. Due to limited space, six discs were arranged for UV-A treatment and three discs for the negative control. The glass panel was installed in a manner that it could be cooled with ice from the lower side during the experiment. During exposure to solar UV-A (one hour), leaf temperature was monitored with a thermoelement thermometer (Tastotherm D 700, Gulton Inc., South Plainfield, USA). Solar radiation was attenuated using a filter combination that was either UV-A transparent or UV excluding as control condition. For attenuation, a DUG11 glass filter (Schott AG, Mainz, Germany) was combined to polyester (Rachow Kunststoff-Folien GmbH) or 226 Lee U.V. foil (LMP Lichttechnik

Vertriebs GmbH, Ibbenbüren, Germany). The irradiance spectra were calculated since the filters were too small to cover the sensor of the double monochromator spectroradiometer. Irradiance spectra were calculated as the product of the solar irradiance spectra, which was recorded with a double monochromator spectroradiometer (DMc150, Bentham instrument Ltd.) and the respective transmittance spectra of applied filters obtained from spectrophotometer measurements. The spectrum of UV-A treatment displayed a half bandwidth from 330 to 375 nm with 30 µmol m^{-2} s^{-1} (11.0 W m^{-2}) in the UV region whereas PFD in the control treatment accounted for less than 1 µmol m^{-2} s^{-1} (0.01 mW m^{-2}). Corresponding PPFDs accounted for 10 µmol m^{-2} s^{-1} (Fig. 2.6).

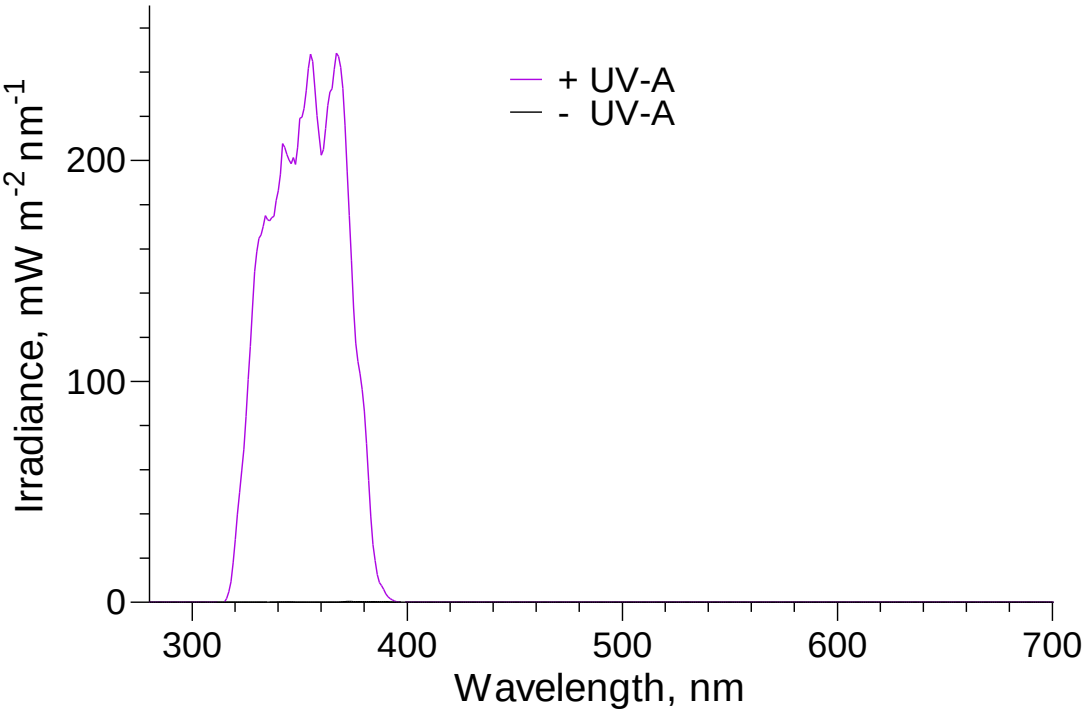

Figure 2.6 Irradiance spectra used for photoinhibtion driven by solar UV-A
For photoinhibition treatment (+ UV-A, violet line; 280-400 nm: 11 W m^{-2}), a UV-A transmitting filter combination (DUG11 + polyester) was used, whereas UV blocking filter (DUG11 + Lee U.V. 226, black line; 280-400 nm: 0.01 W m^{-2}) were used for control treatment. The photoinhibition treatment was conducted on a sunny day (07/27/18) in the Botanical Garden of Kiel. Irradiance spectra were calculated by multiplication of the solar spectrum measured with the double monochromator spectroradiometer and transmittance spectra of the applied filter combinations.

Determination of photoinhibition by a broad UV-A region

For photoinhibition treatment at different UV wavelengths, a dismounted HPLC fluorescence detector (RF551, Shimadzu, Kyoto, Japan) with a Xenon lamp and a manually selectable wavelength range of excitation with a respective half bandwidth of approximately 10 nm was used. One lincomycin treated leaf sample per wavelength region was exposed to a specific UV setting for 10 minutes each. In total, ten different settings with a maximal irradiance (λ_{max}) in 10-nm-steps from 310 to 400 nm were applied. The irradiance spectra of the respective UV settings of the fluorescence detector were recorded with a DMc150 double monochromator spectroradiometer (Bentham instrument Ltd.) (Fig 2.7). Leaf discs of plants with high and low UV transmittance were placed on

moistened filter paper in a sample holder so that the leaf discs were partially irradiated and partially protected from the radiation.

Table 2.7 Photoinhibition settings

λ_{max}, nm	Half bandwidth, nm	UPFD, µmol m^{-2} s^{-1}	Irradiance, W m^{-2}
310	304 – 316	51	20
320	315 – 326	58	22
330	324 – 336	62	22
340	334 – 345	69	26
350	344 – 355	80	27
360	354 – 366	87	29
370	364 – 375	97	31
380	374 – 386	115	36
390	384 – 396	125	38
400	395 – 406	131	39

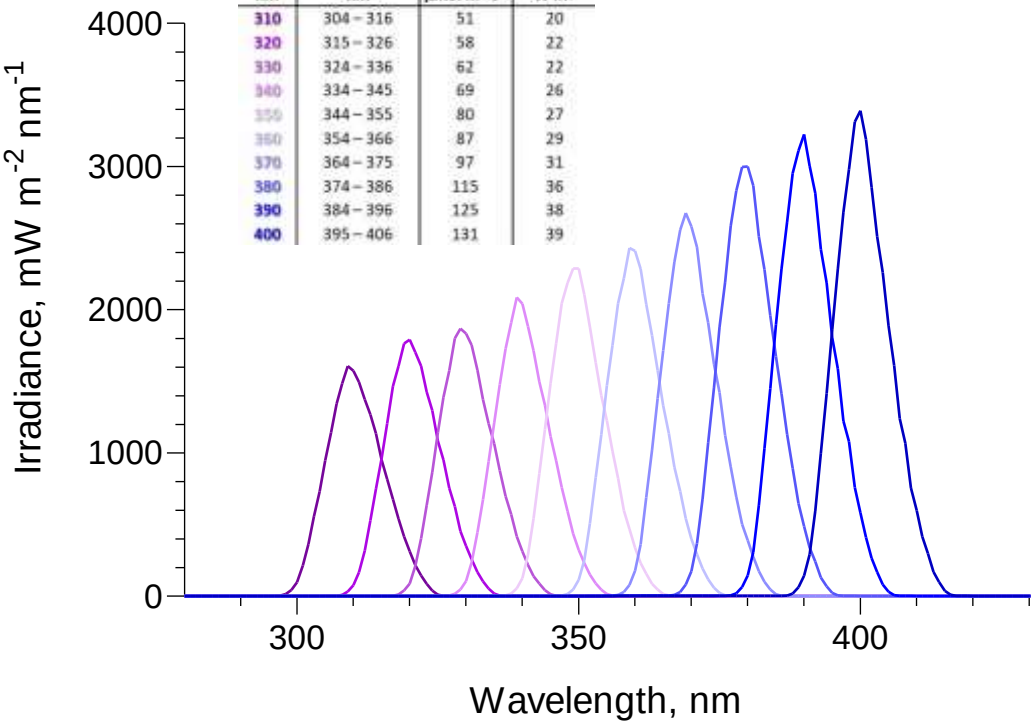

Figure 2.7 Irradiance spectra used for photoinhibtion driven by artificial UV
Leaf discs of high and low light grown plants were exposed to different UV wavebands (310 to 400 nm) with approximately 10 nm halfband width provided by different gratings in front of a Xenon lamp. Irradiance spectra were recorded in technical duplicates with a Bentham double monochromator spectroradiometer. The photon flux density (UPFD) and irradiance over 280 to 400 nm of each setting is summarised in the table 2.7 as inset.

2.8 Fluorescence microscopy

2.8.1 Visualization of caffeoylquinic acids

The blue autofluorescence of caffeoylquinic acid caused by its chromophore caffeic acid upon excitation with UV radiation allows its tissue-specific observation in leaves (Lang et al. 1991). For localization of sunflower CQAs, sections of freshly sampled leaves of high and low light grown plants were prepared directly prior to fluorescence microscopy. Cross-sections of fresh leaves (150 µm thick) were generated with a Hydrax V50 vibratome (Zeiss, Oberkochen, Germany) using 80 Hz blade vibration and a cutting speed of 43 mm s^{-1}. Paradermal sections of upper and lower epidermis were produced manually. Specimens were collected in tap water and analysed under a fluorescence microscope (Axiophot, Zeiss) using magnifications of 200 × or 400 ×. Excitation and emission filter were selected based on the publication of Lang and co-authors (1991), who reported maximal emission for CGA at 440 nm. Accordingly, CQA autofluorescence was induced with a Xenon lamp using excitation at 365 nm for 2 seconds and monitored by a RGB camera either through a 445 nm bandpass filter with a half band width of 50 nm (Zeiss) or through a 420 nm longpass (LP) filter (Zeiss)

allowing simultaneous detection of chlorophyll fluorescence. Corresponding bright field images of identical details were exposed for 1 to 10 ms. Plasmolysis was induced in paradermal sections by a 1M KNO_3-solution.

2.8.2 Visualization of flavonoids with Naturstoff reagent A

Potential occurrence of flavonoids was investigated by staining with Naturstoff reagent A (NA; 2-aminoethoxydiphenyl borate) according to Hutzler et al. (1998). A stock solution with 2.5 % (w/v) Naturstoff reagent A (Carl Roth) in EtOH was freshly prepared. For staining of hand cut sections, the stock solution was diluted to 0.1 % (w/v) with a 0.1 M potassium phosphate buffer (0.0497 M K_2HPO_4 + 0.0503 M KH_2PO_4; pH at 6.8). Hand cut leaf sections were placed in a droplet of 0.1 % Naturstoff reagent A solution on a microscopy slide under a coverslip. After 5 minutes of incubation, the stained samples were washed by soaking of the NA-staining solution with a filter paper and simultaneous addition of the 0.1 M potassium phosphate buffer. UV-induced fluorescence (365 nm; 2 s exposure time) was investigated through the 420 nm LP filter of the fluorescence microscope at identical magnifications as used for CQA visualization.

2.9 Statistical analysis

Obtained raw data was collected in Excel V2016 (Microsoft, Redmond, USA) for subsequent processing such as calculation of UV screening, relative PS II damage, caffeoyl residues, relative content, fold of control or relative gene expression. Processed data was then transferred to GraphPad Prism V5.0 (GraphPad Software, San Diego, USA) for further statistical analysis. Linear regression analysis was used for UV-B absorbance in dependence of growth irradiance and maximal photochemical quantum yield as well as relative PS II damage plotted against UV-A transmittance. Non-linear regression was calculated using a 2^{nd} order polynomial (T(UV-A) vs. T(UV-B) and T(UV-B vs. growth irradiance) or an exponential approach (A(UV-A) or T(UV-A) vs. caffeoyl residues). Data followed a Gaussian distribution ($\alpha = 0.05$) that was tested using the D'Agostino & Pearson omnibus normality test or, if the sample number was below ten (PCR data and HPLC data for UV-B1 experiment), with a Kolmogorov-Smirnov test at a confidence interval of 95 %.

Statistically significant differences between control and treated groups in kinetics of relative epidermal absorbance, HPLC peak areas and relative gene expression for experiments presented in chapter 3.2 were analysed using Two-Way ANOVAS with repeated measures. Two Way ANOVAS without repeated measures were selected for comparative UV-A absorbance data of leaves with different insertion heights. When single values were missing due to sample loss or single values were excluded due to outlier analysis, Two-Way-ANOVAS was conducted based on row means and standard deviations. An unpaired t-test with Welch correction was applied for comparative UV-A absorbance data of control and UV-B treated plants that passed normality test but displayed significantly different variances.

3 Results

3.1 Epidermal UV screening of sunflower leaves

Sunflowers are plants adapted to the exposition of full sunlight. Different sunflower cultivars that grew outdoors in the summer in Kiel, showed high epidermal screening capacity in the UV-B and UV-A range (Hoier 2012). When the present work was initialized, the phenylpropanoids, which provide epidermal UV screening in foliar leaves of sunflower, had not been identified. Although hydroxycinnamic acids were predominantly abundant in foliar leaves of several *Helianthus annuus* accession and different flavonoids were extracted from tubular and ligulate ray flowers of other subspecies (Rieseberg et al. 1987; Saftić-Panković et al. 2006; Hoier 2012), it was not clear whether they serve a UV protecting role. Additionally, no data on the histolocalization of phenylpropanoid in sunflower existed. The aim of the present work was to identify the UV screening pigments in foliar sunflower leaves. It was hypothesized that sunflower leaves accumulate both flavonoids and hydroxycinnamic acids in the epidermal layer as internal UV screening pigments.

3.1.1 Identification of UV absorbing compounds in sunflower leaf extracts

Prior to identification of UV screening pigments in *Helianthus annuus*, the different phenylpropanoids needed to be separated from each other. For compound separation and identification, the profile of phenylpropanoid metabolites extracted from sunflower leaves with high UV screening was analysed by HPLC using a diode array system. The UV chromatograms displayed three dominant peaks at retention times of 13.3 (peak 1), 20.4 (peak 2) and 21.6 minutes (peak 3), respectively (Fig. 3.1A). The corresponding UV absorbance spectra were nearly identical with a maximal extinction at approximately 330 nm and a shoulder at 290 nm (Fig. 3.1B). The peak area of those three peaks contributed to more than 95 % of absorbance at 330 nm in analysed leaf extracts. Throughout different experiments including more than 100 leaf samples with varying epidermal UV screening, chromatogram peaks with UV absorbance spectra characteristic for flavonoids were not detectable. In order to identify the chemical structure responsible for the three peaks, mass spectrometry (MS) analysis was conducted at the Department of Physiology and Cell Biology at the Leibniz Institute of Plant Genetics and Crop Plant Research (IPK) in Gatersleben. MS data obtained from IPK Gatersleben together with comparison of retention times and UV absorbance spectra to that of HPLC standard solutions clearly indicated the three dominant compounds to be caffeoylquinic acid (CQA) esters belonging to the group of hydroxycinnamic acids (supplementary Fig. S7.1). Peak 1 was identified as chlorogenic acid (3-O-mono-CQA) and peaks 2 and 3 were identified as two different isomers of di-CQAs. Whereas the isomeric structure of the compound responsible for peak 2 could not be clarified clearly due to a missing standard, peak 3 was identified unequivocally as 3,5-diCQA. When leaf extracts were highly concentrated, flavonoids were found in minor amounts (Fig. S7.1, Table S7.1).

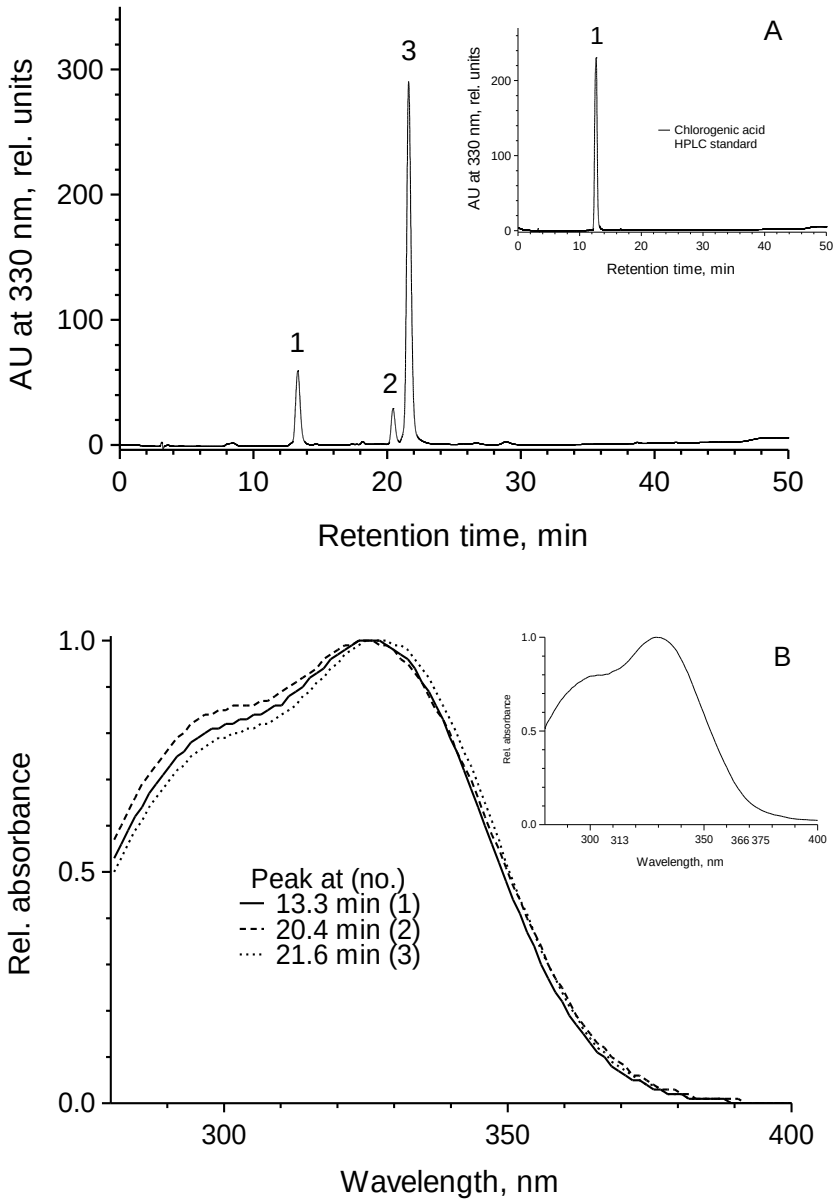

Figure 3.1 Representative chromatograms (A) of an extract of a sunflower leaf grown at an irradiance of 230 µmol m^{-2} s^{-1} PAR and (B) corresponding UV absorbance spectra
UV chromatogram at 330 nm of an aqueous methanolic leaf extract of a sunflower plant (A). The insets shows the chromatograms and normalized UV absorbance of a chlorogenic acid HPLC standard dissolved in 50 % MeOH acidified with 1% HCl. The leaf displayed a UV-A screening of 1.2. Online-determined photodiode array absorbance spectra corresponding to the dominant peaks were normalized to the maximum (B). The graphs are modified from Stelzner et al. (2019).

3.1.2 Linking epidermal UV screening to caffeoylquinic acid content

The UV screening capability of the epidermal layer is expressed as either epidermal transmittance or absorbance giving a measure of how much UV either pass the epidermis or how much UV is attenuated through the outermost layer. Absorbance is linearly correlated to the concentration of absorbing compounds in the optical path according to the Beer-Lambert law whereas transmittance should give a curvilinear relationship. The CQA content differed between sunflower plants grown in high light and low light. It was, thus, hypothesized that (1) the UV screening of sunflower leaves is

variable. Predominant abundance of CQAs in high light grown sunflower leaves indicated these HCAs to contribute substantially to epidermal UV screening. The absence of other UV absorbing compounds such as flavonoids pointed towards CQAs to overtake solely the function of epidermal UV protection. Hence, it was further hypothesized that (2) CQAs are localized in the outermost, epidermal cell layer of UV-protected sunflower leaves and that (3) increasing UV screening depends on an increasing CQA content. In order to test these assumptions, two different methods complementing each other were applied. One approach involved comparative CQA visualization by fluorescence microscopy in leaves generated with high and low UV screening. In the second approach, CQA content was determined via HPLC in sunflower leaves with varying epidermal screening.

3.1.2.1 Relationship between UV screening and growth irradiance

The variability of epidermal UV screening was determined via chlorophyll fluorescence measurements at different UV wavelengths using a Xenon-PAM chlorophyll fluorometer (313 and 366 nm), a combination of UV-A/Mini-PAM fluorometer and the Dualex® device (both at 375 nm) and a spectrofluorometer (300 to 400 nm). Due to the high molar extinction of wavelengths below 315 nm by CQAs, UV-B screening was thought to reflect optimally the potential variability of the foliar epidermal UV screening in sunflower plants. At the same time, epidermal UV-A protection was proposed to be smaller due to weak absorbance by CQAs (Fig. 3.2).

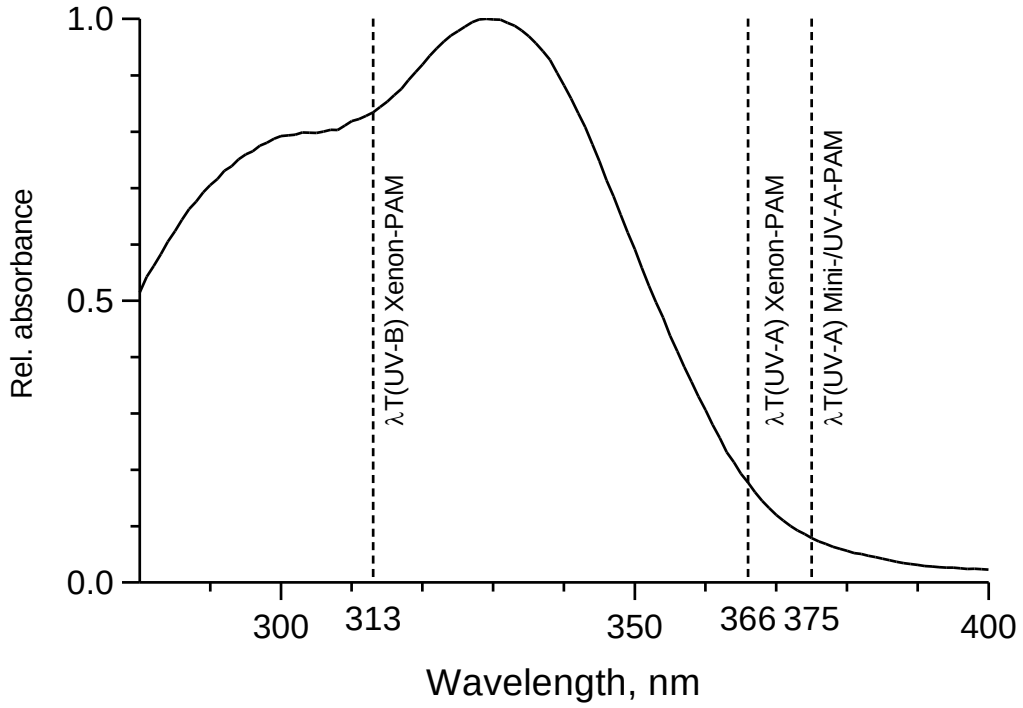

Figure 3.2 UV absorbance spectrum of a chlorogenic acid HPLC standard
The HPLC standard was dissolved in 50 % MeOH acidified with 1% HCl and UV absorbance was determined spectrophotometrically and normalized to the maximal absorbance at 330 nm. The dashed vertical lines display wavelengths at which UV-transmittance is measured via chlorophyll fluorescence using either the Xenon-PAM fluorometer or a combination of UV-A- and Mini-PAM

fluorometer.

The UV screening is determined by surrounding light conditions such as PAR and UV in various higher plants (Pescheck and Bilger 2020) and preliminary HPLC data indicated the same pattern for sunflower plant. In order to analyse the relationship between CQA content and UV screening, plants with different UV screening capacities were required and, thus, grown under a range of PPFDs. Plants grew under four different filter combinations with super low light (SLL), low light (LL), moderate light (ML) and high light (HL). The determination of UV transmittance based on excitation spectra of chlorophyll fluorescence in leaves displayed four distinct spectra (Fig. 3.3).

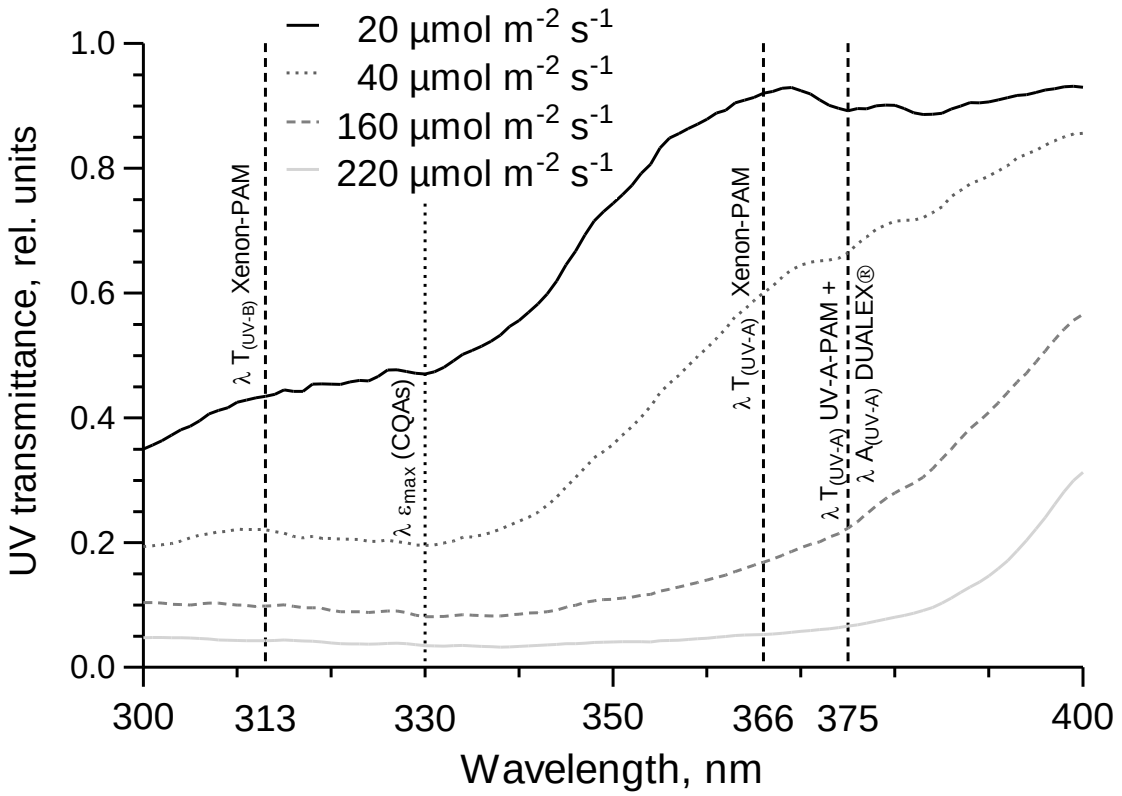

Figure 3.3 UV transmittance spectra of sunflower foliage leaves grown under varying PPFDs
UV transmittance was obtained by measuring excitation spectra of chlorophyll fluorescence at 720 nm in leaves of sunflower plants grown at either super low light (20 µmol m^{-2} s^{-1}, black solid line), low light (40 µmol m^{-2} s^{-1}, dot-dot-dashed line), moderate light (160 µmol m^{-2} s^{-1}, dashed line) or high light (220 µmol m^{-2} s^{-1}, grey solid line). Dashed vertical lines display wavelengths of measurement of UV transmittance and absorbance, respectively. The dotted vertical line displays the wavelength of maximal extinction by caffeoylquinic acids (CQAs). The raw excitation spectra of six leaves per growth irradiance were normalized to 650 nm and referred to the normalized chlorophyll fluorescence excitation spectrum of a suspension of isolated sunflower chloroplasts applied to a piece of filter paper. Afterwards the spectra were smoothened. Chlorophyll fluorescence was detected at 720 nm through a 715 nm long pass filter.

The epidermal transmittance at the distinct UV wavelengths was consistent with the absorbance spectrum of the chlorogenic acid standard (Fig. 3.2). As compared to the UV-A transmittance, the UV-B transmittance at 313 nm displayed the smallest deviation from transmittance at 330 nm, the wavelength at which CQAs absorb maximally for each growth irradiance. High light grown leaves

displayed low transmittance values throughout the UV region (Table 3.1). The range of transmittance at 366 and 375 nm (approximately 0.1 up to 0.9) among plants that grew under different growth irradiances was by far broader than in the UV-B (0.1 up to 0.5) suggesting the measurement in the UV-A range to reflect alterations with a higher signal to noise ratio. Consistently, leaf discs under different PPFDs displayed variable UV transmittance at 366 nm from 0.1 to 0.6 measured with the Xenon-PAM chlorophyll fluorometer.

Table 3.1 Epidermal transmittance at distinct UV wavelengths of sunflower leaves at different growth irradiances

	Growth irradiance			
	HL	**ML**	**LL**	**SLL**
T_{313}	< 0.1 ± 0.0	0.1 ± 0.0	0.2 ± 0.0	0.4 ± 0.1
T_{330}	< 0.1 ± 0.0	0.1 ± 0.0	0.2 ± 0.0	0.5 ± 0.1
T_{366}	< 0.1 ± 0.0	0.2 ± 0.0	0.6 ± 0.1	0.9 ± 0.1
T_{375}	< 0.1 ± 0.0	0.2 ± 0.0	0.7 ± 0.1	0.9 ± 0.1

Transmittance was obtained by measuring excitation spectra of chlorophyll fluorescence as described for Fig. 3.3 in leaves of sunflower plants grown at super low light (SLL, 20 µmol m^{-2} s^{-1}), low light (LL, 40 µmol m^{-2} s^{-1}), moderate light (ML, 160 µmol m^{-2} s^{-1}) and high light (HL, 220 µmol m^{-2} s^{-1}). Values are given as average of six sunflower plants ± standard deviation.

The relative epidermal transmittance of sunflower leaves at 366 nm depended negatively on growth irradiance (Fig. 3.4A). At highest PPFDs, UV-A transmittance accounted to values between 0.05 and 0.06 and increased in a non-linear manner to 0.6 at PPFDs of approximately 20 µmol m^{-2} s^{-1}. The correlation was fitted by an exponential equation with $\mathrm{T(UV_{366})} = 0.8 - 0.06 \times \mathrm{e}^{-0.025 \times \mathrm{GI}} + 0.060$ (R^2 = 0.94; GI = growth irradiance) (Fig. 3.4A). Logarithmic conversion of transmittance into absorbance resulted in a linear correlation with an equation of $\mathrm{A(UV_{366})} = 0.005 \times \mathrm{GI} + 0.25$ (inset of Fig. 3.4A). The epidermal UV-A transmittance, either determined at 366 nm or 375 nm, strongly correlated in a non-linear manner with transmittance at 313 nm (R^2 = 0.99 for $T(UV\text{-}A_{366})/T(UV\text{-}B_{313})$ and R^2 = 0.98 for $T(UV\text{-}A_{375})/T(UV\text{-}B_{313})$). The non-linear correlations were fitted with a modified Michaelis-Menten-equation:

$T(UV_{366}) = \frac{1.558 \times \mathrm{T}(UV_{313})}{0.4112 + \mathrm{T}(UV_{313})} - 0.0967$ with R^2 = 0.99 and

$T(UV_{375}) = \frac{1.771 \times \mathrm{T}(UV_{313})}{0.1495 + \mathrm{T}(UV_{313})} - 0.3152$ with R^2 = 0.98 (Fig. 3.4B).

According to these equations, 75 % of radiation at 366 nm is transmitted when 50 % of UV-B is transmitted through the epidermis. Consistent with the steeply decreasing absorbance in the UV-A region by CQAs, nearly 100 % of radiation at 375 nm is transmitted when 50 % of UV-B are transmitted. These values are in accordance with results of spectrofluorometer measurements (Fig. 3.3.).

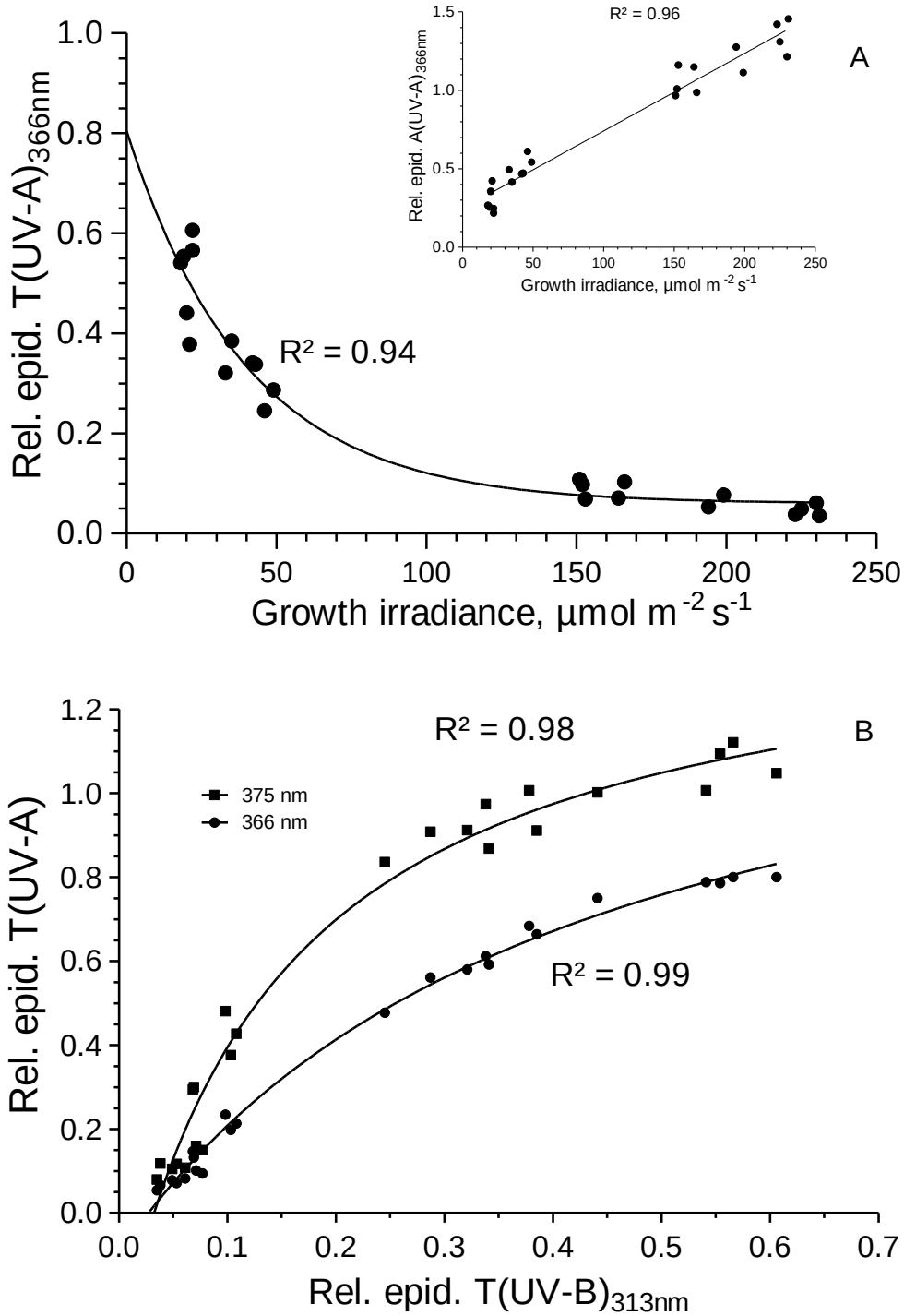

Figure 3.4 Dependence of relative epidermal transmittance at 366 nm on growth irradiance (A) and correlation of epidermal UV-A and UV-B transmittance (B)

Epidermal UV transmittance was determined in discs of sunflower leaves growing under varying PPFDs (A, n=23). Absorbance was obtained by calculating the negative logarithm of transmittance. UV-A transmittance at 366 nm (Xenon-PAM fluorometer; circles) or 375 nm (combination of UV-A/Mini-PAM chlorophyll fluorometers; squares) was determined in leaf discs of 24 sunflower plants grown under variable PPFDs. The correlations for A were fitted with an exponential model for $\mathrm{T(UV_{366})} = 0.8 - 0.06 \times \mathrm{e}^{-0.025 \times \mathrm{GI}} + 0.060$ (R^2 = 0.94) and with a linear regression for $\mathrm{A(UV_{366})} = 0.005 \times \mathrm{GI} + 0.25$ (R^2 = 0.96). Non-linear correlations of B were fitted with a modified Michaelis-Menten-equation: $T(UV_{366}) = \frac{1.558 \times \mathrm{T}(UV_{313})}{0.4112 + \mathrm{T}(UV_{313})} - 0.0967$ with R^2 = 0.99 and $T(UV_{375}) = \frac{1.771 \times \mathrm{T}(UV_{313})}{0.1495 + \mathrm{T}(UV_{313})} - 0.3152$ with R^2 = 0.98. The graph A is modified from Stelzner et al. (2019).

Although the reason is not clear, transmittance values at 366 nm above 0.2 obtained by spectrofluorometer measurements appeared overestimated in comparison to measurements with the Xenon-PAM fluorometer device (Figs. 3.3, 3.4, Table 3.1). Thus, especially transmittance of low light plants appeared too high (Figs. 3.3, 3.4, Table 3.1). It is possible that the deviation was caused by using a suspension of isolated chloroplasts as a 100 % transmittance reference for normalization instead of epidermis-free *Vicia faba* leaves.

3.1.2.2 Localization of phenylpropanoids within sunflower leaves

One prerequisite for the contribution to UV screening is the localization of the UV absorbing compounds to the epidermis. Combining predominant abundance of CQAs as soluble UV absorbing compounds with the variability of UV screening suggests variable amounts of CQAs in the epidermis. In order to test whether CQAs are localized in the epidermis of vegetative sunflower leaves, their characteristic blue-green autofluorescence was induced by UV fluorescence microscopy in leaf sections with intact epidermal cells (Lang et al. 1991). The PPFD-dependence of UV screening was used to generate a positive control with low UV transmittance (high light grown, HL) and a quasi "negative" control in which UV transmittance was high (low light-grown, LL). If CQAs substantially contributed to the epidermal UV screening, the blue autofluorescence should be remarkably stronger in HL than in LL plants.

In cross sections of leaves with high UV screening, strong blue-green fluorescence signals characteristic for CQAs were restrictedly localized to epidermal cells of the adaxial side including trichomes (Figs. 3.5A, C). The abaxial epidermis displayed a much weaker blue fluorescence with a different tone apparently originating from the cuticle or the cell walls (Figs. 3.5A, C). In contrast, the blue-green fluorescence was much fainter if not absent in adaxial epidermal cells and basal cells of trichomes of plants with low UV screening capacities. As for leaves with high UV screening, no comparable fluorescence was seen in abaxial epidermis of leaves with low UV screening (Figs. 3.5B, D).

Comparative fluorescence microscopy of paradermal sections confirmed results obtained from cross sections. As observed before, fluorescence characterizing the presence of CQAs was strong in adaxial epidermal cells of leaves with high UV absorbing capacities except for guard cells of stomata. The signal intensity was apparently homogenously distributed within epidermal cells and absent from cell walls (Fig. 3.6A). No comparable fluorescence signals were localized in leaves with low UV screening and in abaxial leaf sides, irrespective of the degree of UV screening, so that red chlorophyll fluorescence could pass the epidermis from underlying mesophyll (Figs. 3.6B, D). A faint blue fluorescence signal with a different blue tone was found in the inner thick wall of stomata consistently for all samples (Figs. 3.6B–D).

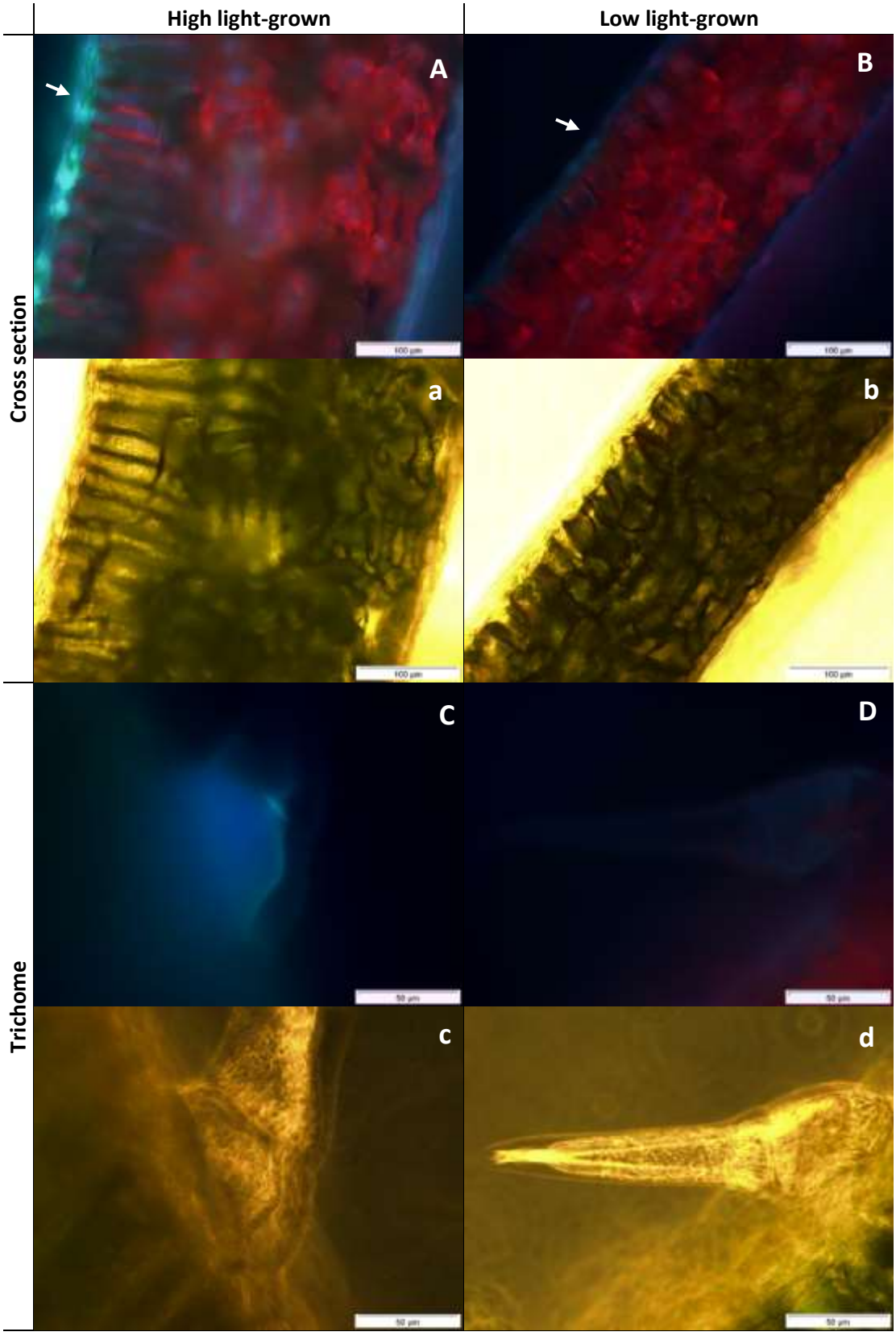

Figure 3.5 Comparative UV excited fluorescence (upper case) and corresponding bright field (lower case) images of sunflower plants grown in high (left) or low (right) light Fluorescence signals were detected through a 420 nm LP filter in cross-sectioned leaves (A, B, a, b) and in intact trichomes (C, D, c, d). Micrographs with lower case letters depict the corresponding bright field images. Arrows mark the respective upper epidermis. Scale bar is depicted in each image.

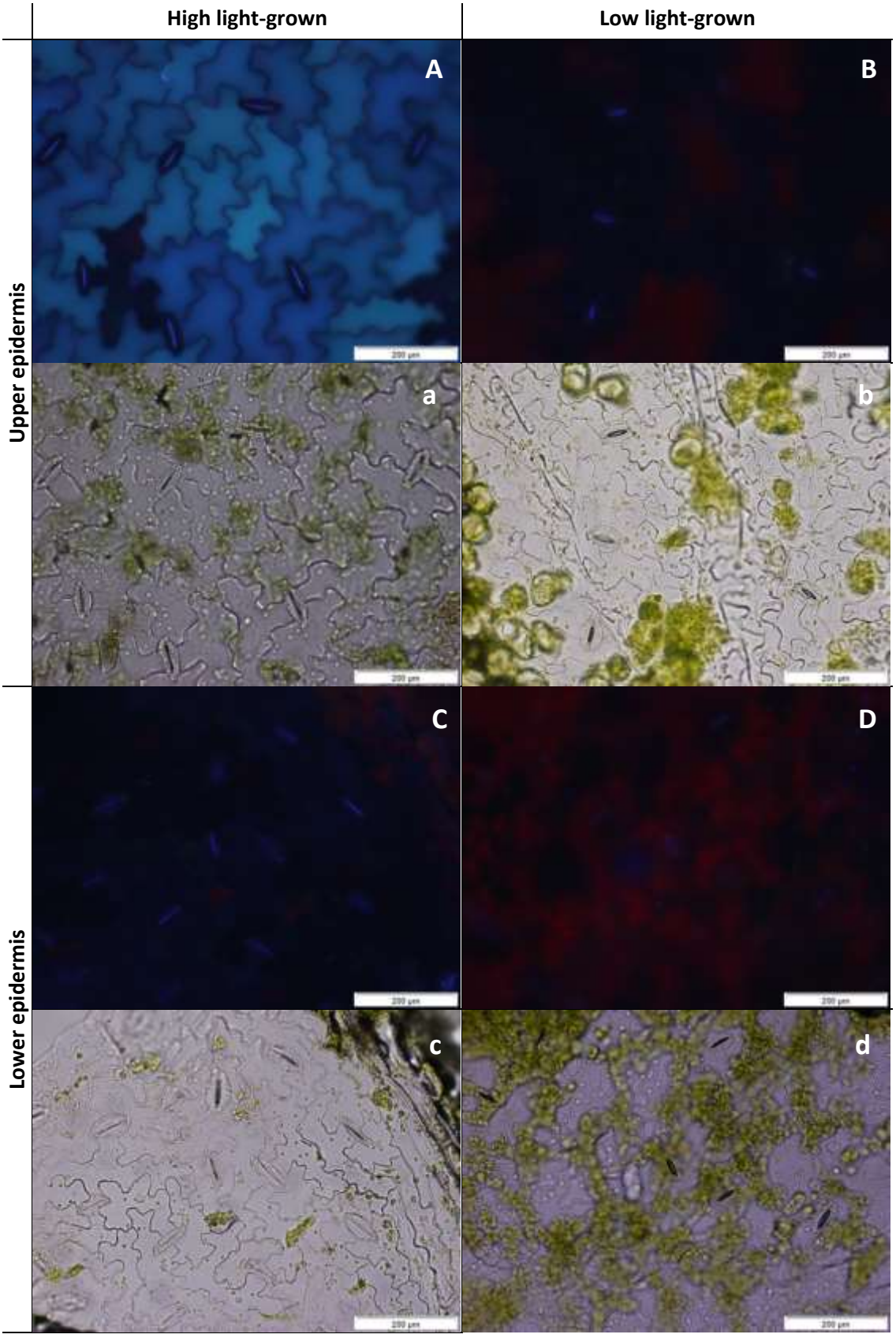

Figure 3.6 Comparative UV excited fluorescence (upper case) and corresponding bright field (lower case) images of the epidermis of high (left) and low (right) light grown sunflower plants Fluorescence signals were detected through a 420 nm LP filter in paradermal sections of the adaxial (A, B, a, b) and abaxial (C, D, c, d) epidermis. Greyscale images of fluorescence micrographs are published in Stelzner et al. (2019). Micrographs with lower case letters depict the corresponding bright field images. Scale bar is depicted in each image.

For a further analysis whether CQA are localized solely intracellularly or also in the cell walls, plasmolysis of epidermal cells was induced by KNO_3 under which the protoplast is detaching from cell walls. After plasmolysis, autofluorescence signals emitted by CQAs were restricted to the protoplast including Hechtian strands verifying absence from cell walls and pointing towards localization in the cytoplasm. However, it cannot be clearly distinguished whether the fluorescence was originating from either the cytoplasm or the vacuole or whether it was localized in both compartments (Figs. 3.7A, B).

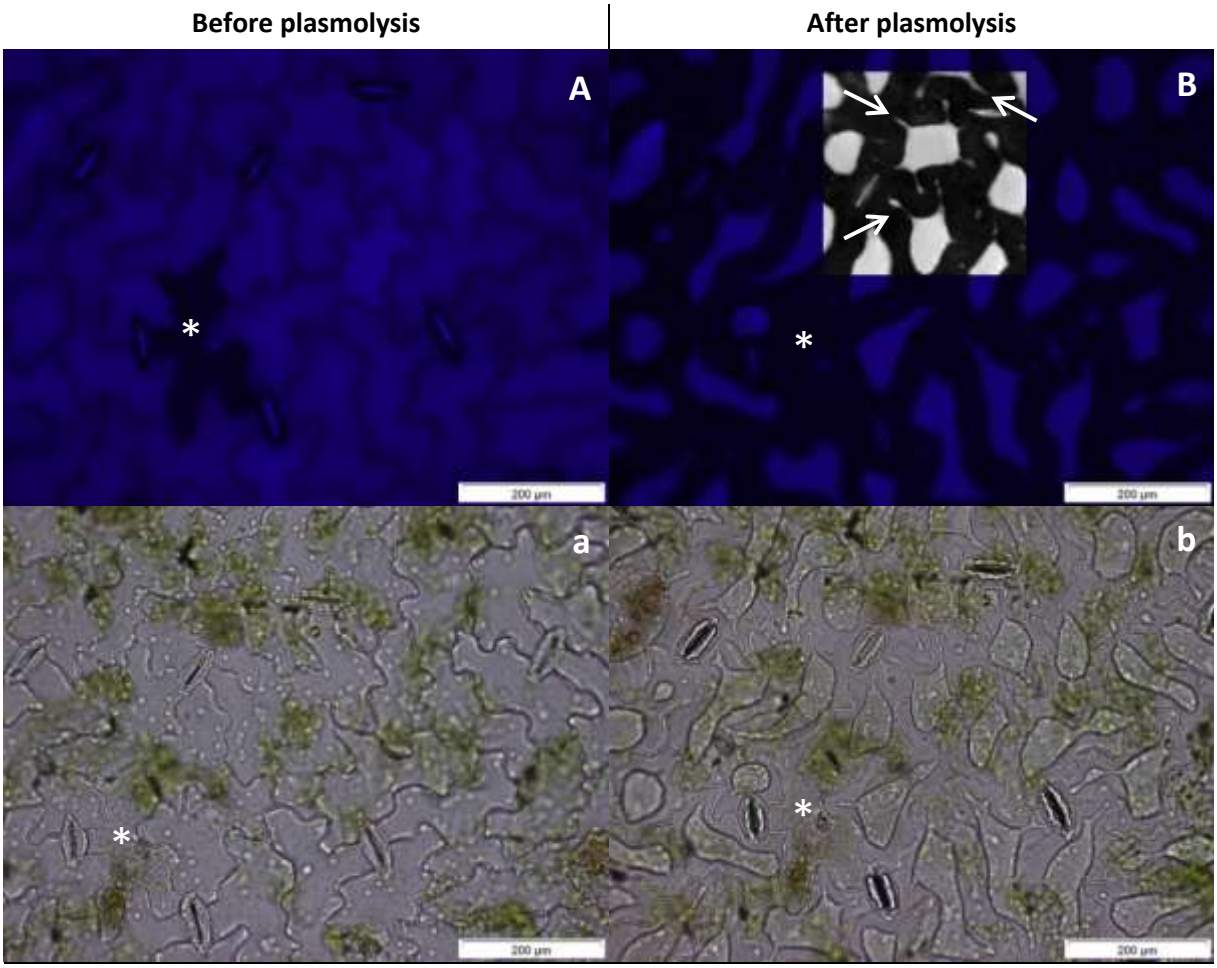

Figure 3.7 Comparative UV excited fluorescence (upper case) and corresponding bright field (lower case) images of the adaxial leaf epidermis of high light grown sunflower plants before (left) and after plasmolysis (right). Autofluorescence of CQAs was detected in paradermal sections using a 445 nm BP filter (A, B). Arrows mark Hechtian strands in a grey converted section (B). Asterisks mark the same leaked cell (A, B, a, b). Micrographs with lower case letters depict the corresponding bright field images. Scale bar is depicted in each image. Greyscale images of fluorescence micrographs are published in Stelzner et al. (2019).

In order to verify absence of flavonoids, Naturstoff reagent A (NA) was used for staining of high light grown plants. The major part of paradermal sections displayed no fluorescence signals characteristic for flavonoids but a bathochromic shift of CQA fluorescence to green was observed. However, the inner cell wall of stomata emitted a yellow-orange fluorescence and unidentified parts of the guard cells showed a reddish signal. In cell walls, a yellow-greenish fluorescence was observed after treatment with Naturstoff reagent A that was not observable in non-treated sections. (Figs. 3.8A, B). A yellow-orange signal was found now and then also in the distal parts of trichomes (Fig.3.8C).

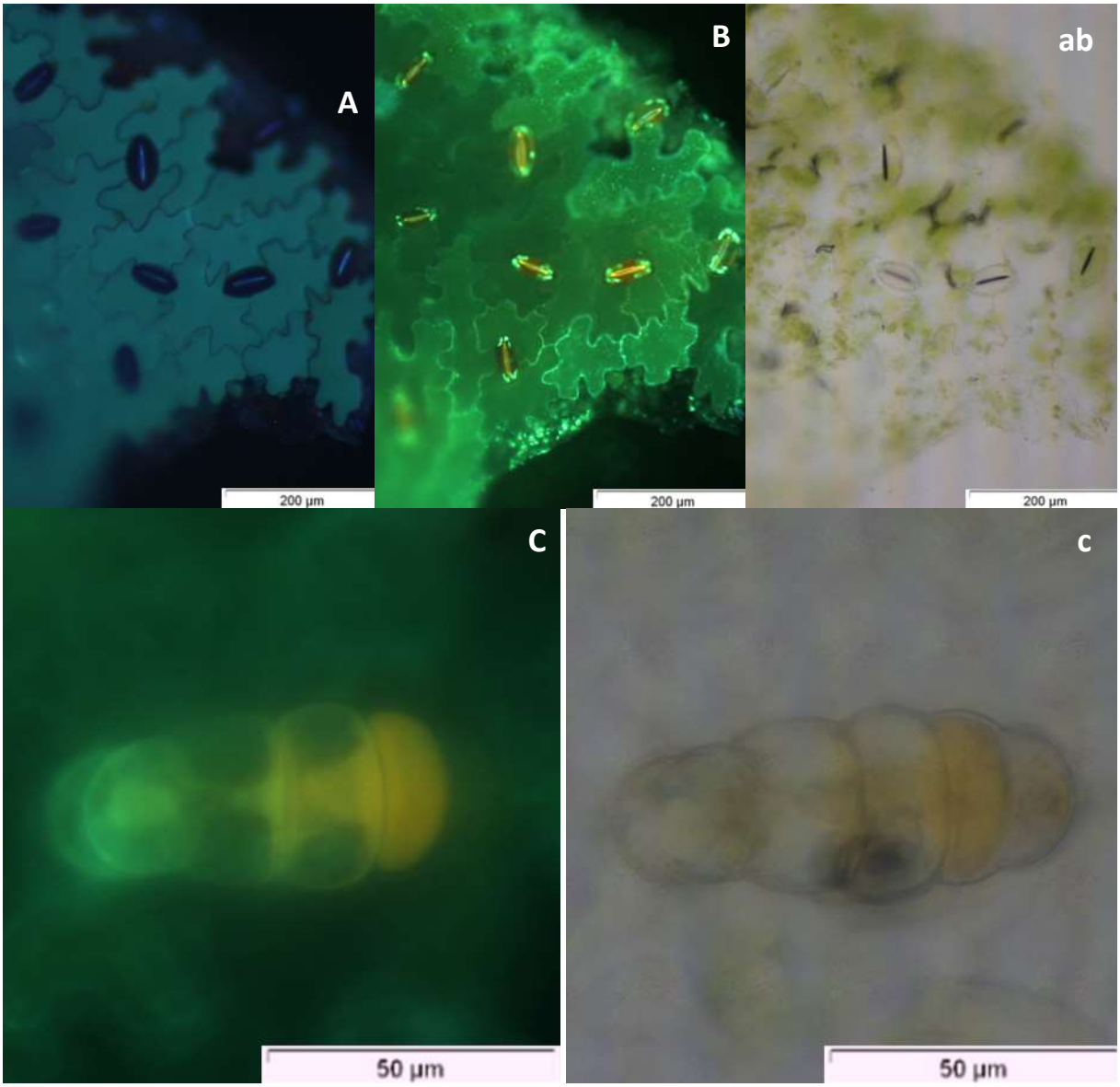

Figure 3.8 UV excited fluorescence microscopy in an epidermis stained with Naturstoff reagent A
Fluorescence signals were detected through a 420 nm LP filter in paradermal sections of the adaxial epidermis of high light grown leaves before (A) and after staining with Naturstoff reagent A (B, C). Micrographs with lower case letters depict the corresponding bright field images. Scale bar is depicted in each image.

Treatment with Naturstoff reagent A resulted in a fluorescence of the cell walls of unknown origin. In order to test whether CQAs could have induced the fluorescence and to search for further potential cell wall-bound phenolics, cell walls were isolated, extracted and analysed via HPLC. The summarised absorbance of phenolic constituents extracted from isolated cell walls at 330 nm approximately accounted for a twentieth of that of leaf extracts although the weight of isolated cell walls was twice as high as the fresh leaf material used for extraction of soluble phenolics (Fig. 3.9). Four major and nine minor peaks occurred. The maximal absorption of major peaks was at 300 nm (peak at 25.7 minutes), 310 nm (24.2 min), 325 nm (19.7 min) or 348 nm (6 min), respectively (inset of Fig. 3.9). None of the peaks displayed absorbance spectra comparable to CQAs. The absorbance spectra of the minor peaks were identical to the spectra of major peaks and are thus, not shown separately.

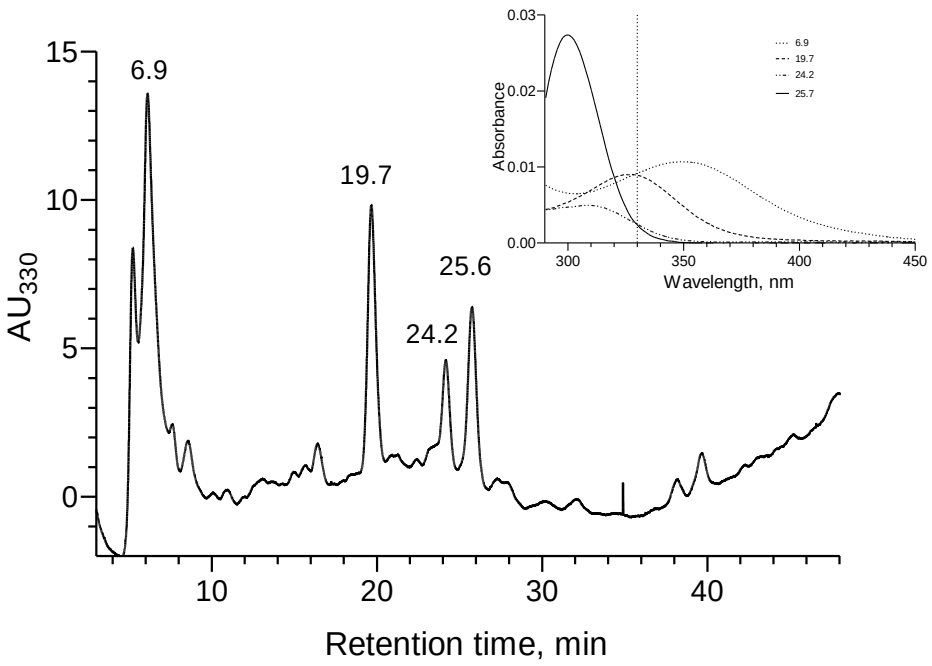

Figure 3.9 HPLC-DAD chromatograms at 330 nm of cell wall extracts
Twelve whole leaves (approximately 4 g dry weight) of four plants grown in high light with epidermal UV-A absorbance around 1.0 were harvested, pooled and used for cell wall extraction and subsequent HPLC analysis according to Harbaum et al. (2008). For extraction, 0.0025 g of isolated cell wall material was enzymatically digested in three technical replicates.

3.1.2.3 Correlating epidermal absorbance to caffeoylquinic acid content

Fluorescence images suggested a close relationship between caffeoylquinic acid content and epidermal UV screening. In order to analyse the contribution of the soluble foliar CQA content to epidermal UV transmittance, both parameters were determined in leaf discs of plants grown for three weeks under a range of PPFDs using high-pressure liquid chromatography (HPLC) and a combination of UV-A- and Mini-PAM fluorometer measurements. Phenylpropanoids in aqueous methanolic leaf extracts displayed comparatively low absorbance at wavelengths above 350 nm. Nevertheless, relative epidermal absorbance at 375 nm showed a strong correlation to the extractable phenylpropanoid contents, consistent with the correlation between UV-B and UV-A transmittance. Again, soluble phenylpropanoids involved mono- and di-caffeoylquinic acids that accounted together for at least 95 % in each sample. The CQA content was calculated based on a HPLC calibration with chlorogenic acid (3-O-mono-caffeoylquinic acid) and was expressed as caffeoyl residues. This calculation includes correction for the molar extinction coefficient of di-CQA, which is twice as high as that of mono-CQA.

Epidermal UV-A absorbance increased in a non-linear manner and strongly correlated with amounts of caffeoyl residues (CR) per cm² leaf area (Fig. 3.10). The correlation between relative epidermal UV-A absorbance and CR was fitted by following Michaelis-Menten equations: $A(UV\text{-}A)_{366} = 2.05 \times CR / (97.82 + CR)$ ($R^2 = 0.96$) and $A(UV\text{-}A)_{375} = 4.41 \times CR / (465.80\ CR)$ ($R^2 = 0.92$). Transmittance decreased in a non-linear manner with amounts of caffeoyl residues (CR) per cm² leaf area and was described by the equations $T(UV\text{-}A)_{366nm} = 0.85 \times e^{(-0.03 \times CR)} + 0.05$ ($R^2 = 0.95$); $T(UV\text{-}A)_{375nm} = 1.19 \times e^{(-0.02 \times CR)} + 0.004$ ($R^2 = 0.96$) (inset of Fig. 3.10).

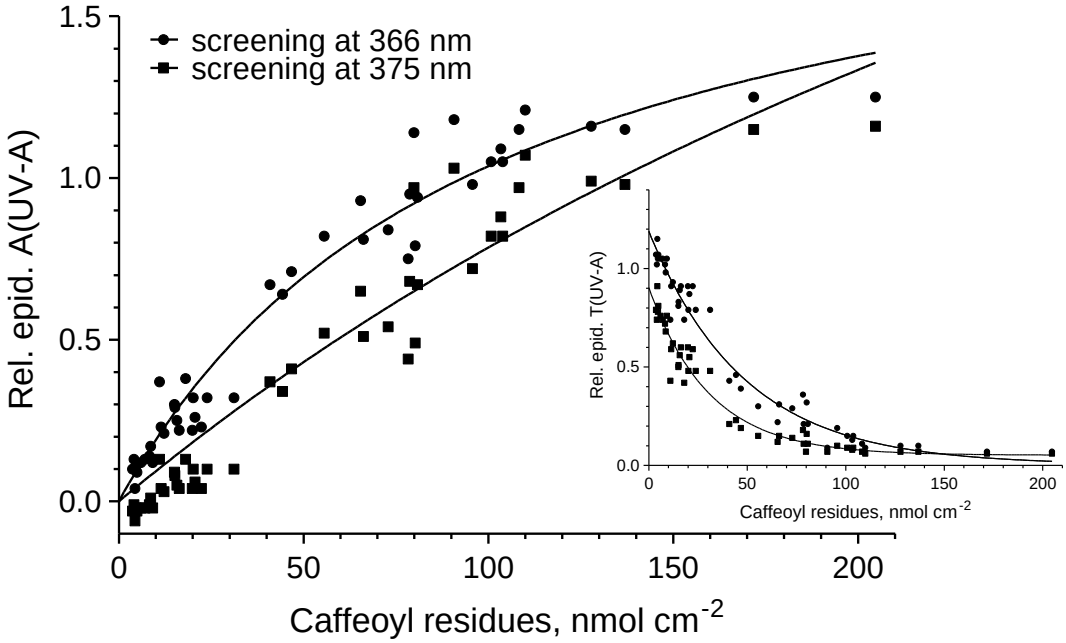

Figure 3.10 Relative epidermal UV-A absorbance and transmittance (inset) in dependence of the caffeoyl residue content

The caffeoyl residue content is referred to the area of the leaf samples (n = 47). Due to HPLC calibration with mono-CQA, each DCQA molecule corresponds to two caffeoyl residues. Regression of absorbance data was done with a modified Michaelis-Menten equation and transmittance data was fitted with an exponential function (one phase decay). Fit equations are: $A(UV\text{-}A)_{366} = 2.05 \times CR / (97.82 + CR)$ ($R^2 = 0.96$) and $A(UV\text{-}A)_{375} = 4.41 \times CR / (465.80\ CR)$ ($R^2 = 0.92$) and $T(UV\text{-}A)_{366nm} = 0.85 \times e^{(-0.03 \times CR)} + 0.05$ ($R^2 = 0.95$); $T(UV\text{-}A)_{375nm} = 1.19 \times e^{(-0.02 \times CR)} + 0.004$ ($R^2 = 0.96$). The graph is modified from Stelzner et al. (2019).

3.1.2.4 Analysis of UV screening efficacy *via* UV-A driven photoinhibition

Results presented in previous sections provided strong evidence for caffeoylquinic acids in sunflower leaves to contribute substantially to epidermal UV-A absorbance, thus, likely acting as UV screening pigments. In order to test whether and to what extent epidermal CQAs protect against UV-A driven photoinhibition, integrity of photosystem II (PS II) was determined in vivo. UV-A-driven photoinhibition is a complex process. The degree of the photoinhibition is determined by the amount of penetrating photons and its wavelength dependent potential (see Fig. 1.2) to damage PS II. The amount of the penetrating radiation is equal to the integrated product of the incident irradiance spectrum and the in vivo transmittance spectrum of a leaf, which is integrated over the UV range. The in vivo transmittance spectrum is affected by different physicochemical factors. For example, it is dependent on the concentration of UV screening compounds in the epidermis and the absorbance spectra of these compounds. The absorbance spectrum of the CQAs, which were extracted from sunflower leaves, is that of CQAs dissolved in aqueous methanol and likely differs from that when CQA is dissolved in the vacuole. The differences are caused on the one hand by e.g. different solvents and pH values and on the other hand by effects of leaf optical properties such as scattering effects. In order to analyse the UV screening efficacy of CQAs in vivo, three individual approaches for photo-inhibition by different sources of ultraviolet radiation were conducted with leaf discs, which differed in their CQA content.

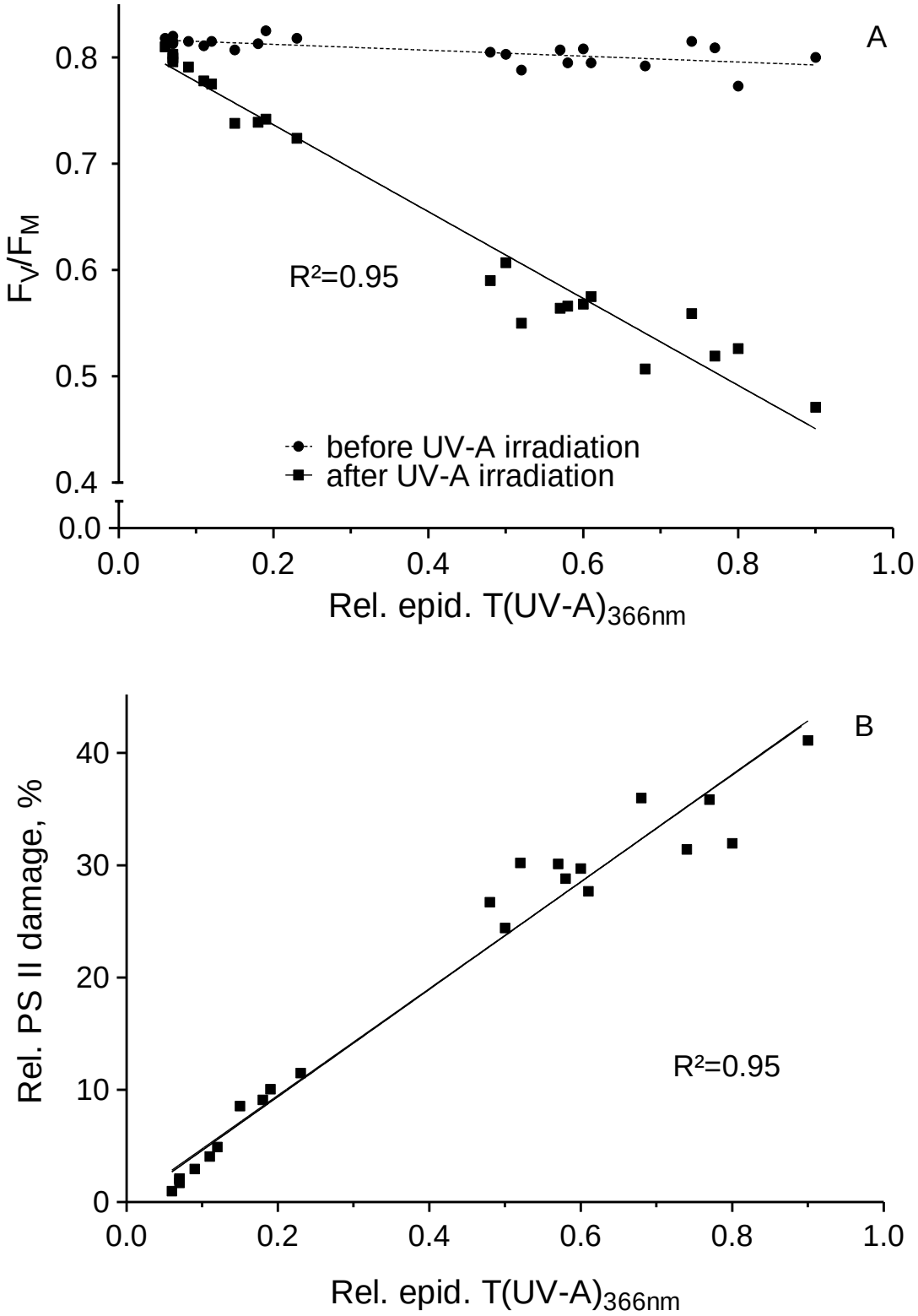

Figure 3.11 PS II integrity (A) and corresponding relative PS II damage (B) after UV-A driven photoinhibition F_V/F_M was determined in lincomycin-treated leaf discs before (circles) and after (squares) irradiation with an artificial UV-A source (n=24). Correlation between F_V/F_M of treated leaf discs was fitted by linear regressions (A: $\frac{F_V}{F_M} = 0.4084 \times \mathrm{T}(UV-A)_{366} + 0.8183$
B: $Rel.PS\ II\ damage = 47.53 \times \mathrm{T}(UV-A)_{366}$; R^2 = 0.95 for both). Relative PS II damage was calculated based on initial and final maximal quantum yield of identical leaf discs. The graph A is modified from Stelzner et al. (2019).

In a first experiment, the dependency between integrity of photosystem II and UV screening was examined using artificial broadband UV-A radiation. After irradiation with UV-A, maximal quantum yield (F_V/F_M) declined strongly dependent on the degree of UV-A screening in lincomycin-treated leaf discs. The linear correlation between F_V/F_M and UV-A transmittance was described by $F_V/F_M = 0.8183 - 0.4085 \times T(UV\text{-}A)$ ($R^2 = 0.95$) (Fig. 3.11A). PS II integrity in leaves with UV-A transmittances below 0.1 decreased by approximately 2 % whereas that in leaves with UV transmittances above 0.6 was reduced by up to 40 % (Fig. 3.11B). Incubation in lincomycin at low light conditions prior to UV-A irradiation yielded in a marginal tendency to decrease with increasing UV-A transmittance ($F_V/F_M = 0.8179 - 0.02778 \times T(UV\text{-}A)$ with a low degree of accuracy ($R^2 = 0.45$)) (Fig. 3.11A). This was nearly identical to leaf discs that were incubated at same light conditions in water ($F_V/F_M = 0.8205 - 0.02255 \times T(UV\text{-}A)$; $R^2 = 0.38$, data not shown).

The determination of the screening efficacy under artificial UV-A gave preliminary data clearly indicating a protective function against UV-A induced PS II damage. The UV-A fluorescence tubes used for photoinhibition emitted a different UV-A spectrum than the sun. In order to determine the screening efficiency under solar UV-A, photoinhibition was conducted outdoors. In the outdoor experiment, the degree of UV-A induced photoinhibition was determined in low and high light grown plants by exposure to filtered sunlight with either blocked ultraviolet radiation or including wavelengths from 330 – 385 nm (50 % cut-on or cut-off wavelength, respectively). Prior to the start of UV-A treatment, equal performance of photosystem II and comparable UV-A transmittance among the different treatment groups was verified. The maximal quantum yield (F_V/F_M) of dark-adapted leaf discs with inhibited D1 repair cycle was nearly identical with values at 0.80 for all treatment groups (Inset Fig. 3.12). Relative transmittance values of low light grown plants assigned to either UV-A or control treatment were at 1.01 ± 0.04 and 1.02 ± 0.04, respectively, and high light grown plants were characterised by comparatively high UV screening with UV-A transmittances at 0.24 ± 0.07 and 0.24 ± 0.14 (Fig. 3.12). After one hour of exposure to solar UV-A, the maximal quantum efficiency in leaf discs of low light grown plants was significantly reduced in contrast to leaf discs of high light grown plants (Figs. 3.13, S7.2). The corresponding relative damage of PS II in lincomycin treated leaf discs with high epidermal transmittance accounted to approximately 30 (± 2) % whereas leaf discs with low UV transmittance displayed damage at around 5 (± 5) % and differed significantly from each other ($p < 0.0001$). Upon exposure to filtered sunlight without UV-A, the relative damage amounted to 8 (± 1) % and 3 (± 2) % in low and high light grown plants, respectively (Fig. 3.13). It is assumed that the negligible proportion of PS II inactivation in control plants is caused by the treatment of leaves such as sampling with a cork borer.

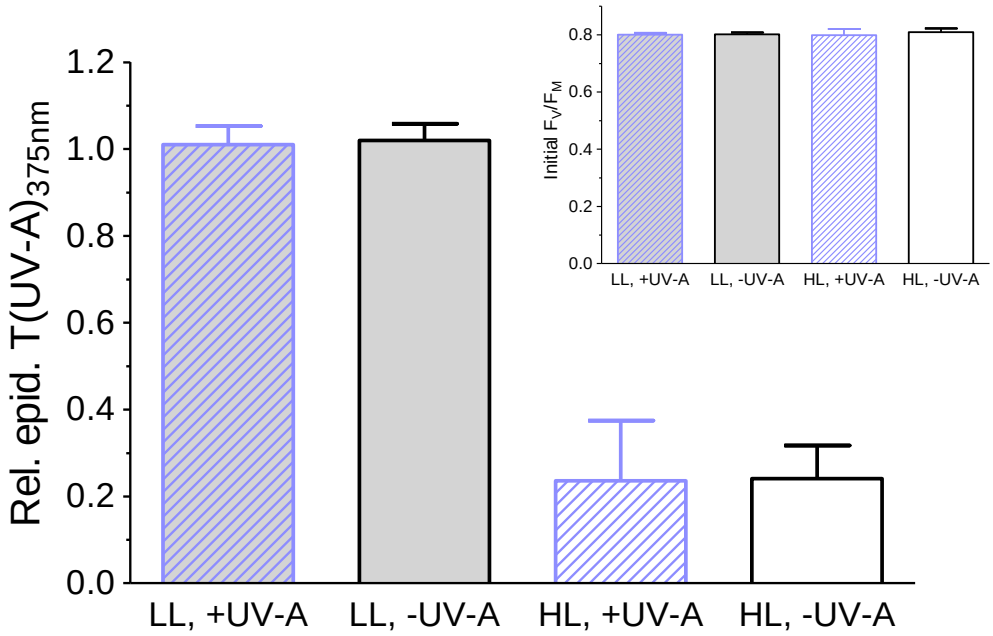

Figure 3.12 Physiological prerequisites of plants in a photoinhibition experiment with solar UV-A

Epidermal transmittance at 375 nm and maximal photochemical quantum yield (inset) was determined in leaf discs of low light (LL) or high light (HL) grown plants prior exposition to solar radiation containing UV-A (+UV-A, n=6) or not (−UV-A, control, n=3). Values are given as average with standard deviation (± SD). Analysis of statistical significance was conducted by comparison high and low light grown plants due to different sample number among the treatment groups.

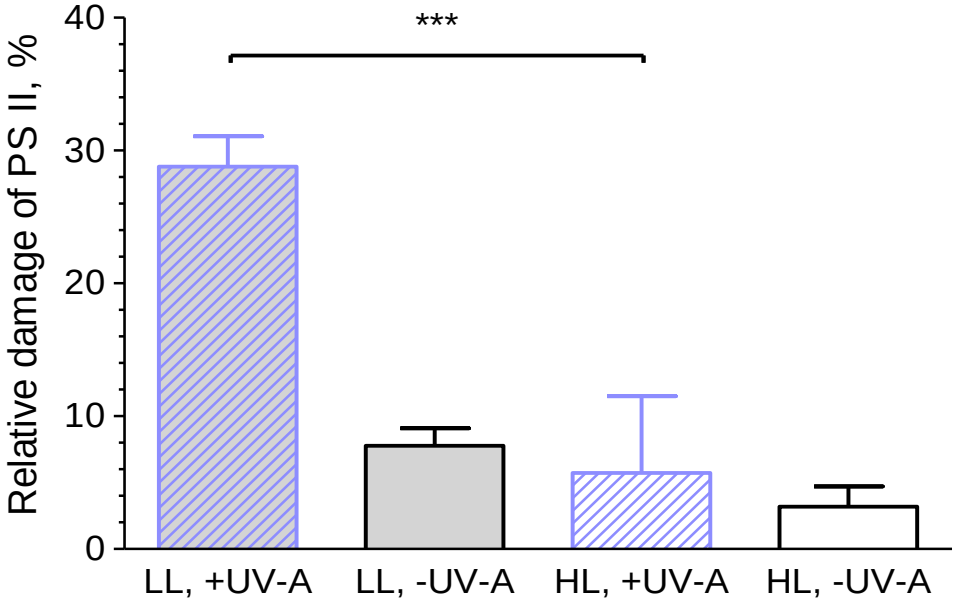

Figure 3.13 Relative damage of PS II of plants in a photoinhibition experiment with solar UV-A

Relative PS II damage after exposure to solar UV-A was calculated based on initial and final maximal quantum yield of identical leaf discs incubated with lincomycin (F_V/F_M, inset) for low (LL) and high light (HL) grown plants exposed to solar UV-A (+ UV-A, n = 6) or not (− UV-A, control, n = 3). Values are given as average with standard deviation (± SD). Analysis of statistical significance was conducted by comparison of high and low light grown plants exposed to UV-A by an unpaired t-test ($p < 0.0001$).

The significant reduction of UV-A induced photoinhibtion in high light grown plants as compared to plants, which were grown in low light, showed a UV-A protection provided by high epidermal CQA concentrations. According to the absorbance spectrum of extracted CQAs, wavelengths of the UV region are differentially attenuated at the epidermis (Fig. 3. 3A) and, thus, UV-induced PS II damage in vivo should differ among different wavebands. In a subsequent experiment, the aim was to obtain a spectrum of the CQA-dependent UV protection in vivo by comparing PS II damage in high and low light-grown plants. Photoinhibition was conducted at different UV wavebands using different filter combined to a Xenon lamp. Prior to UV treatment, the epidermal UV transmittance was determined via chlorophyll fluorescence excitation spectra in leaf discs.

High light grown plants displayed relative epidermal UV transmittance below 0.2 r.u. from wavelengths of 310 to 370 nm. Relative epidermal transmittance above 370 nm increased gradually to approximately 0.5 r.u. in those plants. The relative epidermal transmittance of low light grown plants was significantly higher throughout the wavelengths from 310 to 400 nm ($p < 0.001$). At the same time, the abscissas of the transmittance at 310 to 330 nm were shifted to approximately 0.5 r.u. and increased gradually from 340 to 400 nm to a value of approximately 0.9 r.u. (Fig. 3.14).

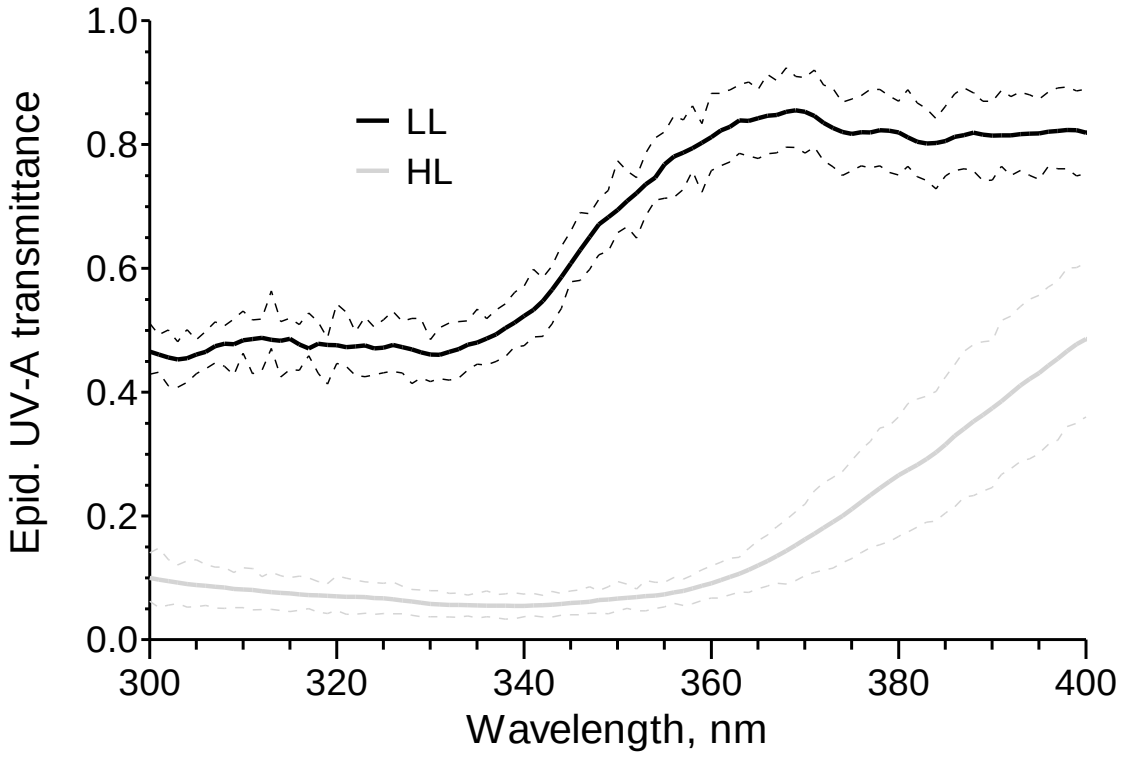

Figure 3.14 Epidermal UV transmittance spectra of high and low light grown sunflower leaves
Transmittance was calculated by referring excitation spectra of chlorophyll fluorescence for leaf discs of high light (HL, solid grey line; 250 µmol $m^{-}2$ s^{-1}) or low light (LL, dashed black line; 35 µmol $m^{-}2$ s^{-1}) grown plants to an excitation spectrum of isolated chloroplasts applied to a piece of filter paper. Excitation spectra of ten sunflower plants per growth condition were recorded in a fluorescence spectrophotometer detecting chlorophyll fluorescence at 720 nm through a 715 nm long pass filter. Solid lines represent the smoothened average of ten leaves ± the 95 % confidence interval that is displayed as dashed lines.

Photoinhibition treatment using the HPLC fluorescence detector involved different photon flux densities (PFD) in the corresponding UV region due to the lamp spectrum. In order to make the relative PS II damage comparable, it was referred to the PFD. After irradiation with monochromatic UV, the maximal quantum yield of PS II in high light grown leaves was especially at wavelengths below 350 nm substantially higher and decreased at radiation from 360 nm and above. F_V/F_M of low light grown plants was below 50 % of controls throughout the tested wavelength region (inset of Fig. 3.15). Statistical tests were not possible due to too low replicate number. Since the photon flux density of the different UV treatments differed (see Fig. 2.5), the damage of photosystem II was normalized to the amount of photons that accumulated during the treatment. The relative and normalized damage of PS II in low light grown plants increased in a non-linear manner with decreasing wavelengths. In contrast, the relative normalized PS II damage in high light grown plants accounted to for a small proportion of that in low light grown plants at UV wavelength below 380 nm. At 380 nm, the damage was similar to each other in high and low light grown plants (Fig. 3.15).

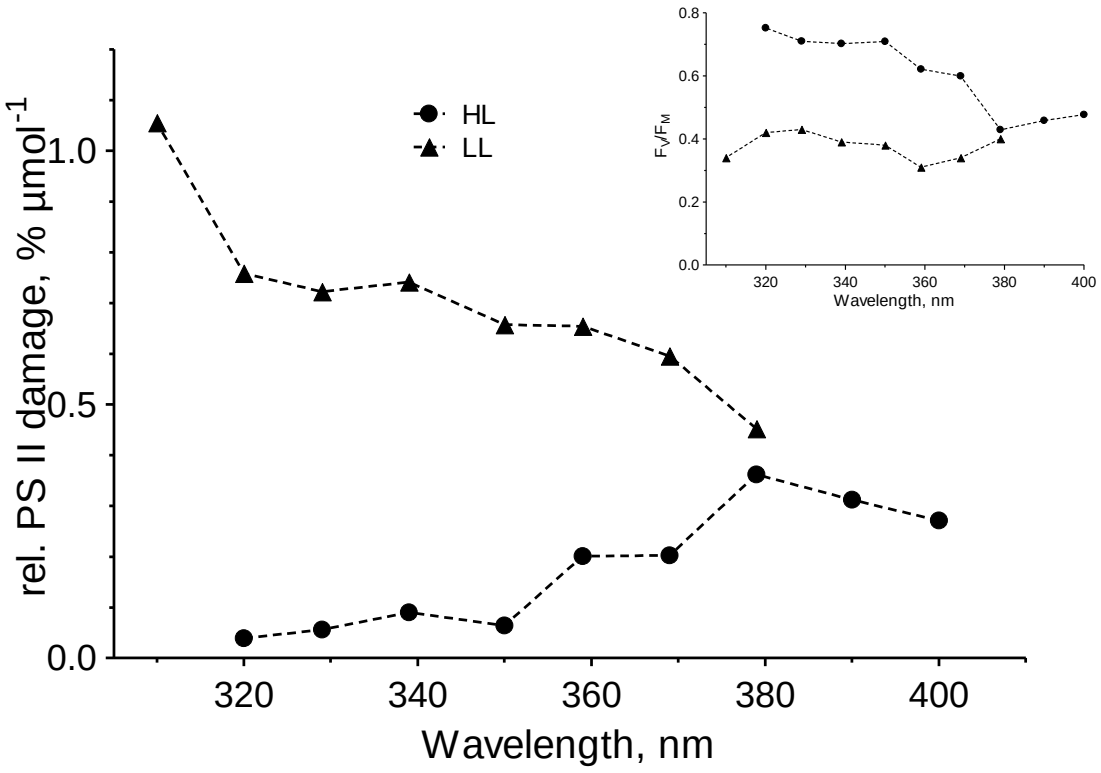

Figure 3.15 Preliminary data for relative damage of PS II in dependence of UV wavelength
Relative damage was calculated for high (HL, circles; 250 µmol m^{-2} s^{-1}) and low light (LL, triangle; 35 µmol m^{-2} s^{-1}) grown plants based on the maximal photochemical quantum yield of UV exposed leaf areas (inset) with non-irradiated areas of the same leaf disc serving as reference for intact PS II. The relative damage was normalized to the amount of photons per m^2, since PFDs differed between the treatments. Data points correspond to values of single leaf discs. No statistical analysis was possible due to low sample number. Photoinhibition treatment with low light leaves at 390 and 400 nm was not possible due to the injury of the epidermis caused by the sampling.

3.2 Induction of changes in foliar epidermal UV screening in sunflower by the abiotic environment

A further thematic section is presented in the following, in which focus of research was on the regulation of sunflower UV screening by different selected abiotic variables. The results presented in chapter 3.1 provide evidence that the caffeoylquinic acids in vegetative leaves of sunflower fulfil a UV screening function of which the degree was variable with changing growth irradiance of wavelengths above 400 nm. The dependence of CQA contents on photosynthetically active radiation suggests the PPFD to act as a regulatory variable as known for flavonoid accumulation. Other selected abiotic variables regulating flavonoid accumulation as well included UV, low temperature and nitrogen depletion. In order to test for the regulatory function of these variables, a set of different shifting experiments was conducted with three to four week old sunflower plants. UV absorbance as well as underlying pigment accumulation and transcription of one key enzyme of CQA biosynthesis was monitored on a short-term scale in one to three leaf generations of shifted and control plants.

3.2.1 Sunflower morphology

In order to facilitate comprehension which leaf generation served for analysis of regulation by abiotic factors presented in the following section, the morphology of four-week-old sunflower plants shall be briefly introduced.

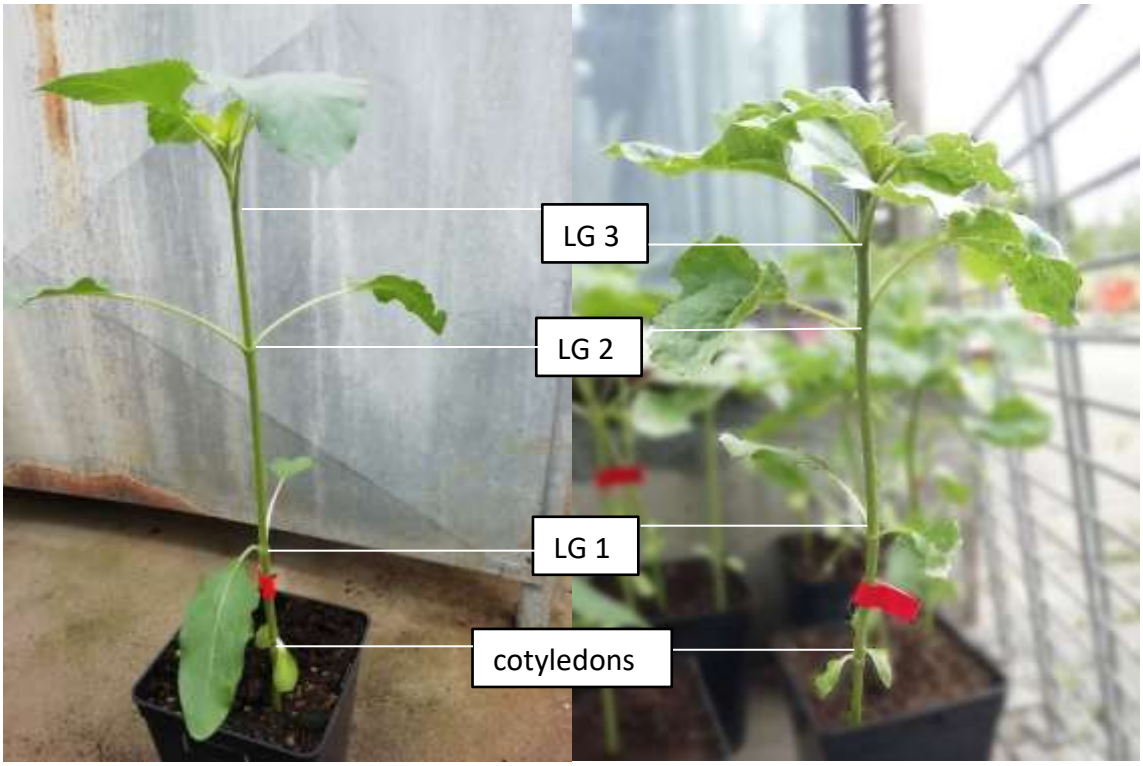

Figure 3.16 Habitus of sunflower plants four weeks after sowing (15/06/2022) and grown in a greenhouse (left) or outside (right) in the Botanical Garden at Kiel University under non-filtered solar radiation with an averaged PPFD of 210 µmol m^{-2} s^{-1} (outside). Lines mark the nodes with the first three consecutive generations of fully-grown leaves (LG) that grew seemingly in leaf pairs.

Sunflower plants were grown for four weeks at a moderate PPFD of 250 µmol m^{-2} s^{-1} with a natural day-night-rhythm and solar radiation filtered through glass. The four-week-old sunflower plants displayed an averaged shoot height of approximately 45 cm that was subdivided into a hypocotyl and four (sometimes five) internodes of unequal length that were shorter towards the top of the plants. The nodes of foliage leaves were at a height of approximately 17, 32, 40 and 43 cm above the soil with three consecutive generations of fully-grown leaves and one generation of growing or emerging leaves.

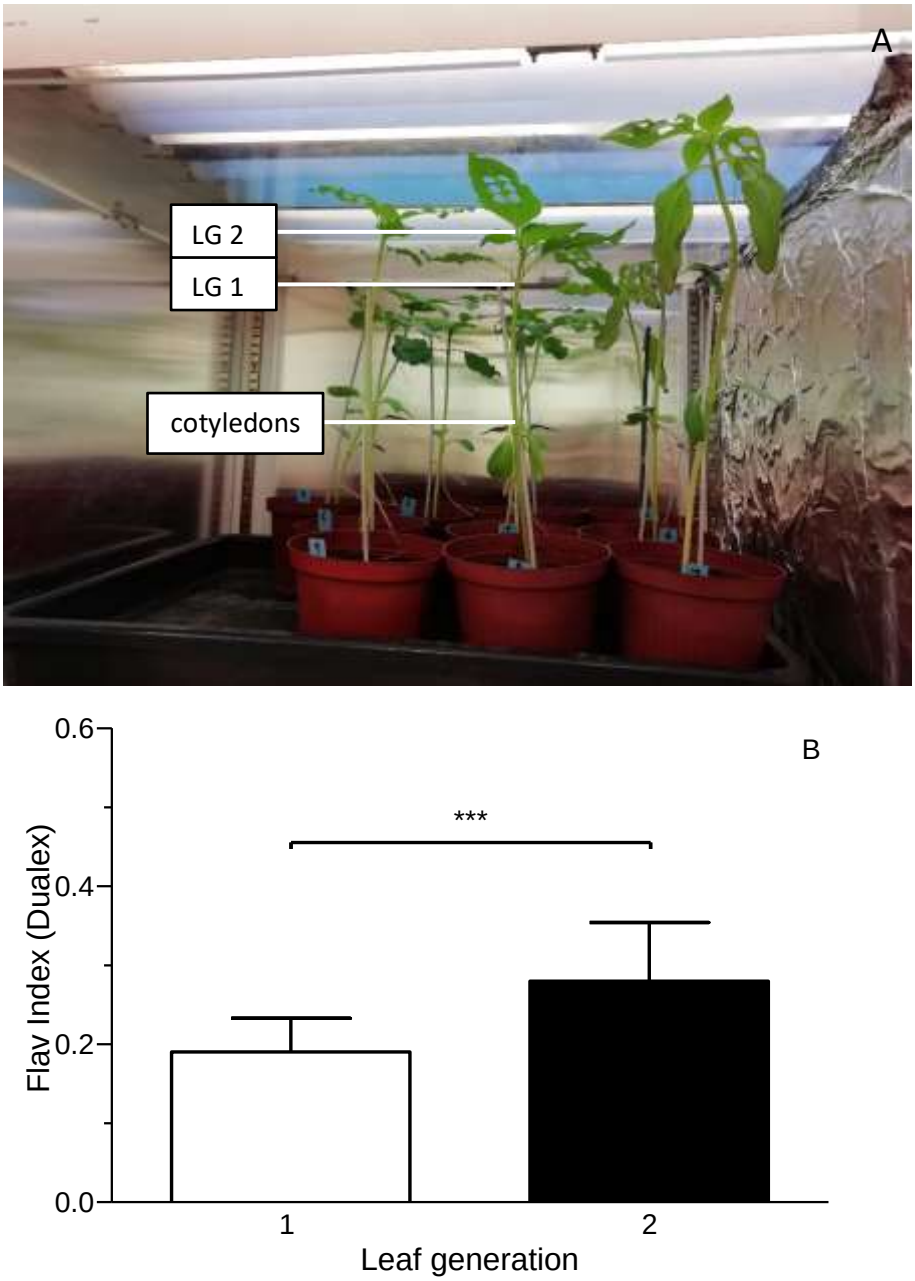

Figure 3.17 Habitus (A) and foliar epidermal absorbance (B) of sunflower plants three weeks after sowing and grown in growth cabinet a 16h/8h day/night rhythm for a shift experiment. Lines mark the cotyledons and nodes with the two consecutive generations of fully expanded leaves (LG 1 and 2) that grew seemingly in leaf pairs. LG 2 was sampled at six consecutive time points. The epidermal absorbance was measured in technical duplicates with a DUALEX device in 32 plants and is averaged for leaf generation 1 and 2 that grew at an average PPFD of 45 ± 11 µmol m^{-2} s^{-1} for both generations. Statistic differences are marked with asterisks (*** for $p < 0.0001$; Mann-Whitney-U-test).

The first three leaf generations will be numbered in the following with generation 1 corresponding to "oldest" and generation 3 corresponding to youngest outgrown leaves. Up to this generation, leaves grew apparently opposite-leaved whereas further leaf generations displayed an alternate, spiral leaf arrangement (Fig. 3.16). When plants grew in a cabinet under controlled climatic conditions with a fixed day/night rhythm of 16 versus 8 hours at a low PPFD of 45 ± 11 µmol m^{-2} s^{-1}, the habitus was slightly different but still comparable to plants grown in the greenhouse. The habitus of growth cabinet plants differed in a way that basal internodes were longer and plants of the same age possessed less leaf generations. The apparent opposite arrangement of leaves remained (Fig. 3.17A). After three weeks, plants possessed two generations of outgrown leaves with LG 1 corresponding to the leaves that had developed first (i.e. the oldest) and LG 2 being the latest developing corresponding to youngest leaves. In an identical set-up with different plants, the insertion height at the stem of both leaf generations was close enough to each other, so that they grew under almost the same irradiance of 45 µmol m^{-2} s^{-1} PPFD. Nevertheless, the epidermal absorbance differed significantly between both leaf generations with 0.2 ± 0.04 and 0.3 ± 0.07. In four-week old plants, one additional leaf generation (LG 3) had emerged.

3.2.2 Induction of changes in the epidermal UV absorbance

3.2.2.1 Induction by solar radiation

In a first attempt, the aim was to analyse the degree of UV screening in foliage leaves under natural conditions. In the following experiments, epidermal absorbance at 375 nm was measured with a DUALEX device, whose results correlated almost perfectly with a slope close to 1 (Flav index =1.01 × A(UV-A_{375}) – 0.054; R^2 = 0.99) to absorbance values converted from transmittance values at 375 nm obtained from UV-A/Mini-PAM fluorometer measurements (shown in section Material & Methods, Fig. 2.7). Thus, the so-called Flav index given by the Dualex device will be used equivalent to epidermal UV-A absorbance in the following sections. Sunflower plants were cultivated in a growth chamber at moderate PAR levels of 250 µmol m^{-2} s^{-1} without UV radiation until three generations of leaves had developed. At this stage, plants were transferred to the field site of the Botanical Garden of Kiel University, where PAR and UV radiation were present at naturally occurring ratios.

In those plants, initial epidermal UV-A absorbance varied with the leaf generation. Leaf generation (LG) 1 exhibited lowest absorbance values of 0.7 (± 0.3) relative units (r.u.) and highest absorbance values above 1.3 (± 0.2) relative units were found for generation 3. The second leaf generation displayed intermediate UV-A absorbance. The plants were transferred to the field site of the Botanical Garden of Kiel University in June 2019 in the morning. After exposition to field-conditions for 54 hours, epidermal UV-A absorbance had increased significantly ($p < 0.001$) in all leaf generations to 1.8 (± 0.1), 1.5 (± 0.1) and 1.3 (±0 .3) r.u., respectively (Fig. 3.18A).

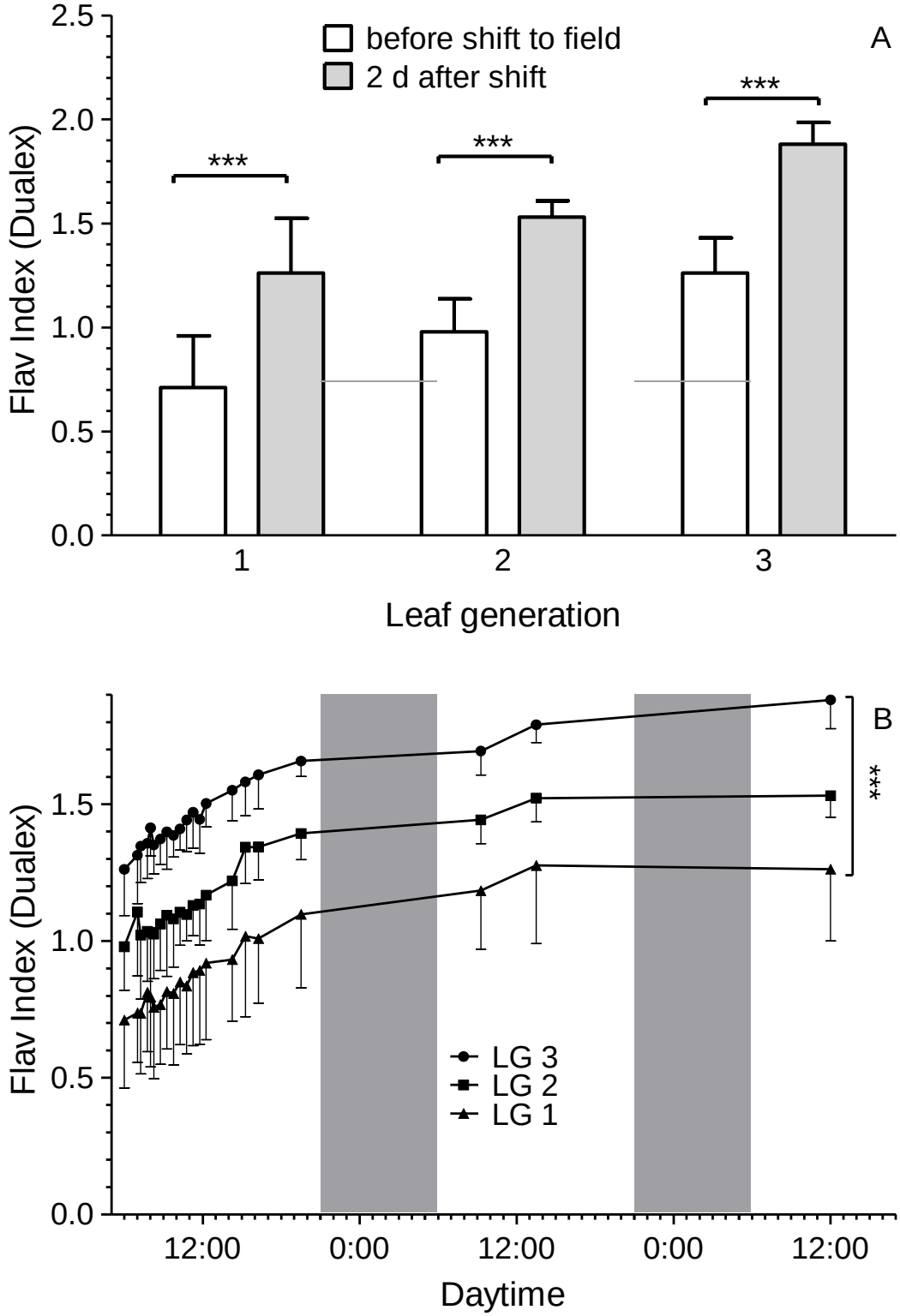

Figure 3.18 Epidermal UV-A screening at growth chamber and field conditions (A) and corresponding short-term response during acclimation to natural field conditions (B)

Initial and final epidermal UV-A absorbance of three consecutive leaf generations (LG 1,2 or 3) of five sunflower plants (n = 5) growing at 250 µmol m^{-2} s^{-1} PPFD without UV radiation (open bars) or 2 days after a shift to a field site of the Botanical Garden of the University Kiel in June 2019 (A). Corresponding short-term kinetic shows the time course of UV-A screening of the same leaves during the 2 days of acclimation with the night period (PPFD < 30 µmol m^{-2} s^{-1}) being marked as grey areas

(B). Statistically significant differences are marked with asterisks (*** for $p < 0.001$; Two-way ANOVA).

Epidermal absorbance increased immediately after the transfer to field conditions within one hour consistently for all leaf generations with a linear and apparently constant slope for the following 10 hours. The slopes of each leaf generation were nearly identical to each other with 0.0313 (LG 1), 0.0311 (LG 2) and 0.0307 (LG 3) h^{-1}. The slopes among the different types did not differ significantly whereas the absolute levels of absorbance did ($p < 0.0001$). In LG 1, the epidermal absorbance approximately doubled, whereas the epidermal absorbance in LG 2 and 3 increased to the 1.5-fold. In the afternoon, the rate of change decreased and during the second day, only minor increases were observed (Fig. 3.18B).

It was conceivable that epidermal absorbance could have been subject to a diurnal rhythm since solar irradiance and spectrum as important abiotic and regulatory parameters change over the day. If a potential diurnal rhythm was present, it could have interfered with and distorted the short-term response kinetic. Thus, in a subsequent approach, epidermal absorbance of field-acclimated plants (7 days of acclimation) was monitored in tight time intervals in the field. No statistically significant differences were observed over the time of monitoring but absorbance values differed significantly among the different insertion heights. Epidermal absorbance values of leaf generation 1, 2 and 3 − averaged over the time − varied slightly around at 1.36 (± 0.25), 1.76 (± 0.33) and 2.11 (± 0.07) r.u., respectively (Fig. 3.19).

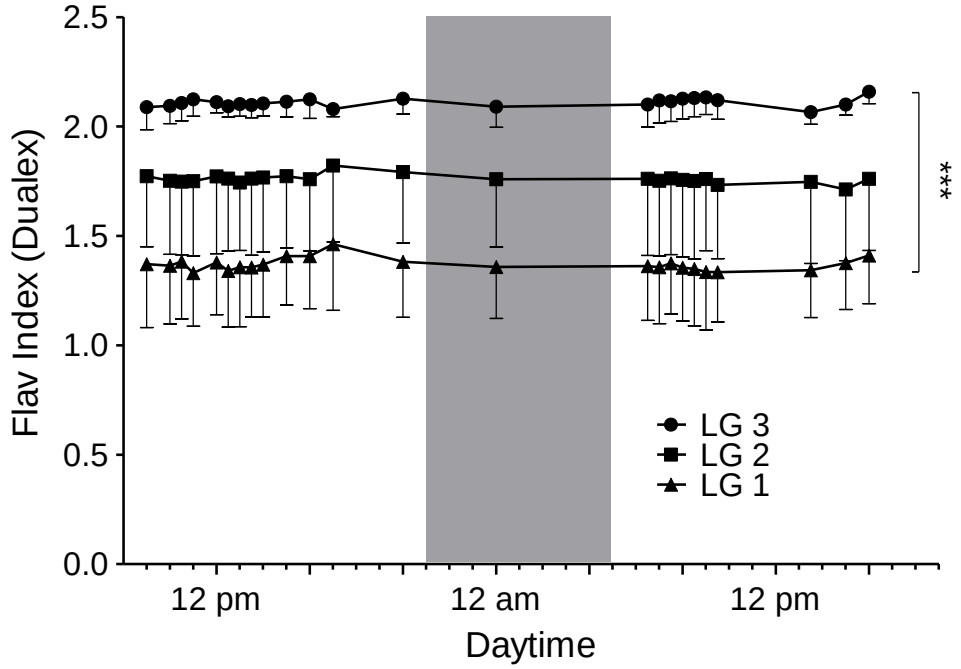

Figure 3.19 Diurnal course of epidermal UV-A screening in leaves of field-acclimated sunflower plants

UV-A absorbance of the consecutive leaf generations was monitored over 31 hours in the Botanical Garden (06/24/2019 to 06/25/2019). The night period (PPFD < 30 µmol m^{-2} s^{-1}) is marked by the grey area. Values are given as average of 5 different sunflower plants ± standard deviation. Statistical differences among leaf generation 1 and 3 were significant during the monitoring and are marked with asterisks (***; $p < 0.001$). Differences over the time or between other leaf generations (LG 1 vs. LG 2, LG 2 vs. LG 3) were tested to be non-significant using two-way ANOVA.

3.2.2.2 Induction by optical radiation, temperature and nitrogen availability

In the previous experiment, foliar epidermal UV absorbance was significantly increased under field conditions compared to the controlled climate indoors. This fact indicates the presence of one or more yet unspecified variables in the field that induce UV screening and that were absent in the growth chamber. Since the temperature was comparable in- and outside, no herbivory or pathogen attack was observed and water as well as nutrient availability was sufficient, likely solar radiation caused the changes in epidermal UV absorbance. One abiotic variable that differed between radiation in the growth chamber and at the field was the presence of UV radiation.

To test whether radiation from 280-400 nm is one abiotic parameter that induces enhanced epidermal UV absorbance in sunflower leaves, plants were cultivated under low PPFDs of 60 µmol m^{-2} s^{-1} without or with supplemental UV radiation at an irradiance of 1.6 W m^{-2} until they possessed three leaf generations. The low growth PPFD resulted in low to moderate UV absorbance with an average at 0.4 ± 0.1 r.u. in leaf generation 2. When plants grew under supplemental UV-B radiation, the epidermal absorbance of top leaves increased significantly to an average absorbance of 0.8 ± 0.2 r.u. ($p < 0.0005$; Fig. 3.20). The UV absorbance in both groups was distributed according to a Gaussian distribution without equal variances.

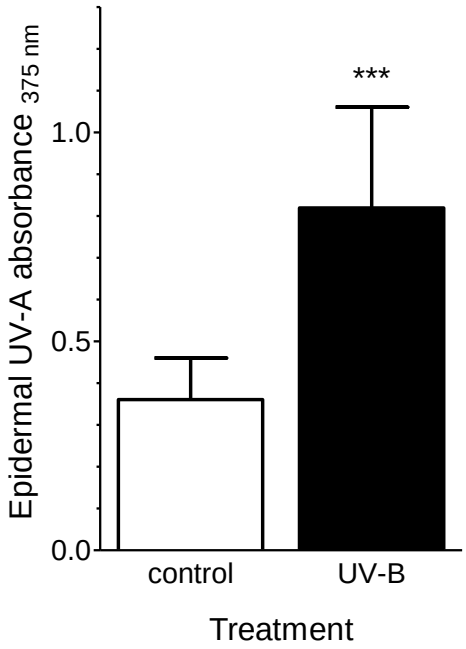

Figure 3.20 Effect of UV-B radiation on epidermal UV-A absorbance
UV absorbance was measured in leaves of generation 2 in four-week-old sunflower plants that grew at 60 µmol m^{-2} s^{-1} without (control, white bar) or with supplemental UV above 280 nm at an irradiance of 1.6 W m^{-2} (UV-B; 1.0 W m^{-2} UV-B + 0.6 W m^{-2} UV-A; black bar). Bars display the average of 10 plants ± standard deviation. Statistically significant differences are marked with asterisks for $p < 0.0001$ (Unpaired t-test with Welch's correction).

The presence of UV-B was clearly identified as a parameter increasing epidermal UV absorbance. However, the measurements were conducted after three weeks of growth at a time point when epidermal absorbance was at steady-state-conditions and differences between the control and treatment group were already significant. The leaves emerged during UV-B treatment and were too

small for measurements at early developmental stages so that the time course of the development of the UV screening capacity remained unknown in this attempt. Besides, the set-up did not allow defining a time point when the treatment started.

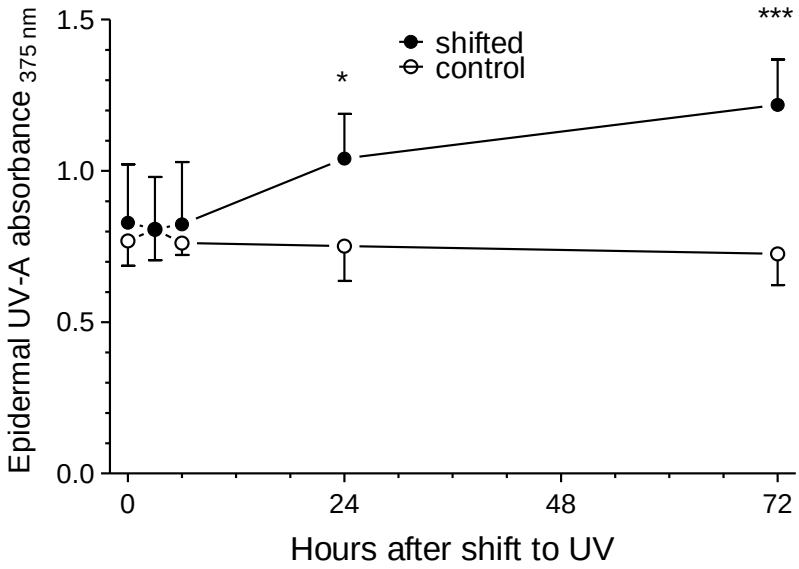

Figure 3.21 Response of epidermal UV-A screening in plants shifted to additional UV
Absorbance was measured in LG 2 of plants that were grown at 55 µmol m^{-2} s^{-1} PAR plus low UV (see chapter 2.2.1). After four weeks, plants were either exposed to additional UV-B (1.1 W m^{-2}) and UV-A (0.7 W m^{-2}) (filled circles) or to UV-A as a negative UV-B control (open circles; 0.8W m^{-2} UV-A). Values are the averages of 5 biological replicates that were measured twice (n = 5). Significant differences between the groups are marked with asterisks (***, $p < 0.001$ and *, $p < 0.01$).

Thus, a further experiment with a treatment and control group was necessary in order to analyse how sunflower plants respond to changes in UV-B levels. For monitoring the short-term kinetic of the UV-B response, both plant groups were grown at conditions with low PPFD at 55 (± 12) µmol m^{-2} s^{-1} and then exposed to the radiation of UV-B fluorescence tubes as described in material and methods (chapter 2.2.1). Initially, control and treatment group displayed moderate and comparable UV screening (0.79 (± 0.08) r.u. vs. 0.83 (± 0.19) r.u.). The minimal difference between the groups was tested as not significant using a Two-Way ANOVA. The partial induction of UV screening was likely caused by low UV doses emitted by non-filtered white fluorescent tubes, which were identical in both groups (0.05 (± 0.01) W m^{-2} UV-B and 0.3 (± 0.04) W m^{-2} UV-A).

When plants had three consecutive leaf generations, UV-B fluorescence tubes, which emit both UV-B and UV-A radiation, were turned on. UV-B fluorescence tubes emit both UV-B and UV-A radiation, of which the latter could not be excluded by a short pass filter without excluding the UV-B region. Thus, the effect in the treatment group could be caused by a combined effect of UV-B and UV-A radiation. In order to distinguish between the effect caused by UV-B from the effect of UV-B and UV-A, the control group was exposed to the UV-A part of the UV-B fluorescence tubes. The treatment group was exposed to 1.1 (± 0.03) W m^{-2} UV-B whereas the control group was exposed to less than a twentieth of the UV-B irradiance of the treatment group. The UV-A irradiance was comparable in both groups (0.9 (± 0.07) W m^{-2} for control vs 0.7 (± 0.02) W m^{-2} in treated plants). After the shift, UV screening remained stable for the first 12 hours and started to increase gradually between 12 and 24

hours after the shift to elevated UV-B in dependence of time. The response yielded in a significant difference 72 after the shift with absorbance values of 1.2 ± 0.2 r.u. ($p < 0.001$). In contrast, control plants had a final absorbance of 0.73 ± 0.1 r.u. and did not show any increment of the epidermal UV absorbance (Fig. 3.21). Whether UV-A would have caused an increased epidermal UV absorbance when plants displayed initially lower absorbance values remained open.

Further abiotic parameters such as different UV wavebands, high PPFD, low temperature and nitrogen availability were tested for their potential to induce UV absorbance (Fig. 3.22). All plants were grown in TKS 2 except for those used for the nitrogen depletion experiment; those were sown in Vermiculite and transferred to hydroponics containing 2 mM NH_4NO_3 when the cotyledons had emerged. In order to begin the time course analysis of epidermal absorbance in plants with non-induced UV screening, initial growth conditions were adjusted in a subsequent set of shift experiments to 50 µmol m^{-2} s^{-1} PAR with blocked ultraviolet radiation and 21 °C. When plants had three consecutive leaf generations, one abiotic parameter per treatment group was changed and LG 2 was used for analysis. The treatment groups were exposed either to UV-B and UV-A (0.05 + 1.1 W m^{-2}, respectively), shortwave UV-A (UV-A_{sw}, >320 nm; 0.5 W m^{-2}) or longwave UV-A (UV-A_{lw}, > 355 nm; 0.09 W m^{-2}), high PPFD (380 µmol m^{-2} s^{-1}), low temperature (9 °C) or nitrogen depletion (0 mM NH_4NO_3).

The initial epidermal UV absorbance was comparatively low in all shift experiments with a total average for all experiments of 0.35 ± 0.14 r.u.. The values ranged from 0.2 ± 0.001 r.u. (0 mM nitrogen, Fig. 3.22D) over 0.3 ± 0.1 (380 µmol m^{-2} s^{-1} PPFD, Fig. 3.22B) to 0.4 ± 0.03 r.u. (9 °C, Fig. 3.22C) and 0.4 ± 0.02 (different UV regions, Fig. 3.22A). Furthermore, a negative control group was introduced in order to test whether sampling or time would have interfering effects on the epidermal UV screening in plants that remain under unchanged initial conditions. Epidermal absorbance values of control groups varied marginally over the time with non-significant differences ($p<0.001$). Corresponding UV absorbance values remained relatively stable at low levels for control plants in all experiments with 0.4 ± 0.03 r.u. (Fig. 3.22A), 0.3 ± 0.1 (Fig. 3.22B), 0.4 ± 0.2 (Fig. 3.22C) and 0.2 ± 0.05 (Fig. 3.22D).

Growth at UV-B, cold and nitrogen deficiency results in smaller leaf areas compared to high light (Jansen et al. 2012; Rodriguez et al. 2015; de Ávila Silva et al. 2021). Thus, comparison of epidermal UV screening and corresponding CQA contents between treated and control plants might have not been fair due to differential growth and size of epidermal cells at the different treatments. If this were the case, it would have been conceivable that extracted CQA concentrations referred to the leaf area differ due to different ratios of CQA containing protoplasts and CQA-free cell walls in the epidermis. Thus, the response of the UV absorbance would have been underestimated in high light treated plants whereas that of plants exposed to UV-B, 9 °C or 0 mM NH_4NO_3 would have been overestimated. However, the leaf length between the different treatment and control groups did not differ from each other (data not shown). It is likely, that the leaf expansion was limited due to the low growth irradiance and the duration of the treatment was too short to cause differences in the growth rate.

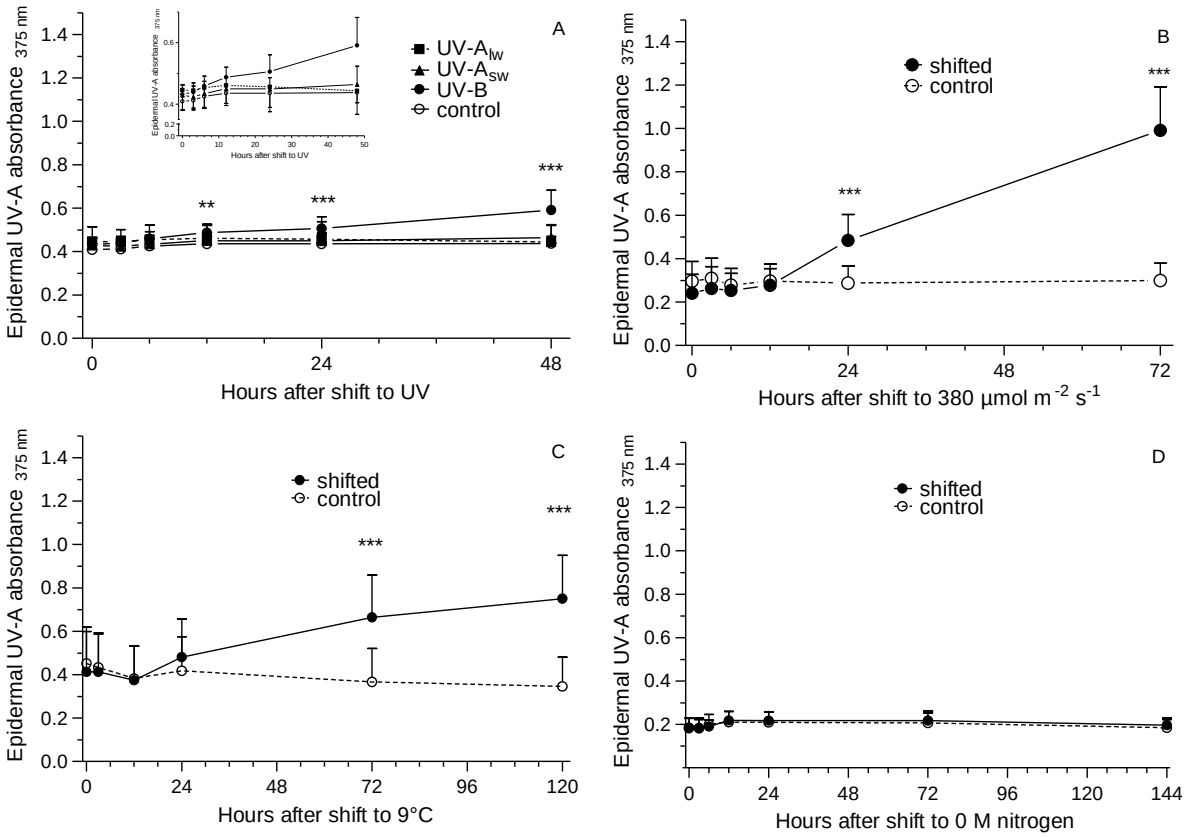

Figure 3.22 Response of epidermal UV-A absorbance in plants shifted to UV radiation (A), high PPFD (B), low temperature (C) and nitrogen deficiency (D)
Absorbance was measured in 2nd generation leaves of sunflower plants. Plants either remained under low PPFDs (control, open circles; 50 µmol m^{-2} s^{-1} PAR without UV, 21 °C) or were shifted to different UV wavelengths (A), high PPFD (B, filled circles: 380 µmol m^{-2} s^{-1}), low temperature (C, filled circles: 9 °C) or nitrogen depletion (D, filled circles: 0 mM nitrogen). UV treatment was either UV-B (filled circles: > 300 nm) shortwave UV-A (UV-A_{sw}; filled triangles: > 320 nm) or longwave UV-A (UV-A_{lw}; filled squares: > 355 nm). For the nitrogen depletion, plants were cultivated in hydroponics with 2 mM NH_4NO_3that was replaced by hydroponic solution with either 0 mM (shifted) or 2 mM NH_4NO_3 (control) after four weeks of growth. Data points display the averages ± standard deviation (n = 10, measured in technical duplicate). Significant differences between control and plants shifted to UV-B are marked with asterisks (A: ** for $p < 0.01$ and *** for $p < 0.001$). Significant differences between control and shifted plants are marked with asterisks (A, B, C: **, $p < 0.01$, ***, $p < 0.001$, Two-Way-ANOVA). No significant differences were found UV-A_{lw} and UV-A_{sw} and nitrogen depletion (A, D).

The shift experiment with further subclasses of UV treatments confirmed findings of the previous experiment with UV radiation. Similarly, the epidermal UV absorbance increased under UV-B with a maximal value of 0.6 ± 0.1 r.u. at the final time point of sampling (48 hours after the shift). In this set-up, the difference between control plants and those shifted to UV-B was significant from 12 hours on after the start of UV exposure. The epidermal UV absorbance remained comparatively stable when longwave UV-A (0.4 ± 0.1 r.u.) or shortwave UV-A (0.5 ± 0.1 r.u.) was applied. At any UV-A treatment, no significant differences in the UV absorbance relative to the control were observed ($p < 0.01$; Fig. 3.22A). Solely applied UV radiation did not result in a similarly large increase of absorbance values as observed in the field experiment (Figs. 3.17, 3.19, 3.22A). Thus, a further, additional abiotic

parameter must have caused the comparatively high absorbance values of approximately 1.5. The comparison between growth conditions in the climate chamber and in the field suggests the higher photon flux density of photosynthetically active radiation (PPFD) to play a crucial role in determining UV screening. Consequently, short-term changes of the epidermal UV absorbance in response to high PPFD were monitored in a further experiment. High PPFD was defined as 380 µmol m^{-2} s^{-1}. Leaves of generation 2 of shifted plants showed an epidermal absorbance that increased gradually from 0.3 ± 0.1 r.u. to 1.0 ± 0.2 r.u. after 72 hours. Epidermal absorbance was significantly higher for the first time 24 hours after the shift than that of control plants ($p < 0.001$) and the increase started between 12 and 24 hours after the transfer. In contrast, during the first 12 hours of the experiment, no noteworthy differences between control and shifted plants were observed (Fig. 3.22B).

Another abiotic environmental variable positively affecting UV screening in higher plants is the presence of low temperature (Bilger et al. 2007). Whether low temperature also affects epidermal absorbance in sunflower plants was tested in another shifting experiment. Unlike the response of epidermal UV absorbance to radiation, epidermal absorbance of shifted plants remained relative stable at initial values for 24 hours and increased subsequently in a gradual manner yielding in significantly higher values at 72 and 120 hours after transfer compared to control plants (0.7 ± 0.2 r.u. and 0.8 ± 0.2 r.u.; $p < 0.001$) (Fig. 3.22C). The slopes after the period of stable absorbance accounted for 0.012 r.u. per hour at high PPFD whereas absorbance increase with a rate of 0.0030 r.u. h^{-1} for UV-B and 0.0028 r.u. h^{-1} for low temperature.

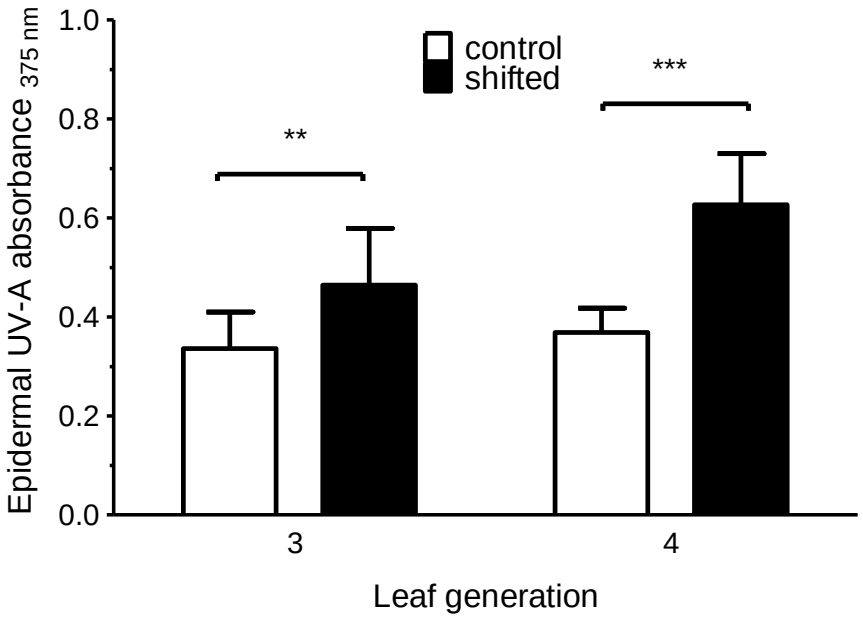

Figure 3.23 Follow-up measurement for the nitrogen shift experiment (Fig. 3.21D) after a change in growth irradiance in hydroponic culture

Absorbance was measured 120 hours after the PPFD was increased to 77 or 82 µmol m^{-2} s^{-1} in leaf generation 3 and 4, respectively, of plants that either remained under stable nitrogen conditions (white bars; 2 mM NH_4NO_3) or were shifted to 0 mM NH_4NO_3 (black bars). Values are the averages ± standard deviation of 10 sunflower plants (n=10). Significant differences between control and shifted plants are marked with asterisks (** for $p < 0.1$ and *** for $p < 0.001$, Two-Way-ANOVA).

The deficiency of nitrogen was a further abiotic parameter that was tested for a regulatory function on epidermal UV absorbance of sunflower leaves. For the treatment group, nitrogen availability was reduced to 0 mM NH_4NO_3 in a hydroponic solution. In contrast to the other experiments, absorbance of shifted plants displayed no change and remained nearly identical to that of the control with low UV absorbance values at an average of 0.2 (± 0.04) r.u., even when the duration of the experiment was prolonged compared to the other approaches (Fig. 3.22D). No statistical differences were found. In the following leaf generation (LG 3), which had emerged during the period of depletion, epidermal UV absorbance was slightly increased compared to the control at the final time point. No significant differences were found between control and shifted plants (data not shown; 0.2 ± 0.05 r.u. vs. 0.2 ± 0.04 r.u.; $p < 0.001$, unpaired t-test). In previous experiments with higher PPFD, UV absorbance of expanding leaves of consecutive generations gradually increased from 0.5 to 0.7 and from 0.7 to 1.0 after six days of depletion (Zink 2018). Although the absorbance in the work by Zink (2018) was determined using a device other than the DUALEX®, the values are approximately comparable. Accordingly, a different behaviour was observed for leaf generation 3 and 4 when the growth irradiance was subsequently increased to approximately 80 µmol m^{-2} s^{-1}. In LG 3, the epidermal UV absorbance was significantly increased in plants shifted to nitrogen deficiency compared to control plants (0.5 ± 0.1 r.u. vs. 0.3 ± 0.1 r.u.). This pattern was even more emphasized in LG 4 that displayed 0.6 ± 0.1 r.u. for shifted and 0.4 ± 0.1 r.u. for control plants (Fig. 3.23).

3.2.3 Induction of changes in the phenylpropanoid content

3.2.3.1 Induction of changes in the phenylpropanoid content by UV, PAR and temperature

The contribution of the predominant HCAs to the epidermal UV-A absorbance has been shown previously and it was also observed for sunflower plants in shift experiments (Figs. 3.4, 3.9, S7.3). Consequently, the kinetic of pigments detected in HPLC analyses AU s at 330 nm should have coincided with that of the epidermal UV absorbance. In order to test whether increasing foliar CQA contents are concomitant with increasing epidermal absorbance, aqueous methanolic leaf extracts were analysed by HPLC. For the analysis, plants that had responded with increasing epidermal UV absorbance values upon a shift in one abiotic parameter were selected. Thus, the analysis was done in the same leaf discs of plants that had been exposed to either elevated PPFD or elevated UV radiation or to low temperature (corresponding to Figs. 3.21, 3.22B, C). Chromatograms and peak areas ($\int\sum AU\ s_{330nm}$) were evaluated at 330 nm, the wavelengths of maximal absorbance for CQAs, for an optimal resolution of the variability of the CQA content. Each chromatogram displayed the three characteristic main peaks at nearly identical retention times as found previously (Fig. 3.1). The caffeoylquinic acids CGA and DCQA were thus hypothesized as main phenylpropanoid components of sunflower leaves. For identification of CQAs and search for further phenylpropanoids that might have been synthesized in response to the shift, chromatograms and corresponding UV spectra of leaf extracts from plants harvested at the beginning and the end of the experiments were compared to each other. Representative chromatograms for the initial and final time point of sampling were

chosen. Those chromatograms displayed $\sum AUs_{330nm}$ closest to the average of ten individuals. The retention times of peaks in representative chromatograms of all treatment groups, initial and final were identical to each other with 12.7 (peak 1), 19.6 (peak 2) and 20.5 (peak 3) minutes (Figs. 3.24A, B). At the beginning of the shift experiments, respective areas of the different peaks were in the same order of magnitude for control and treatment groups (Fig. 3.24A, Table 3.1). At the end of the experiments, the control groups displayed comparable peak areas as well, whereas that of shifted plants displayed remarkable increases (Fig. 3.24B, Table 3.1).

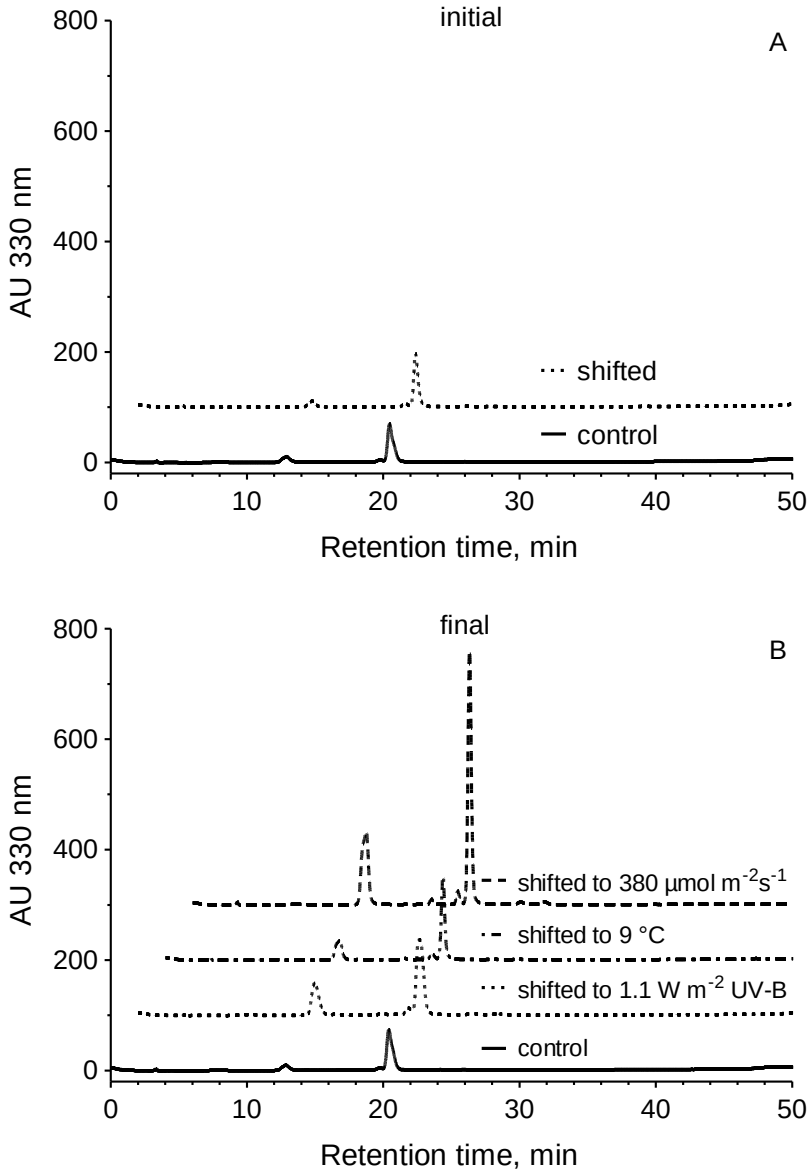

Figure 3.24 Representative UV-DAD chromatograms of aqueous methanolic extracts from leaves sampled at the beginning (A) and the end (B) of selected shift experiments

The samples for HPLC analysis were collected in the same experiments in which epidermal UV absorbance increased as a response to a shift in an abiotic variable (Figs. 3.21A, B, C). Control (solid line) sunflower plants remained at 50 µmol m^{-2} s^{-1} PPFD and 21 °C and treatment group plants (dashed lines) were shifted to either 380 µmol m^{-2} s^{-1} PPFD (dashed line), to 9 °C (dot-dashed line) or to 1.1 W m^{-2} UV-B (dotted line). Initial (0 h) and control chromatograms display the averages of the three shift experiments. Final chromatograms correspond to plants sampled at 72 h after the shift for control, UV-B and PPFD and 120 h after shift to 9 °C. For the sake of clarity, chromatograms are shifted by multiples of 100 AU and 2 minutes.

Table 3.1 Representative peak areas (∫AU(s)) of identified (CGA and DCQA) and other phenylpropanoids

		Extracted phenylpropanoids					
		CGA		DCQA		Other peaks	
		Control	Shifted	Control	Shifted	Control	Shifted
Initial ∫AU(s)	UV-B*	390	500	2800	3300	5	68
	PPFD	250	270	1400	1400	32	4
	LT	550	370	2200	2400	52	52
Final ∫AU(s)	UV-B*	380	2200	3000	5400	24	80
	PPFD	220	4580	1800	8900	81	506
	LT	460	1200	2000	3100	11	110

Initial ∫AU(s) correspond to plants sampled prior to a shift in UV-B, PPFD or temperature (Fig. 3.23A) and final ∫AU(s) correspond to plants sampled at 72 h after the shift for control, UV-B and PPFD and 120 h after shift to 9 °C (Fig. 3.23B). Peaks at 19.7 and 20.6 minutes are summarised due to identical molecular formula (previously confirmed by MS).*In the UV-B shift experiment, the control was exposed to 0.9 W m^{-2} UV-A radiation and did not remain at initial conditions as in the other shift experiments.

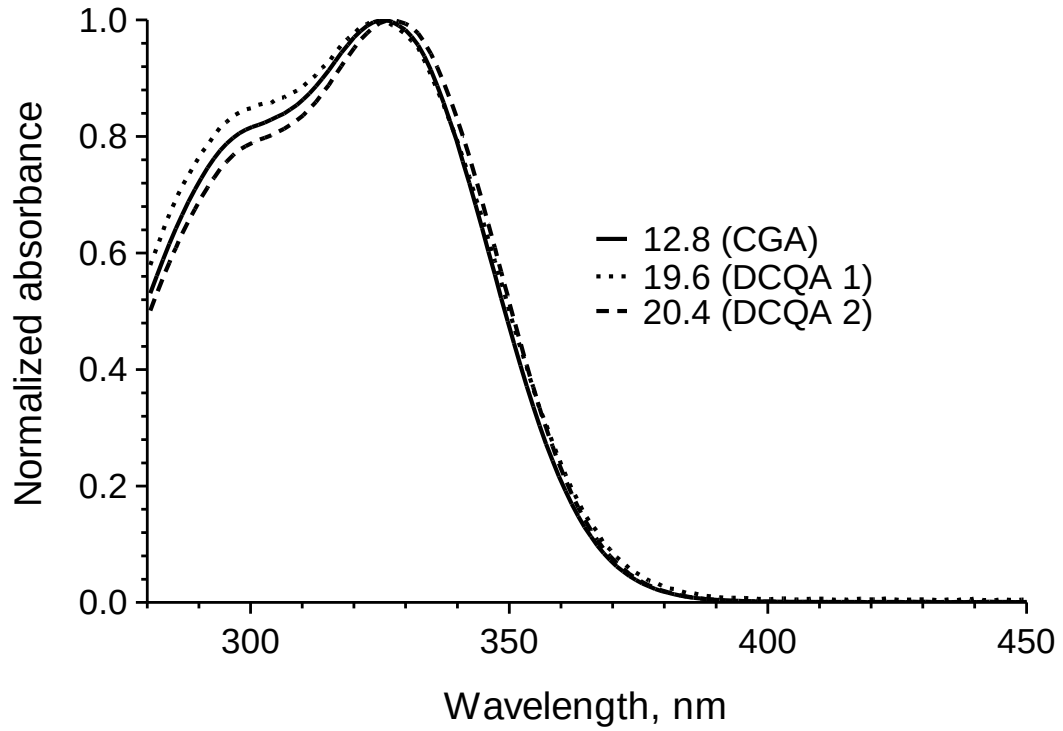

Fig. 3.25 Normalized UV absorbance spectra of prominent and identified phenylpropanoids extracted from leaves exposed in shift experiments
The leaf material was harvested at the final time point (72 or 120 h) of the shift experiment and UV absorbance spectra were averaged of one sample each from the different shift experiments.

Since leaves harvested at the final time point displayed the highest content of phenylpropanoids, those chromatograms were used in order to check whether compounds were identical to the ones previously identified by mass spectrometry. Consistently, the compounds corresponding to the

dominant peaks displayed nearly congruent UV absorbance spectra with a maximal extinction near 330 nm and a shoulder at 290 nm characteristic for CQAs and particularly chlorogenic acid (CGA) (Figs. 3.2, 3.25). According to the retention time of a HPLC chlorogenic acid standard (Fig. 3.1, inset) and in accordance with HPLC data presented in chapter 3.1, peak 1 was assigned to chlorogenic acid and the two other dominant peaks (2 + 3) were identified both as isomers di-caffeoylquinic acids. Hence, both isomers are summarised in the following data. The relative content of CGA and DCQA amounted to at least 95% of total HCAs among the individual samples and treatments confirming both as main components in sunflower leaves. This predominance was observed at any time point of the analysis.

Consistent with the time courses of the epidermal UV absorbance, HPLC-DAD analysis confirmed the hypothesis of significantly increasing total concentrations of caffeoylquinic acids in response to exposure to UV-B radiation, high PPFD or low temperature based on UV chromatograms at 330 nm (Fig. 3.26). The peak areas reflecting the summarized HCA content remained stable for a factor-specific period and then increased with differential rates that accounted for 200 AU s h^{-1} at high PPFD whereas that for UV-B and low temperature were in a smaller order of magnitude with 45 AU s h^{-1} and 16 AU s h^{-1}, respectively (Fig. 3.26). The shift to 1.1 W m^{-2} UV-B caused significantly increased total peak areas compared to plants exposed solely to UV-A ($p < 0.001$) after 72 hours. After six hours of UV-B exposure, the sum of peak areas started to increase gradually with a noticeable but non-significant difference between the treatment and the control groups 24 hours after the shift (Fig. 3.26A).

As observed for the epidermal UV absorbance, a shift to high PPFD yielded in a somewhat different time course. Within the first 12 hours, $\sum AUs_{330nm}$ remained on comparable levels in both shifted and control group. The subsequent gradual increase of peak areas at 330 nm was shifted to a time slot between 12 and 24 hours. Peak areas were significantly higher in shifted plants compared to the control after 24 and 48 hours, respectively (Fig. 3.26B).

For plants shifted to 9 °C, the significant difference relative to control plants was observable later than in the PPFD shifting experiment (Fig. 3.26C). 72 and 120 hours after the shift, total peak areas were significantly higher compared to the control plants ($p < 0.01$ and $p < 0.001$, respectively; Fig. 3.26C). Although in a lower order of magnitude than in the PPFD experiment, the difference between control and the group at low temperature became apparent for the first time 24 hours after the plants had been shifted. An intermediate decline of peak areas, 12 hours after the shift to 9°C was tested to be not significant (Fig. 3.26C). Besides, stable and comparatively low epidermal UV absorbance values in the absence of UV-B, high PPFD or low temperature were congruent with constant and low CQA concentrations in all experiments. Exposure to UV-A radiation alone resulted in stable peak areas, which reflect the generally higher level of epidermal UV absorbance compared to the other negative control groups (Figs. 3.26A, B, C). Besides, initial peak areas of respective treatment plants were in a comparable order of magnitude and corresponded to the descending order of initial epidermal UV absorbance (0.8 vs 0.4 vs 0.3).

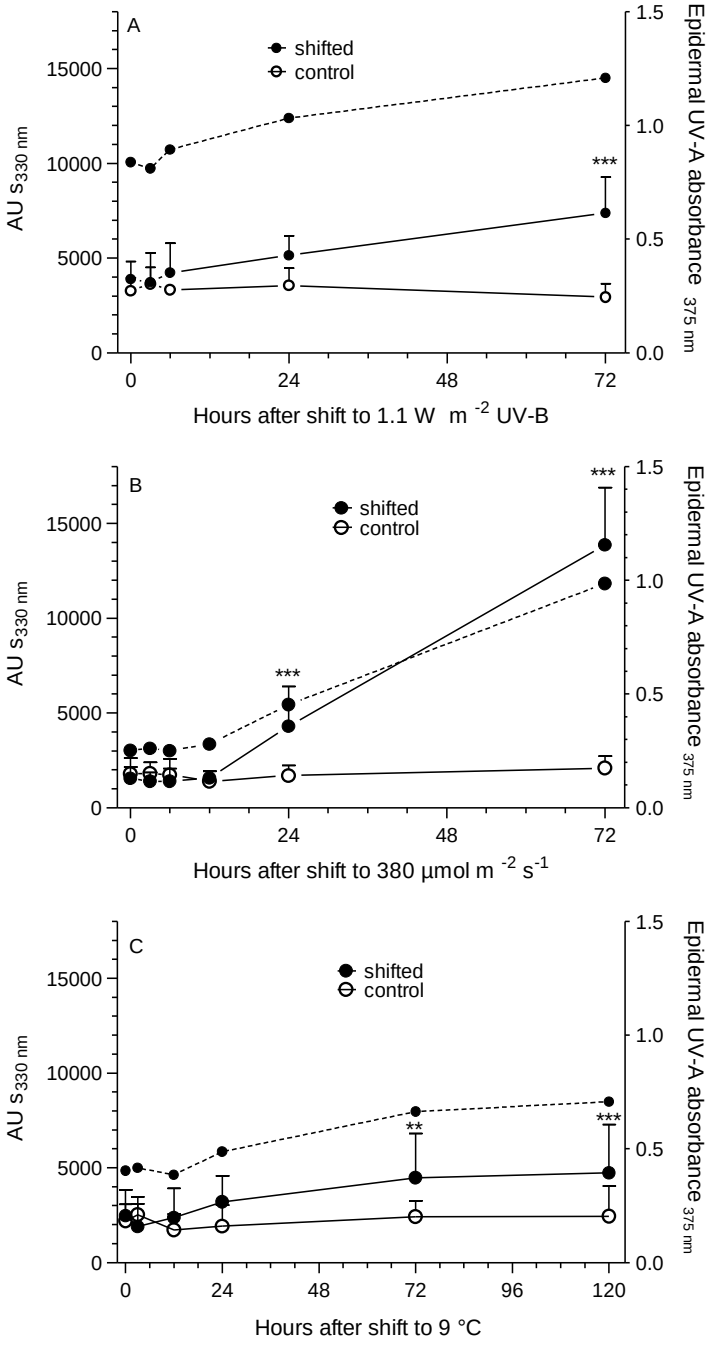

Figure 3.26 Time courses of total peak area at 330 nm of leaf extracts (solid lines) and of epidermal absorbance (dashed lines) in experiments in which plants were shifted to enhanced UV-B radiation (A), increased PPFD (B) and to low temperature (C)

Samples were collected for HPLC analysis in the same experiments shown in Figs 3.21 and 3.22B, C. Control (open circles) sunflower plants remained at 50 µmol m^{-2} s^{-1} PPFD and 21 °C (A, B, C). The negative control of the UV-B experiment was exposed to the UV-A spectrum of UV-B fluorescence tubes (A) and treatment group plants (closed circles) were shifted either to 1.1 W m^{-2} UV-B (A), 380 µmol m^{-2} s^{-1} PPFD (B) or to 9 °C (C). Total peak areas of UV-DAD chromatograms are displayed on the left y-axis. Data points represent means of five (A) or eight to ten (B, C) sunflower plants with standard deviation. Due to loss of samples during the temperature experiment or analysis, the sample number was reduced to five or six for data points representing treated plants 72 hours after the shift and control plants at time point 3 and 120 hours after the shift started. Significant differences between treatment groups are marked with asterisks (** for $p < 0.01$ and ***for $p < 0.001$; Two-Way-ANOVA).

The increase of phenylpropanoid concentration in treated plants (Fig. 3.26) summarizes the three HCA components not taking into account that they changed independently of each other. When plants continued growth at initial conditions or were transferred to UV-A, all components remained stable (Figs. 3.27A–F).

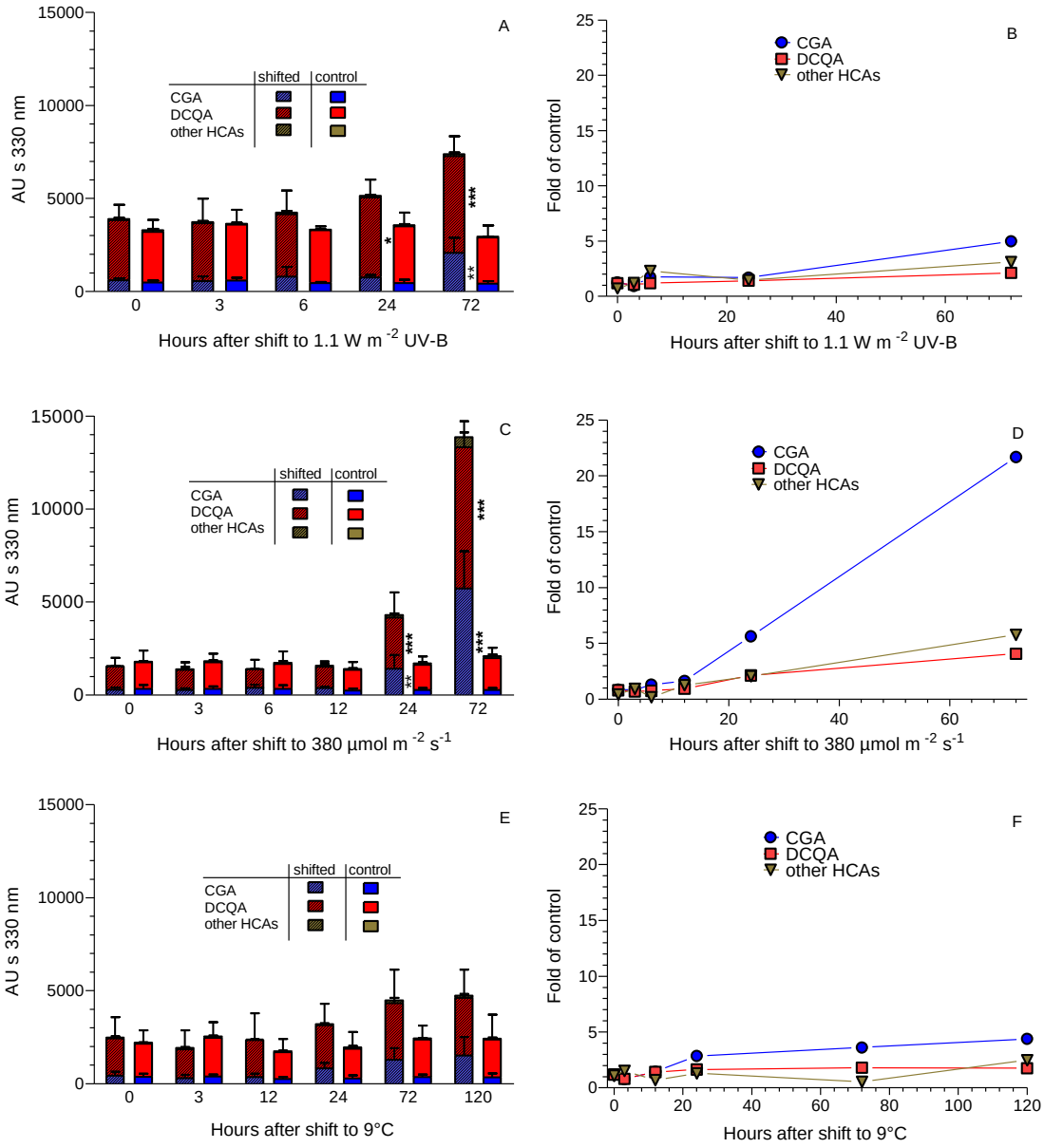

Figure 3.27 Peak area at 330 nm and time course of control-related contents of identified compounds

Compound-specific AU s of mono-CQA (blue), di-CQA (red) and yet unidentified, other HCAs (brown) for the negative control (plane bars, 50 µmol m^{-2} s^{-1} PPFD, 21 °C) and plants shifted to either, 1.1 W m^{-2} UV-B (A; hatched bars), 380 µmol m^{-2} s^{-1} PPFD, or to 9 °C (B, C; hatched bars). Analysis was done in either five (A, B) or eight to ten (C–F) individual sunflowers. Due to loss of samples during the temperature experiment or analysis, the sample number was reduced to five or six for data points representing treated plants 72 hours after the shift and control plants at time point 3 and 120 hours after the shift started. Significant differences between treatment groups are marked with asterisks (*** for $p < 0.001$; ** for $p < 0.01$ and * for $p < 0.05$; TWO-Way-ANOVA). Control-related content of CGA (circles), DCQA (squares) and yet unidentified HCAs (triangles) was not analysed statistically since the calculations are average-based.

With the exception of CGA in the UV-B treated plants, significant higher peak areas were found from 24 hours on after the shifts to UV-B radiation and PPFD for the identified CQAs (Figs. 3.27A, C). After 72 hours of the respective change in radiation, the pool size of CGA accounted to the 5- and 20-fold of that of the reference plants (Figs. 3.27B, D). The dramatic increase of CGA upon high PPFD exposure was consistent with the steep increase in UV absorbance of epidermis and extracted leaves. In general, the multiplication of CGA concentrations compared to reference plants was more emphasized than for DCQA throughout the shift experiments. The latter varied between the 2- and 4-fold and yet unidentified HCAs had increased maximally to the 2- to 6-fold at final harvesting time points (Figs. 3.27B, D, F). Although total HCAs had increased significantly upon treatment with 9 °C and CGA concentrations were 4 times higher than in control plants, the compound-specific increment was not significant (Figs. 3.27E, F).

As a logical consequence, the differential increase of the identified CQAs resulted in a shift in the ratio of CGA and DCQA in treated plants. The ratio of negative control plants did not change significantly. In contrast, plants shifted to either UV-B, high PPFD or low temperature, CGA/DCQA increased in a significant manner to values between 0.40 and 0.76. The shift to high PPFDs resulted as observed for the other parameters in most remarkable and early alterations (Tab. 3.2).

Table 3.2 CGA/DCQA ratios of sunflower leaves at different time points of sampling in the shift experiments

Treatment (n)	CGA/DCQA						
	0 h	**3 h**	**6 h**	**12 h**	**24 h**	**72 h**	**120 h**
Control (7-25)	0.22 (± 0.09)	0.22 (± 0.05)	0.22 (± 0.06)	0.22 (± 0.06)	0.19 (± 0.05)	0.18 (± 0.06)	0.18 (± 0.11)
1.8 W m^{-2} UV-B (5)	0.22 (± 0.05)	0.20 (± 0.07)	0.26 (± 0.15)	--	0.18 (± 0.05)	0.40** (± 0.12)	--
380 µmol m^{-2} s^{-1} (8-10)	0.23 (± 0.05)	0.26 (± 0.05)	0.40*** (± 0.10)	0.37*** (± 0.10)	0.51*** (± 0.15)	0.76*** (± 0.25)	--
9 °C (8-10)	0.21 (± 0.07)	0.21 (± 0.06)	--	0.30 (± 0.11)	0.28*** (± 0.20)	0.44*** (± 0.16)	0.43* (± 0.21)

Values display the means ± standard deviations of the sample number (n) given in brackets in the first column. Mean values were calculated for control plants from the UV, PPFD and temperature shift experiments together. Statistically significant differences were compared to the negative control using a Two-Way ANOVA and are marked with asterisks *** for $p < 0.000$, ** for $p < 0.01$ and * for $p < 0.05$. UV-B shifted plants were compared to plants grown at low UV-A

Areas of other minor peaks increased in leaves of shifted plants harvested at the final time point (Table 3.1, Fig. 3.24). Chromatograms of plants shifted to a high PPFD showed up to seven further small peaks at retention times of 15.8, 16.6, 17.6, 22.6, 24.2, 25.9 and 37.0 minutes with HCA resembling UV absorbance (Figs. 3.28A, S7.4). The highest relative proportions of ∑AU s_{330nm} accounted for 1.1 % (peak 17.6 and 25.9 min) and 0.9 % (24.2 min) (Fig. 3.24). Similarly, eight further tentative phenylpropanoids with small peak areas of maximal 2 % each of total AU s in plants treated for 72 hours with 9 °C were observed at retention times of 14.5, 17.6, 22.6, 23.6, 24.2, 25.9, 37.0, 43.3 minutes (Figs. 3.28, S7.4). Of those, the peaks at 14.5, 17.6 and 25.9 minutes displayed the largest peak areas with 0.5, 1.7 and 2 % of ∑AU s_{330nm}. The relative proportion of the other peaks was

below 0.5 % of total peak area at 330 nm. At the final time point, chromatograms for leaf extracts of plants shifted to elevated UV-B showed up to five further minor peaks with a total relative proportion of 3.4 % of ∑AU s_{330nm} at retention times of 14.5, 17.6, 18.7, 24.2, 25.9 minutes. The areas of peaks at 14.5, 17.6 and 24.2 minutes were equal to 0.8, 1.0 and 1.3 % of ∑AU s_{330nm}. For all further small peaks, an exact identification was not possible and the compounds were tentatively classified based on their UV absorbance spectra. The bulk of the small peaks displayed UV absorbance spectra with a characteristic shape for caffeic acid derivatives except for the peak at 14.5 minutes. This latter peak corresponded to a compound with a maximal extinction at 310 nm (Fig. 3.28A). Two additional peaks with a maximal extinction above 330 nm occurred sporadically in low temperature (peak at 23.6 minutes) or UV-B (peak at 46.5 minutes) treated samples (Fig. 3.28B). With maximal absorbance at 350 nm and 365 nm, respectively, the absorbance spectra of these two peaks resembled those of flavonoids (Fig. 3.28B), but the compounds could not be further identified. The corresponding peak areas were less than 0.5 % and 1.5 % of total absorbance at 360 nm (∑AUs_{360nm}; Fig. S7.5).

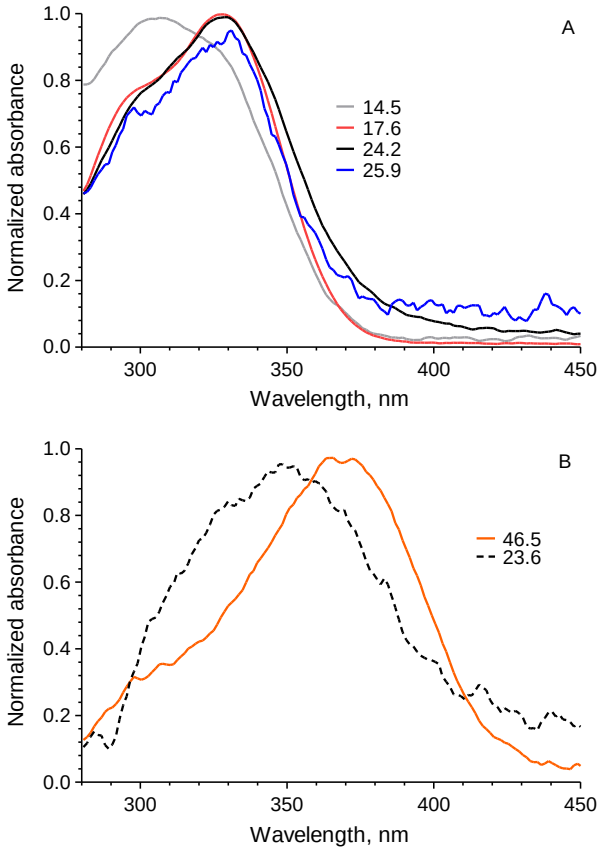

Figure 3.28 Normalized online absorbance spectra of low abundant phenylpropanoids with $\lambda_{max} \leq 330nm$ (A) or $\lambda_{max} > 330$ nm (B) obtained from shift experiments
The leaf material was harvested at the final time point (72 h or 120 h after the shift) of the shift experiment. UV absorbance spectra were smoothened afterwards. Peaks with HCA-resembling UV absorbance at retention times of 14.5 (A, grey line), 17.6 (A, red line), 24.2 (A, black line) and 25.9 (A, blue line) minutes were present in samples shifted to 380 µmol m^{-2} s^{-1}, 9°C and 1.1 W m^{-2} UV-B. The peak that ran at 14.5 minutes (A, dotted line) was present in plants shifted to low temperature and UV-B. Peaks with flavonoid-like UV absorbance spectra were present in low temperature (B, 23.6 min; dashed line) and UV-B (B, 46.5 min, orange line) treated plants.

3.2.3.2 Compounds detected by HPLC in leaves grown under solar radiation

The work of Hoier (2012) provided preliminary results indicating that flavonoids remain absent in sunflower leaves under abiotic stress conditions, but further experiments were needed. In sunflower plants grown under laboratory conditions or exposed to one abiotic stress factor, flavonoids were only found in trace amounts in leaf extracts.

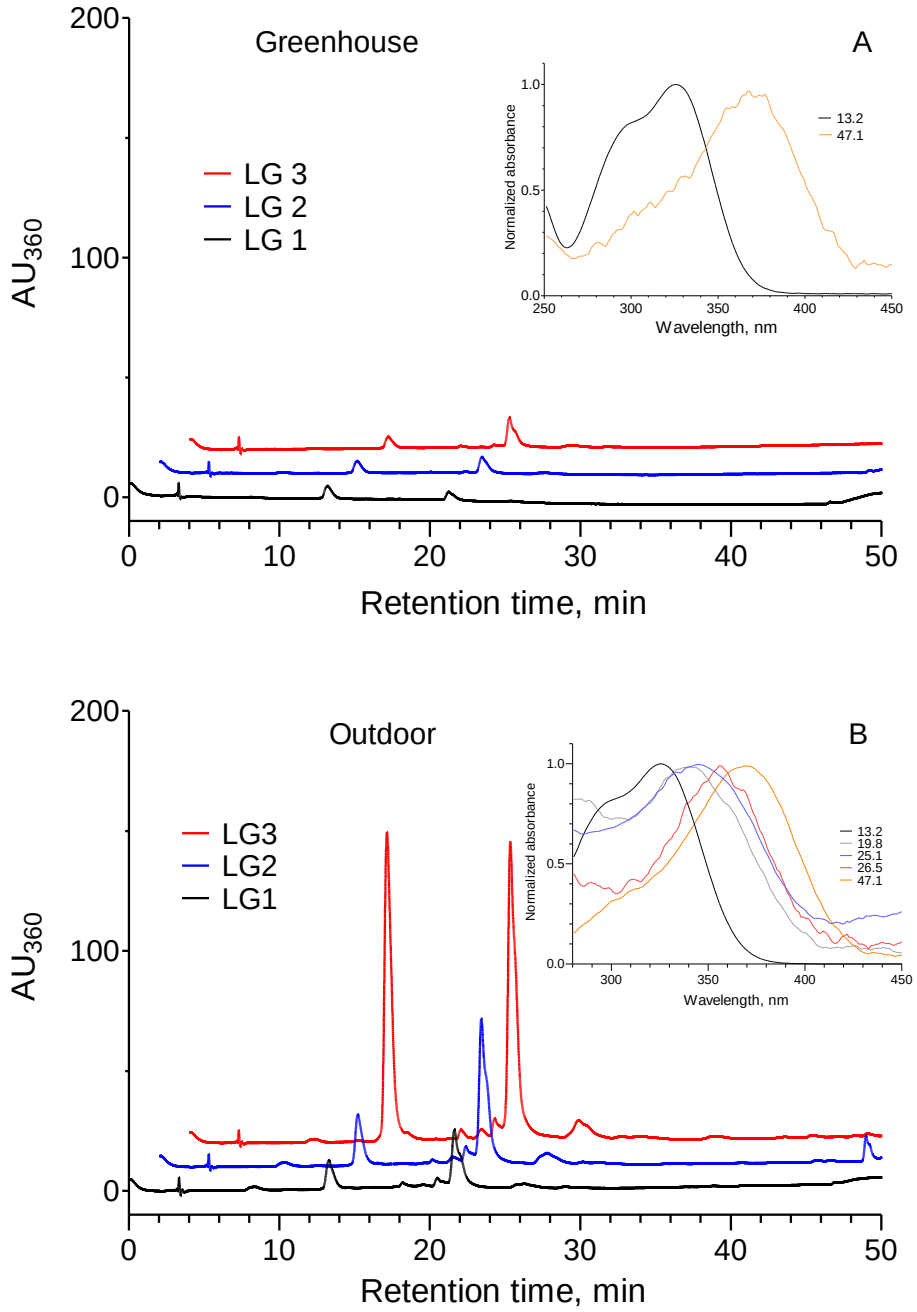

Figure 3.29 HPLC-DAD chromatograms at 360 nm of leaf extracts of greenhouse or outdoor grown sunflower plants. The three leaf generations (black, red and blue line for LG 1 to LG 3) were analyzed from plants either grown in the greenhouse (A) or grown outdoors (B). For HPLC analysis, plants with highest values of UV screening were selected (A: 0.7, 0.9 and 1.2 for LG 1 to 3 and B: 1.5, 2.0 and 2.2 for LG 1 to 3).The insets show the absorbance spectra characteristic for CQA (black solid line) or the different additional peaks with a maximal extinction above 340 nm. Absorbance was normalized to the maximal value and smoothened afterwards.

Based on previous experiments, it remained open, whether flavonoids could accumulate in higher concentrations under more natural conditions with various external stress parameters. In order to search for potentially higher flavonoid contents, two groups of five sunflower plants each were grown either under greenhouse conditions or outside in unfiltered solar radiation during a sunny period in summer (06/15/2022 – 07/18/2022) for five weeks. The averaged epidermal absorbance of leaf generations 1-3 in ascending order of indoor plants was at 0.6 (± 0.0), 0.7 (± 0.1) and 1.0 (± 0.1) and for outdoor grown plants at 1.5 (± 0.3), 1.9 (± 0.3) and 2.0 (± 0.2). The aqueous methanolic leaf extracts were analysed via HPLC-DAD. Plants grown in the greenhouse and grown outside displayed the three characteristic dominant peaks corresponding to CGA and DCQA in leaf generation 1 to 3 also at 360 nm (Fig. 3.29).

Nevertheless, in both plant groups, in total four different compounds with maximal extinction above 340 nm and marginal peak areas were found. The corresponding retention times were 19.7, 25.0, 26.5 or 47.1 minutes. However, the presence of those compounds varied between the different samples so that only one to three out of those four peaks were found per sample in outdoor grown plants. On average, the proportion of summarized peak absorbance accounted to 0.4 (± 0.5) % in LG 1, 6 (± 3) % in LG 2 and 6 (± 3) % in LG 3 of the total absorbance at 360 nm. In sunflower plants grown in the greenhouse, only one additional peak was found only in leaf generations 2 and 3. The peak at 47.1 minutes made up a proportion of approximately 1.5 % of the total absorbance at 360 nm for both leaf generation 2 and 3.

3.2.4 Induction of changes in the gene expression of one key enzyme for chlorogenic acid biosynthesis

It was proposed that the enhanced accumulation of CQAs in sunflower plants, confirmed by phytochemical analysis, was preceded by an activation of CQA biosynthesis. Hydroxycinnamoyl-CoA quinate transferase (HQT) plays a key role in chlorogenic acid biosynthesis that in turn is likely essential for formation of DCQA as well. In order to test whether transcription of *HQT* is upregulated transiently, mRNA levels of the three genes of sunflower hydroxycinnamoyl-CoA quinate transferase (*HQT1–3*) were analysed for identical plants used for determination of epidermal absorbance and phytochemical analysis.

In a first attempt, sunflower plants with a moderately induced CQA biosynthesis (Fig. 3.26A, 3.27A) due to low background UV-B emitted by white light fluorescence tubes were shifted to 1.1 W m^{-2} UV-B. In general, the amount of mRNA of *HQT* accounted to for a small proportion relative to the reference genes *ACT7* and *EiF5A* in control and treatment plants. *HQT1* displayed $2^{-\Delta\Delta CT}$ of 0.07 ± 0.03 r.u., *HQT2* of 0.5 ± 0.2 r.u. and *HQT3* of 0.07 ± 0.07 r.u.. The alterations of the relative transcript levels caused by UV-B appeared so marginal and within the scattering of biological variation, so that tendencies are only potential and have to be interpreted carefully. The differences of plants shifted to UV-B and control plants were tested statistically to be non-significant at any time point of sampling.

However, averaged transcript levels of all three genes in control plants exposed to UV-A were initially at comparable transcript levels. The Initial levels in shifted to UV-B were comparable or slightly lower

(Figs. 3.30A–C). 72 hours after the shift to 1.1 W m^{-2} UV-B, transcript levels of *HQT1* to *HQT3* showed a similar trend to increase marginally to approximately the 1.5-fold (Figs. 3.30A–C). The mRNA levels of all three *HQT* genes in negative control plants exposed to UV-A were stable throughout the experiment (Fig. 3.30C).

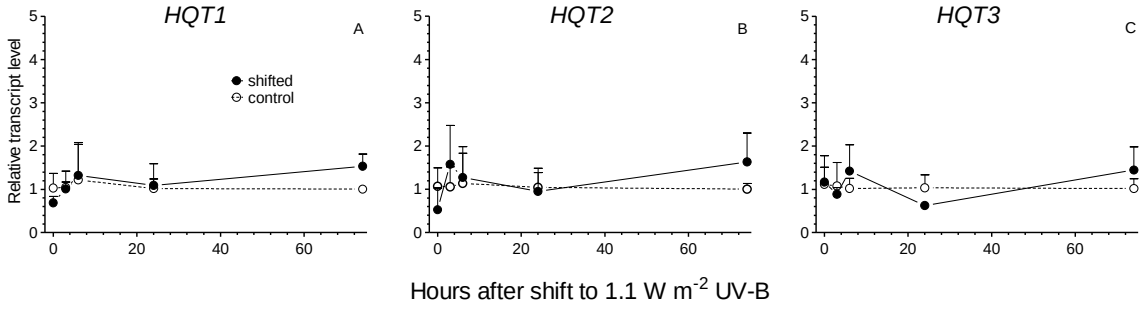

Figure 3.30 Short-term kinetics of relative transcript levels of *HQT1* (A), *HQT2* (B), and *HQT3* (C) in a UV shift experiment
Relative transcript levels ($2^{-\Delta\Delta Ct}$) of the three identified sunflower hydroxycinnamoyl CoA quinate transferase (*HQT*) genes in plants grown at 55 µmol m^{-2} s^{-1} PAR and 0.4 ±0.1 W m^{-2} supplemental UV-B and shifted to UV-A (open circles) or plants that were shifted to 1.1 (± 0.03) W m^{-2} UV-B radiation (filled circles). UV-A irradiance accounted to 0.9 (± 0.07) W m^{-2} in the control and 0.7 (± 0.02) W m^{-2} in shifted plants. Each data point corresponds to the averaged differences of three biological replicates measured in technical duplicates (n = 3). No significant differences between the treatment and control group were found using Two-Way-ANOVA.

Although the epidermal absorbance and CQA content increased in plants shifted to 1.1 W m^{-2} UV-B, no noteworthy alterations in the HQT gene expression were observed. Since the plants displayed a partially induced CQA biosynthesis (Fig. 3.26A, 3.27A), it was hypothesized that the transcriptional upregulation would have been observable in plants with little CQA biosynthesis. When plants with low initial epidermal absorbance were exposed to 1.2 W m^{-2} UV-B, the plants died. Thus, the UV-B shift experiment was repeated with a lower UV-B dose of 0.05 W m^{-2}. The UV-B shift experiment was part for a set of analysis, in which the *HQT* transcript levels of plants shifted to high PPFD or low temperature were analysed in addition in plants with low initial epidermal absorbance below 0.4 r.u.. The relative expression of the HQT genes was a small proportion of that of the reference genes *ACT7* and *EiF5A.* It was about the half of that in the other UV shift experiments with sunflower plants, which were already partially induced before the exposition to 1.1 W m^{-2} UV-B started. In the control plants of all experiments, *HQT2* displayed highest relative gene expression ($2^{-\Delta CT}$) of 0.2 ± 0.1 followed by *HQT1* (0.042 ± 0.01). Expression of *HQT3* in contrast was weakest compared to the reference genes with 0.03 ± 0.02.
For plants shifted to UV-B, high PPFD or low temperature, the short-term response of *HQT* transcript levels was incongruent among the three genes and characterised by relatively strong biological variation at single time points. However, the trend of the time courses, i.e. whether expression was up- or downregulated was identical in all biological replicates of the respective shift experiments.
In the UV-B shift experiment, *HQT2* was the only isoform with significant transcriptional upregulation to the 15-fold (± 16.4; $p < 0.001$; Fig. 3.31B) in plants that have been shifted to 0.05 W m^{-2} UV-B.

Although the mRNA levels increased in all biological replicates, the biological variation was high. The upregulation was gradual and transient until six hours after the shift and then levels decreased gradually approximately to the initial value. A slight transient upregulation of relative *HQT1* gene expression started later to maximally the 3-fold (± 2.5) after 24 hours (Fig. 3.31A). The moderate increase was followed by a subsequent decline. *HQT3* in shifted plants, in contrast, displayed low relative gene expression comparable to control plants with values varying between 1.0 and 2.3 (± 0.3 to 1.2) (Fig. 3.31C). Similarly, the expression pattern of *HQT1* levels after a shift to high PPFD was not significantly altered in transferred plants compared to those at control conditions with values ranging between 0.5 and 1.5 (± 0.1 to 0.6) (Fig. 3.31D). In contrast, the relative transcript abundance of *HQT2* and *HQT3* increased both, albeit differentially with respect to degree and time course (Fig. 3.31E−F). In particular, the mRNA levels of *HQT3* were significantly increased 6 and 24 hours in the shifted group. Respective relative transcript levels gradually increased until they were significantly higher than in control plants six hours after transfer to the 11-fold with a strong variation (± 12.4; $p < 0.01$). The increment was followed by an immediate decline and a further remarkable and significant increase 24 hours after PPFD elevation to 26 (± 7.3; $p < 0.001$), respectively (Fig. 3.31F). The kinetic of relative transcript levels of HQT3 appeared somewhat shifted in time with a weaker response. The relative transcript levels of *HQT2* were significantly increased three hours after plants have been transferred to approximately the 10-fold (± 3.7; $p < 0.01$, Fig. 3.31E). The levels remained comparably high after six hours, followed by a gradual decrease with a temporary minimal level 12 hours after the shift. At 24 hours after transfer, transcript levels increased once more to the 7-fold (± 2.0) without being significantly different from that in control plants (Fig. 3.31E). Consistently with findings for the PAR experiment, *HQT2* and *HQT3* displayed transient upregulation of transcript levels whereas *HQT1* transcript levels did not alter upon a shift to 9°C (Figs. 3.31H−I). At single time points, again, the biological variation was high. For *HQT3* transcript levels, the initial increase was congruent with that of *HQT2* on the time scale although the degree of increment differed. The corresponding transcript levels were significantly higher than in control plants 12 hours after the shift to altered temperature conditions (7.5 (± 6.9, $p < 0.001$) followed by a small decline within the next 12 hours to a stable level of approximately 4. However, 120 hours after the shift, the relative transcript levels increased significantly once more to a value of 6 (± 4.1, $p < 0.05$) (Fig. 3.31I). The trace of the short-term response kinetic of *HQT2* appeared very similar to that observed in the PAR experiment with an immediate and gradual increase between 3 and 12 hours after the shift to the 4- (± 2.0) and 5-fold (± 3.7), respectively (Fig. 3.31H).

The relative gene expression of the three *HQT* isoforms in control plants among the three shift experiments was relatively stable. In the control group of the UV-B shift experiment relative gene expression accounted to values from 1.0 to 1.3 (± 0.2 - 0.9). Relative transcript levels averaged over the time for control plants in the PPFD experiment accounted for 1.0 (± 0.2; *HQT1*), 1.3 (± 0.9; *HQT2*) and 1.1 (± 0.5; *HQT3*) for the respective isoforms. Transcript levels of control plants in the temperature shift experiment remained for the most part stable at low values between 1.0 and 1.4 (± 0.1 – 1.0) (Figs. 3.31G−I). The initial relative *HQT* expression was comparable in control and shifted plants, so that both groups had similar prerequisites. Initial relative transcript levels for the different

HQT isoforms in the UV-B experiment of control plants (1.0 to 1.2 (± 0.2 – 1.0)) varied less than in the shift group. In the latter, *HQT1* mRNA levels were at 1.4 (± 0.2) whereas levels of *HQT2* accounted to 2.9 (± 1.2) and that of *HQT3* displayed higher, albeit not significantly different initial transcript levels and 2.3 (± 1.1). Initial transcript levels in the PPFD experiment were in a comparable order of magnitude with averages between 1.0 and 1.5 (± 0.2 - 0.9) relative units except for *HQT3* in shifted plants that displayed 2.8 (± 0.5), respectively (Figs. 3.31D−F). In the temperature experiment, initial transcript levels in control plants displayed levels from 1.0 to 1.4 (± 0.2 – 1.0) throughout the different isoforms whereas those in the shift group were slightly lower but still comparable (1.0 (±0.6; *HQT1*), 0.9 (±0.5; *HQT2*) and 0.9 (± 0.5; *HQT3*) (Figs. 3.31G−I).

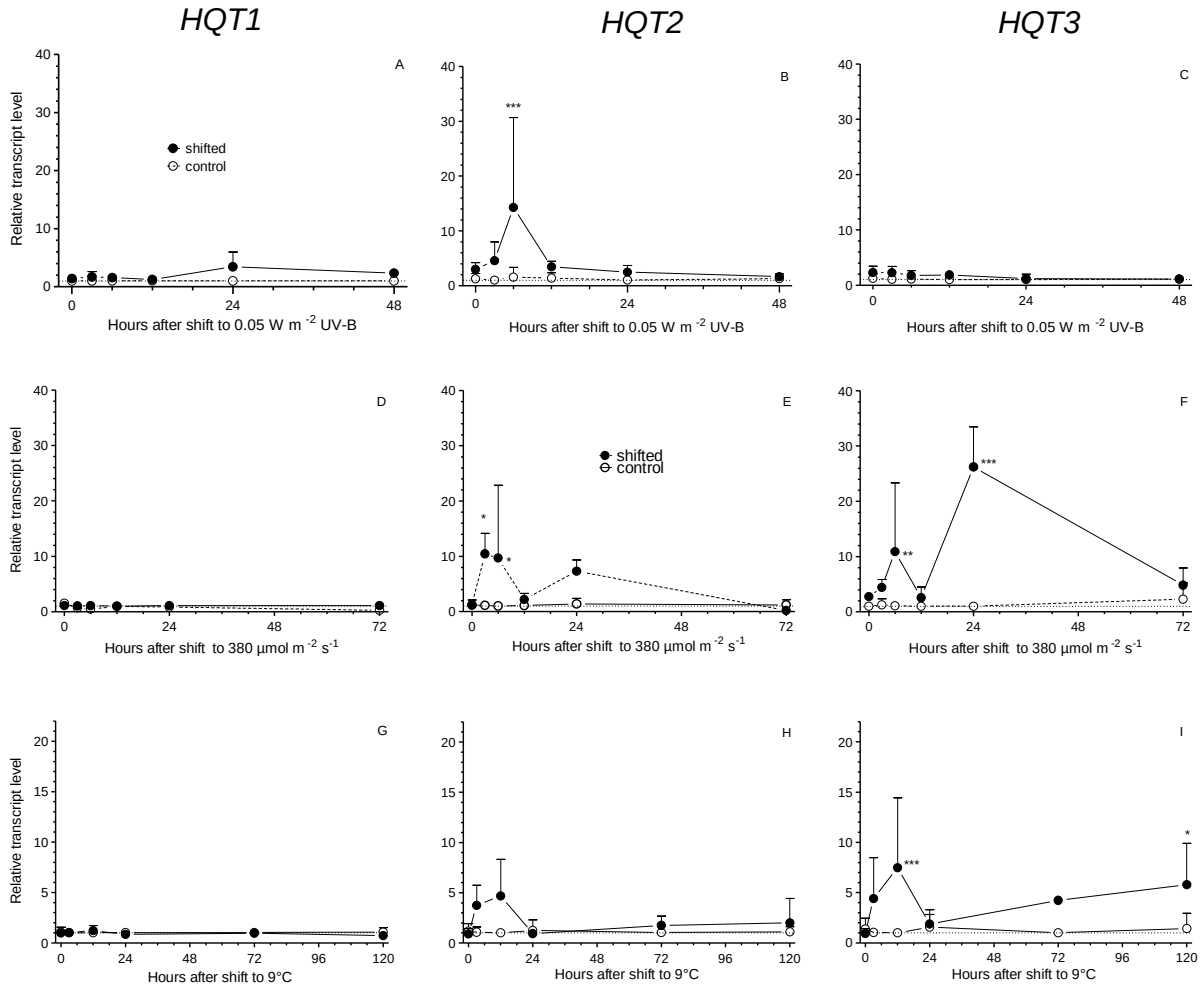

Figure 3.31 Short-term kinetics of relative transcript levels of *HQT1-3* in three shift experiments
The second leaf generation of sunflower plants used for analysis of epidermal UV absorbance was sampled for analysis of relative gene expression of three identified sunflower hydroxycinnamoyl CoA quinate transferase (*HQT*) isoforms. Relative gene expression of *HQT1* (A, D, G), *HQT2* (B, E, H) and *HQT3* (D, F, I) was calculated as $2^{-\Delta\Delta Ct}$ and is given in dependence of time after an alteration in one respective abiotic variable as average ± standard deviation for three biological replicates measured in technical duplicates (n = 3). Control plants (open circles) remained at initial growth conditions (50 µmol m^{-2} s^{-1} PAR without UV, 21 °C) and the shift group was transferred to either 0.05 (± 0.02) W m^{-2} UV-B (A–C, filled circles: > 300 nm, 1.1 (± 0.5) W m^{-2} UV-A), high PPFD (D–F, filled circles: 380 µmol m^{-2} s^{-1}), low temperature (G–I, filled circles: 9 °C). Significant differences between control and shifted plants are marked with asterisks (** for $p < 0.01$ and *** for $p < 0.001$; Two-Way-ANOVA).

4 Discussion

4.1 Phenylpropanoid profile of sunflower foliage leaves

4.1.1 Predominance of caffeoylquinic acids

Leaves of higher plants are characterised most often by a variety of different flavonoids and hydroxycinnamic acids (HCAs) (Shirley 1996; Agati et al. 2009; Karakas and Turker 2013; Kolarević et al. 2021). Based on the available information at the time when the present study was conducted, data on specific secondary metabolites in vegetative leaves of *Helianthus annuus* was either qualitatively or quantitatively fragmentary (Rieseberg et al. 1987; Mason et al. 2016; Fernandez et al. 2019). The phenylpropanoid profile presented in this thesis includes a detailed and complete report on specific isomers of the dominant caffeoylquinic acids in leaves of the oilseed sunflower cultivar Peredovick grown under a broad variety of environmental conditions. The profile was dominated by chlorogenic acid (CGA) and di-caffeoylquinic acid (DCQA) with both constituting approximately 95 % of total phenolics (Figs. 3.1, 3.24–3.27, S7.1, Table 3.1, S7.1). These two particular CQAs were accompanied by other hydroxycinnamic acids − mainly with UV absorbance, retention times and mass to charge ratios characteristic for caffeoyl derivatives − in proportions below 5 % (Figs. 3.1, 3.2, 3.24, 3.27, 3.28A, S7.1, S7.4, Table 3.1, S7.1). The absorbance of the other HCAs corresponded to approximately 0.05 nmol of chlorogenic acid equivalents (CAE) per cm^2 of leaf area in non-stressed plants and up to 0.5 nmol cm^{-2} CAEs in stressed plants (Table 3.1). Considering the potentially broad spectrum of phenylpropanoids within one plant species, the phenolic profile of the analysed sunflower cultivar appeared rather narrow because other phenylpropanoids occurred in negligible amounts. In particular, flavonoids were almost entirely lacking. In the presented work, more than 200 samples of *Helianthus annuus* cv. Peredovick (sunflower) leaves have been analysed phytochemically. Even in stressed plants, no other compounds than CGA and DCQA were found in proportions higher than 5 %. The qualitative and quantitative occurrence of the other caffeoyl derivatives differed between biological replicates. The occurrence was not found to be subjected to any pattern indicating no stress-induced accumulation of compounds alternative to CGA and DCQA via shifted and differentially regulated biosynthesis routes. When plants were exposed to abiotic stress, the foliar phenolic profile differed mainly in the concentrations of mono-and di-CQAs, whereas the qualitative composition of the compounds remained nearly constant throughout different growth irradiances, irradiance spectra, temperatures, and availability of nitrogen (Figs. 3.24–3.25, 3.27, Tables 3.1–3.2). Sunflower plants growing for several weeks under inducing field conditions in summer with high PPFD and UV levels displayed identical dominant peaks in the chromatograms (Fig. 3.29). Furthermore, the phenolic profiles did not alter among different ages of analysed plants or leaves and were not affected in plants cultivated in hydroponics either (Fig. 3.29). The consistent dominance of CGA and DCQA is in accordance with previous analyses conducted in this lab by Bargholz (2012), Hoier (2012), Zink (2018) and Greßmann (2019) and other authors (see below). The specific isomers corresponding to the dominant peaks were identified as 3-mono-O- and 3,5-di-O-caffeoylquinic acid (Fig. S7.1, Table S7.1). Assuming a similar phenolic profile throughout the

plant, the predominance of one 3-mono-O- and 3,5-di-O-caffeoylquinic acid is in line with published results on secondary metabolites of sunflower aerial parts (Gai et al. 2020). Furthermore, the abundance of additional isomers of mono- and dicaffeoylquinic acids (including neochlorogenic, cryptochlorogenic, 3,4-di-O-caffeoylquinic and 4,5-di-O-caffeoylquinic acid) in lower amounts has also been reported earlier (Mason et al. 2016; Gai et al. 2020). It was not possible to identify the isomeric structure of the minor peak at a retention time of approximately 20 minutes unequivocally as 3,4- or 4,5-DCQA using HPLC standards (Fig. S7.1, Table S7.1). It is likely, that this peak corresponds with yet another isomeric form. Cheevarungnapakul and colleagues (2019) have found 1,5-DCQA in young sunflower sprouts that might correspond to this minor peak. However, the predominance of esters of quinic and hydroxycinnamic acids occurs throughout the life cycle of sunflowers. They are present in seeds, sprouts and aerial parts of flowering plants (Dorrell 1976a; Jan et al. 2018; Cheevarungnapakul et al. 2019; Gai et al. 2020). In addition to that, the high abundance of hydroxycinnamoylquinic acids has been confirmed for several different species of the tribe *Helianthus* (Mason et al. 2016; Fernandez et al. 2019). In contrast, one study on two specific sunflower lines did not detect di-caffeoylquinic acids but remarkable amounts of chlorogenic acid and other cinnamic acid derivatives in minor amounts (Saftić-Panković et al. 2006).

Interestingly, the foliar phenolic profiles of other Asteracean species resembled each other in that caffeic acid derivatives are the predominant extractable phenolics (Moglia et al. 2008; Hoier 2012; Mai and Glomb 2013; Legrand et al. 2016). In a previous analysis in this lab, CQAs were found in dominant proportions in several sunflower cultivars, in *Helianthus debilis*, *Helianthus tuberosus* and in two *Senecio* species (Hoier 2012). Similarly, both, globe artichoke (*Cynara cardunculus,* subfamily Carduoidea) and sunflowers (subfamily Heliantheae), contained isomers of mono- and di-CQAs (Moglia et al. 2008). Likewise, phenolics in chicory (*Cichorium intybus,* subfamily Cichorioideae) included the mono-CQAs chlorogenic and caftaric acid and the DCQA chicoric acid (Legrand et al. 2016). In lettuce (*Lactuca sativa*, subfamily Cichorioideae) the mono-CQA chlorogenic and phaseolic acid, the DCQAs chicoric and isochlorogenic acid were detected together with some flavonoids in minor amounts (Mai and Glomb 2013; Taulavuori et al. 2016).

Other more distantly related eudicotyledons containing high amounts of caffeic acid derivatives in leaves, especially chlorogenic acid, are for example tobacco (*Nicotiana tabacum*, Solanaceae) and tomato (*Solanum lycopersicum*, Solanaceae). The same applies to the phylogenetically far more distant species creeping barberry (*Mahonia repens*, Berberidaceae), (Sheen and Calvert 1969; Grace et al. 1998; Clé et al. 2008). Especially Solanaceaen species such as tobacco, tomato and potato are of particular importance in this research context since they have formed the basis for comprehension of biosynthesis routes of chlorogenic acid and involved enzymes as well as corresponding genes (Clé et al. 2008; Hoffmann et al. 2003, 2004; Niggeweg et al. 2004; Payyavula et al. 2015). Phylogenetically, species of the families Solanaceae and Asteraceae both belong to the monophyletic clade of asterids, which is comparatively young in the evolutionary history of angiosperms (Gemeinholzer 2018). The biosynthesis routes and underlying genetics in both families might display enough similarities for *in silico* sequence analysis due to relicts of the common ancestor.

4.1.2 Involvement of the key enzyme HQT in the biosynthesis of caffeoylquinic acids

To this day, the entirety of consecutive steps of chlorogenic acid biosynthesis remains ambiguous (Villegas and Kojima 1986; Niggeweg et al. 2004; Moglia et al. 2016; Cheevarungnapakul et al. 2019). At least three distinct routes are proposed for the biosynthesis of chlorogenic acid depending on plant species and the subsequent reaction mechanism for the biosynthesis of di-CQA is not yet fully understood (Niggeweg et al. 2004; Moglia et al. 2016). One proposed route of chlorogenic acid biosynthesis, which has been found in tomato and tobacco involves the activity of the key enzyme hydroxycinnamoyl-CoA quinate transferase (HQT) (Niggeweg et al. 2004; Clé et al. 2008). HQT mediates the transfer of quinate to caffeic acid and has recently been discovered in sunflower as well (Niggeweg et al. 2004; Clé et al. 2008; Cheevarungnapakul et al. 2019). The corresponding HQT protein sequences of sunflower and the Solanacean species share about 70 % sequence identity (Niggeweg et al. 2004; Cheevarungnapakul et al. 2019). HQT also catalysed DCQA synthesis, likely by the addition of two CGA molecules under the release of a quinate (Moglia et al. 2014). However, *HQT* overexpression in tomato increased solely CGA levels and in sunflower, two of three DCQA isomers were not affected by RNA interference manipulation of *HQT* (Niggeweg et al. 2004; Cheevarungnapakul et al. 2019).

Presented phytochemical and molecular data on transcript abundance confirm the key role of HQT in CGA biosynthesis (Figs. 3.24−3.31). The significant transcriptional upregulation of *HQT2* and *HQT3* occurring before the enhanced CGA accumulation (Figs. 3.26, 3.27, 3.31, Table 3.2) provides evidence for these genes to be substantially involved in CGA biosynthesis in outgrown young sunflower leaves in response to changes in different abiotic variables. Previous reports had indicated *HQT2* to be the only isoform responsible for CGA biosynthesis in sunflower, as relative expression levels of *HQT1* and *HQT3* were low in leaves (Cheevarungnapakul et al. 2019). The subordinate role of *HQT1* was confirmed in the present work since its relative expression was not or just barely affected in sunflower leaves with enhanced accumulation of CGA (Figs. 3.26, 3.27, 3.31, Table 3.2). However, in this thesis, *HQT3* was upregulated by high PPFD and low temperature but not by UV-B, whereas relative gene expression of *HQT2* increased in response to all three different stress conditions, which were tested (Fig. 3.31). This is in line with findings of Moglia et al. (2016) who observed high transcript levels of *HQT2* and *HQT3* in vegetative tissue as well as the stem whereas *HQT1* expression was restricted to bracts in the closely related globe artichoke. The analysis of Cheevarungnapakul and colleagues (2019) was conducted in young sunflower sprouts. It is likely that expression in older plants differs from that in young ones.

4.1.3 Minor amounts of flavonoids

In contrast to the high amounts of caffeoylquinic acids, flavonoids were detected only in highly concentrated extracts or rather seldom in plants that grew under suboptimal conditions (Figs. 3.28, 3.29, S7.1, S7.5). In unstressed plants, the abundance of in total putative 11 flavonoids was below the detection limit except when measured in concentrated leaf extracts (Figs. 3.28B, S7.1, Table S7.1). In

sunflowers that grew for several weeks under particular stress conditions, minor peaks with flavonoid-like absorbance spectra were found sporadically in addition to the characteristic dominant CQA-peaks (Fig. 3.29). When plants were cultivated outdoors and exposed to several variables, especially high PAR and UV radiation, compounds with a maximal extinction at 343, 357 or 369 nm were found (Fig. 3.29B). However, the relative proportion of absorbance at 360 nm of flavonoid-like peaks was below 1.5 % in each stressed plant (Fig. S7.5). According to their absorbance spectra and with reference to mass spectrometry data of highly concentrated leaf extracts, these compounds are likely glycosides of quercetin, kaempferol and luteolin. Apparently, noteworthy amounts of epidermal flavonoids have also not been detected in any other analysed sunflower cultivars in the previously cited studies of Saftić-Panković et al. (2006), Cheevarungnapakul and co-authors (2019) or of Gai et al. (2020). In contrast to CQA-dominated publications, one report on eight epicuticular flavonoids and internal flavonoid aglycones exists but no quantitative data was available (Rieseberg et al. 1987). In the latter study, leaves of *Helianthus annuus* had been extracted using considerably higher amounts of plant material and acetone instead of aqueous methanol so that a difference in extraction methods might have caused the divergence in flavonoid presence. However, the extraction and detection method used in the present study revealed the presence of flavonoids when used in other higher plants including tomato and several *Helianthus* species (Hoier 2012; Bergmann 2021). In a study investigating the presence of foliar flavonoids of other *Helianthus* species, several flavonoids were detected when using 10-fold of the plant material used in the present work (Schilling 1983, 1983; Schilling et al. 1987). Although the authors found specific flavonoids, the pattern of specific flavonoid derivatives varied remarkably among one subgroup of the Heliantheae tribe (Schilling 1983). Consistently, in addition to the CQAs, Hoier (2012) also found quercetin- and kaempferol derivatives in further species belonging to the Heliantheae tribe such as *Zinnia elegans* and *Tagetes patula*. For certain *Helianthus* species, a reduced variation together with small concentrations of flavonoids were reported and aglycones of specific polyhydroxyflavones with a similar hydroxylation pattern to quercetin were present only in glandular trichomes (Schilling and Mabry 1981; Schilling 1983). In accordance with this pattern, the Peredovick cultivar in the present work showed an orange fluorescence restricted to trichomes using Neu's Naturstoff reagent A (Fig. 3.8). In addition, yellow-orange fluorescence was observed in guard cells of stomata, indicating the presence of flavonoids (Fig. 3.8B). These colours of fluorescence are reported specifically for polyhydroxyflavone and derivatives such as glycosides of quercetin, luteolin or apigenin after derivatization with Naturstoff reagent A (Pirvu et al. 2014; Nile and Park 2015). At the same time, autofluorescence due to CQAs that underwent a bathochromic shift upon treatment with Naturstoff reagent A was absent in stomatal guard cells (Takahama 1988; Mondolot et al. 2006).

On the one hand, visualization with Neu's reagent did not imply the presence of remarkable amounts of foliar flavonoids (Figs. 3.8B, C). On the other hand, the phenolic profile of the *H. annuus* flower part including bracts, ray and disc floret contained caffeic acid esters as well as small but detectable amounts of flavonoids (Figs. S7.6, S7.7). The presence of flavonoids in leaves and floral tissue (Figs. S7.5−S7.7), although in minor amounts, implies that flavonoid accumulation is possible in *Helianthus annuus* cv. Peredovick in principle. Thus, the gene sequences for flavonoid biosynthesis enzymes

must be present in sunflower without undergoing a mutation yielding in one or more non-functional biosynthesis enzymes. Preliminary data of *in silico* research imply the existence of a large number of more than 50 gene sequences, which resemble that of chalcone synthase and are worth considering for their role in flavonoid formation (data not shown). It is likely that these genes are underlying a tissue-specific, so far unknown, regulation mechanism that has been silenced in the leaves. A potentially delayed substantial flavonoid formation after the sampling of leaves cannot be ruled out but appears improbable since sunflowers that grew outdoors for a few weeks did not show induced flavonoid accumulation. Flavonoid biosynthesis is considered a core component of vascular plants that has evolved during land colonialization, likely as a strategy of establishing an epidermal UV shield (Davies et al. 2020). The contribution of individual phenolic compounds to epidermal UV protection can differ among species and even among varieties with similar genetic background (Taulavuori et al. 2016; Cetinkaya et al. 2017; Szopa et al. 2017). Although the strategies of establishing an epidermal UV shield are manifold among the plant kingdom, the deviating response of CQA levels in sunflower as compared to other higher plants and especially the missing inducibility of flavonoids appear exceptional.

4.2 Hydroxycinnamic acids in sunflower as UV-A screening pigments

Results of the presented work have shown that the hydroxycinnamic acids in sunflower serve as UV screening pigments (Figs 3.5−3.15). Four criteria that compounds have to meet in order to be considered screening pigments were established more than twenty years ago (Cockell and Knowland 1999). According to two of these criteria, molecules functioning as UV pigments must, in the first place, absorb UV radiation, and secondly, attenuate the radiation in a manner that is physiologically effective. With respect to a physiologically effective screening, the localization of the pigments is of high importance. Attenuation of UV by screening compounds is optimal if they are localized in the outermost layer of the leaves preventing the energetic radiation to reach the tissue where essential biochemical processes are localized (Hutzler 1998; Takahashi and Badger 2011). One further prerequisite of Cockell and Knowland (1999) is fulfilled, when the survival rate under UV radiation of plants with the UV absorbing compound is higher as compared to plants without the UV absorbing compound. The fourth criterion is met, when the biosynthesis of a UV absorbing compound is inducible by UV radiation. This last criterion is facultative.

4.2.1 Epidermal localization of HCAs in sunflower leaves

The present work provides strong evidence for the CQAs to be present predominantly as soluble compounds in cells of the adaxial epidermis of sunflower foliage leaves in variable concentrations, contributing substantially to epidermal UV absorbance (Figs. 3.5−3.10, S7.3). UV screening parameters reflecting epidermal concentrations of UV absorbing compounds and foliar content of soluble caffeoyl residues were closely correlated, albeit in a non-linear manner (Figs. 3.10, S7.3). Consistently, the trend of growing UV-A absorbance was accompanied by increasing CQA contents in the same leaves (Figs. 3.22, 3.26−3.28). The linear relationship between concentration and

absorbance according to the Beer-Lambert law was apparent up to a threshold concentration of approximately 50 nmol per cm² of leaf area and absorbance values of approximately 1.2 (Fig. 3.10). The degree of correlation of UV absorbance or transmittance and CQA content might have been even closer to 1 if the abaxial leaf sides had been taken into account as well (Burchard et al. 2000). Above the threshold concentration, optical effects such as molecular interactions and scattering in and on the leaf tissue likely contributed to the divergence from the theoretical linearity and caused the curvilinear relationship (Day 1993; Day et al. 1994; Kolb and Pfündel 2005; Tolbin et al. 2017). Especially the lack of screening compounds in the epidermal cell walls sets a minimum of transmittance, which cannot be undercut (Day et al. 1993, 1994; Kolb et al. 2001). The inhomogeneous distribution of UV absorbing compounds among the leaf surface as caused by the absence in cell walls. Blue autofluorescence of CQAs was shown to be restricted to epidermal protoplasts (Figs. 3.5, 3.7) but treatment with Neu's Naturstoff reagent A stained cell walls with a greenish-yellow UV-induced fluorescence (Fig. 3.8), which has been reported for ferulic acid (Bachmann 1978). However, absence of HCAs in cell walls, causing the so-called sieve effect, was confirmed by HPLC analysis after enzymatic digestion of cell walls and subsequent extraction (Fig. 3.9).

The level of correlation between epidermal absorbance and extracted phenylpropanoids is generally dependent on the species-specific phenolic profile and compound pattern (Kolb et al. 2005). The close correlation with UV screening determined either at 366 or 375 nm (Figs. 3.5−3.7; $R^2 = 0.94$ or 0.96 respectively) is plausible since the phenylpropanoid extracts were a mixture of UV absorbing compounds with a uniform absorbance spectrum, which was particularly based on the chromophore caffeic acid (Figs. 3.1−3.2). No phenolic compounds, such as flavonoids, whose divergent UV absorbance would have potentially interfered with that of the CQAs were detectable (Kolb et al. 2005). Since the variable compounds were consistently caffeic acid derivatives, the absorbance spectrum should remain congruent when UV screening is increasing. Thus, absorbance at different wavelengths should correlate with each other until spectral flattening results in stable values where absorbance is high and in increasing values where absorbance is weak (Tolbin et al. 2017). In consequence, the mainly identical qualitative phenylpropanoid profile allows quantification of the CQA content via chlorophyll fluorescence measurements in sunflower leaves *in situ* when a HPLC calibration with a known concentration of CQAs is available. The high degree of accuracy suggests the non-invasive determination of CQA content is suitable for other species, in which hydroxycinnamic acids occur preferentially in the upper epidermis (Figs. 3.5−3.7). In addition, the comparatively weak molar extinction of CQAs in the UV-A allows to assess CQA contents quantitatively up to relatively high concentrations.

Current indices reflecting HCA content based on chlorophyll fluorescence measurements need to be corrected for flavonoid contents and no direct correlation on epidermal absorbance with HCA content has been found so far (Latouche et al. 2013; Morales et al. 2013). So far, reports on epidermally localized hydroxycinnamic acids, as for sinapoylmalate in *Arabidopsis* plants, are sporadical (Chapple et al. 1992; Franke et al. 2002). No reports were found on the localization of CQAs in leaves of sunflower but the isolated leaf epidermis of the monocotyledon *Tradescantia*

virginiana contained flavonoids, caffeic and ferulic acid (Takahama 1988). In accordance with the findings of Takahama, the respective GFP constructs of the three genes encoding hydroxycinnamoyl CoA quinate transferase (HQT) – isolated from sunflower or artichoke – have been reported to be localized in the cytosol of epidermal cells after transient ectopic expression (Moglia et al. 2016; Cheevarungnapakul et al. 2019). Thus, the localization of biosynthesis is consistent with the localization of the CQAs in sunflower leaves found in the present work

4.2.2 Protection efficacy of caffeoylquinic acids in sunflower leaves

The localization of the caffeoylquinic acids in the adaxial epidermal layer and consequent contribution to the epidermal UV screening suggests these molecules to function as UV protecting pigments, comparable to flavonoids (Reuber et al. 1996; Cockell 1997; Cockell and Knowland 1999; Burchard et al. 2000). One further criterion of physiologically effective screening is given when plants accumulate a specific compound in sufficiently high concentrations so that plants have a survival benefit (Cockell and Knowland 1999). Whether UV absorbing compounds can be taken into account to serve as UV protecting pigments also depends on how efficient the respective compounds prevent damage from UV-susceptible physiological processes such as photosynthesis compared to plants that do not contain the corresponding compound (Cockell 1997; Cockell and Knowland 1999; Takahashi and Badger 2011).

A high protection efficacy was found for the CQAs in photoinhibition experiments using different sources of UV radiation with diverging emission spectra when the hydroxycinnamic acids were present in high concentrations (Figs. 3.11–3.15). Each experiment provided important implications that complemented each other. Tendencies of the three approaches were consistent, although the extent of the damage was not comparable among the different experiments due to divergent UV spectra and PFDs applied for induction of photoinhibtion. Photoinhibition by PAR is considered as negligible in the different photoinhibition treatments. In the photoinhibition treatments, the PPFDs were below 10 µmol m^{-2} s^{-1}, except for the photoinhibition treatment with the HPLC fluorescence detector at 400 nm. The PPFD was at 75 µmol m^{-2} s^{-1}. Because low light grown plants were injured during sampling, this latter treatment was solely applied to high light grown plants, which were adapted to three times higher PPFDs. It is conceivable, that the damage caused by PPFD would have been higher in low light grown leaves. In those low light acclimated plants, more photon energy might have been excessive due to a reduced capacity of photosynthesis, caused by e.g. a smaller pool size of the photosynthetic enzyme RUBISCO (Seemann 1989). However, this hypothesis requires the conduction of further experiments.

Photochemical quantum yields in non-irradiated leaf discs were nearly identical in a range from 0.79 to 0.81 (± 0.01-0.02) (Figs. 3.11 (inset), 3.15A) confirming similar preconditions such as intact photosystems II and non-stressed plants prior to UV irradiation (Björkman and Demmig 1987; Lichtenthaler et al. 2005). In all three approaches, leaves with high UV screening capacity displayed reduced PS II damage compared to leaves with low UV screening after UV exposure. In plants with UV-A transmittances (375 nm) below 0.25, the extent of PS II inactivation was reduced by a factor of 5 compared to plants with low UV screening capacity under solar UV-A (Figs. 3.11–3.12). The foliar

content corresponding to that 5-fold protection was equivalent to the accumulation of CQAs of at least 75 nmol per cm² leaf area (Fig. 3.10). Compared to that, exposure to artificial UV radiation required 60 nmol CQAs per cm² leaf area for a reduction of PS II damage by a factor of five (Figs. 3.10, 3.15). Thus, slightly higher amounts of CQAs were required under solar UV-A radiation for the same degree of protection than under artificial UV-A. It is likely, that the divergent extent of damage was caused by exposure to different wavelengths during photoinhibition. Plants exposed to artificial UV radiation were exposed to wavebands from 350 to 400 nm. The irradiance of the artificial UV-A spectrum included 25 W m^{-2}, which is equal to the irradiance in the same waveband region on a sunny day. In contrast, photoinhibition by solar UV-A included a comparatively broader spectrum from 320 to 400 nm (Figs. 2.5−2.7, 3.11−3.12). Although the filter combinations in the experiment with solar radiation caused lower UV-A irradiance of 11 W m^{-2}, more than 40 % of that irradiance was in the region from 320 to 350 nm with more energetic radiation, thus having more damaging potential (Takahashi et al. 2010). The CQA concentration as cause for protection against UV-induced damage was also confirmed by presented data on photoinhibition implying a spectrum of protection that is corresponding to the absorbance spectrum of CQAs (Figs. 3.1, 3.13, 3.14). Plants with high UV screening capacity were particularly well protected up to wavelengths of 370 nm. Under irradiances, which were 3 to 5 times higher than in the solar irradiance spectrum, high light grown plants displayed PS II damages below 10 % in plants with an inhibited D1 repair cycle. Thus, the screening by CQA is supposed to be sufficient to prevent PS II damage under natural conditions.

Presented data are in line with the well-known model of dose-dependency, according to which the degree of PS II damage positively correlates with the cumulative dose of ultraviolet radiation (Cullen and Lesser 1991; Vass et al. 1996). Indeed, the relative PS II inactivation was directly proportional to the UV transmittance ($Inactivation_{PS\ II} = 47.53 \times T(UV\text{-}A)_{366nm}$; Fig. 3.15B), the latter reflecting the number of photons of a particular wavelength that can pass through the epidermis and hit a photosystem II complex.

A further option to test the physiological effectiveness of the sunflower UV screening would have been possible by determining whether the accumulation of CQAs would have prevented UV-B induced DNA damage. This topic was not included in the present work. It was not possible to grow plants with more than 40 % UV-B transmittance due to the efficient screening by the CQAs in that region. So far, the prevention of UV-B induced DNA damage by chlorogenic acid has been shown for human cells and explained by the combination of UV absorption and strong antioxidant capacity (Cha et al. 2014).

4.2.3 UV-inducibility of CQAs in sunflower

According to Cockell and Knowland (1999), three out of four UV screening pigment criteria were fulfilled by CQAs in sunflower leaves. Another and final criterion, which is not mandatory but has been interpreted as strong evidence for a UV protective function, is the inducibility of the accumulation of a specific compound by UV radiation (Cockell and Knowland 1999). In the present work, the adjustment of CQA content in sunflower leaves in response to UV-B radiation could be shown (Figs. 3.24, 3.26A, 3.27A, B, Table 3.1). Consistently, the UV screening capacity *of Helianthus*

annuus leaves increased significantly and rapidly upon continuous solar and artificial UV-B radiation (Figs. 3.18, 3.20–3.22A). However, exposure to UV-A, irrespective of short- or longwave UV-A radiation, did neither cause alteration in UV screening nor in CQA content although a protective function was found for these wavebands (Figs. 3.21, 3.22A). One could transfer the criterion of Cockell and Knowland to specific UV regions so that evidence for a UV-A protective function would be given if UV-A had enhanced CQA accumulation. However, data on photoinhibition clearly indicate protection against UV-B and UV-A (Figs. 3.11–3.15). Action spectra of photodamage had shown that a protection against UV-A is as important as against UV-B (Thimijan et al. 1978; Takahashi et al. 2010; Schultze 2011). Since the presence of UV-A has always been accompanied by that of UV-B during the evolution of regulatory pathways, the activation of CQA accumulation by UV-B was likely sufficient to also cause an efficient protection in the UV-A region. Thus, an additional regulation by UV-A would have been redundant not conferring a benefit of survival.

In an extensive literature research in November 2022, only one report on the upregulation of chlorogenic acid in sunflower by UV radiation was found (del Moral 1972). An additional and similar report on UV-inducibility exists on the induction of DCQA in the globe artichoke, which is a closely related species to the sunflower (Moglia et al. 2008). These studies are difficult to compare with the presented data since duration and dose of the applied UV radiation as well as irradiance spectra differed substantially. For example, the UV radiation was given either once for 20 minutes or discontinuously for 1 month. The corresponding emission spectra were not reported but UV radiation was provided by germicidal mercury lamps (del Moral 1972; Moglia et al. 2008). These lamps usually emit maximally in the UV-C (254 nm) with a small proportion of emission in the UV-B and UV-A region (manufacturer information of Atlantic Ultraviolet Corporation®, New York, USA). Based on the UV experiment in the presented work, the observed increases in the CQA contents are most likely assignable to the presence of UV-B (Figs. 3.24, 3.26A, 3.27 A, B, Table 3.1).

4.3 Induction of UV screening by the abiotic environment

A significantly enhanced upregulation of epidermal UV-absorbance in mature leaves (LG 2) of *Helianthus annuus* after exposure to high PPFD, low temperature, UV-B radiation or nitrogen depletion combined to moderate PPFDs was observed after a short period of comparatively stable values (Figs. 3.18, 3.20–3.22). The increase of epidermal UV absorbance in response to a changing abiotic environment and its magnitude is consistent with findings for other higher plants (Cartelat et al. 2005; Meyer et al. 2006; Bilger et al. 2007; Agati et al. 2011b; Barnes et al. 2013; Laureau et al. 2015; Pescheck and Bilger 2020). However, these studies focussed on the final values after several days and did not investigate the kinetics of epidermal absorbance upon the environmental change, so that comparable short-term data is missing.

It is conceivable that short-term kinetics can be influenced by additional factors besides the shifted abiotic parameters. Barnes and co-authors for example have shown, that epidermal UV screening in several field-grown species including okra and tomato underlies diurnal adjustment according to the increasing need of protection at midday when radiation levels are high (Barnes et al. 2016a). The extent of this adjustment varied greatly among different species and accounted for less than 5 % in

sunflower leaves (Barnes et al. 2016a, 2016b). Corresponding phytochemical data are not yet existent for sunflower (Barnes et al. 2016a, 2016b). In our hands, during the summer cultivation of sunflower plants in the Botanical Garden of Kiel, no diurnal dynamics could be observed based on epidermal UV absorbance. Since most experiments of this thesis were conducted in climate cabinets without gradual changes of radiation, it seems unlikely that a circadian rhythm could have interfered with the induction of epidermal absorbance and UV pigment accumulation. Another factor that was taken into account in the experimental design was a potential response of pigment content due to wounding. Dixon and Paiva (1995) summarised that chlorogenic acid levels increase when plant tissue is injured. As responses of individual phenolic compounds are highly species-specific, it is likely that presence and degree of a wounding-response is dependent on underlying genetics as well. However, a potential interference by any of the named factors can be ruled out since absorbance, pigment content and transcript levels of HQT isomers in control plants remained stable during the whole duration of experiments (results in chapter 3.2), although the control leaves were wounded for sampling in an identical manner as the treated leaves.

4.3.1 Induction of enhanced CQA accumulation by abiotic variables

The time course of the epidermal UV screening capacity was well reflected by the absorbance of leaf extracts determined by HPLC, when both parameters were determined simultaneously. During periods in which epidermal absorbance remained stable, the CQA contents were stable as well (Fig. 3.26). The enhancement of UV screening capacity in response to changing UV, PPFD or temperature was accompanied by the increasing accumulation of the predominant chlorogenic and di-caffeoylquinic acid in sunflower (Figs. 3.22−3.27). At this point, it should be noted, that the rates of absorbance change reflect the changes in foliar concentrations of the caffeoyl moiety in CGA and DCQA together. Therefore, epidermal absorbance can be taken as a means to follow the kinetics of CQA biosynthesis without the need for destructive sampling as used for plants under nitrogen depletion combined to moderate PPFD. For those plants, small leaves did not allow consecutive sampling for phytochemical analysis.

Because CGA and DCQA do not contribute equally to the total extract absorbance due to their divergent molar extinction coefficients and changing content ratios, compound-specific changes may differ from changes in the total absorbance of extracts. In plants shifted to 9 °C the absorbance of the total peak area was twice as high after 72 hours, whereas the CGA content had doubled within 20 hours and the content of DCQA had not doubled at all (Fig. 3.27E, F). A doubling of the CGA content occurred 12 hours after a transfer to high PPFD and took more than 30 hours after a shift to UV-B.

The increase rates of the total HPLC peak areas also differed in magnitude. Additionally, they were temporally shifted to each other indicating different rates of underlying biosynthesis. The fastest response occurred in UV-B shifted plants after 4.5 hours with a rate of 170 AU per hour. The strongest increase was observed in PPFD shifted plants after 18 hours with a rate of 230 AU per hour. For plants shifted to low temperature, the response started latest with the smallest rates of absorbance change compared to both other abiotic factors. In the majority of published studies on environmental regulation, phytochemical analysis was conducted several days to weeks after plants

were transferred to an altered abiotic environment so that short-term changes remained undetected (Vogt et al. 1991; Hofmann et al. 2003; Løvdal et al. 2010; Morales et al. 2010; Agati et al. 2011b; Latouche et al. 2013; Rai et al. 2019). Responses to an altered abiotic environment were most often observed for flavonoid concentrations (which consistently increased), but not for HCA levels (Hofmann et al. 2003; Morales et al. 2010; Latouche et al. 2013; Neugart et al. 2013, 2019; Rai et al. 2019). In *Betula pendula* and *Ligustrum vulgare*, the enhancement of UV screening was assigned to epidermally located flavonoids, whereas contents of hydroxycinnamic acids were not correlated to the increase in epidermal UV absorbance or were less responsive at the same time (Morales et al. 2010; Agati et al. 2011b). In *Arabidopsis*, HCA contents even decreased, although epidermal absorbance increased (Morales et al. 2013). However, in leaves of the evergreen shrubs *Mahonia* and *Aronia,* for example, it has been shown, that CQA concentrations fluctuate seasonally (Grace et al. 1998; Szopa et al. 2017). Highest amounts were found when temperature was low or when leaves were fully exposed to the sunlight (Grace et al. 1998; Szopa et al. 2017). These findings are consistent with the PPFD and temperature shift experiments. However, in field studies, plants are experiencing multifactorial dynamics of the abiotic environment. Therefore, the specific factors responsible for changes in the phenylpropanoid contents cannot be specified in field studies.

Further data on environmental regulation of the CQA content refer to other plants than sunflower accumulating monocaffeic and dicaffeic acid esters, most often together with flavonoids. Growing birch seedlings with UV-B, for example, resulted in a simultaneous increase of CGA together with specific flavonol glycosides by a factor of 1.5 to 2 (Tegelberg et al. 2004). In globe artichoke and yerba mate, exposure to UV increased especially DCQA content to the two- to threefold (Moglia et al. 2008; Lewinski et al. 2015). In tomato, high PAR and growth below 15 °C approximately doubled caffeoyl derivatives and flavonoids in tomato (Løvdal et al. 2010). Additional nitrogen depletion enhanced the increment once more (Løvdal et al. 2010). When external nitrate was reduced without adjustment of other abiotic parameters, CGA increased to the fourfold in tobacco (Fritz et al. 2006). In a similar manner, CGA as well as dicaffeoyltartaric acid and flavonoid contents increased differentially in two lettuce cultivars under nitrogen depletion by factors of approximately 2 and 5, respectively (Becker et al. 2015). Kinetics data, comparable to presented results (Figs. 3.22−3.27) on the specific responsivity of CGA and DCQA to different abiotic parameters and complementing data on UV screening, are not publicly available yet. It may be hypothesized, that the results on the induction of the secondary metabolism in sunflower are transferable to other CQA containing plants.

4.3.2 Induction of enhanced gene expression of a key enzyme of caffeoylquinic acid biosynthesis by abiotic variables

One prerequisite for an enhanced accumulation of secondary plant products such as phenylpropanoids is obviously the preceding enhanced biosynthesis of those phenolic compounds. During increased flavonoid biosynthesis, several specific key enzymes such as PAL, 4CL and CHS show increased activity (Hahlbrock and Wellmann 1970; Ragg et al. 1981; Chappell and Hahlbrock 1984; Beggs and Wellmann 1994). The increased enzyme activity is caused by an upregulated transcription and higher protein levels (Chappell and Hahlbrock 1984; Schmelzer et al. 1988; Beggs and Wellmann

1994). The high transcription rate lasts over a short period of time and is inducible by abiotic factors such as UV, PAR, low temperature and nitrogen depletion (Schmelzer et al. 1988; Kubasek et al. 1992; Beggs and Wellmann 1994; Christie et al. 1994; Coronado et al. 1995). In comparison to flavonoid biosynthesis, HCA biosynthesis and especially its environmental regulation is far less understood, although both classes of UV pigments are chemically related to each other and share biosynthetic enzymes such as PAL, 4CL and C4H. Due to the shared biosynthetic routes of hydroxycinnamic acids and flavonoids, I hypothesized that upregulation of hydroxycinnamoyl CoA quinate transferase (HQT) – analogous to flavonoid key enzymes – occurs transiently and on a transcriptional level – before changes in CQA contents become apparent.

The data of qRT-PCR was in line with the hypothesis. RNA integrity, C_T-dependent fluorescence time courses, melting curves and raw C_T values of the reference genes for actin (*ACT7*) and eukaryotic translation initiation factor 5A (*eIF5A*) were checked for plausibility prior to calculation of relative expression of HQTs (Figs. S7.8–S7.11). Within one day after alteration of abiotic factors, rapid changes of UV screening and foliar CQA contents became evident. Responses of epidermal absorbance at high PPFD and low temperature showed a flattening at time points later than 24 hours indicating that maximal activity of CQA biosynthesis had already passed at this time (Figs. 3.22, 3.26, 3.27). For all abiotic factors, the enhanced accumulation of CQAs was preceded by a transcriptional upregulation of at least one gene of *HQT* that started 3 hours after the shift. The exact time courses and magnitudes of upregulation were different between *HQT2* and *HQT3,* whereas *HQT1* transcripts showed only minimal alteration at UV-B and no response at the other conditions (Fig. 3.31). This pattern was also found, when plants were exposed to nitrogen depletion and moderate PPFD (Negwer 2022). At UV-B, high PPFD and low temperature, gene expression of *HQT2* was maximal within 12 hours suggesting a key role for *HQT2* in CQA biosynthesis (Figs. 3.31B, E, H). This has also been proposed by Cheevarungnapakul et al. (2019). For UV-B irradiation, epidermal absorbance increased just moderately as compared to high PPFD and low temperature. It is possible that less CQA biosynthesis occurred compared to both other shifts due to a shorter period of high *HQT2* transcript levels (Figs. 3.31B, E, H). Interestingly, in plants, which initially had already moderate CQA levels, responses of all *HQT* genes were absent after treatment with UV-B, although pigment levels continued to increase remarkably (Figs. 3.26, 3.30). This observation is probably explainable by an enzyme pool that had been synthesized earlier – potentially in response to the low UV-B radiation emitted by the fluorescence tubes used for white light – and that was large enough for further CQA accumulation.

Furthermore, a short-term induction was observed for *HQT3* expression in both latter conditions in addition to a long-term upregulation after 24 hours indicating *HQT3* to be likewise relevant for CQA biosynthesis (Figs. 3.31 F, I). Interestingly, upregulation of CQAs in response to nitrogen depletion and moderate light within 24 hours followed short-term-upregulation of *HQT3* expression*,* whereas mRNA of *HQT2* had not yet increased at that time. The long-term changes for both genes were found in a manner similar to high irradiance and low temperature (Negwer 2022). It is possible, that two distinct regulation mechanisms, one for short-term and one for long-term changes, for the *HQT* genes exist, which are differentially activated by the different parameters.

The slow response of CQA content and UV absorbance at low temperatures was consistent with lower relative gene expression of *HQTs* than at high PPFD or UV-B (Figs. 3.22, 3.26−3.27, 3.31). The mRNA and protein levels of HQT were found to correlate with CGA biosynthesis in flowers of *Lonicera japonica,* but this is so far the only report linking the different levels of gene expression (Li et al. 2019). The link between gene expression of the biosynthetic enzymes and their phytochemical products at different abiotic conditions is by far more complex. Gene transcription is often slower at low temperatures than at higher ones but other regulatory processes such as RNA degradation may compensate for differences in RNA levels such that protein levels stay constant (Casal and Balasubramanian 2019).. Experiments in this work do not include protein analysis, so that the time courses of the HQT protein level and enzyme activity in plants of shifting experiments have yet to be shown using Western Blotting or an enzyme assay of leaf extracts. Thus, it cannot be ruled out that temperature-dependent differences were present on the protein levels or in relation to enzyme activity. Little is known on *in vivo* protein synthesis at low temperature and its regulation is proposed to be complex (Yan et al. 2006). However, publications consistently report inhibited rates of translation in fungi, bacteria and plants after chilling due to reduced biogenesis of ribosomes or instability of the polysome (Martegani and Alberghina 1977; Broeze et al. 1978; Grennan and Ort 2007; Hang et al. 2018). It is conceivable that not only a smaller pool of *HQT* caused slower rates of CQA biosynthesis. In plants shifted to 9 °C, the weaker response in the pigment concentration might have also been caused by slower turn-over rates of biosynthetic enzymes at low temperature (Sharpe and DeMichele 1977; DeLong et al. 2017).

The presented kinetics of CQA biosynthetic enzymes may be transferable to other CQA containing plants, too. They may also hold true for flavonoid metabolism in other species and vice versa and may create awareness of potential pitfalls when interpreting published results with a focus on the interaction between secondary metabolism and the environment. Recent reports on environmental regulation of the flavonoid biosynthesis seem often in conflict with established principles such as the central dogma of molecular biology or the sequential upregulation of biosynthetic enzymes (Ragg et al. 1981; Schmelzer et al. 1988; Christie et al. 1994; Kubasek et al. 1998; Løvdal et al. 2010; Neugart et al. 2013, 2016; Schulz et al. 2015). In some studies, mRNA analysis of enzymes of the flavonoid biosynthesis was not consistent with phytochemical analysis (Løvdal et al. 2010; Neugart et al. 2013, 2016). Early flavonoid biosynthetic enzymes such as PAL and CHS were transcriptionally upregulated, whereas mRNA levels of enzymes responsible for downstream flavonol formation were not enhanced although the flavonol content was increased (Løvdal et al. 2010; Neugart et al. 2013, 2016). In other cases, transcript levels of biosynthetic enzymes were not reflected on the protein level or by enzyme activity. For example, high light treatment of tomatoes enhanced PAL activity, although the corresponding transcription was not affected at all (Løvdal et al. 2010). The presented data (Figs. 3.18−3.31) on the abiotic stress response of CQA biosynthesis together with published kinetics suggest, that the factor time is the relevant key to data inconsistency (Ragg et al. 1981; Schmelzer et al. 1988; Ohl et al. 1989; Christie and Jenkins 1996). The environmental inducibility of flavonoid biosynthesis is often examined focussing on long-term changes of enzyme mRNA levels ranging from one day to several days up to weeks (Olsen et al. 2008; Løvdal et al. 2010; Neugart et al. 2013, 2016;

Schulz et al. 2015; Qian et al. 2019). The presented results, however, implicate sampling earlier than 24 hours as essential in order to observe environmental regulation of gene expression at all, which is a prerequisite for its understanding (Figs. 3.30−3.31). The early response was reported for several flavonoid key enzymes, whose expression increased gradually after 1 to 4 hours by UV, high PPFD and low temperature to a transient maximum within the next 24 hours (Ragg et al. 1981; Kreuzaler et al. 1983; Schmelzer et al. 1988; Ohl et al. 1989; Christie and Jenkins 1996; Rai et al. 2019). In some cases, long term upregulations ranging from 2 to 14 days, especially after induction by cold, were also found (Christie et al. 1994; Leyva et al. 1995; Schulz et al. 2016; Qian et al. 2019). However, repeated sampling showed that alterations in flavonoid-related gene expression no longer detectable after several days in many cases (Ragg et al. 1981; Qian et al. 2019; Rai et al. 2019). It may be concluded that the adjustment of the gene expression of CQA biosynthetic enzymes during environmental changes is dynamic and far away from steady state during acclimation. Furthermore, the response may occur on short- and long-term scale.

In order to promote a comprehensive understanding of CQA biosynthesis and its positive regulation by abiotic stress, transcriptome analysis of CQA accumulating species is a promising approach. The sunflower seems as an appropriate model, since other biosynthesis pathways are not substantially included in the regulation. For understanding the coordination of the positive regulation by signal transduction cascades of the whole CQA biosynthetic pathway, several suitable snapshots − thus, sampling time points − are necessary since each sampling provides a single snapshot of mRNA and/or protein levels for metabolic routes. Currently, selected samples used in the shift experiments of this thesis have been sent in a follow-up-project for RNA sequencing. Subsequent analysis will provide data of the transcript levels of CQA biosynthetic enzymes at several consecutive time points after shifts to high PPFD, low temperature and UV-B. It will likely reveal differences in the transcriptome of plants of the control and shifted group. The differences might simplify the search for yet unidentified enzymes involved in DCQA synthesis. Additionally, it is not known whether the gene expression of identified consecutive enzymes in CQA biosynthesis is temporally shifted in relation to one another. Furthermore, missing transcripts of flavonoid biosynthetic enzymes, which are presumably present on the genomic level, would explain the absence of flavonoids in sunflower. More importantly, the differences are expected to indicate transcriptional changes, which mediate responses to a changing abiotic environment.

4.3.3 Signal perception and transduction

The results of the shifting experiments showed that caffeoylquinic acid biosynthesis in sunflower was upregulated in response to PAR, UV-B and low temperature (and to some extent to low nitrogen) (Figs. 3.18−3.31). For the three parameters, there was a period in which absorbance increased minimally, if at all, prior to the enhancement. A prerequisite for the adjustment of the secondary metabolism is the perception and integration of a particular stimulus into the primary and secondary metabolism via signal transduction. In particular, the transformation of an external physical stimulus into biochemical signals needs time. Depending on the parameter, the duration of that lag period took six to twelve hours indicating the signalling cascades to take place (Figs. 3.21−3.23, 3.26, 3.27).

The search for overlapping differences induced by UV, high PAR and low temperature could reveal, which components could act as signalling messengers.

Although analysis of signal perception and subsequent perception was not included in the present work, it is worth to keep an eye on it with respect to interpretation and evaluation of data consistency. To date, no empirical data exist on how signal perception and subsequent transduction mediates the biosynthesis of CQAs in sunflower. However, literature provides data on regulatory factors of CQA biosynthesis for other euasterids than sunflower (Koeppe et al. 1970; Moglia et al. 2008; Johkan et al. 2010; Løvdal et al. 2010; Agati et al. 2011b). In some species, the abiotic parameters which induce flavonoid and CQA biosynthesis overlap indicating some general principles (Hofmann et al. 2003; Olsen et al. 2008; Løvdal et al. 2010; Agati et al. 2011b; Neugart et al. 2013; Schulz et al. 2015; Rai et al. 2019). The results suggest the involvement of the same receptors and transcription factors for both biosynthetic pathways. A direct link between the UV-B receptor UVR8 and the phenylpropanoid metabolism, especially the UV-B mediated positive regulation of flavonoid biosynthesis, has been shown for different UVR8 mutants of *Arabidopsis thaliana* (Kliebenstein et al. 2002; Brown et al. 2005; Brown and Jenkins 2008; Demkura and Ballaré 2012; Rai et al. 2019). There exist different UVR8 proteins, which appear to be at least partially functionally redundant, since *UVR8* transcripts were still detectable in mutants although UV-B tolerance was impaired (Kliebenstein et al. 2002). Interestingly, the hydroxycinnamic acid levels were either downregulated or not altered at the same time, apparently dependent on which *UVR8* allele was mutated (Kliebenstein et al. 2002; Demkura and Ballaré 2012; Morales et al. 2013; Rai et al. 2019). Comparable data for sunflower or related species with a predominant accumulation of HCAs are missing to date and are only inferable with restrictions from other plants due to the high diversity of the phenylpropanoid biosynthetic pathway and its regulation among different species. However, the gene annotation of UVR8 receptor protein in sunflower has recently been updated by the International Consortium for Sunflower Genomics. The enhanced accumulation of CQA induced by UV-B suggests one signal transduction pathway to begin via the UVR8 receptor. The involvement of the blue light receptor cryptochrome in the adjustment of epidermal UV screening appears less consistent and potentially more variable depending on the species (Siipola et al. 2015; Rai et al. 2019). For instance, in different species of *Aronia*, a plant accumulating various phenolic acids and flavonoids, blue light increased the content per dry weight of CGA approximately to the three fold whereas the increment in flavonoid content was not as high (Szopa et al. 2018). On the contrary, in lettuce and basil, CGA levels were not affected by blue light, but pools of specific quercetin glucosides and chicoric acid were increased after 12 days of exposure (Taulavuori et al. 2016). In a different lettuce cultivar, CGA increased under blue light (Johkan et al. 2010). In addition, recent findings indicate that cryptochrome activity interferes with that of UVR8 in a complex manner (Rai et al. 2019; Palma et al. 2021). Whereas phenylpropanoid contents in cucumber increased under blue and white light when no UV was applied, presence of UV caused decreasing contents under these light qualities (Palma et al. 2021).

Interestingly, light receptors may also be involved in temperature sensing (Casal and Balasubramanian 2019). Recent findings showed that the red light receptor phytochrome B

undergoes temperature-dependent conformational changes making it a suitable candidate for sensing temperature (Legris et al. 2016; Casal and Balasubramanian 2019). A key role of the transcription factor PHYTOCHROME INTERACTING FACTOR (PIF4) in thermo-morphogenesis supports the involvement of phytochrome as internal thermometer (Johansson et al. 2014; Quint et al. 2016). Nevertheless, the *phyB* mutant still responds to temperature changes, indicating further sensory systems (Casal and Balasubramanian 2019). By now, plenty of cellular components and processes with light-independent features have been suggested for the perception of temperature (Minorsky 1989; Penfield 2008; Casal and Balasubramanian 2019). The sensing may occur via changes in membrane fluidity, protoplasmic streaming, levels of regulatory RNAs and phytohormones as well as cytoskeleton stability (Minorsky 1989; Penfield 2008; Ruelland and Zachowski 2010; Casal and Balasubramanian 2019).

Which parameter(s) could act as concrete signals in terms of nitrogen sensing, is likewise under research (Coruzzi and Zhou 2001; O'Brien et al. 2016; Gent and Forde 2017; Xuan et al. 2017). In general, two main signals exist: an external and an internal one (Gent and Forde 2017). On the one hand, the roots are surrounded by inorganic nitrogen in form of nitrate and (NO_3^-) and ammonium (NH_4^+) (Coruzzi and Zhou 2001; Xuan et al. 2017). The perception of NO_3^- and NH_4^+ is suggested to occur via specific membrane proteins, which simultaneously function as receptor and transporter, so-called transceptors (O'Brien et al. 2016; Xuan et al. 2017). On the other hand, sensing of the endogenous nitrogen status appears crucial for the feedback-regulation of nitrogen uptake (Coruzzi and Zhou 2001; Gent and Forde 2017; Xuan et al. 2017). The internal perception of nitrogen in plants is not yet understood (Coruzzi and Zhou 2001; Gent and Forde 2017). Of particular importance for nitrogen dependent responses is the internal carbon/nitrogen balance since nitrogen metabolism is closely linked to carbon metabolism and vice versa (Coruzzi and Zhou 2001; Gent and Forde 2017). The information on the nitrogen status is likely provided by amino acids such as glutamine and leucine whereas sugars like glucose and sucrose are utilized for sensing the carbon level (Coruzzi and Zhou 2001; Hannah et al. 2010; Gent and Forde 2017). However, determination of the C/N ratio requires the integration of the various molecular signals at the same time likely resulting in a highly complex mechanism (Coruzzi and Zhou 2001; Gent and Forde 2017).

Likewise, the biochemical mechanisms that couple sensing of PAR, UV, temperature and nitrogen status to the phenylpropanoid metabolism are presumably highly complex and the elucidation of full pathways probably requires extensive research. Nevertheless, the common response of enhanced phenylpropanoid biosynthesis implicates downstream signalling cascades to overlap at least partially although perception of PAR, UV, nitrogen and temperature is distinct from each other (Delker et al. 2014; Quint et al. 2016; Song et al. 2017). Indeed, all downstream pathway(s) share transcription factors belonging to the MYB/PAP family (Lea et al. 2007; Schulz et al. 2015; Song et al. 2017; Rai et al. 2020; Bhatia et al. 2021). In addition, PAR, UV and cold induce changes for the signalling components COP1 and HY5, which are well known to interact with MYB/PAP (Song et al. 2017; Rai et al. 2020; Bhatia et al. 2021). However, involvement of HY5 has been shown for nitrogen signalling under depleted conditions, but the link to the regulation of the secondary metabolism is still missing (Huang et al. 2015).

Consistent with current knowledge on flavonoid biosynthesis, *in silico* promoter analysis of sunflower *HQT2* and *HQT3* revealed binding regions for MYB transcription factors that are involved in activation of phenylpropanoid and, in other species, flavonoid biosynthetic enzymes (Hemm et al. 2001; Docimo et al. 2013; Cheevarungnapakul et al. 2019). Different MYB isoforms of eggplant, *Arabidopsis* or rice promoted chlorogenic acid biosynthesis via *HQT* activation upon transient ectopic overexpression and UV-B exposure. In carrot, enhanced chlorogenic acid biosynthesis following UV-B exposure was associated with enhanced levels of HY5 and MYB (Luo et al. 2008; Docimo et al. 2013, 2016; Bartley et al. 2016). The involvement of further transcription factors known from the regulation of the flavonoid biosynthetic pathway is to date speculative and requires further research. Whether the signalling cascades are distinct from each other or whether they are integrated at one central regulatory point remains an important issue of current research on phenylpropanoid biosynthesis.

Independent of whether the internal or the external nitrogen status – or both in interaction – mediate the upregulation of the CQA biosynthesis, the downstream signalling cascade is apparently co-regulated by PAR (Figs. 3.22D and 3.23). These results together with findings of Zink (2018) and Negwer (2022) imply that the speed and magnitude of the response are dependent on the applied photon dose. At nitrogen depletion and at a PPFD of 150 µmol m^{-2} s^{-1}, the epidermal UV absorbance in sunflower had doubled after six days (Zink 2018), whereas at 200 µmol m^{-2} s^{-1} an increase of the absorbance began within one day (Negwer 2022). The latter change was more moderate and did not exceed 20 % in the first three days (Negwer 2022). It is conceivable that the response would have been even more pronounced after a longer period of nitrogen depletion. The interfering (cross talking) regulatory role of nitrogen supply and PAR in terms of the phenylpropanoid biosynthesis exists in other plants as well (Lea et al. 2007; Løvdal et al. 2010; Fallovo et al. 2011). In tomato, nitrogen limitation under low light resulted in remarkably less foliar phenylpropanoids than under high light (Løvdal et al. 2010). In *Arabidopsis* under nitrogen depletion, anthocyanins were not detectable in dim light but under high light (Lea et al. 2007). Consistently, the flavonoid concentration of kale increased gradually with decreasing plant nitrogen content and increasing PPFDs (Fallovo et al. 2011). The interaction of nitrogen availability and light suggests a further crosstalk of distinct signalling pathways, which are integrated at a central regulation point orchestrating the response of phenylpropanoid metabolism. Since light is a driving force of carbon metabolism, a potential way to integrate both pathways is the carbon/nitrogen balance for which HY5 was found to act regulatory (Gent and Forde 2017). In future experiments, different abiotic parameters could be coupled to a multifactorial design for the analysis of a potential cross-talking regulation of CQA biosynthesis. Identifying the molecular components of this regulatory mechanism is a further important task for future research.

4.4 Ecological functions of CQAs

CQA has proven as UV-A protecting pigment and in view of its even stronger UV-B absorption, one must expect that it provides an even better UV-B protection (Figs. 3.3−3.7, 3.10−3.15). The chlorophyll fluorescence measurements indicate that UV-B attenuation by CQAs in the epidermis can

be up to three times higher than that of UV-A (Fig. 3.3, 3.4, Table 3.1). However, accumulation induced by high PPFD and low temperature raises the question of the function(s) of the UV screening pigment biosynthesis under these conditions (Figs. 3.18−3.31, Table 3.2).

The function of UV screening is considered as important under these conditions, too, taking into account, that repair processes are impaired under high PPFD and low temperature (Takahashi and Badger 2011; Pescheck and Bilger 2020). Repair counteracts UV-induced DNA damage such as CPD formation or inactivation of photosystem II, both of which are unavoidable under sunlight (Sinha and Häder 2002; Takahashi and Murata 2008; Campbell and Tyystjärvi 2012). In field-acclimated plants, the rates of repair do not fully compensate the rates of damage resulting in an accumulation of non-functional PS II and DNA, albeit the accumulation takes place on comparatively small levels (Stapleton et al. 1997; Coffey et al. 2017; Pescheck and Bilger 2019). At low temperature, the rates of the respective enzymatically mediated repair processes decrease (Ihle and Laasch 1996; Takeuchi et al. 1996; He and Chow 2003; Allakhverdiev and Murata 2004; Li et al. 2004). Reduction of repair rates of inactive PS II by approximately 30 % was observed in different studies with shifts from 25 °C to 15 ° (Takeuchi et al. 1996; Allakhverdiev and Murata 2004; Li et al. 2004). When leaves were treated with high irradiance or UV-B radiation at temperatures below 10 °C, the rate of PS II repair did not exceed 50 % relative to that at 20 °C (Ihle and Laasch 1996; Allakhverdiev and Murata 2004; Schultze and Bilger 2018). The repair of CPDs was inhibited in a manner similar to that of non-functional PSII (Takeuchi et al. 1996; Li et al. 2004). The rate of CPD repair, also called photorepair due to its activation by blue light, showed a light dependency, which increased in a curvilinear manner until 120 µmol m^{-2} s^{-1} (Takeuchi et al. 1996). In another publication similar repair rates at 50 and 350 m^{-2} s^{-1} were observed (Hidema et al. 1999). The impact of higher PPFDs on the rate of CPD repair seems to be unknown, yet. However, the rates of PS II repair declined by approximately 20 % at a photon irradiance above 1200 µmol m^{-2} s^{-1}, as compared to moderate PPFD levels between 350 and 700 µmol m^{-2} s^{-1} (He and Chow 2003). On the other hand, low temperature and high PAR levels just marginally reduced – if at all – rates of UV-driven damage of DNA or PS II (Takeuchi et al. 1996; Allakhverdiev and Murata 2004; Li et al. 2004; Schultze and Bilger 2018). As a consequence, more sites damaged by UV would accumulate if higher pigment concentrations did not mitigate the UV radiation under high light and low temperature conditions (Coffey et al. 2017; Schultze and Bilger 2018; Pescheck and Bilger 2019).

According to Campbell and Tyystjärvi (2012), mitigation of UV radiation under high visible light may also reduce photoinhibition through the protection of repair processes against UV. High PAR inhibits PS II as UV does, although through a different molecular process (Aro et al. 1993; Vass 2012). However, the resulting molecular damage is also recovered via the PSII repair cycle (Sass et al. 1997; Pescheck and Bilger 2020). The cycle is likely UV-susceptible, as it is dependent on several enzymes (Nixon et al. 2010; Campbell and Tyystjärvi 2012; Theis and Schroda 2016). UV-B can cause enzyme inactivation by photolysis of aromatic structures, disulfide or hydrogen bonds, which are relevant for the catalysing function (Setlow 1960; McLaren and Luse 1961; Cockell 1997). Furthermore, different reactive oxygen species (ROS), which are UV-inducible, highly oxidative by-products, promote PS II damage and inhibit PS II repair (Pospíšil et al. 2004; Murata et al. 2007; Vass 2012; Tyystjärvi 2013). If

not attenuated in the epidermis, penetrating UV-B radiation could impair repair via enzyme inactivation and ROS formation. However, repair rates under UV radiation are difficult to quantify, since on-going damage interferes. Thus, it remains speculative whether proposed mechanisms are physiologically relevant.

CQAs may not only prevent ROS formation by UV screening, but also scavenge ROS by their antioxidant function (Rice-Evans et al. 1996, 1997; Grace et al. 1998; Agati et al. 2013). Increased ROS formation can be detected in plants, when PPFD is high or temperature is low (Dreyer and Dietz 2018; Pescheck and Bilger 2020). If not scavenged, ROS can cause severe cellular damage at essential sites such as the D1 protein or organellar and nuclear DNA (Aro et al. 1993; Roldán-Arjona and Ariza 2009). Many of the phenylpropanoids including flavonoids as well as hydroxycinnamic acids can serve as radical scavengers (Rice-Evans et al. 1996, 1997; dos Santos Nascimento et al. 2020). Chlorogenic acid has an antioxidant potential for specific radicals exceeding that of ascorbic acid and comparable to that of kaempferol (Rice-Evans et al. 1997; Grace et al. 1998). It was shown to reduce oxidative stress induced by the herbicide paraquat *in vivo* (Niggeweg et al. 2004). Furthermore, the antioxidant activity of 3,5-DCQA, the abundant isomer in sunflower, was found to be in a comparable range to that of chlorogenic acid (Shang et al. 2010). In the present work, analysis of the antioxidant properties of CQAs in sunflowers was not conducted. In order to estimate, whether the CQAs function as antioxidants, it is worth to compare their localization with that of ROS formation. ROS are small, short-lived and highly reactive with other cellular components (Pospíšil 2016). Thus, their way of diffusion from their origin in the chloroplasts or other organelles through the cell is very likely to be short (Pospíšil 2016). If the CQAs played an essential role in radical scavenging, their localization should be spatially much closer to that of ROS formation than it is. However, ROS may diffuse into epidermal vacuoles if the main antioxidant systems such as the glutathione-ascorbate cycle are working on its limits of capacity (Noctor and Foyer 1998; Samson et al. 2020). Under certain conditions, CQAs of sunflower leaves were oxidised, even resulting in a loss of epidermal UV absorbance (Samson et al. 2020). However, comparatively high concentrations of paraquat were used for the induction of oxidative stress (Böger and Kunert 1978; Niggeweg et al. 2004; Samson et al. 2020). Applied concentrations completely blocked photosynthesis within one hour so that a massive excess of electrons likely caused massive ROS production and, thus, massive oxidative stress exceeding the capacity of other antioxidant systems (Böger and Kunert 1978).

The different possible functions imply phenylpropanoids, such as CQAs, to have several functions. As plants are constantly exposed to various abiotic and biotic stressors, which simultaneously exert selection pressure, it appears easily conceivable that metabolites fulfil more than one function.

4.5 Possible consequences for sunflower cultivation

Sunflower oil is used for many applications in our everyday life including food industry, individual nutrition or cosmetics making sunflower a crop of major importance. The hydroxycinnamic acids, especially chlorogenic acid, in sunflower possess a strong antioxidative as well as health-promoting potential (Nabavi et al. 2017; Santana-Gálvez et al. 2017; Tajik et al. 2017). These secondary compounds are – besides the vegetative tissue – detectable in sunflower seeds, their flour and oil

(Sabir et al. 1974; Dorrell 1976a; Pedrosa et al. 2000; Romani et al. 2017; Jan et al. 2018). The optimisation of sunflower oil with respect to health beneficial compounds, thus, the (up)regulation of these secondary compounds is one important issue for food production but also of interest for the pharmaceutical and cosmetic industry. It has been shown that treatment of parental sunflowers with different elicitors also affects the CQA content in seeds (Jan et al. 2018). Assuming that regulation of CQA content in seeds upon different environmental conditions follows the same rules as it does in other plant parts, presented results can be useful for possible deductions for sunflower cultivation. Although the link between secondary metabolism and abiotic environment is well known for other phenylpropanoids in higher plants, the present work reports an analogous link between secondary metabolism and abiotic environment for CQA levels in sunflower.

Cultivation of sunflower as one of the important oil crops includes both, field- and greenhouse growth (Berglund et al. 2007; FAOSTAT 2023). The cultivation of sunflower in fields and greenhouses has been conducted since long time and is well established with respect to specific needs of the industry. Since field conditions include various abiotic (and biotic) variables that induce accumulation of mono- and di-caffeoylquinic acid, it does not seem surprising that outdoor grown plants contain high levels of these compounds (Figs. 3.18−3.19, 3.29) so that the data presented do not imply the need for any changes in the cultivation of these plants. Furthermore, the shown data result from mechanistic approaches with artificial growth conditions that are hardly comparable to the complex network of parameters in the field environment.

However, the presented work together with current state of public knowledge might provide indications for potential further optimisation of growth conditions of greenhouse-cultivated sunflowers. The glass or plastic of greenhouses most often blocks a considerable part − if not all − of the terrestrial UV-B radiation. Thus, greenhouse cultivation results in a lack of UV-B radiation, which effectively induced CQAs in sunflower (Figs. 3.20−3.27, 3.30−3.31). Plants and seeds may also contain potentially low, suboptimal levels of CQAs when cultivated year-round in greenhouses in moderate latitudes. This particularly applies during seasons when PAR levels are low, as implied by low pigment content of control plants (Figs. 3.20, 3.22, 3.24 and 3.26). Although UV-B radiation can severely impair humans' health and inhibit the plant's photosynthesis even in plants with high UV screening (Caldwell and Flint 1994; Cockell 1997; Flint and Caldwell 2003; Cechin et al. 2007; Takahashi et al. 2010; Pfeifer and Besaratinia 2012), its presence in greenhouses might be the easiest way to optimise sunflowers' CQA levels. Low doses of UV-B radiation emitted by white fluorescent tubes were already sufficient to induce CQA biosynthesis remarkably (Fig. 3.21). Without taking the risk of harmful doses which cause photoinhibition and yield loss, light in greenhouses could be provided by e.g. fluorescence tubes that emit a small amount of UV-B radiation in addition to white light (manufacturer's data, see also inset of Fig. 2.1B). Another possibility to apply low-dose UV-B would be the use of alternative materials for the greenhouses transparent for UV-B radiation.

Application of other abiotic stress such as low temperature or low nitrogen supply, which do not directly affect humans, appears inconvenient in greenhouses since these conditions strongly reduce biomass production (Cechin and de Fátima Fumis 2004; Bai et al. 2016). Their application would require careful consideration and testing of the trade-off between high CQA levels and reduction of

biomass. This testing would include further fine and co-ordinated, thus laborious, establishment of either concrete temperatures, nitrogen levels or a combination of these variables in order to find a reasonable balance between CQA accumulation and produced biomass. It is conceivable, that low temperature for example could be applied for a short period in order to induce the fast-responsive CQA accumulation but prevent yield loss at the same time. However, the approach of cooling down a greenhouse does not appear to be cost- and energy-efficient.

Furthermore, the present work provides strong evidence, that the foliar content of CQAs can be determined and monitored non-invasively by measuring the relative epidermal absorbance via chlorophyll fluorescence. In sunflower, the correlation is much stronger than for phenolic acids in other plants, likely due to predominant epidermal localization and absence of interfering absorbance by flavonoids (Burchard et al. 2000; Sytar et al. 2015). Portable chlorophyll-fluorometers could be used *in situ* to determine pre-harvest CQA levels.

4.6 Implications for future research

As discussed in more detail in chapter 4.3, reports on the positive regulation of phenylpropanoid biosynthesis by abiotic parameters such as UV, high PPFD and low temperature show the induction to be highly complex (Lillo et al. 2008; Løvdal et al. 2010; Pescheck and Bilger 2019, 2020; Palma et al. 2021). There does not to exist a uniform pattern across the different species on how the different classes of phenylpropanoids are regulated.

Rather, three distinct pattern types of how phenylpropanoid biosynthesis is coupled to a response mediating signalling cascade may be classified. Type 1 includes species, in which the flavonoid biosynthesis is positively regulated by the environment, whereas biosynthesis of HCAs is not or little affected. The type 1 pattern is found in species such as *Secale cereale* (Burchard et al. 2000), *Betula pendula* (Morales et al. 2010), *Vitis vinifera* (Kolb et al. 2001), *Salix myrsinifolia* (Nybakken et al. 2012), *Arabidopsis thaliana* (Neugart et al. 2019; Rai et al. 2019) and *Brassica oleracea* (Neugart et al. 2013). Whereas the first species belong to monocotyledons, the others belong to families of dicots including Betulaceae, Vitaceae and Brassicaceae. In species responding to abiotic stress according to the pattern of type 2, not only flavonoid levels but also HCA levels increase. Species in which both biosynthetic pathways are positively regulated together are for example *Solanum lycopersicum*, *Nicotiana tabacum* and *Solanum tuberosum, Lactuca sativa, Helianthus tuberosus, Zinnia elegans* and *Tagetes patula* (Fritz et al. 2006; André et al. 2009; Løvdal et al. 2010; Hoier 2012; Larbat et al. 2012b; Torras-Claveria et al. 2012; Becker et al. 2015; Martinez et al. 2016). These species belong to the euasterids I with the first three species as members of the family of Solanaceae followed by species of the Asteraceae family. In species of the pattern of type 3, the HCA biosynthesis is positively regulated, whereas biosynthesis of flavonoids is not or little affected. This type was found in species such as *Helianthus annuus, Helianthus debilis* or *Cynara cardunculus* (Figs. 3.24–3.29; Moglia et al. 2008; Hoier 2012). Hence, type 3 is found especially in the Asteraceae family.

Although current knowledge is by far not sufficient in order to establish a classification, the pattern types appear to coincide with the current taxonomical classification and thus, understanding of evolution. The pattern type 1 occurs in species of the rosidae clade whereas pattern type 2 is found

in species of the euasterid I clade. Whereas species of the euasterid I families Solanaceae and Asteraceae constantly show the pattern 2, the position of another family of the euasterid I clade appears exceptional. Within the Oleaceae, phenylpropanoids of *Ligustrum vulgare* respond according to pattern I (Agati et al. 2011a) and that of *Phyllirea latifolia* corresponds to type 2 pattern (Agati et al. 2011b). The pattern type 3 is found only in euasterids II. The assignment suggests that, during the evolution of the core eudicotyledons, specific events might have taken place, in which a particular signalling cascade (or part of it) was coupled to that of CQA biosynthesis and potentially later uncoupled from flavonoid biosynthesis.

Transcriptome analysis of type 2 species, in which flavonoid and CQA biosynthesis are positively regulated together, may show general principles of and potential analogies between flavonoid biosynthesis and that of CQAs and other HCAs. The potential analogy might include the homology of the components of the signal transduction cascade. Furthermore, transcriptome analysis of different CQA accumulating species, which are phylogenetically close relatives, may be of high potential in order to confine when shifts of coupling between biosynthesis and signalling cascades had taken place on an evolutionary scale. Sequence data may even allow reconstructing which events had taken place.

5 Summary

Most angiosperms accumulate flavonoids as UV-A screening pigments and hydroxycinnamic acids (HCAs) as UV-B screening pigments in their epidermis for their protection against UV induced damage in the underlying tissue. This thesis was initiated when preliminary phytochemical analysis of leaves of *Helianthus annuus* L. (sunflower) cv. Peredovick showed absence of flavonoids, indicating a different strategy of UV resistance in sunflower plants. The first aim of this thesis was to identify which compounds serve as foliar UV-A screening pigments in sunflower. For the identification, determination of epidermal UV-A absorbance via chlorophyll fluorescence was combined to analysis of high-pressure liquid chromatography and mass spectrometry. In the phenolic profiles of leaves with high UV-A absorbance, caffeoylquinic acids (CQAs), a group of hydroxycinnamic acids (HCAs), were identified as the only candidates for UV screening compounds. In extracts of the well-protected leaves, chlorogenic acid (CGA) and two isomers of di-caffeoylquinic acid (DCQA) were detected. In order to check, whether the CQAs were localized in the epidermal layer, fluorescence microscopy was conducted. The CQA-specific autofluorescence showed predominant accumulation in the protoplasts of epidermal cells suggesting the CQAs to provide the UV-A screening. The staining of leaf sections with Naturstoff reagent A confirmed absence of flavonoids.

When gradually protected sunflower leaves were analysed, the results showed that the epidermal UV-A absorbance was correlated in a non-linear manner to the foliar contents of the CQA moieties with a high coefficient of determination. The analysis of UV-A screening efficacy included photoinhibition experiments with the sunflower plants. When CQAs were abundant in high concentrations, they reduced the photoinhibitory potential of solar and artificially generated UV-A radiation by more than 90 % and ensured PS II protection up to wavelengths of circa 380 nm. The results of the photoinhibition experiments provide strong evidence for the CQAs to be effective UV-A screening compounds.

In the majority of flavonoid accumulating angiosperms, epidermal UV screening is induced by abiotic environmental parameters such as high UV-B levels, high photon flux densities of photosynthetically active radiation (PPFD), low temperature and nitrogen deficiency. In order to test, whether this pattern is transferable to sunflower, plants with initially low UV screening, which were shifted to either UV-B, high PPFD, low temperature or nitrogen deficiency using determination of epidermal UV screening via chlorophyll fluorescence. The epidermal UV screening in sunflower increased quickly under high UV-B, high PPFD and low temperature. In contrast, nitrogen depletion under low light conditions had no effect. Due to the close correlation of the epidermal UV screening to CQAs, it was hypothesized that the levels of the CQAs were regulated positively. For all inducing parameters, parallel HPLC analysis showed that the pool of CGA increased to the highest extent, followed by that of unidentified hydroxycinnamic acids and DCQAs. Sporadically, one to two flavonoids were induced in shifted plants, but they appeared in trace amounts. Coincident to the epidermal UV-A absorbance, the CQA accumulation started within the first 12 to 24 hours. The rate of change was dependent on the changed parameter, with UV-B inducing the fastest response and low temperature the slowest.

The enhanced accumulation of flavonoids is preceded by a transient transcriptional upregulation of biosynthetic key enzymes. In order to search for a transient transcriptional upregulation prior to the CQA accumulation, the mRNA abundance of three genes of hydroxycinnamoyl quinate CoA transferase (*HaHQT1-3*), one of the key enzymes responsible for CGA formation, was analysed by qRT-PCR at several time point after the shifts. For UV-B, high PPFD and low temperature, the mRNA levels of *HQT2* increased to a transient maximum. The increase started within the first 6 hours after the shift of all inducing parameters. After shifts in PPFD or temperature, the relative expression of the *HQT3* gene was increased transiently, too, but differentially to *HQT2*, whereas mRNA levels of *HQT1* displayed no changes. Under UV-B, the relative gene expression of *HQT3* was not affected, whereas *HQT1* increased slightly but not significantly. The pattern of the transient upregulation of mRNA levels suggests the underlying biosynthesis to be quickly responsive to the shifts and *HQT2* as the main gene responsible for the CQA biosynthesis.

In summary, this work promotes the understanding of the UV-A protecting mechanism of the sunflower (*Helianthus annuus* L. cv. Peredovick). Analysis of shifting experiments showed a quick positive regulation of this UV protecting mechanism by high UV-B levels, high PPFD and low temperature within one day. Preliminary data on the positive regulation by nitrogen depletion point towards a key role of the prevailing PPFD and towards a crosstalk of both parameters. Taken together, this work suggests – at least partially – an analogy between HCAs in *Helianthus annuus* and flavonoids in other angiosperms. This analogy concerns both, the UV protective function and the regulation by the analyzed abiotic parameters and opens a door to new research implications. Future research may reveal whether this analogous regulation coincides with a homologous signalling cascade.

6 Zusammenfassung

Die meisten Angiospermen akkumulieren Flavonoide als UV-A-Schutzpigmente und Hydroxyzimtsäuren als UV-B-Schutzpigmente in der Epidermis, um die physiologischen Prozesse im darunterliegenden Gewebe vor UV-induzierten Schäden zu schützen. Die vorliegende Arbeit wurde initiiert, als vorläufige phytochemische Analysen von Blättern von *Helianthus annuus* L. cv. Peredovick zeigten, dass keine Flavonoide vorhanden waren. Das Fehlen der Flavonoide deutete darauf hin, dass die Sonnenblume einen anderen Schutzmechanismus gegen UV-A als die meisten Angiospermen ausweist. Das erste Ziel dieser Arbeit war, die UV-A Schutzpigmente in der Sonnenblume zu identifizieren. Für die Identifikation wurde die Bestimmung der epidermalen UV-A-Abschirmung via Chlorophyllfluoreszenz mit phytochemischen Analysen durch High Pressure Liquid Chromatography (HPLC) und Massenspektrometrie kombiniert. In den phenolischen Profilen von Blättern mit hoher UV-A-Abschirmung wurden Derivate der Kaffeoylchinasäure, eine Gruppe der Hydroxyzimtsäuren, als einzige mögliche Kandidaten für den UV-A-Schutz identifiziert. In den Extrakten dieser Blätter wurde vor allem Chlorogensäure und Di-Kaffeoylchinasäure gefunden. Die epidermale UV-A-Abschirmung korrelierte mit einem hohen Bestimmtheitsmaß mit den Blattgehalten an Resten der Kaffeoylchinasäure. Um nachzuprüfen, ob sich die Derivate der Kaffeoylchinasäure in der Blattepidermis befinden, wurde Fluoreszenzmikroskopie eingesetzt. Die für Kaffeoylchinasäure spezifische Autofluoreszenz wurde vor allem in den Protoplasten epidermaler Zellen gefunden. Das Einsetzen von Naturstoffreagenz A bestätigte das Fehlen von Flavonoiden. Um die Effektivität des UV-A-Schutzes durch die Kaffeoylchinasäurederivate zu analysieren, wurden verschiedene Photoinhibitions-Experimente an Blättern mit unterschiedlicher UV-A-Abschirmung durchgeführt. Das Potential zur Photoinhibtion von solarer und künstlich erzeugter UV-A-Strahlung wurde um bis zu 90 % reduziert, wenn die Kaffeoylchinasäuren in hoher Konzentration vorhanden waren. Der Schutz von Photosystem II vor Strahlung mit Wellenlängen bis zu 380 nm war gewährleistet. Die Ergebnisse der Photoinhibitions-Experimente legen nahe, dass die Kaffeoylchinasäurederivate einen hinreichend guten UV-A Schutz bieten.

In den meisten der Angiospermen, die Flavonoide akkumulieren, wird die epidermale UV Abschirmungdurch abiotische Umweltfaktoren wie UV-B-Strahlung, eine hohe Photonenflussdichte im photosynthetisch aktiven Bereich (PPFD), niedrige Temperaturen oder Stickstoffmangel induziert. Um zu überprüfen, ob dieses Muster auch auf Kaffeoylchinasäurederivate in der Sonnenblume zutrifft, wurden Pflanzen mit eingangs geringer UV-Abschirmung den induzierenden Bedingungen ausgesetzt. Dafür wurden Pflanzen unter Schwachlicht angezogen und nach 3 bis 4 Wochen UV-B, einer hohen PPFD, einer niedrigen Temperatur oder Stickstoffmangel ausgesetzt. Der zeitliche Verlauf der epidermalen Abschirmung wurde mittels Chlorophyllfluoreszenz zu unterschiedlichen Zeitpunkten nach Veränderung des entsprechenden Faktors ermittelt. Die epidermale UV-A-Abschirmung stieg bei UV-B, hoher PPFD und niedriger Temperatur innerhalb von 24 Stunden an. Stickstoffmangel unter Schwachlicht-Bedingungen dagegen brachte keine Veränderung der Abschirmung mit sich. Wegen der hohen Korrelationsgüte zwischen der Abschirmung und der Blattgehalte an Kaffeoylchinasäurenderivaten, wurde angenommen, dass ein Anstieg der Gehalte der

Kaffeoylchinasäurederivatve für den Anstieg der Abschirmung verantwortlich war. Diese Hypothese wurde mittels HPLC überprüft. Für alle induziernden Faktoren zeigte die HPLC-Analyse, dass vor allem der Gehalt an Chlorogensäure anstieg, gefolgt von dem von nicht näher identifizierten Hydroxyzimtsäuren und Di-Kaffeoylchinasäure. Zeitgleich mit der epidermalen UV-Abschirmung begann die Akkumulation der Kaffeoylchinasäurederivate 12 bis 24 Stunden nach dem Umsetzen der Pflanzen. Die Änderungrate hing von dem veränderten Parameter ab. UV-B induzierte die schnellste Veränderung, die niedrige Temperatur die langsamste. Vereinzelt wurden ein bis zwei verschiedene Flavonoide in den umgesetzten Pflanzen entdeckt. Diese waren aber nur in sehr geringen Gehalten zu finden.

Der verstärkten Akkumulation von Flavonoiden geht eine transiente transkriptionalle Hochregulierung der Schlüsselenzyme der Biosynthese voran. Um zu untersuchen, ob vor der Akkumulation von Kaffeoylchinasäurederivaten ebenfalls eine transiente Hochregulierung eines Schlüsselenzyms stattfindet, wurden die relative Genexpression von drei Genen für die Hydroxycinnamoyl-Quinate-CoA-Transferase (HaHQT1-3) mittels qRT-PCR auf Transkriptebene zu unterschiedlichen Zeitpunkten nach dem Transfer analysiert. Unter UV-B, hoher PPFD und der niedrigen Temperatur stiegen die relativen Transkriptlevel von *HQT2* auf ein vorrübergehendes Maximum an. Für alle drei Parameter begann dieser Anstieg innerhalb der ersten 6 Stunden nach dem Transfer. Unter einer hohen PPFD oder einer niedrigen Temperatur stiegen auch die relativen Transkriptlevel von *HQT3* vorrübergehend an, allerdings sah der zeitliche Verlauf anders als bei *HQT2* aus. Die relativen Transkriptlevel von *HQT1* zeigten unter hoher PPFD oder niedrigen Temperature keine Veränderungen. Nach UV-B-Exposition blieben die relativen Transkriptlevel von *HQT3* unverändert, während die von *HQT1* schwach, aber in nicht-signifikanter Weise, anstieg. Das Muster der transienten Hochregulierung deutet darauf hin, dass die Biosynthese der Kaffeoylchinasäurederivate schnell auf abrupte Veränderungen der UV-B-Strahlung, zu hoher PPFD oder niedriger Temperatur im PPFD reagieren kann. Außerdem scheint vor allem die Genexpression von *HQT2* entscheidend für die Biosynthese der Kaffesäurederivate zu sein.

Zusammenfassend trägt diese Arbeit zum Verständnis des Schutzmechanimus vor UV-A-Strahlung in der Sonnenblume (*Helianthus annuus* L. cv. Peredovick) bei. Die Umsetzversuche zeigten eine schnell einsetzende positive Regulierung dieses Schutzmechanismus als Reaktion auf UV-B, hohe PPFD und eine niedrige Temperatur innerhalb eines Tages. Vorläufige Daten zur positiven Regulation durch Stickstoffmangel implizieren eine wichtige Rolle für die photosynthetisch aktive Strahlung und legen einen Crosstalk zwischen der Regulierung durch das Stickstofflevel und der vorherrschenden PPFD nahe. Abschließend legten die Ergebnisse dieser Arbeit nahe, dass es − zumindest teilweise − Analogien zwischen Hydroxyzimtsäuren in der Sonnenblume und Flavonoiden in vielen Angiospmern bestehen. Diese Analogien betreffen sowohl den UV-A-Schutzmechanismus als auch die positive Regulierung durch UV-B, hohe PPFD oder eine niedrige Temperature und eröffnen neue Fragestellungen für die Forschung.

7 References

Agati G, Azzarello E, Pollastri S, Tattini M (2012) Flavonoids as antioxidants in plants: Location and functional significance. Plant Sci 196: 67–76

Agati G, Biricolti S, Guidi L, Ferrini F, Fini A, Tattini M (2011a) The biosynthesis of flavonoids is enhanced similarly by UV radiation and root zone salinity in *L. vulgare* leaves. J Plant Physiol 168: 204–212

Agati G, Brunetti C, Di Ferdinando M, Ferrini F, Pollastri S, Tattini M (2013) Functional roles of flavonoids in photoprotection: New evidence, lessons from the past. Plant Physiol Biochem 72: 35–45

Agati G, Cerovic ZG, Pinelli P, Tattini M (2011b) Light-induced accumulation of ortho-dihydroxylated flavonoids as non-destructively monitored by chlorophyll fluorescence excitation techniques. Environ Exp Bot 73: 3–9

Agati G, Stefano G, Biricolti S, Tattini M (2009) Mesophyll distribution of 'antioxidant' flavonoid glycosides in *Ligustrum vulgare* leaves under contrasting sunlight irradiance. Ann Bot 104: 853–861

Agati G, Tattini M (2010) Multiple functional roles of flavonoids in photoprotection. New Phytol 186: 786–793

Alfonso L, Ai G, Spitale RC, Bhat GJ (2014) Molecular targets of aspirin and cancer prevention. Br J Cancer 111: 61–67

Allakhverdiev SI, Murata N (2004) Environmental stress inhibits the synthesis de novo of proteins involved in the photodamage–repair cycle of Photosystem II in Synechocystis sp. PCC 6803. Biochim Biophys Acta 1657: 23–32

André CM, Schafleitner R, Legay S, Lefèvre I, Aliaga CAA, Nomberto G, Hoffmann L, Hausman J-F, Larondelle Y, Evers D (2009) Gene expression changes related to the production of phenolic compounds in potato tubers grown under drought stress. Phytochemistry 70: 1107–1116

Arias DM, Rieseberg LH (1995) Genetic relationships among domesticated and wild sunflowers (*Helianthus annuus*, Asteraceae). Econ Bot 49: 239–248

Aro E-M, Virgin I, Andersson B (1993) Photoinhibition of Photosystem II. Inactivation, protein damage and turnover. Biochim Biophys Acta BBA - Bioenerg 1143: 113–134

de Ávila Silva L, Omena-Garcia RP, Condori-Apfata JA, Costa PM de A, Silva NM, DaMatta FM, Zsögön A, Araújo WL, de Toledo Picoli EA, Sulpice R, Nunes-Nesi A (2021) Specific leaf area is modulated by nitrogen via changes in primary metabolism and parenchymal thickness in pepper. Planta 253: 16

Bachmann KM, Ebbert V, Adams III WW, Verhoeven AS, Logan BA, Demmig-Adams B (2004) Effects of lincomycin on PSII efficiency, non-photochemical quenching, D1 protein and xanthophyll cycle during photoinhibition and recovery. Funct Plant Biol 31: 803–13

Bachmann O (1978) Distribution of phenolic acids and flavonoids in Vitaceae. Vitis 17: 234–257

Badouin H, Gouzy J, Grassa CJ, Murat F, Staton SE, Cottret L, Lelandais-Brière C, Owens GL, Carrère S, Mayjonade B, Legrand L, Gill N, Kane NC, Bowers JE, Hubner S, Bellec A, Bérard A, Bergès H, Blanchet N, Boniface M-C, Brunel D, Catrice O, Chaidir N, Claudel C, Donnadieu C, Faraut T,

Fievet G, Helmstetter N, King M, Knapp SJ, Lai Z, Le Paslier M-C, Lippi Y, Lorenzon L, Mandel JR, Marage G, Marchand G, Marquand E, Bret-Mestries E, Morien E, Nambeesan S, Nguyen T, Pegot-Espagnet P, Pouilly N, Raftis F, Sallet E, Schiex T, Thomas J, Vandecasteele C, Varès D, Vear F, Vautrin S, Crespi M, Mangin B, Burke JM, Salse J, Muños S, Vincourt P, Rieseberg LH, Langlade NB (2017) The sunflower genome provides insights into oil metabolism, flowering and Asterid evolution. Nature 546: 148–152

Bai L, Deng H, Zhang X, Yu X, Li Y (2016) Gibberellin is involved in inhibition of cucumber growth and nitrogen uptake at suboptimal root-zone temperatures. PLOS ONE 11: e0156188

Bargholz L (2012) Induktion der Chlorogensäure-biosynthese durch Umweltfakturen bei *Helianthus annuus*. Diploma thesis. Christian-Albrechts-Universität, Kiel

Barnes PW, Flint SD, Tobler MA, Ryel RJ (2016a) Diurnal adjustment in ultraviolet sunscreen protection is widespread among higher plants. Oecologia 181: 55–63

Barnes PW, Kersting AR, Flint SD, Beyschlag W, Ryel RJ (2013) Adjustments in epidermal UV-transmittance of leaves in sun-shade transitions. Physiol Plant 149: 200–213

Barnes PW, Tobler MA, Keefover-Ring K, Flint SD, Barkley AE, Ryel RJ, Lindroth RL (2016b) Rapid modulation of ultraviolet shielding in plants is influenced by solar ultraviolet radiation and linked to alterations in flavonoids: Rapid modulation of UV sunscreen protection. Plant Cell Environ 39: 222–230

Bartley GE, Avena-Bustillos RJ, Du W-X, Hidalgo M, Cain B, Breksa AP (2016) Transcriptional regulation of chlorogenic acid biosynthesis in carrot root slices exposed to UV-B light. Plant Gene 7: 1–10

Becker C, Urlić B, Jukić Špika M, Kläring H-P, Krumbein A, Baldermann S, Goreta Ban S, Perica S, Schwarz D (2015) Nitrogen limited red and green leaf lettuce accumulate flavonoid glycosides, caffeic acid derivatives, and sucrose while losing chlorophylls, β-carotene and xanthophylls. PLoS ONE 10: (11): e0142867

Beggs CJ, Wellmann E (1994) Photocontrol of flavonoid biosynthesis. In: Kendrick RE, Kronenberg GHM (eds) Photomorphogenesis in Plants. Springer Netherlands, Dordrecht, pp. 733–751

Bennett RN, Wallsgrove RM (1994) Tansley Review No. 72. Secondary metabolites in plant defence mechanisms. New Phytol 127: 617–633

Bentley R (1997) Secondary metabolites play primary roles in human affairs. Perspect Biol Med 40: 197–221

Berglund DR, Ashley R, Bradley C, Brewer G, Charlet L, Endres G, Flaskerud G, Franzen D, Gulya T, Hanzel J, Hellevang Kenneth, Hofman VL, Kleingartner L, Knodel J, Lardy G, Linz G, Markell S, Miller J, Sandbakken J, Scherer T, Tanaka D, Zollinger R (2007) Sunflower Production. NDSU (North Dakota State University) Extentsion Service and North Dakota (N.D.) Agricultural Experiment Station

Bergmann S (2021) Die Dynamik der epidermalen UV-Abschirmung von *Solanum lycopersicum* im Tagesverlauf. Bachelor thesis. Christian-Albrechts-Universität zu Kiel, Kiel

Bernal M, Llorens L, Badosa J, Verdaguer D (2013) Interactive effects of UV radiation and water availability on seedlings of six woody Mediterranean species. Physiol Plant 147: 234–247

Bhatia C, Gaddam SR, Pandey A, Trivedi PK (2021) COP1 mediates light-dependent regulation of flavonol biosynthesis through HY5 in *Arabidopsis*. Plant Sci 303: 110760

Bhatia C, Pandey A, Gaddam SR, Hoecker U, Trivedi PK (2018) Low temperature-enhanced flavonol synthesis requires light-associated regulatory components in *Arabidopsis thaliana*. Plant Cell Physiol 59: 2099–2112

Biała W, Jasiński M (2018) The phenylpropanoid case – It is transport that matters. Front Plant Sci 9: 1610

Bidel LPR, Meyer S, Goulas Y, Cadot Y, Cerovic ZG (2007) Responses of epidermal phenolic compounds to light acclimation: In vivo qualitative and quantitative assessment using chlorophyll fluorescence excitation spectra in leaves of three woody species. J Photochem Photobiol B 88: 163–179

Bidel LPR, Meyer S, Talhouët A-C, Baudin X, Daniel C, Cazals G, Streb P (2020) Epidermal UVA screening capacity measured in situ as an indicator of light acclimation state of leaves of a very plastic alpine plant *Soldanella alpina* L. Plant Physiol Biochem 151: 10–20

Bilger W, Johnsen T, Schreiber U (2001) UV-excited chlorophyll fluorescence as a tool for the assessment of UV-protection by the epidermis of plants. J Exp Bot 52: 2007–2014

Bilger W, Rolland M, Nybakken L (2007) UV screening in higher plants induced by low temperature in the absence of UV-B radiation. Photochem Photobiol Sci 6: 190

Bilger W, Veit M, Schreiber L, Schreiber U (1997) Measurement of leaf epidermal transmittance of UV radiation by chlorophyll fluorescence. Physiol Plant 101: 754–763

Björkman O, Demmig B (1987) Photon yield of O_2 evolution and chlorophyll fluorescence characteristics at 77 K among vascular plants of diverse origins. Planta 170: 489–504

Björn LO (2015) Ultraviolet-A, B, and C. UV4Plants Bull 2015: 17–18

Böger P, Kunert KJ (1978) Phytotoxic action of paraquat on the photosynthetic apparatus. Z Für Naturforschung C 33: 688–694

Bornman JF, Barnes PW, Robson TM, Robinson SA, Jansen MAK, Ballaré CL, Flint SD (2019) Linkages between stratospheric ozone, UV radiation and climate change and their implications for terrestrial ecosystems. Photochem Photobiol Sci 18: 681–716

Böttcher C (2020) Induktionskinetik der transkriptlevel der Hydroxycinnamoyl-CoA Quinat Hydroxycinnamoyl Tranferase bei starkem Weißlicht in *Helianthus annuus* (L.). Bachelor thesis. Christian-Albrechts-Universität, Kiel

Bouguyon E, Gojon A, Nacry P (2012) Nitrate sensing and signaling in plants. Semin Cell Dev Biol 23: 648–654

Brauch D, Porzel A, Schumann E, Pillen K, Mock H-P (2018) Changes in isovitexin-O-glycosylation during the development of young barley plants. Phytochemistry 148: 11–20

Broeze RJ, Solomon CJ, Pope DH (1978) Effects of low temperature on in vivo and in vitro protein synthesis in *Escherichia coli* and *Pseudomonas fluorescens*. J Bacteriol 134: 861–874

Brown BA, Cloix C, Jiang GH, Kaiserli E, Herzyk P, Kliebenstein DJ, Jenkins GI (2005) A UV-B-specific signaling component orchestrates plant UV protection. Proc Natl Acad Sci 102: 18225–18230

Brown BA, Jenkins GI (2008) UV-B signaling pathways with different fluence-rate response profiles are distinguished in mature *Arabidopsis* leaf tissue by requirement for UVR8, HY5, and HYH. Plant Physiol 146: 576–588

Brown NF, Anderson RC, Caplan SL, Foster DW, McGarry JD (1994) Catalytically important domains of rat carnitine palmitoyltransferase II as determined by site-directed mutagenesis and chemical modification. Evidence for a critical histidine residue. J Biol Chem 269: 19157–19162

Burchard P, Bilger W, Weissenböck G (2000) Contribution of hydroxycinnamates and flavonoids to epidermal shielding of UV-A and UV-B radiation in developing rye primary leaves as assessed by ultraviolet-induced chlorophyll fluorescence measurements. Plant Cell Environ 23: 1373–1380

Caldwell MM, Flint SD (1994) Stratospheric ozone reduction, solar UV-B radiation and terrestrial ecosystems. Clim Change 28: 375–394

Caldwell MM, Robberecht R, Flint SD (1983) Internal filters: Prospects for UV-acclimation in higher plants. Physiol Plant 58: 445–450

Campbell DA, Tyystjärvi E (2012) Parameterization of photosystem II photoinactivation and repair. Biochim Biophys Acta -Bioenerg 1817: 258–265

Cartelat A, Cerovic ZG, Goulas Y, Meyer S, Lelarge C, Prioul J-L, Barbottin A, Jeuffroy M-H, Gate P, Agati G, Moya I (2005) Optically assessed contents of leaf polyphenolics and chlorophyll as indicators of nitrogen deficiency in wheat (*Triticum aestivum* L.). Field Crops Res 91: 35–49

Casal JJ, Balasubramanian S (2019) Thermomorphogenesis. Annu Rev Plant Biol 70: 321–346

Catalá R, Medina J, Salinas J (2011) Integration of low temperature and light signaling during cold acclimation response in *Arabidopsis*. Proc Natl Acad Sci 108: 16475–16480

Cechin I, de Fátima Fumis T (2004) Effect of nitrogen supply on growth and photosynthesis of sunflower plants grown in the greenhouse. Plant Sci 166: 1379–1385

Cechin I, Fumis T de F, Dokkedal AL (2007) Growth and physiological responses of sunflower plants exposed to ultraviolet-B radiation. Ciênc Rural 37: 85–90

Cetinkaya H, Kulak M, Karaman M, Karaman HS, Kocer F (2017) Flavonoid accumulation behavior in response to the abiotic stress: Can a uniform mechanism be illustrated for all plants? In: Justino GC (ed) Flavonoids - From Biosynthesis to Human Health. IntechOpen Limited., London

Cha JW, Piao MJ, Kim KC, Yao CW, Zheng J, Kim SM, Hyun CL, Ahn YS, Hyun JW (2014) The polyphenol chlorogenic acid attenuates UVB-mediated oxidative stress in human HaCaT keratinocytes. Biomol Ther 22: 136–142

Chappell J, Hahlbrock K (1984) Transcription of plant defence genes in response to UV light or fungal elicitor. Nature 311: 76–78

Chapple CC, Vogt T, Ellis BE, Somerville CR (1992) An *Arabidopsis* mutant defective in the general phenylpropanoid pathway. Plant Cell 4: 1413–1424

Cheevarungnapakul K, Khaksar G, Panpetch P, Boonjing P, Sirikantaramas S (2019) Identification and functional characterization of genes involved in the biosynthesis of caffeoylquinic acids in sunflower (*Helianthus annuus* L.). Front Plant Sci 10: 968

Christie JM, Jenkins GI (1996) Distinct UV-B and UV-A/blue light signal transduction pathways induce chalcone synthase gene expression in Arabidopsis cells. Plant Cell 8: 1555–1567

Christie PJ, Alfenito MR, Walbot V (1994) Impact of low-temperature stress on general phenylpropanoid and anthocyanin pathways: Enhancement of transcript abundance and anthocyanin pigmentation in maize seedlings. Planta 194: 541–549

CIE, International Commission on Illumination (2014) Rationalizing nomenclature for UV doses and effects on humans. CIE Central Bureau, Vienna

Clé C, Hill LM, Niggeweg R, Martin CR, Guisez Y, Prinsen E, Jansen MAK (2008) Modulation of chlorogenic acid biosynthesis in *Solanum lycopersicum*; consequences for phenolic accumulation and UV-tolerance. Phytochemistry 69: 2149–2156

Clifford MN (1999) Chlorogenic acids and other cinnamates - nature, occurrence and dietary burden. J Sci Food Agric 79: 362–372

Cockell CS (1997) Ultraviolet radiation, evolution and the π-electron system. Biol J Linn Soc 63: 449–457

Cockell CS, Knowland J (1999) Ultraviolet radiation screening compounds. Biol Rev Camb Philos Soc 74: 311–345

Coffey A, Prinsen E, Jansen M a. k., Conway J (2017) The UVB photoreceptor UVR8 mediates accumulation of UV-absorbing pigments, but not changes in plant morphology, under outdoor conditions. Plant Cell Environ 40: 2250–2260

Comino C, Hehn A, Moglia A, Menin B, Bourgaud F, Lanteri S, Portis E (2009) The isolation and mapping of a novel hydroxycinnamoyltransferase in the globe artichoke chlorogenic acid pathway. BMC Plant Biol 9: 30

Comino C, Lanteri S, Portis E, Acquadro A, Romani A, Hehn A, Larbat R, Bourgaud F (2007) Isolation and functional characterization of a cDNA coding a hydroxycinnamoyltransferase involved in phenylpropanoid biosynthesis in *Cynara cardunculus* L. BMC Plant Biol 7: 14

Coronado C, Zuanazzi Jas, Sallaud C, Quirion JC, Esnault R, Husson HP, Kondorosi A, Ratet P (1995) Alfalfa root flavonoid production Is nitrogen regulated. Plant Physiol 108: 533–542

Coruzzi GM, Zhou L (2001) Carbon and nitrogen sensing and signaling in plants: emerging 'matrix effects'. Curr Opin Plant Biol 4: 247–253

Cramer GR, Urano K, Delrot S, Pezzotti M, Shinozaki K (2011) Effects of abiotic stress on plants: a systems biology perspective. BMC Plant Biol 11: 163

Cronn R, Brothers M, Klier K, Bretting PK, Wendel JF (1997) Allozyme variation in domesticated annual sunflower and its wild relatives: Theor Appl Genet 95: 532–545

Crozier A, Jaganath IB, Clifford MN (2009) Dietary phenolics: chemistry, bioavailability and effects on health. Nat Prod Rep 26: 1001–1043

Crozier A, Lean MEJ, McDonald MS, Black C (1997) Quantitative analysis of the flavonoid content of commercial tomatoes, onions, lettuce, and celery. J Agric Food Chem 45: 590–595

Csepregi K, Coffey A, Cunningham N, Prinsen E, Hideg É, Jansen MAK (2017) Developmental age and UV-B exposure co-determine antioxidant capacity and flavonol accumulation in *Arabidopsis* leaves. Environ Exp Bot 140: 19–25

Cullen JJ, Lesser MP (1991) Inhibition of photosynthesis by ultraviolet radiation as a function of dose and dosage rate: Results for a marine diatom. Mar Biol 111: 183–190

Davies KM, Jibran R, Zhou Y, Albert NW, Brummell DA, Jordan BR, Bowman JL, Schwinn KE (2020) The Evolution of Flavonoid Biosynthesis: A Bryophyte Perspective. Front Plant Sci 11: 7

Day TA (1993) Relating UV-B radiation screening effectiveness of foliage to absorbing-compound concentration and anatomical characteristics in a diverse group of plants. Oecologia 95: 542–550

Day TA, Howells BW, Rice WJ (1994) Ultraviolet absorption and epidermal-transmittance spectra in foliage. Physiol Plant 92: 207–218

Day TA, Martin G, Vogelmann TC (1993) Penetration of UV-B radiation in foliage: evidence that the epidermis behaves as a non-uniform filter. Plant Cell Environ 16: 735–741

Delker C, Sonntag L, James GV, Janitza P, Ibañez C, Ziermann H, Peterson T, Denk K, Mull S, Ziegler J, Davis SJ, Schneeberger K, Quint M (2014) The DET1-COP1-HY5 pathway constitutes a multipurpose signaling module regulating plant photomorphogenesis and thermomorphogenesis. Cell Rep 9: 1983–1989

DeLong JP, Gibert JP, Luhring TM, Bachman G, Reed B, Neyer A, Montooth KL (2017) The combined effects of reactant kinetics and enzyme stability explain the temperature dependence of metabolic rates. Ecol Evol 7: 3940–3950

Demain AL, Fang A (2000) The natural functions of secondary metabolites. In: Fiechter A (ed) History of modern biotechnology I. Springer Berlin Heidelberg, Berlin, Heidelberg

Demkura PV, Ballaré CL (2012) UVR8 mediates UV-B-induced *Arabidopsis* defense responses against *Botrytis cinerea* by controlling sinapate accumulation. Mol Plant 5: 642–652

Dixon RA, Paiva NL (1995) Stress-induced phenylpropanoid metabolism. Plant Cell 7: 1085–1097

Docimo T, Francese G, Ruggiero A, Batelli G, De Palma M, Bassolino L, Toppino L, Rotino GL, Mennella G, Tucci M (2016) Phenylpropanoids accumulation in eggplant fruit: characterization of biosynthetic genes and regulation by a MYB transcription factor. Front Plant Sci 6: 1233

Docimo T, Mattana M, Fasano R, Consonni R, de Tommasi N, Coraggio I, Leone A (2013) Ectopic expression of the Osmyb4 rice gene enhances synthesis of hydroxycinnamic acid derivatives in tobacco and clary sage. Biol Plant 57: 179–183

Dorrell DG (1976a) Chlorogenic acid content of sunflower seed flour as affected by seeding and harvest date. Can J Plant Sci 56: 901–905

Dorrell DG (1976b) Chlorogenic acid content of meal from cultivated and wild sunflowers. Crop Sci 16: 422–424

Dreyer A, Dietz K-J (2018) Reactive oxygen species and the redox-regulatory network in cold stress acclimation. Antioxidants 7: 169

Duan S-B, Li Z-L, Tang B-H, Wu H, Tang R (2014) Direct estimation of land-surface diurnal temperature cycle model parameters from MSG–SEVIRI brightness temperatures under clear sky conditions. Remote Sens Environ 150: 34–43

Engelsma G (1974) On the mechanism of the changes in phenylalanine ammonia-lyase activity induced by ultraviolet and blue light in gherkin hypocotyls. Plant Physiol 54: 702–705

Engelsma G, Meijer G (1965) The influence of light of different spectral regions on the synthesis of phenolic compounds in gherkin seedlings in relation to photomorphogenesis. Acta Bot Neerlandica 14: 54–72

Fallovo C, Schreiner M, Schwarz D, Colla G, Krumbein A (2011) Phytochemical changes induced by different nitrogen supply forms and radiation levels in two leafy *Brassica* species. J Agric Food Chem 59: 4198–4207

FAOSTAT (2023) Crops and livestock products. Available At https://www.fao.org/faostat/en/#data/QCL (accessed 6 April 2022)

Fernandez O, Urrutia M, Berton T, Bernillon S, Deborde C, Jacob D, Maucourt M, Maury P, Duruflé H, Gibon Y, Langlade NB, Moing A (2019) Metabolomic characterization of sunflower leaf allows discriminating genotype groups or stress levels with a minimal set of metabolic markers. Metabolomics 15: 56

Flint SD, Caldwell MM (2003) A biological spectral weighting function for ozone depletion research with higher plants. Physiol Plant 117: 137–144

Franke R, Humphreys JM, Hemm MR, Denault JW, Ruegger MO, Cusumano JC, Chapple C (2002) The *Arabidopsis* REF8 gene encodes the 3-hydroxylase of phenylpropanoid metabolism. Plant J 30: 33–45

Fritz C, Palacios-Rojas N, Feil R, Stitt M (2006) Regulation of secondary metabolism by the carbon–nitrogen status in tobacco: nitrate inhibits large sectors of phenylpropanoid metabolism. Plant J 46: 533–548

Fuglevand G, Jackson JA, Building B (1996) UV-B, UV-A, and blue light signal transduction pathways interact synergistically to regulate chalcone synthase gene expression in *Arabidopsis*. Plant Cell 8: 2347–2357

Gai F, Karamać M, Janiak MA, Amarowicz R, Peiretti PG (2020) Sunflower (*Helianthus annuus* L.) plants at various growth stages subjected to extraction—comparison of the antioxidant activity and phenolic profile. Antioxidants 9: 535

Gao Q, Garcia-Pichel F (2011) Microbial ultraviolet sunscreens. Nat Rev Microbiol 9: 791–802

Garcia-Pichel F, Castenholz RW (1991) Characterization and biological implications of scytonemin, a cyanobacterial sheath pigment. J Phycol 27: 395–409

Gemeinholzer B (2018) Systematik der Pflanzen kompakt. Springer Berlin Heidelberg, Berlin, Heidelberg

Gent L, Forde BG (2017) How do plants sense their nitrogen status? J Exp Bot 68: 2531–2539

Ghetti F, Herrmann H, Häder D-P, Seidlitz HK (1999) Spectral dependence of the inhibition of photosynthesis under simulated global radiation in the unicellular green alga *Dunaliella salina*. J Photochem Photobiol B 48: 166–173

Goulas Y, Cerovic ZG, Cartelat A, Moya I (2004) Dualex: a new instrument for field measurements of epidermal ultraviolet absorbance by chlorophyll fluorescence. Appl Opt 43: 4488

Govindjee R, Rabinowitch E, Govindjee (1968) Maximum quantum yield and action spectrum of photosynthesis and fluorescence in *Chlorella*. Biochim Biophys Acta - Bioenerg 162: 539–544

Grace SC, Logan BA, Adams WW (1998) Seasonal differences in foliar content of chlorogenic acid, a phenylpropanoid antioxidant, in *Mahonia repens*. Plant Cell Environ 21: 513–521

Greenberg BM, Gaba V, Canaani O, Malkin S, Mattoo AK, Edelman M (1989) Separate photosensitizers mediate degradation of the 32-kDa photosystem II reaction center protein in the visible and UV spectral regions. Proc Natl Acad Sci 86: 6617–6620

Grennan AK, Ort DR (2007) Cool temperatures interfere with D1 synthesis in tomato by causing ribosomal pausing. Photosynth Res 94: 375–385

Greßmann H (2019) Die Auswirkung niedriger Temperaturen auf die epidrmale UV-Abschirmung in den Blättern von *Helianthus annuus*. Bachelor thesis. Christian-Albrechts-Universität, Kiel

Grundy J, Stoker C, Carré IA (2015) Circadian regulation of abiotic stress tolerance in plants. Front Plant Sci 6: 648

Guidi L, Brunetti C, Fini A, Agati G, Ferrini F, Gori A, Tattini M (2016) UV radiation promotes flavonoid biosynthesis, while negatively affecting the biosynthesis and the de-epoxidation of xanthophylls: Consequence for photoprotection? Environ Exp Bot 127: 14–25

Gutierrez E, García-Villaraco A, Lucas JA, Gradillas A, Gutierrez-Mañero FJ, Ramos-Solano B (2017) Transcriptomics, targeted metabolomics and gene expression of blackberry leaves and fruits indicate flavonoid metabolic flux from leaf to red fruit. Front Plant Sci 8:

Hahlbrock K, Wellmann E (1970) Light-induced flavone biosynthesis and activity of phenylalanine ammonia-lyase and UDP-apiose synthetase in cell suspension cultures of *Petroselinum hortense*. Planta 94: 236–239

Hakala M (2006) Photoinhibition of manganese enzymes: insights into the mechanism of photosystem II photoinhibition. J Exp Bot 57: 1809–1816

Hakala M, Tuominen I, Keränen M, Tyystjärvi T, Tyystjärvi E (2005) Evidence for the role of the oxygen-evolving manganese complex in photoinhibition of photosystem II. Biochim Biophys Acta BBA - Bioenerg 1706: 68–80

Hakala-Yatkin M, Mäntysaari M, Mattila H, Tyystjärvi E (2010) Contributions of visible and ultraviolet parts of sunlight to photoinhibition. Plant Cell Physiol 51: 1745–1753

Hang R, Wang Z, Deng X, Liu C, Yan B, Yang C, Song X, Mo B, Cao X (2018) Ribosomal RNA Biogenesis and Its Response to Chilling Stress in *Oryza sativa*. Plant Physiol 177: 381–397

Hannah MA, Caldana C, Steinhauser D, Balbo I, Fernie AR, Willmitzer L (2010) Combined Transcript and Metabolite Profiling of Arabidopsis Grown under Widely Variant Growth Conditions Facilitates the Identification of Novel Metabolite-Mediated Regulation of Gene Expression. Plant Physiol 152: 2120–2129

Harbaum B, Hubbermann EM, Zhu Z, Schwarz K (2008) Free and bound phenolic compounds in leaves of pak choi (*Brassica campestris* L. ssp. *chinensis* var. *communis*) and Chinese leaf mustard (*Brassica juncea* Coss). Food Chem 110: 838–846

Harborne JB (2007) Role of secondary metabolites in chemical defence mechanisms in plants. In: Chadwick DJ, Marsh J (eds) Novartis Foundation Symposia. John Wiley & Sons, Ltd., Chichester, UK

He J, Chow WS (2003) The rate coefficient of repair of photosystem II after photoinactivation. Physiol Plant 118: 297–304

Heiser C, Lentz DL, Pohl MED, Pope KO (2001) About Sunflowers... [with Author's Reply]. Econ Bot 55: 470–472

Heiser, CBJunior (1951) The sunflower among the North American Indians. Proc Am Philos Soc 95: 432–448

Hemm MR, Herrmann KM, Chapple C (2001) AtMYB4: a transcription factor general in the battle against UV. Trends Plant Sci 6: 135–136

Herms DA, Mattson WJ (1992) The dilemma of plants: To grow or defend. Q Rev Biol 67: 283–335

Herrmann H, Häder D-P, Ghetti F (1997) Inhibition of photosynthesis by solar radiation in *Dunaliella salina*: relative efficiencies of UV-B, UV-A and PAR. Plant Cell Environ 20: 359–365

Hidema J, Kang H-S, Kumagai T (1999) Changes in cyclobutyl pyrimidine dimer levels in rice (*Oryza sativa* L.) growing indoors and outdoors with or without supplemental UV-B radiation. J Photochem Photobiol B 52: 7–13

Hoffmann L (2004) Silencing of hydroxycinnamoyl-Coenzyme A shikimate/quinate hydroxycinnamoyltransferase affects phenylpropanoid biosynthesis. PLANT CELL ONLINE 16: 1446–1465

Hoffmann L, Besseau S, Geoffroy P, Ritzenthaler C, Meyer D, Lapierre C, Pollet B, Legrand M (2004) Silencing of hydroxycinnamoyl-Coenzyme A shikimate/quinate hydroxycinnamoyltransferase affects phenylpropanoid biosynthesis. Plant Cell 16: 1446–1465

Hoffmann L, Maury S, Martz F, Geoffroy P, Legrand M (2003) Purification, cloning, and properties of an acyltransferase controlling shikimate and quinate ester intermediates in phenylpropanoid metabolism. J Biol Chem 278: 95–103

Hofmann RW, Campbell BD, Bloor SJ, Swinny EE, Markham KR, Ryan KG, Fountain DW (2003) Responses to UV-B radiation in *Trifolium repens* L. - physiological links to plant productivity and water availability: Acclimation to UV-B linked to productivity and drought. Plant Cell Environ 26: 603–612

Hoier S (2012) Akkumulation von Polyphenolen bei Asteraceen mit unterschiedlicher Beziehung zur Gattung *Helianthus*. Bachelor thesis. Christian-Albrechts-Universität, Kiel

Hollósy F (2002) Effects of ultraviolet radiation on plant cells. Micron 33: 179–197

Huang L, Zhang H, Zhang H, Deng XW, Wei N (2015) HY5 regulates nitrite reductase 1 (NIR1) and ammonium transporter1;2 (AMT1;2) in Arabidopsis seedlings. Plant Sci 238: 330–339

Hussein RA, El-Anssary AA (2018) Chapter 2: Plants secondary metabolites: The key drivers of the pharmacological actions of medicinal plants. In: F. Builders P (ed) Herbal Medicine. IntechOpen (London)

Hutzler P (1998) Tissue localization of phenolic compounds in plants by confocal laser scanning microscopy. J Exp Bot 49: 953–965

Hutzler P, Fischbach R, Heller W, Jungblut TP, Reuber S, Schmitz R, Veit M, Weissenbock G, Schnitzler J-P (1998) Tissue localization of phenolic compounds in plants by confocal laser scanning microscopy. J Exp Bot 49: 953–965

Ihle C, Laasch H (1996) Inhibition of Photosystem II by UV-B Radiation and the Conditions for Recovery in the Liverwort Conocephalum conicum Dum. Bot Acta 109: 199–205

Inada K (1976) Action spectra for photosynthesis in higher plants. Plant Cell Physiol 17: 355–365

Jaakola L, Määttä-Riihinen K, Kärenlampi S, Hohtola A (2004) Activation of flavonoid biosynthesis by solar radiation in bilberry (*Vaccinium myrtillus* L.) leaves. Planta 218: 721–728

Jan AU, Hadi F, Zeb A, Islam Z (2018) Identification and quantification of phenolic compounds through reversed phase HPLC-DAD method in sunflower seeds under various treatments of potassium nitrate, zinc sulphate and gibberellic acid. J Food Meas Charact 12: 269–277

Jansen MAK, Ač A, Klem K, Urban O (2022) A meta-analysis of the interactive effects of UV and drought on plants. Plant Cell Environ 45: 41–54

Jansen MAK, Coffey AM, Prinsen E (2012) UV-B induced morphogenesis: Four players or a quartet? Plant Signal Behav 7: 1185–1187

Jansen MAK, Gaba V, Greenberg BM (1998) Higher plants and UV-B radiation: balancing damage, repair and acclimation. Trends Plant Sci 3: 131–135

Järvi S, Suorsa M, Aro E-M (2015) Photosystem II repair in plant chloroplasts — Regulation, assisting proteins and shared components with photosystem II biogenesis. Biochim Biophys Acta BBA - Bioenerg 1847: 900–909

Jenkins GI (2014) The UV-B photoreceptor UVR8: From structure to physiology. Plant Cell 26: 21–37

Jenkins GI, Long JC, Wade HK, Shenton MR, Bibikova TN (2001) UV and blue light signalling: pathways regulating chalcone synthase gene expression in *Arabidopsis*: Research review. New Phytol 151: 121–131

Johansson H, Jones HJ, Foreman J, Hemsted JR, Stewart K, Grima R, Halliday KJ (2014) Arabidopsis cell expansion is controlled by a photothermal switch. Nat Commun 5: 4848

Johkan M, Shoji K, Goto F, Hashida S, Yoshihara T (2010) Blue light-emitting diode light irradiation of seedlings improves seedling quality and growth after transplanting in red leaf lettuce. HortScience 45: 1809–1814

Kalemba D, Kunicka A (2003) Antibacterial and antifungal properties of essential oils. Curr Med Chem 10: 813–829

Kaling M, Kanawati B, Ghirardo A, Albert A, Winkler JB, Heller W, Barta C, Loreto F, Schmitt-Kopplin P, Schnitzler J-P (2015) UV-B mediated metabolic rearrangements in poplar revealed by non-targeted metabolomics: Poplar metabolome under UV stress. Plant Cell Environ 38: 892–904

Karakas FP, Turker AU (2013) An efficient in vitro regeneration system for Bellis perennis L. and comparison of phenolic contents of field-grown and in vitro-grown leaves by LC-MS/MS. Ind Crops Prod 48: 162–170

Kataria S, Guruprasad KN, Ahuja S, Singh B (2013) Enhancement of growth, photosynthetic performance and yield by exclusion of ambient UV components in C3 and C4 plants. J Photochem Photobiol B 127: 140–152

Kliebenstein DJ, Lim JE, Landry LG, Last RL (2002) *Arabidopsis UVR8* regulates ultraviolet-B signal transduction and tolerance and contains sequence similarity to human *Regulator of Chromatin Condensation 1*. Plant Physiol 130: 234–243

Koeppe DE, Rohrbaugh LM, Rice EL, Wender SH (1970) The Effect of Age and Chilling Temperature on the Concentration of Scopolin and Caffeoylquinic Acids in Tobacco. Physiol Plant 23: 258–266

Kolarević T, Milinčić DD, Vujović T, Gašić UM, Prokić L, Kostić AŽ, Cerović R, Stanojevic SP, Tešić ŽLj, Pešić MB (2021) Phenolic compounds and antioxidant properties of field-grown and in vitro leaves, and calluses in blackberry and blueberry. Horticulturae 7: 420

Kolb CA, Käser MA, Kopecky J, Zotz G, Riederer M, Pfundel EE (2001) Effects of natural intensities of visible and ultraviolet radiation on epidermal ultraviolet screening and photosynthesis in grape leaves. Plant Physiol 127: 863–875

Kolb CA, Pfündel EE (2005) Origins of non-linear and dissimilar relationships between epidermal UV absorbance and UV absorbance of extracted phenolics in leaves of grapevine and barley. Plant Cell Environ 28: 580–590

Kolb CA, Schreiber U, Gademann R, Pfündel EE (2005) UV-A screening in plants determined using a new portable fluorimeter. Photosynthetica 43: 371–377

Kreuzaler F, Ragg H, Fautz E, Kuhn DN, Hahlbrock K (1983) UV-induction of chalcone synthase mRNA in cell suspension cultures of *Petroselinum hortense*. Proc Natl Acad Sci 80: 2591–2593

Krizek DT, Mirecki RM, Britz SJ (1997) Inhibitory effects of ambient levels of solar UV-A and UV-B radiation on growth of cucumber. Physiol Plant 100: 886–893

Kubasek WL, Ausubel FM, Shirley BW (1998) A light-independent developmental mechanism potentiates flavonoid gene expression in *Arabidopsis* seedlings. Plant Mol Biol 37: 217–223

Kubasek WL, Shirley BW, McKillop A, Goodman HM, Briggs W, Ausubel FM (1992) Regulation of flavonoid biosynthetic genes in germinating *Arabidopsis* seedlings. Plant Cell 1229–1236

Kuhn DN, Chappell J, Boudet A, Hahlbrock K (1984) Induction of phenylalanine ammonia-lyase and 4-coumarate:CoA ligase mRNAs in cultured plant cells by UV light or fungal elicitor. Proc Natl Acad Sci 81: 1102–1106

Lambers H, Oliveira RS (2019) Photosynthesis, Respiration, and Long-Distance Transport: Photosynthesis. Plant Physiological Ecology, 3rd Ed. Springer International Publishing, Cham

Landry LG, Chapple C, Last RL (1995) *Arabidopsis* mutants lacking phenolic sunscreens exhibit enhanced ultraviolet-B injury and oxidative damage. Plant Physiol 109: 1159–1166

Lang M, Stober F, Lichtenthaler HK (1991) Fluorescence emission spectra of plant leaves and plant constituents. Radiat Environ Biophys 30: 333–347

Larbat R, Le Bot J, Bourgaud F, Robin C, Adamowicz S (2012a) Organ-specific responses of tomato growth and phenolic metabolism to nitrate limitation. Plant Biol 14: 760–769

Larbat R, Olsen KM, Slimestad R, Løvdal T, Bénard C, Verheul M, Bourgaud F, Robin C, Lillo C (2012b) Influence of repeated short-term nitrogen limitations on leaf phenolics metabolism in tomato. Phytochemistry 77: 119–128

Larbat R, Robin C, Lillo C, Drengstig T, Ruoff P (2016) Modeling the diversion of primary carbon flux into secondary metabolism under variable nitrate and light/dark conditions. J Theor Biol 402: 144–157

Latouche G, Bellow S, Poutaraud A, Meyer S, Cerovic ZG (2013) Influence of constitutive phenolic compounds on the response of grapevine (*Vitis vinifera* L.) leaves to infection by *Plasmopara viticola*. Planta 237: 351–361

Laureau C, Meyer S, Baudin X, Huignard C, Streb P (2015) In vivo epidermal UV-A absorbance is induced by sunlight and protects *Soldanella alpina* leaves from photoinhibition. Funct Plant Biol 42: 599

Lea US, Slimestad R, Smedvig P, Lillo C (2007) Nitrogen deficiency enhances expression of specific MYB and bHLH transcription factors and accumulation of end products in the flavonoid pathway. Planta 225: 1245–1253

Legrand G, Delporte M, Khelifi C, Harant A, Vuylsteker C, Mörchen M, Hance P, Hilbert J-L, Gagneul D (2016) Identification and characterization of five BAHD acyltransferases involved in hydroxycinnamoyl ester metabolism in chicory. Front Plant Sci 7:

Legris M, Klose C, Burgie ES, Rojas CCR, Neme M, Hiltbrunner A, Wigge PA, Schäfer E, Vierstra RD, Casal JJ (2016) Phytochrome B integrates light and temperature signals in *Arabidopsis*. Science 354: 897–900

Lepelley M, Cheminade G, Tremillon N, Simkin A, Caillet V, McCarthy J (2007) Chlorogenic acid synthesis in coffee: An analysis of CGA content and real-time RT-PCR expression of HCT, HQT, C3H1, and CCoAOMT1 genes during grain development in *C. canephora*. Plant Sci 172: 978–996

Levitt J (1980) Responses of plants to environmental stresses - Water, radiation, salt, and other stresses, 2d Ed. Academic Press, New York

Lewinski CS, Gonçalves IL, Piovezan Borges AC, Dartora N, de Souza LM, Valduga AT (2015) Effects of UV light on the physic-chemical properties of yerba-mate. Nutr Food Sci 45: 221–228

Leyva A, Jarillo JA, Salinas J, Martinez-Zapater JM (1995) Low temperature induces the accumulation of phenylalanine ammonia-lyase and chalcone synthase mRNAs of *Arabidopsis thaliana* in a light-dependent manner. Plant Physiol 108: 39–46

Li J, Ou-Lee TM, Raba R, Amundson RG, Last RL (1993) Arabidopsis flavonoid mutants are hypersensitive to UV-B irradiation. Plant Cell 5: 171–179

Li S, Wang Y, Björn LO (2004) Effects of temperature on UV-B-induced DNA damage and photorepair in Arabidopsis thaliana. J Environ Sci China 16: 173–176

Li Y, Kong D, Bai M, He H, Wang H, Wu H (2019) Correlation of the temporal and spatial expression patterns of HQT with the biosynthesis and accumulation of chlorogenic acid in Lonicera japonica flowers. Hortic Res 6: 73

Lichtenthaler HK, Buschmann C, Knapp M (2005) How to correctly determine the different chlorophyll fluorescence parameters and the chlorophyll fluorescence decrease ratio R_{Fd} of leaves with the PAM fluorometer. Photosynthetica 43: 379–393

Lillo C (2008) Signalling cascades integrating light-enhanced nitrate metabolism. Biochem J 415: 11–19

Lillo C, Lea US, Ruoff P (2008) Nutrient depletion as a key factor for manipulating gene expression and product formation in different branches of the flavonoid pathway. Plant Cell Environ 31: 587–601

Liou KN (2002a) Chapter 1 - Fundamentals of Radiation for Atmospheric Applications. International Geophysics. Academic Press, Cambridge

Liou KN (2002b) Chapter 2 - Solar Radiation at the Top of the Atmosphere. International Geophysics. Academic Press, Cambridge

Liou KN (2002c) Chapter 3 - Absorption and Scattering of Solar Radiation in the Atmosphere. International Geophysics. Academic Press, Cambridge

Liu J, Osbourn A, Ma P (2015a) MYB transcription factors as regulators of phenylpropanoid metabolism in plants. Mol Plant 8: 689–708

Liu L, Gregan S, Winefield C, Jordan B (2015b) From UVR8 to flavonol synthase: UV-B-induced gene expression in Sauvignon blanc grape berry: UV-B-induced gene expression. Plant Cell Environ 38: 905–919

Livak KJ, Schmittgen TD (2001) Analysis of relative gene expression data using Real-Time quantitative PCR and the 2−ΔΔCT method. Methods 25: 402–408

Løvdal T, Olsen KM, Slimestad R, Verheul M, Lillo C (2010) Synergetic effects of nitrogen depletion, temperature, and light on the content of phenolic compounds and gene expression in leaves of tomato. Phytochemistry 71: 605–613

Lüders K, Pohl RW (eds) (2006) Energie der Strahlung und Bündelbegrenzung. Pohls Einführung in die Physik - Band 2: Elektrizitätslehre und Optik, 23rd Ed. Springer, Berlin, Heidelberg

Luengo Escobar AL, Magnum de Oliveira Silva F, Acevedo P, Nunes-Nesi A, Alberdi M, Reyes-Díaz M (2017) Different levels of UV-B resistance in *Vaccinium corymbosum* cultivars reveal distinct backgrounds of phenylpropanoid metabolites. Plant Physiol Biochem 118: 541–550

Luo J, Butelli E, Hill L, Parr A, Niggeweg R, Bailey P, Weisshaar B, Martin C (2008) AtMYB12 regulates caffeoyl quinic acid and flavonol synthesis in tomato: expression in fruit results in very high levels of both types of polyphenol. Plant J 56: 316–326

Lüttge U, Scarano FR (2004) Ecophysiology. Rev Bras Botânica 27: 1–10

Mai F, Glomb MA (2013) Isolation of phenolic compounds from iceberg lettuce and impact on enzymatic browning. J Agric Food Chem 61: 2868–2874

Markstädter C, Queck I, Baumeister J, Riederer M, Schreiber U, Bilger W (2001) Epidermal transmittance of leaves of *Vicia faba* for UV radiation as determined by two different methods. Photosynth Res 67: 17–25

Marquardt J, Hanelt D (2004) Carotenoid composition of *Delesseria lancifolia* and other marine red algae from polar and temperate habitats. Eur J Phycol 39: 285–292

Martegani E, Alberghina L (1977) Low-temperature restriction of the rate of protein synthesis in Neurospora crassa. Exp Mycol 1: 339–351

Martinez V, Mestre TC, Rubio F, Girones-Vilaplana A, Moreno DA, Mittler R, Rivero RM (2016) Accumulation of Flavonols over Hydroxycinnamic Acids Favors Oxidative Damage Protection under Abiotic Stress. Front Plant Sci 7: 838

Mason CM, Bowsher AW, Crowell BL, Celoy RM, Tsai C-J, Donovan LA (2016) Macroevolution of leaf defenses and secondary metabolites across the genus *Helianthus*. New Phytol 209: 1720–1733

McCree KJ (1972) The action spectrum, absorptance and quantum yield of photosynthesis in crop plants. Agric Meteorol 9: 191–216

McLaren AD, Luse RA (1961) Mechanism of inactivation of enzyme proteins by ultraviolet light. Science 134: 836–837

Mecherikunnel ATM, Richmond JC (1980) Spectral distribution of solar radiation (NASA technical memorandum 82021)

Medina-Sánchez JM, Villar-Argaiz M, Carrillo P (2002) Modulation of the bacterial response to spectral solar radiation by algae and limiting nutrients. Freshw Biol 47: 2191–2204

Meyer S, Cerovic ZG, Goulas Y, Montpied P, Demotes-Mainard S, Bidel LPR, Moya I, Dreyer E (2006) Relationships between optically assessed polyphenols and chlorophyll contents, and leaf mass per area ratio in woody plants: a signature of the carbon-nitrogen balance within leaves? Plant Cell Environ 29: 1338–1348

Minorsky PV (1989) Temperature sensing by plants: a review and hypothesis. Plant Cell Environ 12: 119–135

Moglia A, Acquadro A, Eljounaidi K, Milani AM, Cagliero C, Rubiolo P, Genre A, Cankar K, Beekwilder J, Comino C (2016) Genome-wide identification of BAHD acyltransferases and in vivo characterization of HQT-like enzymes involved in caffeoylquinic acid synthesis in globe artichoke. Front Plant Sci 7: 1424

Moglia A, Comino C, Menin B, Portis E, Acquadro A, Beekwilder J, Hehn A, Bourgaud F, Lanteri S (2013) Caffeoylquinic acids biosynthesis and accumulation in *Cynara cardunculus*: State of the art. Acta Hortic 401–406

Moglia A, Lanteri S, Comino C, Acquadro A, de Vos R, Beekwilder J (2008) Stress-induced biosynthesis of dicaffeoylquinic acids in globe artichoke. J Agric Food Chem 56: 8641–8649

Moglia A, Lanteri S, Comino C, Hill L, Knevitt D, Cagliero C, Rubiolo P, Bornemann S, Martin C (2014) Dual Catalytic Activity of Hydroxycinnamoyl-Coenzyme A Quinate Transferase from Tomato Allows It to Moonlight in the Synthesis of Both Mono- and Dicaffeoylquinic Acids. Plant Physiol 166: 1777–1787

Mondolot L, La Fisca P, Buatois B, Talansier E, De Kochko A, Campa C (2006) Evolution in caffeoylquinic acid content and histolocalization during *Coffea canephora* leaf development. Ann Bot 98: 33–40

del Moral R (1972) On the variability of chlorogenic acid concentration. Oecologia 9: 289–300

Morales LO, Brosché M, Vainonen J, Jenkins GI, Wargent JJ, Sipari N, Strid Å, Lindfors AV, Tegelberg R, Aphalo PJ (2013) Multiple roles for UV RESISTANCE LOCUS8 in regulating gene expression and metabolite accumulation in *Arabidopsis* under solar ultraviolet radiation. Plant Physiol 161: 744–759

Morales LO, Tegelberg R, Brosche M, Keinanen M, Lindfors A, Aphalo PJ (2010) Effects of solar UV-A and UV-B radiation on gene expression and phenolic accumulation in *Betula pendula* leaves. Tree Physiol 30: 923–934

Mu X, Huang A, Wu Y, Xu Q, Zheng Y, Lin H, Fang D, Zhang X, Tang Y, Cai S (2021) Characteristics of the precipitation diurnal variation and underlying mechanisms over Jiangsu, Eastern China, during warm season. Front Earth Sci 9:703071:

Mulligan RM, Chory J, Ecker JR (1997) Signaling in plants. Proc Natl Acad Sci 94: 2793–2795

Murata N, Takahashi S, Nishiyama Y, Allakhverdiev SI (2007) Photoinhibition of photosystem II under environmental stress. Biochim Biophys Acta BBA - Bioenerg 1767: 414–421

Murray JD, Liu C-W, Chen Y, Miller AJ (2017) Nitrogen sensing in legumes. J Exp Bot 68: 1919–1926

Nabavi SF, Tejada S, Setzer WN, Gortzi O, Sureda A, Braidy N, Daglia M, Manayi A, Nabavi SM (2017) Chlorogenic acid and mental diseases: From chemistry to medicine. Curr Neuropharmacol 15: 471–479

Nayak L, Biswal B, Ramaswamy NK, Iyer RK, Nair JS, Biswal UC (2003) Ultraviolet-A induced changes in photosystem II of thylakoids: effects of senescence and high growth temperature. J Photochem Photobiol B 70: 59–65

Negwer E (2022) Induction of UV-screening compounds by N-deficiency in *Helianthus annuus*. Master thesis. Christian-Albrechts-Universität zu Kiel, Kiel

Nenadis N, Llorens L, Koufogianni A, Díaz L, Font J, Gonzalez JA, Verdaguer D (2015) Interactive effects of UV radiation and reduced precipitation on the seasonal leaf phenolic content/composition and the antioxidant activity of naturally growing *Arbutus unedo* plants. J Photochem Photobiol B 153: 435–444

Neugart S, Fiol M, Schreiner M, Rohn S, Zrenner R, Kroh LW, Krumbein A (2013) Low and moderate photosynthetically active radiation affects the flavonol glycosides and hydroxycinnamic acid derivatives in kale (*Brassica oleracea* var. *sabellica*) dependent on two low temperatures. Plant Physiol Biochem 72: 161–168

Neugart S, Krumbein A, Zrenner R (2016) Influence of light and temperature on gene expression leading to accumulation of specific flavonol glycosides and hydroxycinnamic acid derivatives in kale (*Brassica oleracea* var. *sabellica*). Front Plant Sci 7: 326

Neugart S, Tobler MA, Barnes PW (2019) Different irradiances of UV and PAR in the same ratios alter the flavonoid profiles of *Arabidopsis thaliana* wild types and UV-signalling pathway mutants. Photochem Photobiol Sci 18: 1685–1699

Neugart S, Zietz M, Schreiner M, Rohn S, Kroh LW, Krumbein A (2012) Structurally different flavonol glycosides and hydroxycinnamic acid derivatives respond differently to moderate UV-B radiation exposure. Physiol Plant 145: 582–593

Nichelmann L, Schulze M, Herppich WB, Bilger W (2016) A simple indicator for non-destructive estimation of the violaxanthin cycle pigment content in leaves. Photosynth Res 128: 183–193

Niggeweg R, Michael AJ, Martin C (2004) Engineering plants with increased levels of the antioxidant chlorogenic acid. Nat Biotechnol 22: 746–754

Nile SH, Park SW (2015) HPTLC densitometry method for simultaneous determination of flavonoids in selected medicinal plants. Front Life Sci 8: 97–103

Nixon PJ, Michoux F, Yu J, Boehm M, Komenda J (2010) Recent advances in understanding the assembly and repair of photosystem II. Ann Bot 106: 1–16

Noctor G, Foyer CH (1998) Ascorbate and glutathione: Keeping active oxygen under control. Annu Rev Plant Physiol Plant Mol Biol 49: 249–279

Norval M, Lucas RM, Cullen AP, de Gruijl FR, Longstreth J, Takizawa Y, van der Leun JC (2011) The human health effects of ozone depletion and interactions with climate change. Photochem Photobiol Sci 10: 199–225

Nybakken L, Bilger W, Johanson U, Björn LO, Zielke M, Solheim B (2004) Epidermal UV-screening in vascular plants from Svalbard (Norwegian Arctic). Polar Biol 27: 383–390

Nybakken L, Hörkkä R, Julkunen-Tiitto R (2012) Combined enhancements of temperature and UVB influence growth and phenolics in clones of the sexually dimorphic Salix myrsinifolia. Physiol Plant 145: 551–564

O'Brien JA, Vega A, Bouguyon E, Krouk G, Gojon A, Coruzzi G, Gutiérrez RA (2016) Nitrate transport, sensing, and responses in plants. Mol Plant 9: 837–856

Ochogavía AC, Novello MA, Picardi LA, Nestares, Picardi LA, IICAR, UNR, CONICET (Instituto de Investigaciones en Ciencias Agrarias de Rosario, Universidad Nacional de Rosario, Consejo Nacional de Investigaciones Científicas y Técnicas), Zavalla, Santa Fe, Argentina, CIUNR (Consejo de Investigaciones de la Universidad Nacional de Rosario), Argentina (2017) Identification of suitable reference genes by quantitative real-time PCR for gene expression normalization in sunflower. Plant Omics 10: 210–218

Oertel A, Matros A, Hartmann A, Arapitsas P, Dehmer KJ, Martens S, Mock H-P (2017) Metabolite profiling of red and blue potatoes revealed cultivar and tissue specific patterns for anthocyanins and other polyphenols. Planta 246: 281–297

Ohad I, Kyle DJ, Arntzen CJ (1984) Membrane protein damage and repair: removal and replacement of inactivated 32-kilodalton polypeptides in chloroplast membranes. J Cell Biol 99: 481–485

Ohl S, Hahlbrock K, Schäfer E (1989) A stable blue-light-derived signal modulates ultraviolet-light-induced activation of the chalcone-synthase gene in cultured parsley cells. Planta 177: 228–236

Oliveira RR, Viana AJC, Reátegui ACE, Vincentz MGA (2015) Short Communication An efficient method for simultaneous extraction of high-quality RNA and DNA from various plant tissues. Genet Mol Res 14: 18828–18838

Olsen KM, Lea US, Slimestad R, Verheul M, Lillo C (2008) Differential expression of four *Arabidopsis* PAL genes; PAL1 and PAL2 have functional specialization in abiotic environmental-triggered flavonoid synthesis. J Plant Physiol 165: 1491–1499

Olsen KM, Slimestad R, Lea US, Brede C, Lovdal T, Ruoff P, Verheul M, Lillo C (2009) Temperature and nitrogen effects on regulators and products of the flavonoid pathway: experimental and kinetic model studies. Plant Cell Environ 32: 286–299

Paik I, Huq E (2019) Plant photoreceptors: Multi-functional sensory proteins and their signaling networks. Semin Cell Dev Biol 92: 114–121

Palma CFF, Castro-Alves V, Morales LO, Rosenqvist E, Ottosen C-O, Strid Å (2021) Spectral composition of light affects sensitivity to UV-B and photoinhibition in Cucumber. Front Plant Sci 11: 610011

Panagopoulos I, Bornman JF, Björn LO (1990) Effects of ultraviolet radiation and visible light on growth, fluorescence induction, ultraweak luminescence and peroxidase activity in sugar beet plants. J Photochem Photobiol B 8: 73–87

Payyavula RS, Shakya R, Sengoda VG, Munyaneza JE, Swamy P, Navarre DA (2015) Synthesis and regulation of chlorogenic acid in potato: Rerouting phenylpropanoid flux in *HQT* -silenced lines. Plant Biotechnol J 13: 551–564

Pedrosa MM, Muzquiz M, García-Vallejo C, Burbano C, Cuadrado C, Ayet G, Robredo LM (2000) Determination of caffeic and chlorogenic acids and their derivatives in different sunflower seeds. J Sci Food Agric 80: 459–464

Penfield S (2008) Temperature perception and signal transduction in plants. New Phytol 179: 615–628

Pereira A (2016) Plant abiotic stress challenges from the changing environment. Front Plant Sci 7:1123:

Pescheck F (2019) UV-A screening in *Cladophora* sp. lowers internal UV-A availability and photoreactivation as compared to non-UV screening in *Ulva intestinalis*. Photochem Photobiol Sci 18: 413–423

Pescheck F, Bilger W (2019) High impact of seasonal temperature changes on acclimation of photoprotection and radiation-induced damage in field grown *Arabidopsis thaliana*. Plant Physiol Biochem 134: 129–136

Pescheck F, Bilger W (2020) UV-B resistance of plants grown in natural conditions. Annu Plant Rev Online 2020: 337–398

Petersen M, Abdullah Y, Benner J, Eberle D, Gehlen K, Hücherig S, Janiak V, Kim KH, Sander M, Weitzel C, Wolters S (2009) Evolution of rosmarinic acid biosynthesis. Phytochemistry 70: 1663–1679

Petridis A, Döll S, Nichelmann L, Bilger W, Mock H-P (2016) *Arabidopsis thaliana* G2-LIKE FLAVONOID REGULATOR and BRASSINOSTEROID ENHANCED EXPRESSION1 are low-temperature regulators of flavonoid accumulation. New Phytol 211: 912–925

Pfeifer GP, Besaratinia A (2012) UV wavelength-dependent DNA damage and human non-melanoma and melanoma skin cancer. Photochem Photobiol Sci 11: 90–97

Pfündel EE, Agati G, Cerovic ZG (2006) Optical properties of plant surfaces. In: Riederer M, Mller C (eds) Biology of the plant cuticle. Blackwell Publishing Ltd, Oxford, UK, pp. 216–249

Pierrehumbert RT (2004) Warming the world. Nature 432: 677–677

Piersma T, Drent J (2003) Phenotypic flexibility and the evolution of organismal design. Trends Ecol Evol 18: 228–233

Pirvu L, Hlevca C, Nicu I, Bubueanu C (2014) Comparative studies on analytical, antioxidant, and antimicrobial activities of a series of vegetal extracts prepared from eight plant species growing in Romania. J Planar Chromatogr – Mod TLC 27: 346–356

Pospíšil P (2016) Production of reactive oxygen species by photosystem II as a response to light and temperature stress. Front Plant Sci 7:1950:

Pospíšil P, Arató A, Krieger-Liszkay A, Rutherford AW (2004) Hydroxyl radical generation by photosystem II. Biochemistry 43: 6783–6792

Price C, Michaelides S, Pashiardis S, Alpert P (1999) Long term changes in diurnal temperature range in Cyprus. Atmospheric Res 51: 85–98

Qian M, Kalbina I, Rosenqvist E, Jansen MAK, Teng Y, Strid Å (2019) UV regulates the expression of phenylpropanoid biosynthesis genes in cucumber (*Cucumis sativus* L.) in an organ and spectrum dependent manner. Photochem Photobiol Sci 18: 424–433

Quaite FE, Sutherland BM, Sutherland JC (1992) Action spectrum for DMA damage in alfalfa lowers predicted impact of ozone depletion. Nature 358: 576–578

Quint M, Delker C, Franklin KA, Wigge PA, Halliday KJ, van Zanten M (2016) Molecular and genetic control of plant thermomorphogenesis. Nat Plants 2: 15190

Ragg H, Kuhn DN, Hahlbrock K (1981) Coordinated regulation of 4-coumarate:CoA ligase and phenylalanine ammonia-lyase mRNAs in cultured plant cells. J Biol Chem 256: 10061–10065

Rai N, Neugart S, Yan Y, Wang F, Siipola SM, Lindfors AV, Winkler JB, Albert A, Brosché M, Lehto T, Morales LO, Aphalo PJ (2019) How do cryptochromes and UVR8 interact in natural and simulated sunlight? J Exp Bot 70: 4975–4990

Rai N, O'Hara A, Farkas D, Safronov O, Ratanasopa K, Wang F, Lindfors AV, Jenkins GI, Lehto T, Salojärvi J, Brosché M, Strid Å, Aphalo PJ, Morales LO (2020) The photoreceptor UVR8 mediates the perception of both UV-B and UV-A wavelengths up to 350 nm of sunlight with responsivity moderated by cryptochromes. Plant Cell Environ 43: 1513–1527

Reuber S, Bornman JF, Weissenböck G (1996) Phenylpropanoid compounds in primary leaf tissues of rye (*Secale cereale*). Light response of their metabolism and the possible role in UV-B protection. Physiol Plant 97: 160–168

Rice-Evans C, Miller N, Paganga G (1997) Antioxidant properties of phenolic compounds. Trends Plant Sci 2: 933–956

Rice-Evans CA, Miller NJ, Paganga G (1996) Structure-antioxidant activity relationships of flavonoids and phenolic acids. Free Radic Biol Med 20: 933–956

Rieseberg LH, Harter AV (2006) Chapter 2: Molecular evidence and the evolutionary history of the domesticated sunflower. Darwin's Harvest. Columbia University Press, New York City, pp. 31–48

Rieseberg LH, Seiler GJ (1990) Molecular evidence and the origin and development of the domesticated sunflower (*Helianthus annuus*, Asteraceae). Econ Bot 44: 79–91

Rieseberg LH, Soltis DE, Arnold Doug (1987) Variation and localization of flavonoid aglycones in *Helianthus annuus* (Compositae). Am J Bot 74: 224–233

Rintamäki E, Salo R, Lehtonen E, Aro E-M (1995) Regulation of D1-protein degradation during photoinhibition of photosystem II in vivo: Phosphorylation of the D1 protein in various plant groups. Planta 195: 379–386

Robberecht R, Caldwell MM (1978) Leaf epidermal transmittance of ultraviolet radiation and its implications for plant sensitivity to ulraviolet-radiation induced injury. Oecologia 32: 277–287

Rodriguez V, Soengas P, Alonso-Villaverde V, Sotelo T, Cartea M, Velasco P (2015) Effect of temperature stress on the early vegetative development of *Brassica oleracea* L. BMC Plant Biol 15: 145

Roldán-Arjona T, Ariza RR (2009) Repair and tolerance of oxidative DNA damage in plants. Mutat Res Mutat Res 681: 169–179

Romani A, Pinelli P, Moschini V, Heimler D (2017) Seeds and oil polyphenol content of sunflower (*Helianthus annuus* L.) grown with different agricultural management. Adv Hortic Sci 85–88

Roth GJ, Stanford N, Majerus PW (1975) Acetylation of prostaglandin synthase by aspirin. Proc Natl Acad Sci 72: 3073–3076

Rozema J, Björn LO, Bornman JF, Gaberščik A, Häder D-P, Trošt T, Germ M, Klisch M, Gröniger A, Sinha RP, Lebert M, He Y-Y, Buffoni-Hall R, de Bakker NVJ, van de Staaij J, Meijkamp BB (2002) The role of UV-B radiation in aquatic and terrestrial ecosystems—an experimental and functional analysis of the evolution of UV-absorbing compounds. J Photochem Photobiol B 66: 2–12

Ruelland E, Zachowski A (2010) How plants sense temperature. Environ Exp Bot 69: 225–232

Ryan KG, Swinny EE, Markham KR, Winefield C (2002) Flavonoid gene expression and UV photoprotection in transgenic and mutant *Petunia* leaves. Phytochemistry 59: 23–32

Sabir MA, Sosulski FW, Kernan JA (1974) Phenolic constituents in sunflower flour. J Agric Food Chem 22: 572–574

Saftić-Panković D, Veljović-Jovanović S, Pucarević M, Radovanović N, Mijić A (2006) Phenolic compounds and peroxidases in sunflower near-isogenic lines after downy mildew infection. Helia 29: 33–42

Samson G, Cerovic ZG, El Rouby WMA, Millet P (2020) Oxidation of polyphenols and inhibition of photosystem II under acute photooxidative stress. Planta 251: 16

Santana-Gálvez J, Cisneros-Zevallos L, Jacobo-Velázquez DA (2017) Chlorogenic acid: Recent advances on its dual role as a food additive and a nutraceutical against metabolic syndrome. Mol Basel Switz 22: E358

dos Santos MD, Almeida MC, Lopes NP, de Souza GEP (2006) Evaluation of the anti-inflammatory, analgesic and antipyretic activities of the natural polyphenol chlorogenic acid. Biol Pharm Bull 29: 2236–2240

dos Santos Nascimento LB, Brunetti C, Agati G, Lo Iacono C, Detti C, Giordani E, Ferrini F, Gori A (2020) Short-term pre-harvest UV-B supplement enhances the polyphenol content and antioxidant capacity of *Ocimum basilicum* leaves during storage. Plants 9: 797

Sarvikas P, Hakala M, Pätsikkä E, Tyystjärvi T, Tyystjärvi E (2006) Action spectrum of photoinhibition in leaves of wild type and npq1-2 and npq4-1 mutants of *Arabidopsis thaliana*. Plant Cell Physiol 47: 391–400

Sass L, Spetea C, Máté Z, Nagy F, Vass I (1997) Repair of UV-B induced damage of Photosystem II via de novo synthesis of the D1 and D2 reaction centre subunits in *Synechocystis* sp. PCC 6803. Photosynth Res 54: 55–62

Sauer D, Burroughs R (1986) Desinfection of seed surfaces with sodium hypochlorite. Phytopathology 76: 745–749

Scalbert A, Williamson G (2000) Dietary intake and bioavailability of polyphenols. J Nutr 8: S2073–S2085

Schachtman DP, Shin R (2007) Nutrient sensing and signaling: NPKS. Annu Rev Plant Biol 58: 47–69

Schilling EE (1983) Flavonoids of *Helianthus* series *Angustifolii*. Biochem Syst Ecol 11: 341–344

Schilling EE, Mabry TJ (1981) Flavonoids of *Helianthus* series *Corona-solis*. Biochem Syst Ecol 9: 161–163

Schilling EE, Panero JL, Storbeck TA (1987) Flavonoids of *Helianthus* series *Microcephali*. Biochem Syst Ecol 15: 671–672

Schmelzer E, Jahnen W, Hahlbrock K (1988) In situ localization of light-induced chalcone synthase mRNA, chalcone synthase, and flavonoid end products in epidermal cells of parsley leaves. Proc Natl Acad Sci 85: 2989–2993

Schultze M (2011) Die Funktion von UV-Schutzpigmenten bei Kühle in *Arabidopsis thaliana*. PhD Thesis. Christian-Albrechts-Universität, Kiel

Schultze M, Bilger W (2018) Acclimation of Arabidopsis thaliana to low temperature protects against damage of photosystem II caused by exposure to UV-B radiation at 9 °C. Plant Physiol Biochem 134: 73–80

Schulz E, Tohge T, Zuther E, Fernie AR, Hincha DK (2015) Natural variation in flavonol and anthocyanin metabolism during cold acclimation in *Arabidopsis thaliana* accessions. Plant Cell Environ 38: 1658–1672

Schulz E, Tohge T, Zuther E, Fernie AR, Hincha DK (2016) Flavonoids are determinants of freezing tolerance and cold acclimation in *Arabidopsis thaliana*. Sci Rep 6:34027:

Seemann JR (1989) Light Adaptation/Acclimation of Photosynthesis and the Regulation of Ribulose-1,5-Bisphosphate Carboxylase Activity in Sun and Shade Plants. Plant Physiol 91: 379–386

Setlow R (1960) Ultraviolet Wave-Length-Dependent Effects on Proteins and Nucleic Acids. Radiat Res Suppl 2: 276

Setlow RB (1974) The wavelengths in sunlight effective in producing skin cancer: A theoretical analysis. Proc Natl Acad Sci 71: 3363–3366

Sha Valli Khan PS, Nagamallaiah GV, Dhanunjay Rao M, Sergeant K, Hausman JF (2014) Abiotic stress tolerance in plants. Emerging technologies and management of crop stress tolerance. Elsevier, pp. 23–68

Shang YF, Kim SM, Song D-G, Pan C-H, Lee WJ, Um B-H (2010) Isolation and identification of antioxidant compounds from *Ligularia fischeri*. J Food Sci 75: C530–C535

Sharpe PJ, DeMichele DW (1977) Reaction kinetics of poikilotherm development. J Theor Biol 64: 649–670

Sheahan JJ (1996) Sinapate esters provide greater UV-B attenuation than flavonoids in *Arabidopsis thaliana* (Brassicaceae). Am J Bot 83: 679–686

Sheen SJ, Calvert J (1969) Studies on polyphenol content, activities and isozymes of polyphenol oxidase and peroxidase during air-curing in three tobacco types. Plant Physiol 44: 199–204

Shevela D, Björn LO, Govindjee (2013) Oxygenic photosynthesis. In: Razeghifard R (ed) Natural and artificial photosynthesis. John Wiley & Sons Inc., Hoboken, NJ, USA, pp. 13–63

Shirley BW (1996) Flavonoid biosynthesis: 'new' functions for an 'old' pathway. Trends Plant Sci 1: 377–382

Sicora C, Szilárd A, Sass L, Turcsányi E, Máté Z, Vass I (2006) UV-B and UV-A radiation effects on photosynthesis at the molecular level. In: Ghetti F, Checcucci G, Bornman JF (eds) Environmental UV radiation: Impact on ecosystems and human health and predictive models. Springer-Verlag, Berlin/Heidelberg, pp. 121–135

Siipola SM, Kotilainen T, Sipari N, Morales LO, Lindfors AV, Robson TM, Aphalo PJ (2015) Epidermal UV-A absorbance and whole-leaf flavonoid composition in pea respond more to solar blue light than to solar UV radiation: Flavonoids in sunlight. Plant Cell Environ 38: 941–952

Sinha RP, Häder D-P (2002) UV-induced DNA damage and repair: a review. Photochem Photobiol Sci 1: 225–236

Song J, Liu Q, Hu B, Wu W (2017) Photoreceptor PhyB Involved in Arabidopsis Temperature Perception and Heat-Tolerance Formation. Int J Mol Sci 18: 1194

Sonnante G, D'Amore R, Blanco E, Pierri CL, De Palma M, Luo J, Tucci M, Martin C (2010) Novel hydroxycinnamoyl-Coenzyme A quinate transferase genes from artichoke are involved in the synthesis of chlorogenic acid. Plant Physiol 153: 1224–1238

Stapleton AE, Thornber CS, Walbot V (1997) UV-B component of sunlight causes measurable damage in field-grown maize (*Zea mays* L.): developmental and cellular heterogeneity of damage and repair. Plant Cell Environ 20: 279–290

St-Pierre B, Laflamme P, Alarco A-M, De Luca V (1998) The terminal O-acetyltransferase involved in vindoline biosynthesis defines a new class of proteins responsible for coenzyme A-dependent acyl transfer. Plant J 14: 703–713

Stracke R, Favory J-J, Gruber H, Bartelniewoehner L, Bartels S, Binkert M, Funk M, Weisshaar B, Ulm R (2010) The *Arabidopsis* bZIP transcription factor HY5 regulates expression of the PFG1/MYB12 gene in response to light and ultraviolet-B radiation. Plant Cell Environ 33: 88–103

Strid Å, Chow WS, Anderson JM (1994) UV-B damage and protection at the molecular level in plants. Photosynth Res 39: 475–489

Sytar O, Bruckova K, Hunkova E, Zivcak M, Konate K, Brestic M (2015) The application of multiplex fluorimetric sensor for the analysis of flavonoids content in the medicinal herbs family Asteraceae, Lamiaceae, Rosaceae. Biol Res 48: 5

Szopa A, Kokotkiewicz A, Kubica P, Banaszczak P, Wojtanowska-Krośniak A, Krośniak M, Marzec-Wróblewska U, Badura A, Zagrodzki P, Bucinski A, Luczkiewicz M, Ekiert H (2017) Comparative analysis of different groups of phenolic compounds in fruit and leaf extracts of *Aronia* sp.: *A. melanocarpa*, *A. arbutifolia*, and *A. ×prunifolia* and their antioxidant activities. Eur Food Res Technol 243: 1645–1657

Szopa A, Starzec A, Ekiert H (2018) The importance of monochromatic lights in the production of phenolic acids and flavonoids in shoot cultures of *Aronia melanocarpa*, *Aronia arbutifolia* and *Aronia × prunifolia*. J Photochem Photobiol B 179: 91–97

Tajik N, Tajik M, Mack I, Enck P (2017) The potential effects of chlorogenic acid, the main phenolic components in coffee, on health: a comprehensive review of the literature. Eur J Nutr 56: 2215–2244

Takahama U (1988) Hydrogen peroxide-dependent oxidation of flavonoids and hydroxycinnamic acid derivatives in epidermal and guard cells of *Tradescantia virginiana* L. Plant Cell Physiol 29: 475–481

Takahashi S, Badger MR (2011) Photoprotection in plants: a new light on photosystem II damage. Trends Plant Sci 16: 53–60

Takahashi S, Milward SE, Yamori W, Evans JR, Warwick Hillier, Badger MR (2010) The solar action spectrum of photosystem II damage. Plant Physiol 153: 988–993

Takahashi S, Murata N (2008) How do environmental stresses accelerate photoinhibition? Trends Plant Sci 13: 178–182

Takeuchi Y, Murakami M, Nakajima N, Kondo N, Nikaido O (1996) Induction and Repair of Damage to DNA in Cucumber Cotyledons Irradiated with UV-B. Plant Cell Physiol 37: 181–187

Takshak S, Agrawal SB (2019) Defense potential of secondary metabolites in medicinal plants under UV-B stress. J Photochem Photobiol B 193: 51–88

Taulavuori K, Hyöky V, Oksanen J, Taulavuori E, Julkunen-Tiitto R (2016) Species-specific differences in synthesis of flavonoids and phenolic acids under increasing periods of enhanced blue light. Environ Exp Bot 121: 145–150

Tegelberg R, Julkunen-Tiitto R, Aphalo PJ (2004) Red : far-red light ratio and UV-B radiation: their effects on leaf phenolics and growth of silver birch seedlings. Plant Cell Environ 27: 1005–1013

Teixeira A, Toorop PE, Iannetta PPM (2020) Differential interspecific adaptation to abiotic stress by *Plantago* Species. Front Plant Sci 11: 573039:

Tezuka T, Hotta T, Watanabe I (1993) Growth promotion of tomato and radish plants by solar UV radiation reaching the Earth's surface. J Photochem Photobiol B 19: 61–66

Tezuka T, Yamaguchi F, Ando Y (1994) Physiological activation in radish plants by UV-A radiation. J Photochem Photobiol B 24: 33–40

Theis J, Schroda M (2016) Revisiting the photosystem II repair cycle. Plant Signal Behav 11: e1218587

Thekaekara MP (1974) Solar energy monitor in space (SEMIS) (NASA technical memorandum 70623)

Thimijan RW, Carns HR, Campbell LE (1978) Radiation Sources and Related Environmental Control for Biological and Climatic Effects of UV Research (BACER). Beltsville Agricultural Research Center, United States. Environmental Protection Agency, Beltsville

Tohge T, Watanabe M, Hoefgen R, Fernie AR (2013) The evolution of phenylpropanoid metabolism in the green lineage. Crit Rev Biochem Mol Biol 48: 123–152

Tolbin AYu, Pushkarev VE, Tomilova LG, Zefirov NS (2017) Threshold concentration in the nonlinear absorbance law. Phys Chem Chem Phys 19: 12953–12958

Torras-Claveria L, Jáuregui O, Codina C, Tiburcio AF, Bastida J, Viladomat F (2012) Analysis of phenolic compounds by high-performance liquid chromatography coupled to electrospray ionization tandem mass spectrometry in senescent and water-stressed tobacco. Plant Sci 182: 71–78

Turcsányi E, Vass I (2000) Inhibition of photosynthetic electron transport by UV-A radiation targets the photosystem II complex. Photochem Photobiol 72: 513–20

Tyystjärvi E (2008) Photoinhibition of photosystem II and photodamage of the oxygen evolving manganese cluster. Coord Chem Rev 252: 361–376

Tyystjärvi E (2013) Photoinhibition of Photosystem II. International Review of Cell and Molecular Biology. Elsevier, pp. 243–303

U.S. Department of Energy (DOE)/NREL/ALLIANCE (2003) ASTM G173-03 reference spectra derived from SMARTS v. 2.9.2

Vane JR (1971) Inhibition of prostaglandin synthesis as a mechanism of action for Aspirin-like drugs. Nature New Biol 231: 232–235

Vass I (2012) Molecular mechanisms of photodamage in the photosystem II complex. Biochim Biophys Acta-Bioenerg 1817: 209–217

Vass I, Sass L, Spetea C, Bakou A, Ghanotakis DF, Petrouleas V (1996) UV-B-induced inhibition of photosystem II electron transport studied by EPR and chlorophyll fluorescence. Impairment of donor and acceptor side components. Biochemistry 35: 8964–8973

Vass I, Turcsányi E, Touloupakis E, Ghanotakis D, Petrouleas V (2002) The mechanism of UV-A radiation-induced inhibition of photosystem II electron transport studied by EPR and chlorophyll fluorescence. Biochemistry 41: 10200–10208

Veit M, Bilger W, Mühlbauer T, Brummet W, Winter K (1996) Diurnal Changes in Flavonoids. J Plant Physiol 148: 478–482

Verdaguer D, Jansen MAK, Llorens L, Morales LO, Neugart S (2017) UV-A radiation effects on higher plants: Exploring the known unknown. Plant Sci 255: 72–81

Verpoorte R (2000) Secondary metabolism. In: Verpoorte R, Alfermann AW (eds) Metabolic engineering of plant secondary metabolism. Springer Netherlands, Dordrecht, pp. 1–29

Villegas RJ, Kojima M (1986) Purification and characterization of hydroxycinnamoyl D-glucose. Quinate hydroxycinnamoyl transferase in the root of sweet potato, Ipomoea batatas Lam. J Biol Chem 261: 8729–8733

Vogt T (2010) Phenylpropanoid biosynthesis. Mol Plant 3: 2–20

Vogt T, Gülz P-G, Reznik H (1991) UV radiation dependent flavonoid accumulation of *Cistus laurifolius* L. Z Für Naturforschung C 46: 37–42

Wilson KE, Thompson JE, Huner NPA, Greenberg BM (2001) Effects of ultraviolet-A exposure on ultraviolet-B–induced accumulation of specific flavonoids in *Brassica napus*. Photochem Photobiol 73: 678

Xiong FS, Day TA (2001) Effect of solar ultraviolet-B radiation during springtime ozone depletion on photosynthesis and biomass production of antarctic vascular plants. Plant Physiol 125: 738–751

Xuan W, Beeckman T, Xu G (2017) Plant nitrogen nutrition: sensing and signaling. Curr Opin Plant Biol 39: 57–65

Yan S-P, Zhang Q-Y, Tang Z-C, Su W-A, Sun W-N (2006) Comparative Proteomic Analysis Provides New Insights into Chilling Stress Responses in Rice. Mol Cell Proteomics 5: 484–496

Yu X, Liu H, Klejnot J, Lin C (2010) The cryptochrome blue light receptors. Arab Book 8:e0135: 1–27

Zink LL (2018) Induktion von Chlorogensäure unter Stickstoffmangel bei *Helianthus annuus* . Bachelor thesis. Christian-Albrechts-Universität, Kiel

8 Supplement

8.1 Idetification of phenylpropanoids

Aqueous methanolic leaf extracts of sunflowers with strong UV screening were analysed by a combination of HPLC and MS/MS analysis in the Department of Physiology and Cell Biology at the Leibniz Institute of Plant Genetics and Crop Plant Research (IPK) in Gatersleben after evaporation. In these highly concentrated leaf extracts, further isomers of mono- and dicaffeoylquinic acids including 5-O-CQA, 4-O-CQA, 3,4-di-O-CQA and 4,5-di-O-CQA as well as one caffeoylhexoside were found. Besides, several flavonoids were abundant in inferior amounts. These flavonoids were identified as glycosides of flavonols of which quercetin was the most common (Fig. S7.1, Table S7.1).

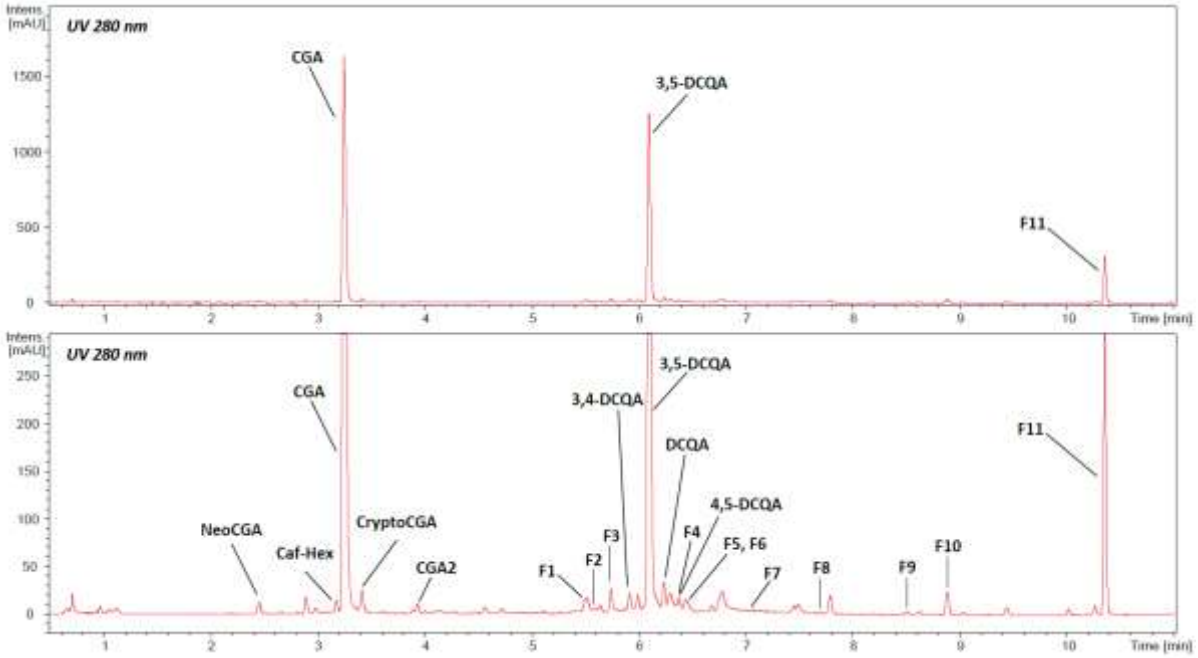

Fig. S7.1 HPLC-DAD chromatogram at 280 nm of a highly concentrated sunflower (*Helianthus annuus* cv. Peredovick) leaf extract as published in Stelzner et al. (2019). Aqueous methanolic leaf extracts of high light grown sunflowers (230 µmol m^{-2} s^{-1})was evaporated and analysed by HPLC-PDA-ESI-QTOF-MS/MS.

			Positive ion mode					Aglycone (flavonoids)			
Poly-phenol	**Abbre-viation**	**Rt (min)**	**Precursor (m/z)**	**Fragments (M/z)**	**Annotation**	**Molecular formula**	**Monoisotopic mass**	**Tentative aglycone**	**Molecular formula**	**Monoisotopic mass**	**Reference**
1	NeoCGA	2.46	355.1008	163.03, 145.02, 135.04	5-O-Caffeoyl quinic acid (Neochlorogenic acid)	$C_{16}H_{18}O_9$	354.0951	—	—	—	Authentic standard. Confirmed by MS/MS and Rt.
2	Caf-Hex	3.19	343.1015	325.09, 307.08,181.04, 163.03, 145.02, 135.04	Caffeoyl-hexoside	$C_{15}H_{18}O_9$	342.298	—	—	—	Not available.
3	CGA	3.25	355.1028	337.09, 163.03,145.02, 135.04	3-*O*-Caffeoyl quinic acid (Chlorogenic acid)	$C_{16}H_{18}O_9$	354.0951	—	—	—	Authentic standard. Confirmed by MS/MS and Rt.
4	CryptoCGA	3.41	355.1026	163.03, 135.04	4-*O*-Caffeoylquinic acid (Cryptochlorogenic acid)	$C_{16}H_{18}O_9$	354.0951	—	—	—	Authentic standard. Confirmed by MS/MS and Rt.
5	CGA2	3.96	355.1026	163.03, 145.02,135.04	*O*-Caffeoyl quinic acid	$C_{16}H_{18}O_9$	354.0951	—	—	—	Authentic standard. Confirmed by MS/MS.
6	F1	5.52	641.1793	495.11, 333.06,**318.03**	Pentahydroxy-methoxyflavone-deoxyhexoside	$C_{28}H_{32}O_{17}$	640.1639	Flavonol	$C_{15}H_{10}O_8$	318.0376	Not available.
7	F2	5.6	465.0952	**303.04**	Pentahydroxyflavone-hexoside	$C_{21}H_{20}O_{12}$	464.0955	Quercetin	$C_{15}H_{10}O_7$	302.0427	Schilling et al., 1981; 1983; 1987
8	F3	5.74	495.1154	333.06, **318.03**	Pentahydroxy-methoxyflavonehexoside	$C_{22}H_{22}O_{13}$	494.106	Flavonol	$C_{15}H_{10}O_8$	318.0376	Not available.
9	3,4-DCQA	5.92	517.1346	499.12, 163.03	3,4-Di-*O*-Caffeoyl quinic acid	$C_{25}H_{24}O_{12}$	516.1268	—	—	—	Authentic standard. Confirmed by MS/MS and Rt.
10	3,5-DCQA	6.11	517.1337	499.12, 319.08,163.03, 145.02, 135.04	3,5-Di-*O*-Caffeoyl quinic acid	$C_{25}H_{24}O_{12}$	516.1268	—	—	—	Authentic standard. Confirmed by MS/MS and Rt.
11	DCQA	6.24	517.1347	499.12, 163.03, 145.02, 135.04	Di-*O*-Caffeoyl quinic acid	$C_{25}H_{24}O_{12}$	516.1268	—	—	—	Authentic standard. Peak 2
12	F4	6.36	551.1089	**303.05**	Pentahydroxyflavone-malonylhexoside	$C_{24}H_{22}O_{15}$	550.0959	Quercetin	$C_{15}H_{10}O_7$	302.0427	Schilling et al., 1981; 1983; 1987
13	4,5-DCQA	6.38	517.1344	499.12, 163.03	4,5-Di-*O*-Caffeoyl quinic acid	$C_{25}H_{24}O_{12}$	516.1268	—	—	—	Authentic standard. Confirmed by MS/MS and Rt.
14	F5	6.42	581.1203	333.06, **318.03**	Pentahydroxy-methoxyflavonemalonyl-hexoside	$C_{25}H_{24}O_{16}$	580.1064	Flavonol	$C_{15}H_{10}O_8$	318.0376	Not available
15	F6	6.49	565.1192	479.11, 317.06,**302.04**	Tetrahydroxy-methoxyflavonemalonyl-hexoside	$C_{25}H_{24}O_{15}$	564.1115	Quercetin	$C_{15}H_{10}O_7$	302.0427	Schilling et al., 1981; 1983; 1987
16	F7	7.04	549.1216	463.14, 301.07,**286.04**	Trihydroxy-methoxyflavonemalonyl-hexoside	$C_{25}H_{24}O_{14}$	548.1166	Kaempferol/ Lutelin	$C_{15}H_{10}O_6$	286.0477	Schilling et al., 1981; Rieseberg et al., 1987
17	F8	7.71	317.0656	**302.04**	Tetrahydroxy-methoxyflavone	$C_{16}H_{12}O_7$	316.0583	Quercetin	$C_{15}H_{10}O_7$	302.0427	Schilling et al., 1981; 1983; 1987
18	F9	8.5	301.0708	**286.04**	Trihydroxy-methoxyflavone	$C_{16}H_{12}O_6$	300.0634	Kaempferol/ Lutelin	$C_{15}H_{10}O_6$	286.0477	Schilling et al., 1981; Rieseberg et al.,1987
19	F10	8.88	361.0921	346.04, 331.04,**316.02**	Trihydroxy-trimethoxyflavone	$C_{18}H_{17}O_8$	361.0923	Flavonol	$C_{15}H_{10}O_8$	318.0376	Not available
20	F11	10.33	345.0969	30.07, 315.05,**300.06**	Dihydroxy-trimethoxyflavone	$C_{18}H_{16}O_7$	344.0896	Quercetin	$C_{15}H_{10}O_7$	302.0427	Schilling et al., 1981; 1983; 1987

Table S7.1 Phenylpropanoids of sunflower leaves

List of polyphenolic compounds in highly concentrated sunflower leaf extracts corresponding to chromatogram (Fig.S7.1) with MS data and method of identification

8.2 Photoinhibition data

After one hour of exposure to solar UV-A (5.7 W m^{-2} for λ from 280-400 nm), the maximal quantum efficiency in leaf discs of low light grown plants was significantly reduced to 0.57 ± 0.01 in contrast to leaf discs of high light grown plants that displayed F_V/F_M of 0.76 ± 0.2 (Fig. S7.2). One hour of – UV-A treatment included a residual UV irradiance of 0.4 W m^{-2} that did not lower the maximal photochemical quantum yield in a significant manner. Corresponding F_V/F_M values were at 0.74 ± 0.1 for low light grown plants and 0.78 ± 0.01 for those grown in high light.

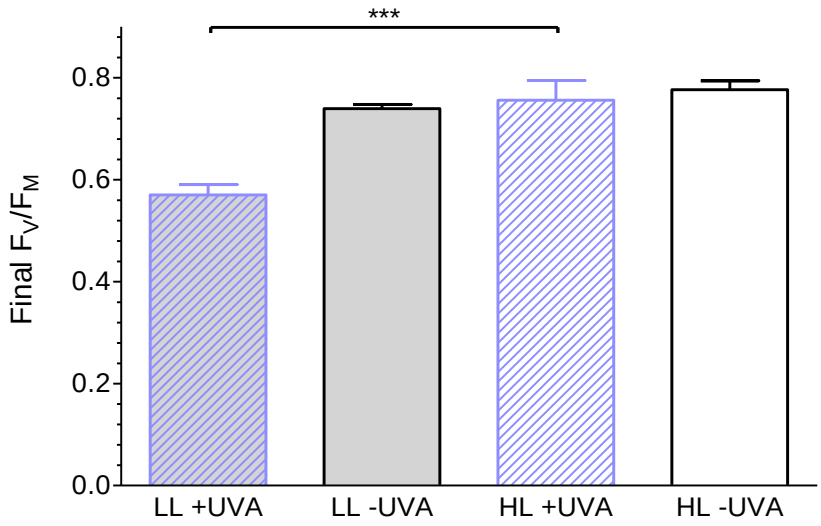

Fig. S7.2 Final maximal photochemical quantum yield after one hour of exposure to solar UV-A UV-A treatment (5.7 W m^{-2}) was conducted with lincomycin-treated leaf discs of six different sunflower plants whereas three biological replicates were used for − UV-A due to limited space below filters. Each treatment was conducted with low (LL; $T_{UV\text{-}A}$ = 1.01 ± 0.04) and high light (HL; $T_{UV\text{-}A}$ = 0.24 ± 0.12) grown plants. Values are given as average with standard deviation (± SD). Analysis of statistical significance was conducted by comparison of high and low light grown plants exposed to UV-A by an unpaired t-test ($p<0.0001$).

After one hour of exposure to solar UV-A (5.7 W m^{-2} for λ from 280-400 nm), the maximal quantum efficiency in leaf discs of low light grown plants was significantly reduced to 0.57 ± 0.01 in contrast to leaf discs of high light grown plants that displayed F_V/F_M of 0.76 ± 0.2 (Fig. S7.2). One hour of – UV-A treatment included a residual UV irradiance of 0.4 W m^{-2} that did not lower the maximal photochemical quantum yield in a significant manner. Corresponding F_V/F_M values were at 0.74 ± 0.1 for low light grown plants and 0.78 ± 0.01 for those grown in high light.

8.3 Contribution of CQAs to foliar UV-A screening in sunflower exposed to abiotic stress

The shift experiments allowed a further correlation of determined epidermal UV-A absorbance with caffeoyl residues obtained by HPLC data and CGA-based calibration. Again, a curvi-linear correlation with a comparatively high degree of accuracy was found (Fig. S7.3).

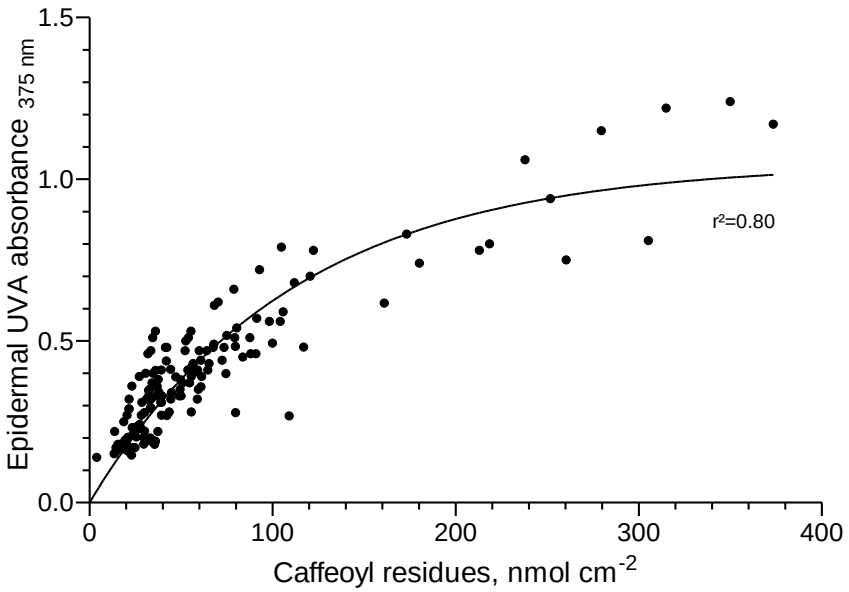

Fig. S7.3 Correlation of epidermal UV-A absorbance and molar amount of caffeoyl moieties
Epidermal absorbance was determined during shift experiments via DUALEX ® leaf discs that were analysed in parallel by HPLC. Data of PPFD and temperature shift experiments is shown including measurments of 151 leaf discs of 40 sunflower individuals. Caffeoyl moieties were calculated for a leaf area of 1 cm² as described in material and methods including correction for DCQA absorbance. The data was fitted with non-linear regression: $A_{UV\text{-}A} = 1.05 \times (1 - e^{-0.009025\,x})$ ($R^2 = 0.80$).

8.4 Presence of further unidentified low abundant phenylpropanoids in sunflower exposed to abiotic stress

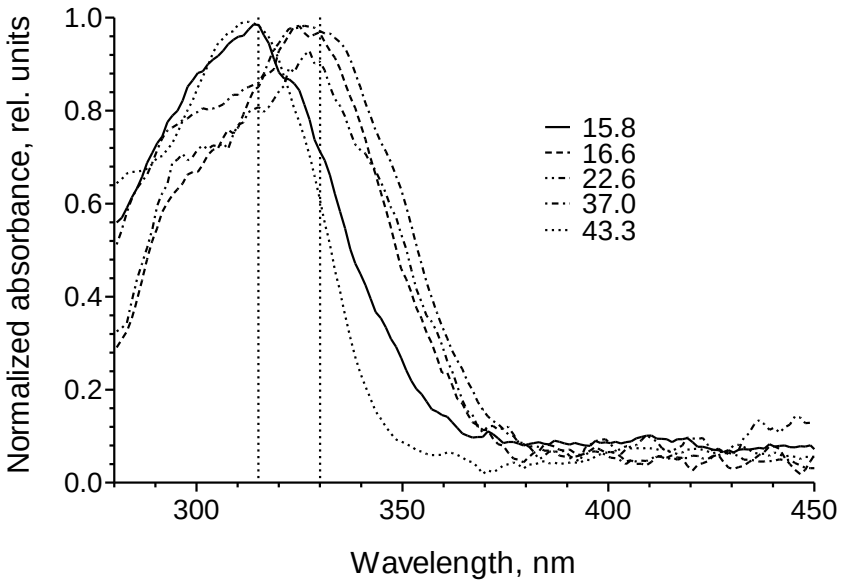

Fig. S7.4 Normalized UV absorbance spectra of very low abundant phenylpropanoids extracted from plants shifted to abiotic stress conditions
The leaf material was harvested at the final time point (72 h or 120 h after the shift). UV absorbance spectra were smoothened afterwards. Peaks with retention times of 22.6 (dot-dot-dashed line) and 37.0 (dot-dashed line) minutes were present in extracts from plants shifted to 380 µmol m^{-2} s^{-1} and to 9°C. Peaks at 15.8 (solid black line), 16.6 (dashed line) and 22.6 minutes were found in plants shifted to high PPFD whereas peak at 43.3 minutes was solely abundant in low temperature treated plants. Dashed vertical lines mark 315 and 330 nm.

Very low abundant phenylpropanoids with absorbance below 0.5 % of the total peak area at 330 nm displayed mainly UV absorbance spectra very similar to that of predominant caffeoylquinic acids with maximal absorbance at approximately 330 nm (Peaks at 16.6, 22.6 and 37.0 minutes). Peaks with retention times at 15.8 and 43.3 minutes showed a slightly deviating UV absorbance with a maximum at 315 nm (Fig. S7.4). The two peaks with a maximal extinction near 360 nm occurred sporadically in low temperature or UV-B treated samples. The corresponding areas of the peaks at 23.6 minutes and 46.5 minutes did not exceed 0.5 % and 1.5 % of total absorbance at 360 nm in any sample (Fig. S7.5).

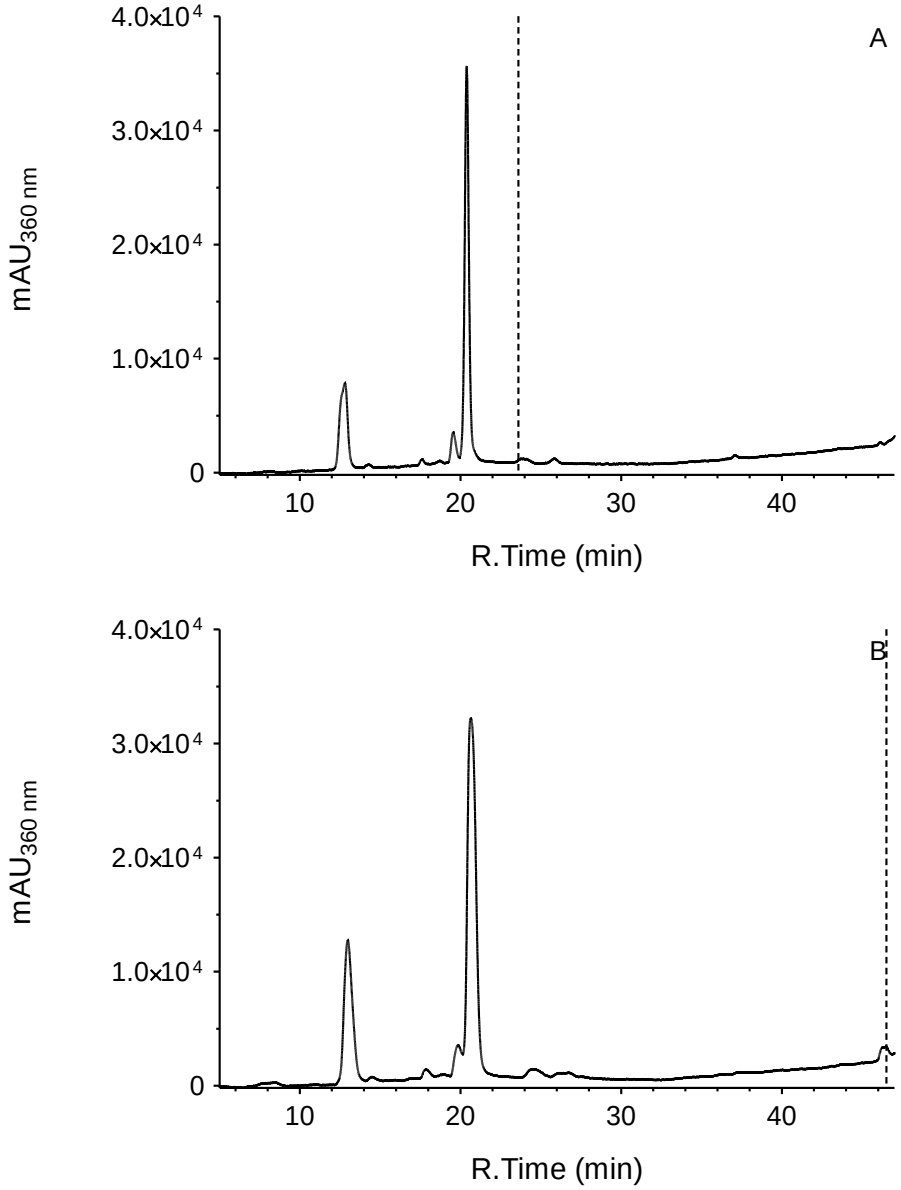

Fig. S7.5 Representative UV-DAD chromatograms at 360 nm of aqueous methanolic extracts from leaves sampled at the end of the temperature (A) or UV-B (B) shift experiment
In total, two peaks with a maximal extinction above 330 nm occurred sporadically in low temperature (peak at 23.6 minutes) or UV-B (peak at 46.5 minutes) treated samples. The peak with a retention time of 23.6 minutes displayed maximal absorbance at 350 nm and the peak at 46.5 minutes showed maximal extinction at 365 nm. The corresponding areas of the peaks at 23.6 minutes and 46.5 minutes were less than 0.5 % and 1.5 % of total absorbance at 360 nm.

8.5 Phenylpropanoids in floral tissues

In order to test whether flavonoids are principally abundant in other aerial parts of the sunflower cultivar Peredovick than in foliar leaves and can be found by the used methods, flower parts including bracts, tubular and ligulet florets were extracted and analysed by HPLC as described for foliar leaves (Fig. S7.6). UV-DAD chromatograms of flower parts showed mono- and dicaffeoylquinic acid as dominant phenolic constituents but displayed a slightly more diverse phenylpropanoid pattern than foliar leaves.

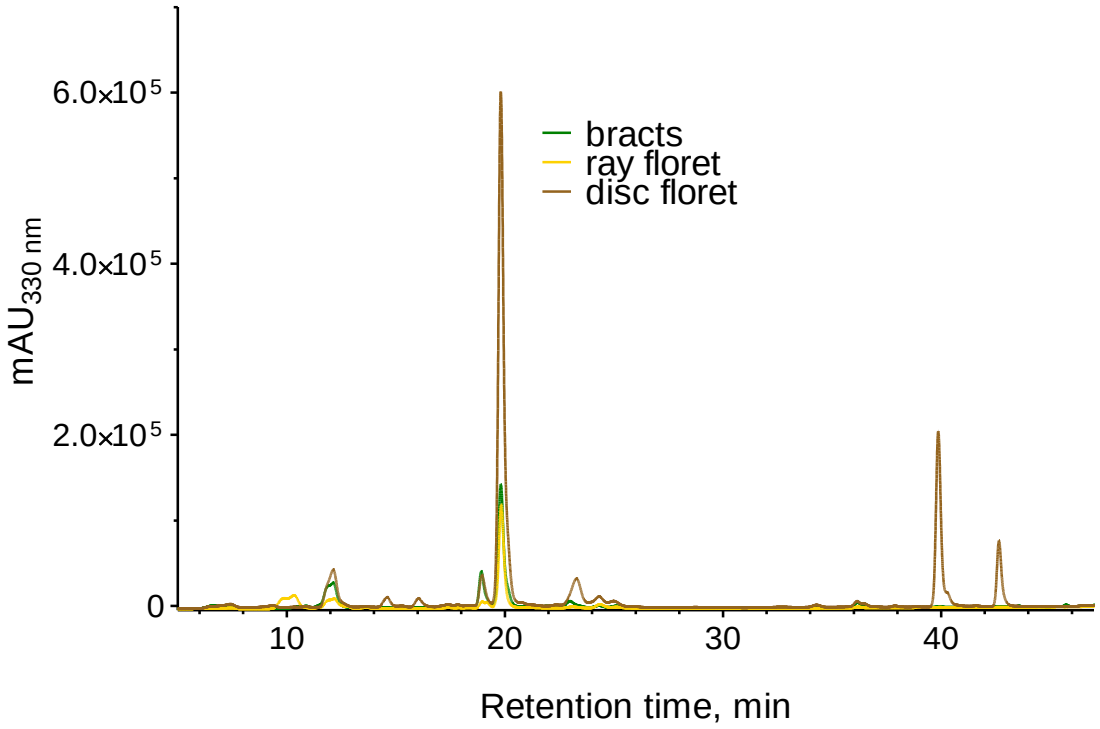

Fig. S7.6 UV-DAD chromatogram at 330 nm of aqueous methanolic extract of flower parts
Bracts (green), tubular (yellow) and ligulet (brown) florets of five sunflowers grown at 230 µmol m^{-2} s^{-1} PAR were extracted as described for foliar leaves and analysed in technical triplicates via HPLC.

Bracts contained similarly to foliar leaves mainly phenylpropanoids that were classified solely as hydroxycinnamic acid esters according to their absorbance spectra. In ligulate and tabulate flower extracts, several phenolics with maximal extinction above 350 nm up to 375 nm were found (Fig. S7.7).

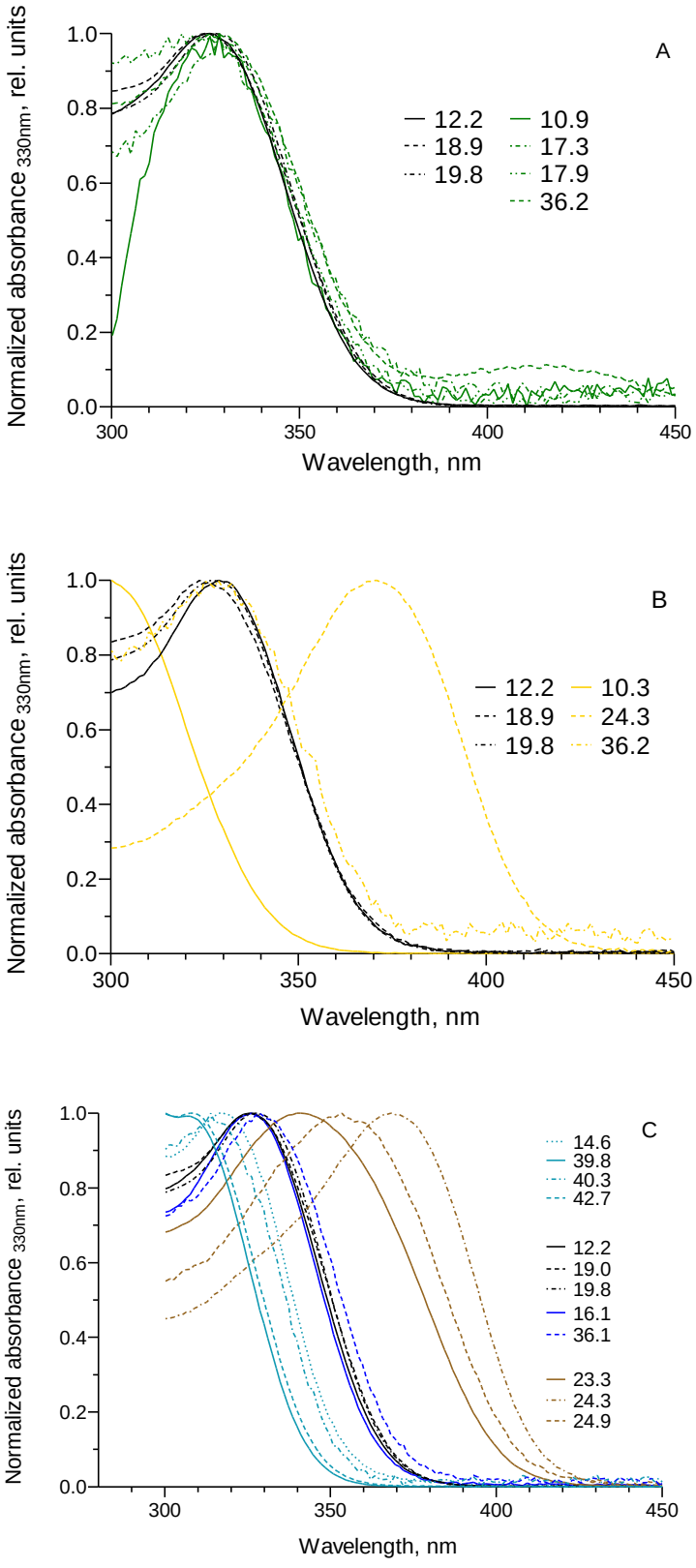

Fig. S7.7 Online UV absorbance spectra of phenolics extracted from bracts (A), tubular (B) and ligulet (C) florets

Floral parts of sunflowers grown at 230 µmol m^{-2} s^{-1} PAR were extracted as described for foliar leaves. Identified HCAs (CGA: black solid line, DCQA: dashed and dot-dashed black line) and unidentified phenylpropanoids (A, green lines; B, yellow lines and C turquoise, blue and brown lines).

8.6 RNA integrity

RNA integrity was checked prior to cDNA synthesis in randomly selected samples by agarose gel electrophoresis (Fig. S7.8). Each sample showed five distinct bands with comparable signal intensity of fluorescence. These five bands very likely correspond – in descending order – to 28S-, 18S-ribosomal and plastid RNA as published for nucleotide extraction for different higher plant species suggesting the RNA quality to have been suitable for subsequent PCR analysis (Oliveira et al. 2015). The diffuse bands at the lower part of the gel might come from partially degraded RNA. However, the calculation of relative gene expression corrects for amounts of degraded RNA.

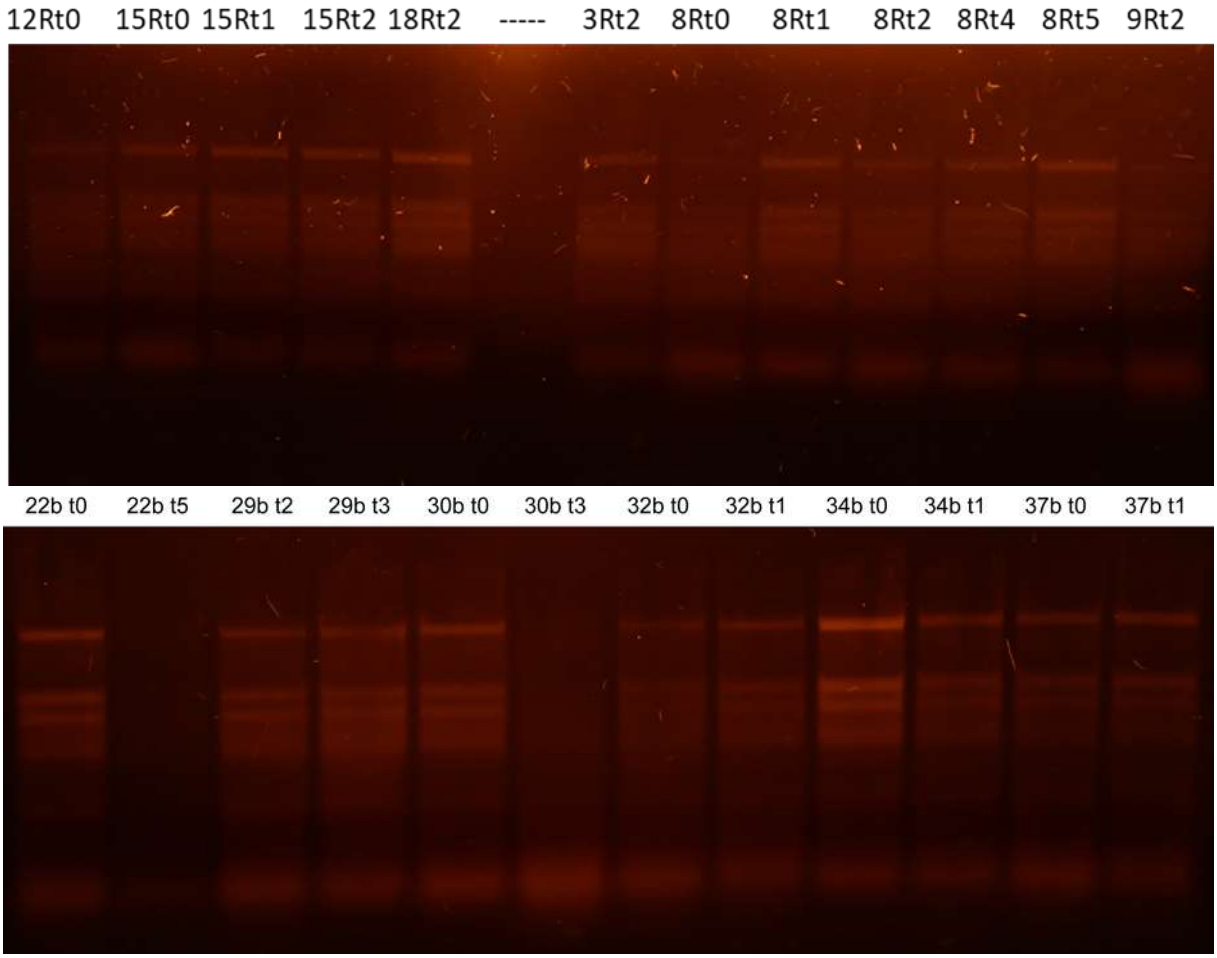

Fig. S7.8 RNA integrity gel of selected samples
An amount of 300 ng RNA per sample was added to a MOPS-based loading buffer mixed with ethidium bromide and used to check for integrity by running electrophoresis at 70 V for 45 min on an agarose gel (1 %; Carl Roth GmbH & Co KG). Afterwards 3.6 µL of ethidium bromide (1 % stock solution, Carl Roth GmbH & Co. KG) was added to 500 µL of loading buffer.

8.7 Melting curves and reference gene stability

The different qRT-PCR runs displayed similar curves of SYBR green fluorescence indicating successful RNA extraction, cDNA synthesis and amplification of desired amplicons. Template samples displayed threshold cycles (C_Ts) ranging from 24 cycles (*ACT7*) to 35 (*HQT3*). Non-template samples displayed constantly very low fluorescence during the PCR runs (Fig. S7.9).

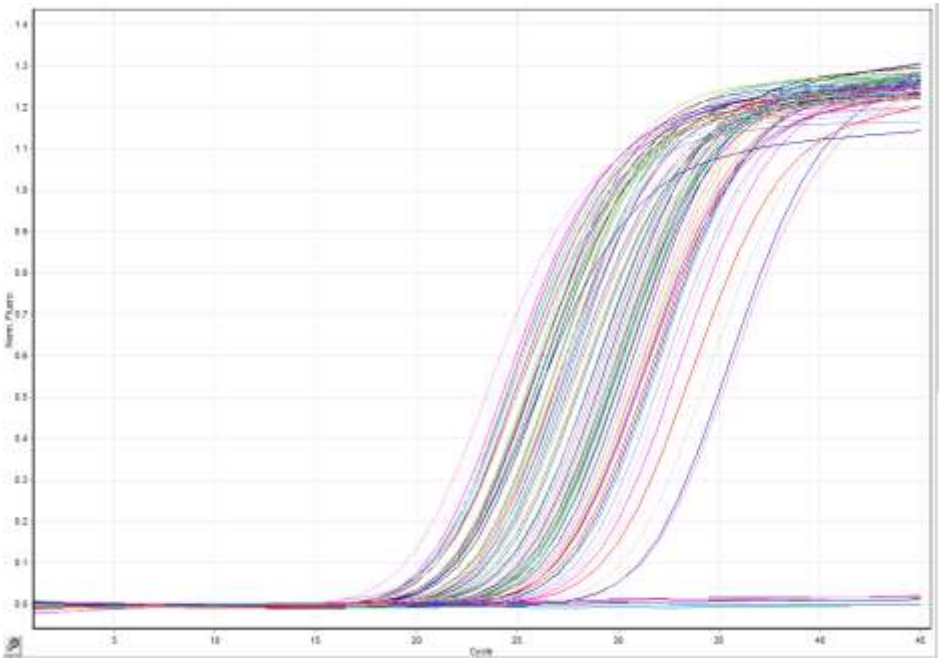

Fig. S7.9 Representative fluorescence curves of qRT-PCR
Normalized fluorescence on a linear scale of the SYBR Green fluorescence monitored in the green channel of a representative qRT-PCR used for analysis of relative gene expression and regulation by abiotic variables, respectively. The chart displays all samples of one qRT-PCR run including control, treated and non-template samples for the two reference genes and three genes of interest (HQT1 to 3).

Melting curves showed single products for each primer pair indicating specific amplification and no artefact production caused by primer dimers. The amplicons had melting points between 82.3 to 82.5 °C for *ACT7*, 81.3 to 81.5 °C for eIF5A, 84.3 to 84.5 °C for *HQT1*, 83.0 to 83.2 °C for *HQT2* and 81.0 to 81.2 °C for *HQT3* (Figs. S7.10A –E). Non-template controls showed consistently no peaks.

In order to verify the suitability of chosen reference genes with respect to its stable expression during abiotic stress, the C_T-values of *ACT7* and *eIF5A* were averaged for control and shifted plants separately at the different time points of sampling for each shift experiment (Figs. S7.11A-D). The averaged C_T-values of the reference genes differed neither between control and shifted plants nor between the different time points of sampling in a significant manner, with one exception (Fig. S7.11A).

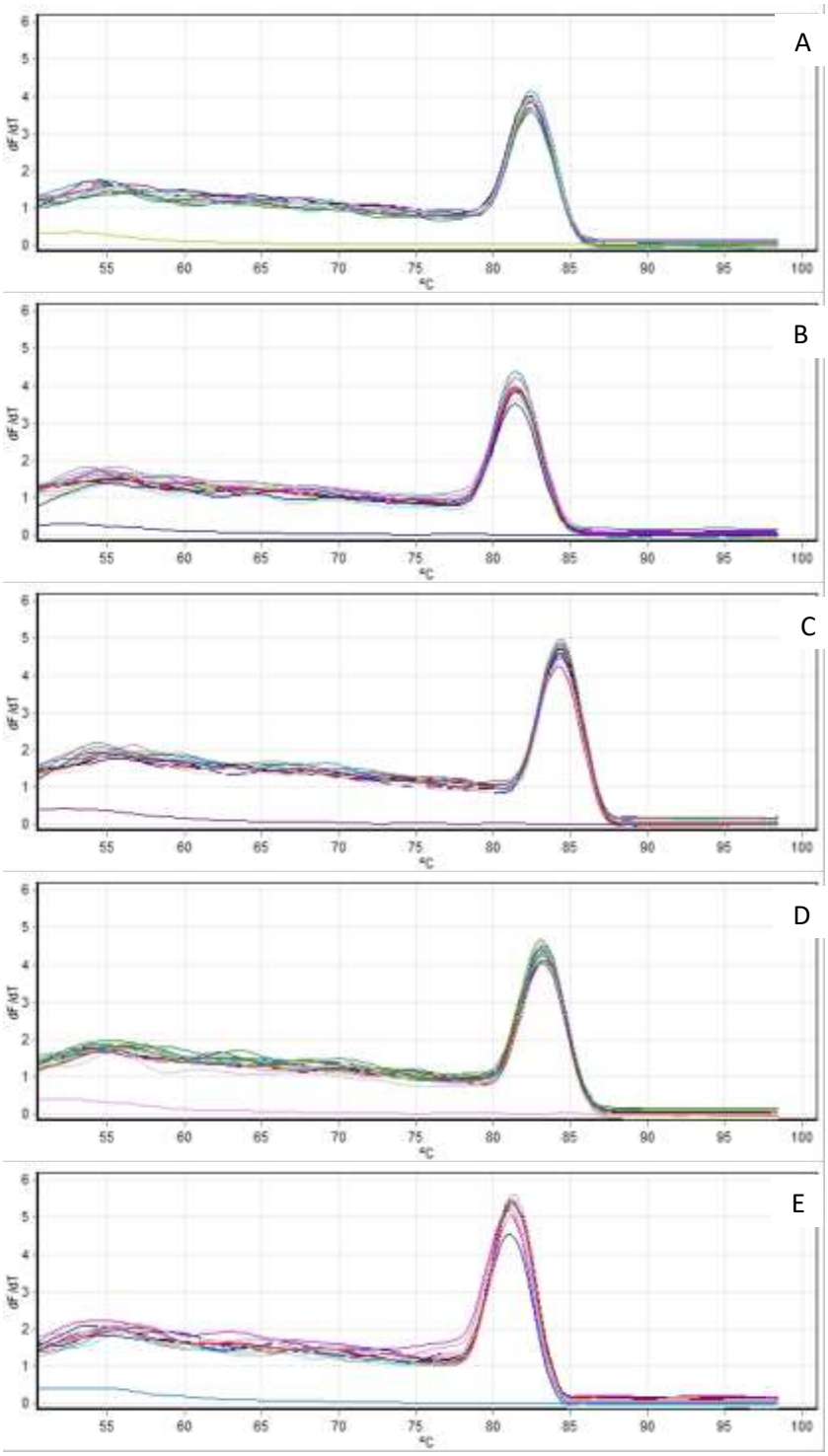

Fig. S7.10 Representative melting curves for the qRT-PCR runs
Melting curves displayed amplicons for primer pairs of *ACT7* (A), *eIF5A* (B), *HQT1* (C), *HQT2* (D) and *HQT3* (E). The averaged melting points of respective amplification were at 82.5 °C for *ACT7*, 81.5 °C for *eIF5A*, 84.5 °C for *HQT1*, 83.2 °C for *HQT2* and 81.2 °C for *HQT3* throughout analysed samples.

At the final time point (72 hours) in the PPFD experiment, the average relative expression of *ACT7* of shifted plants was significantly higher ($p < 0.0001$) than in control plants. For this time point, the averaged C_T values differed by approximately three units between shifted and control plants. All other averaged C_T-values deviated between 0.2 and 0.9 units from the overall average. A stable expression of *ACT7* and *eIF5A* has been determined previously in a different PPFD shift experiment as

described in more detail in the discussion (Böttcher 2020). The difference was not observed – neither for *ACT7* nor for *eIF5A* – in analysis of transcript levels under high PPFD on a comparable time scale at 0, 2, 6, 24, 72 and 96 hours (Böttcher 2020). Based on data of Carolin Böttcher, *ACT7* was evaluated as suitable reference gene, due to slight differences between C_T values of control and treated plants (between 0.1 and 0.8). Due to the suspicious deviation at 72 hours an outlier search was conducted according to the "1.5 × IQR"-rule. Two outliers were found for *ACT7* and were excluded when $2^{-\Delta\Delta C_T}$ of *HQT* was calculated. A similar inconsistence was observed in the UV-B shift (0.05 W m^{-2}) experiment (Fig. S7.11C). A search for outliers found five outliers that were excluded in the calculation of relative gene expression of *HQT* genes. This deviation for *ACT7* was not replicable in the other UV-B experiment. There, expression of *ACT7* remained stable, confirming outlier status of the deviating data points (Fig. S7.11D). For *eIF5A*, no deviation after either PPFD or UV shift was observed. The transcript levels of both reference genes have not been affected by low temperature at any time point (Fig. S7.11B).

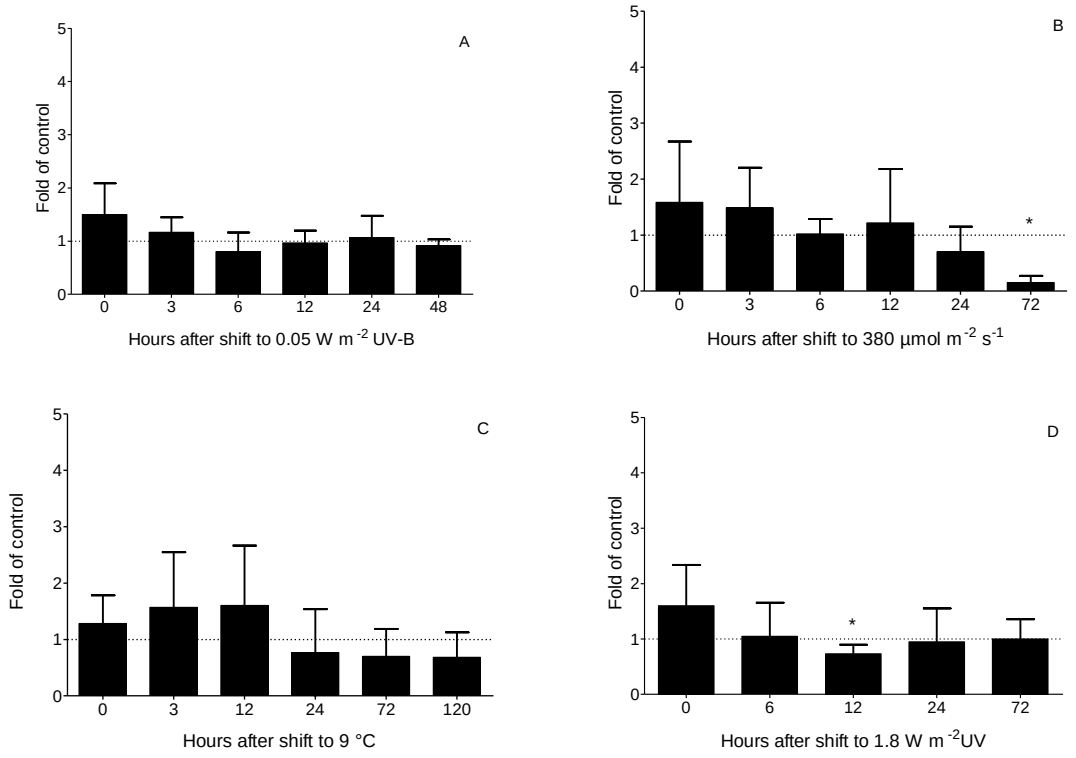

Fig. S7.11 Relative expression of **the reference genes in shifted plants**
Relative expression as fold of control ($2^{-\Delta CT}$) of the reference genes *ACT7* and *eIF5A* is shown in dependence of time in shifted plants. Plants were shifted to either 0.05 W m^{-2} UV-B (A), 380 µmol m^{-2} s^{-1} (B), to 9 °C (B) or to 1.6 W m^{-2} UV-B (D). The control plants for D were exposed to small amount of UV-B during growth. Data points represent the averages of three biological replicates analysed in technical duplicates and is given with standard deviation (n=3). Horizontal dotted lines represent equal reference gene expression in shifted and control plants. The gene expression was not significantly different from one except for values that are marked with asterisks (Wilcoxon Signed Rank Test, $p < 0.05$). These values imply requirement of further reference gene analysis and were excluded in the calculation of ΔC_T.and $\Delta\Delta C_T$ for *HQT* expression.

9 Eidestattliche Erklärung

Jana Stelzner
Jahnstraße 8
24116 Kiel

Hiermit versichere ich an Eides statt, dass ich die vorliegende Dissertation selbständig verfasst habe und sie – abgesehen von der Beratung durch meinen Supervisor – nach Inhalt und Form meine eigene Arbeit ist und nur mit den angegebenen Hilfsmitteln verfasst wurde. Die Arbeit ist unter Einhaltung der Regeln guter wissenschaftlicher Praxis der Deutschen Forschungsgemeinschaft entstanden. Ich erkläre außerdem, dass die in dieser Dissertation zusammengefassten Daten an keiner anderen Stelle im Rahmen eines anderen Prüfungsverfahrens vorgelegt wurden. Teile der Dissertation sind unter dem Titel „Hydroxycinnamic acids in sunflower leaves serve as UV-A screening pigments“ in dem Journal „Photochemical & Photobiological Sciences” (Volume 18, pp 1649–59; DOI: 10.1039/c8pp00440d) veröffentlicht.
Ferner wurde mir kein akademischer Grad entzogen.

Kiel, den _____ _____

(Jana Stelzner)